Palabras Clave:

Ácido *N*-acetilneuramínico aldolasa, enzima acoplada, cinética, ensayo espectrofotométrico, lactato deshidroganasa, evolución dirigida, nicotinaminidasa, glutamato deshidroganasa, nicotinamida mononucleotido desaminasa, modelado de estructuras protéicas, filogenia, mutagénesis, metabolismo NAD.

Resumen en Español:

El objetivo de esta tesis fue la búsqueda de nuevas aldolasas y nicotin desaminasas bacterianas con características mejoradas para la producción de compuestos con interés farmacéutico y biotecnológico. En primer lugar, se clonó y caracterizó una ácido *N*-acetilneuramínico aldolasa de *Lactobacillus plantarum*, que se utilizó como molde para la creación de librerías de evolución dirigida. Se desarrollo un método de ensayo de alto rendimiento para esta librería de evolución dirigida, utilizando una L-lactato deshidrogenasa de *Bacillus halodurans* como enzima acoplada. 2 nuevas enzimas involucradas en el metabolismo del NAD se clonaron y caracterizaron: una nicotinaminidasa y una nicotinamida mononucleótido (NMN) desaminasa, ambas obtenidas del extremófilo *Oceanobacillus iheyensis* HTE831. Se desarrollo también un método de cribado de alto rendimiento para nicotinaminidasas, basado en el uso de una glutamato deshidrogenasa clonada de *Bacillus halodurans*. Además, se describió por primera vez un método de medida espectrofotométrico para la NMN desaminasa.

Resumen en Inglés:

The main objective was the search for new bacterial aldolases and nicotin deamidases with improved characteristics for the production of compounds with pharmaceutical and biotechnological interest. In first instance, the cloning and characterization of the novel *N*-acetylneuraminic acid aldolase from *Lactobacillus plantarum* was achieved and it was used as template for directed evolution experiments. A high-throughput screening method for this directed evolution library was developed using a novel L-lactate dehydrogenase from *Bacillus halodurans* as coupling enzyme. Two novel enzymes

involved in the NAD^+ metabolism were also cloned and characterized: a nicotinamidase and a nicotin mononucleotide (NMN) deamidase, both from the extremophile *Oceanobacillus iheyensis* HTE831. A high-throughput screening method for nicotinamidases was also developed, based on the use of a cloned glutamate dehygrogenase from *Bacillus halodurans.* Furthermore, a novel spectrophotometric screening method was described for the first time for the enzyme nicotinamide mononucleotide deamidase.

UNIVERSIDAD DE MURCIA
FACULTAD DE BIOLOGÍA

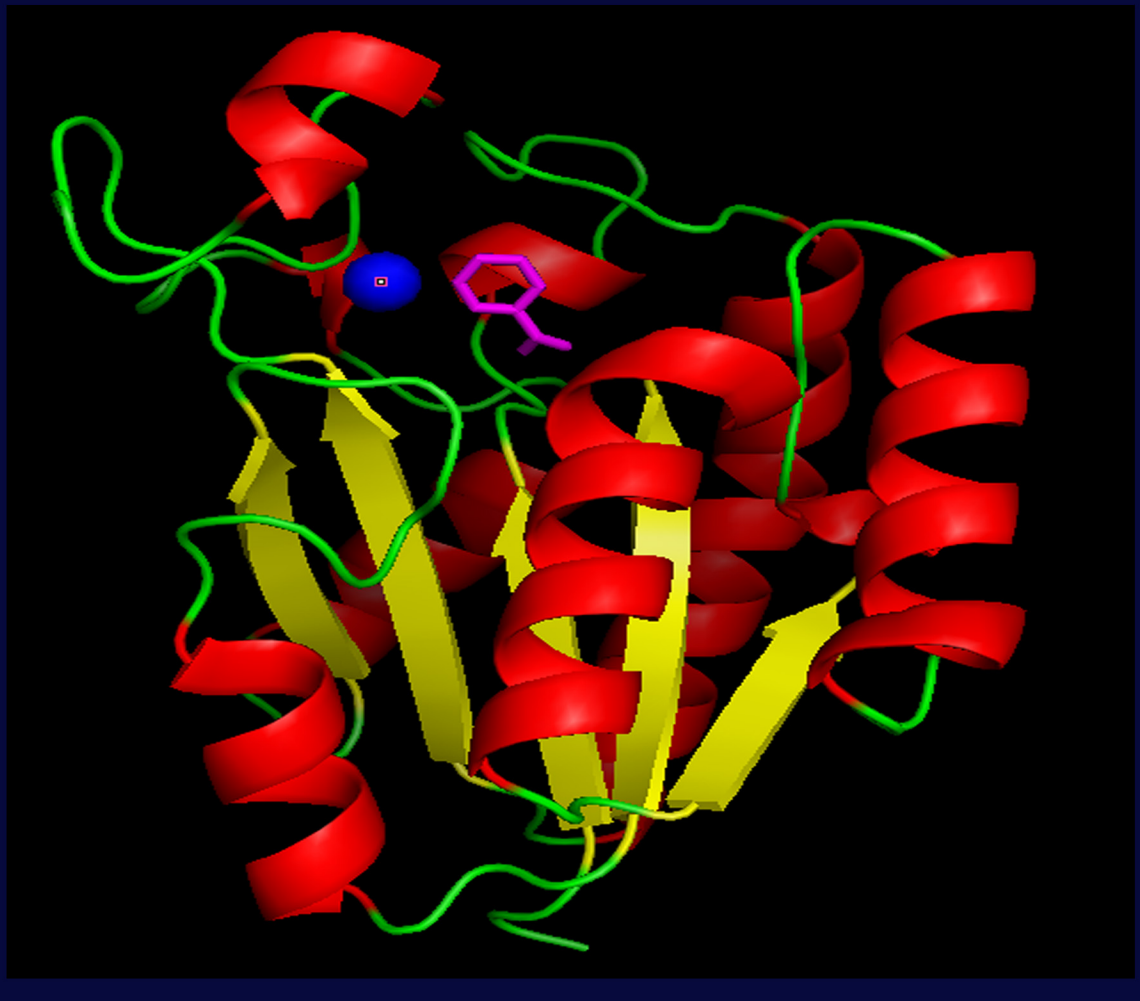

“Caracterización cinetica y molecular de nicotin desaminasas y aldolasas mediante enzimas acopladas”

Guiomar Sánchez Carrón

2012

UNIVERSIDAD DE MURCIA

FACULTAD DE BIOLOGÍA

"Caracterización cinética y molecular de nicotin desaminasas y aldolasas mediante enzimas acopladas"

Guiomar Sánchez Carrón

2012

UNIVERSIDAD DE MURCIA

FACULTAD DE BIOLOGÍA

"Caracterización cinética y molecular de nicotin desaminasas y aldolasas mediante enzimas acopladas"

"Kinetic and molecular characterization of nicotin deamidases and aldolases using couple enzymes"

Memoria presentada para aspirar al título de

Doctor por la Universidad de Murcia

Guiomar Sánchez Carrón

2012

UNIVERSIDAD DE
MURCIA

D. Álvaro Sánchez Ferrer y **D. Francisco García Carmona,** Catedráticos de Universidad del área de Bioquímica y Biología Molecular en el Departamento de Bioquímica y Biología Molecular-A,

AUTORIZAN

La presentación de la Tesis Doctoral titulada **"Caracterización cinética y molecular de nicotin desaminasas y aldolasas mediante enzimas acopladas",** realizada por **Dª. Guiomar Sánchez Carrón,** bajo nuestra inmediata dirección y supervisión en el departamento de Bioquímica y Biología Molecular-A, y que presenta para la obtención del grado de Doctor por la Universidad de Murcia.

En Murcia, a 25 de Julio de 2012

Fdo. Álvaro Sánchez Ferrer

Fdo. Francisco García Carmona

UNIVERSIDAD DE
MURCIA

Dª. Teresa Soto Pino, Profesora Titular de Universidad del Área de Microbiología y **Presidente Comisión Académica programa doctorado** * en Biología Molecular y Biotecnología, INFORMA:

Que una vez evaluado, de conformidad con el procedimiento establecido en el artículo 21 del Reglamento de doctorado de la Universidad de Murcia, el expediente completo de la tesis doctoral titulada "Caracterización cinética y molecular de nicotin desaminasas y aldolasas mediante enzimas acopladas", realizada por D. Guiomar Sánchez Carrón, bajo la inmediata dirección y supervisión de D. Álvaro Sánchez Ferrer y D. Francisco García Carmona, esta Comisión Académica, en sesión celebrada en fecha de 25 de Julio de 2012 , ha dado su autorización para su presentación ante la Comisión General de Doctorado.

Murcia, a 25 de Julio de 2012

TERESA SOTO PINO

MASTER Y DOCTORADO EN BIOLOGÍA MOLECULAR Y BIOTECNOLOGÍA · UNIVERSIDAD DE MURCIA

Los trabajos de investigación recogidos en la presente Memoria han sido financiados por los siguientes proyectos:

- "Metagenómica y Evolución dirigida de las enzimas usadas en la síntesis de intermedios antivirales derivados del ácido siálico" (BIO2007-625510) financiado por el Ministerio de Educación y Ciencia.
- "Generación de nuevas enzimas/proteínas con aplicación industrial mediante evolución dirigida" (004541/GERM/06) del Programa de Ayuda a Grupos de Excelencia de la Región de Murcia de la Fundación Séneca (Plan Regional de Ciencia y Tecnología 2007/2010).
- "Metagenómica y Evolución Dirigida de Sirtuinas y nicotinamidasas bacterianas (EVOSIRT)" (BIO2010-22225-C02-01) financiado por el Ministerio de Ciencia e Innovación.

La firmante de la presente Memoria ha disfrutado de una beca predoctoral del Programa de Formación de Profesorado Universitario (FPU) (MICIIN, ahora competencia de Ministerio de Educación, Cultura y Deporte).

Murcia, a de Julio de 2012

Fdo. Guiomar Sánchez Carrón

Los contenidos de esta Tesis Doctoral han sido parcialmente publicados o están en proceso de revisión:

- **Sánchez-Carrón G.**, García-García M.I., López-Rodríguez A. B., Jiménez-García S., Sola-Carvajal A., García-Carmona F., Sánchez-Ferrer A.
  Molecular characterization of a novel N-acetylneuraminate lyase from Lactobacillus plantarum *WCFS1.*
  Applied Environmental Microbiology. 2011. 77(7):2471-8
  Impact factor: 3.829

- **Sánchez-Carrón G.**, García-Carmona F., Sánchez-Ferrer A.
  High yield production and characterization of a novel L-lactate dehydrogenase from Bacillus halodurans *C-125. Application in a high-throughput assay.*
  Protein Expression and Purification. (Enviado).
  Impact factor: 1.58

- **Sánchez-Carrón G.**, García-García M.I., Martínez-Moñino A. B., Takami H., García-Carmona F., Sánchez-Ferrer A.
  Characterization and classification of a novel Oceanobacillus iheyensis *HTE831 nicotinamidase.*
  Applied Environmental Microbiology. (Enviado).
  Impact factor: 3.829

- **Sánchez-Carrón G.**, García-Carmona F., Sánchez-Ferrer A.
  High yield production and characterization of a novel glutamate dehydrogenase from Bacillus halodurans *C-125. Application in a high-throughput assay.*
  Protein Expression and Purification. (Enviado).
  Impact factor: 1.58

- **Sánchez-Carrón G.**, Sola-Carvajal A., Zapata-Pérez R., Takami H., García-Carmona F., Sánchez-Ferrer A.
- *Development of a novel spectrophotometric method for the measurement of nicotinamide mononucleotide deamidase and its application in the characterization of the enzyme from* Oceanobacillus iheyensis *HTE831.*
  Journal of Bacteriology. (Enviado).
  Impact factor: 3.825

Son muchas las personas que de una forma u otra han contribuido a la realización de esta Tesis Doctoral, y a quienes quiero expresar mi gratitud:

En primer lugar a los Catedráticos D. Álvaro Sánchez Ferrer y D. Francisco García Carmona que han dirigido esta tesis. A Álvaro quiero agradecerle su confianza y su constante esfuerzo y dedicación para que esta Tesis saliera adelante. Gracias por tus brillantes ideas, tus dosis extra de paciencia conmigo y por tratar que aprendiera de tu experiencia a ser una buena investigadora. A Paco he de agradecerle que me permitiera realizar la Tesis en su grupo de investigación y su disposición a ayudarme siempre que lo he necesitado durante la realización de la tesis.

A las profesoras y profesores del Ala-C del departamento de Bioquímica y Biología Molecular-A, a Juany, Pepa, Manoli, Mercedes y Jose Manuel por vuestra amabilidad y simpatía. A Fernando por ser como un hermano mayor, siempre dispuesto a echarme una mano con mis dudas. A los profesores y compañeros de las distintas alas del departamento por tratarme siempre tan bien.

A mis compañeros de laboratorio. A los que me ayudaron en mis comienzos, (Irene, Pepe, Ana, Inma, Silvia). A Silvia por esas horas que pasamos codo con codo, que fueran todas buenas, por tus consejos y tu amistad. A todos los que durante más o menos tiempo fuisteis compañeros de comidas y descansos (Lorena, Marta, Pili, Lili, Marian, Antonio, Pedro), gracias por dejarme disfrutar de vuestra compañía y por tantos buenos ratos y risas. A Rubén y Anabel, los jóvenes "padawanes", porque vuestra compañía este último año de mi tesis ha sido un regalo. Y a los que más tiempo han pasado conmigo durante estos años, a María por tu sinceridad y ayuda cuando lo he necesitado. A Sofía, porque te echo de menos cada día, tal ha sido tu apoyo en esta tesis y a Agustín, porque sobran las palabras, estos diez años jamás habrían sido lo mismo sin ti.

Al personal de apoyo del CAID. A Almudena, a César, a Jose y especialmente a María del Mar por ser la alegría hecha persona.

A mi gente de Murcia (Miguel, Diana, Mery, Pili, Santi, Elena B, Pili, Rebeca, Eva, Carmen, y Elena K), de Cartagena (Edu, Pablo, Jose, Álvaro, Juanma, Andrés, etc…) y de Albacete (Inés, Sheila y Clara), agradezco vuestra amistad y que estéis ahí por encima de todo.

Por supuesto a mi familia, así como a la familia de Adrián por tratarme siempre como a una más.

A mi hermana porque no hay nadie más fuerte que tú y es un orgullo ser tu hermana pequeña. A mi hermano y a su recién estrenada familia, porque es genial tener a alguien tan próximo a quien admirar.

A mis padres, que me habéis dado todo y porque confiáis tantísimo en mi, gracias por haber intentado hacer de mi una gran persona, sois excepcionales y solo llegar a parecerme a vosotros sería más de lo que puedo pedir. Gracias.

A Adrián, por ser mi otra mitad, porque yo ya no soy solo yo, somos tú y yo y porque nos queda mucho por vivir juntos. Esta tesis es tan tuya como mía y por eso es para ti.

A mis padres y hermanos

A Adrián

Abbreviations

Amp	Ampicillin
AbPncC	*Acinetobacter baumanii* nicotinamide mononucleotide deamidase
BSA	Bovine Serum Albumin
BhGDH	*Bacillus halodurans* glutamate dehydrogenase
BhLDH	*Bacillus halodurans* lactate dehydrogenase
CBD	Chitin binding domain
CHES	2-(Cyclohexylamino) ethane sulfonic acid
Chlor	Chloramphenicol
cinA	Competence/damage-inducible protein
CIP	Calf intestinal phosphatase
CLEAs	Cross-linking enzyme aggregates
CMAH	Cytidine monophosphate *N*-acetylneuraminic acid hydroxilase
CMP	Cytidine5'–monophosphate
CMP-Siasynthetase	CMP-sialic acid synthetase
CV	Coefficient of Variation
DAH	7-P3-deoxy-d-arabino-heptulosanate 7-phosphate
DHAP	Dihydroxiacetone phosphate
DHDPS	Dihydrodipicolinate synthase
DMS	Dimethyl suberimidate
DMSO	Dimethyl sulfoxide
DNaseI	Deoxyribonuclease I
dNTPs	Deoxyribonucleotides
EcNAL	*E.coli* recombinant *N*-acetylneuraminate lyase
EDTA	Ethylene diamine tetraacetic acid
EGTA	Ethyleneglycol-bis(2-aminoethylether)-N,N,N',N'-tetraacetic acid
ELAM-1	Endothelium leukocyte adhesión molecule-1
ELISAs	Enzyme-linked immunosorbent assays
ELSD	Evaporative light scattering detector
epPCR	Error prone PCR
epEcNAL	Error prone library of LpNAL
FBP	Fructose-1
FPLC	Fast Protein liquid chromatography
gdbA	*Bacillus halodurans* glutamate dehydrogenase gene
GDH	Glutamate dehydrogenase
GlcNAc	*N*-acetylglucosamine
GlcNAc-6P	*N*-acetylglucosamine6-phosphate
GST	Glutathione S-transferase
HEPES	4-(2-Hydroxyethyl)piperazine-1-ethanesulfonic acid

HiNAL	Recombinant acetylneuraminate lyase from *Haemophilus influenzae*
HMO	Human milk oligosaccharides
HPLC	Highp erformance liquid chromatography
HTS	High-throughput screening
hSIRT	Human sirtuin
IPTG	Isopropil-β-D-1-thiogalactopyranoside
ICP-OES	Inductively Coupled Plasma-Optical Emission Spectometer
kan	Kanamycin
DGDH	D-5keto-4-deoxyglucarate
KDN	2-keto-3-deoxy-d-glycero-D-galacto2-nonulosolicacid
KDO	3-deoxy-D-manno-octulosonicacid
LB	Luria Bertani medium
lctE	*Oceanobacillusiheyensis* lactatae dehydrogenase gene
LIC	Ligase Independent Cloning
LDH	Lactate dehydrogenase
LOS	Lipooligosaccharides
pNAL	*Lactobacillusplantarum* WCFS1 recombinant *N*-acetylneruaminate lyase
ManNAc	*N*-acetylmannosamine
MocF	Molybdopterin binding domain
MRSbroth	Man´s Rogosa and Sharpe broth
NA	Nicotinic acid
NaAD	Nicotinic acid adenine dinucleotide
NAD	Nicotinamide adenine dinucleotide
NADH	Nicotinamide adenine dinucleotide reduced form
NADP	Nicotinamide adenine dinucleotide phosphate
NADPH	Nicotinamide adenine dinucleotide phosphate reduced form
NadD	NMN adenyltransferase
NadE	NAD synthetase
NAM	Nicotinamide
NaMN	Nicotinic acid mononucleotide
nanA	*Lactobacillus plantarum* Neu5Ac aldolase gene
NAL	*N*-acetylneuraminate lyase
NAMDH	*N*-acetyl-D-mannosamine dehydrogenase
NCAMs	Neural cell adhesión molecules
NCBI	National Center For Biotechnology Information
Neu5Ac	*N*-Acetylneuraminic acid/Sialic acid
Neu5Gc	*N*-glycolylneuraminic acid
NJ	Neighbour joining
NMN	Nicotinamide mononucleotide

NmR	Nicotinamide ribose
OiNIC	*Oceanobacillus iheyensis* nicotinamidase
OiPncC	*Oceanobacillus iheyensis* NMN deamidase
PCR	Polymerase chain reaction
PEP	Phosphoenol pyruvate
PH999	*Pyrococcus horikoshii* nicotinamidase
Pnc1	*Saccharomyces cerevisiae* nicotinamidase
PncA	(*Mycobacterium tuberculosis*) nicotinamidase
PncB	Nicotinic acid phosphorybosiltransferase
PNC	Pyridine Nucleotide Cycle
PncC	NMN deamidase
PSA	Polysialic acid
PZA	Pyrazinamide
QA	Quinolinic acid
RmLDH	Rabbit muscle LDH
rtPCR	Real time PCR
Sarkosyl	Sodium lauroyl sarcosinate
SD	Standard deviation
SDM	Site directed mutagenesis
SDS	Sodium dodecyl sulfate
SDS-PAGE	SDS-Polyacrylamide gel electrophoresis
Sir2	Silent information regulator of *S. cerevisiae*
SIRT	Sirtuin
SpNIC	*Streptococcus pneumoniae* nicotinamidase
TB	Terrific Broth
TEMED	N,N,N',N'-Tetramethyl ethylene diamine
TFA	Trifluoroacetic acid
Tm	Melting temperatura
TSA	Thermal shift assay

Esta tesis doctoral está sometida a procesos de protección o transferencia de tecnología o de conocimiento, por lo que los siguientes contenidos están inhibidos en la publicación en los repositorios institucionales:

-Chapter V

-Chapter VII

-Chapter VIII

Autorizado por la Comisión General de Doctorado de la Universidad de Murcia con fecha 15 de Febrero de 2013.

GENERAL INDEX

Contenido inhibido autorizado por Comisión General de Doctorado de fecha 15 de Febrero de 2013.

FIGURES AND TABLES INDEX

INTRODUCTION

MATERIALS AND METHODS

CHAPTER IV

I. GENERAL INTRODUCTION

1. ENZYME BIOTECHNOLOGY

Enzymes are remarkable catalysts: capable of accepting a wide array of complex molecules as substrates, and exquisitely selective, catalysing reactions with unparalleled chiral (enantio-) and positional (regio-) selectivities. As a result, biocatalysts can be used in both simple and complex transformations without the need for the tedious blocking and deblocking steps that are common in enantio- and regioselective organic synthesis. Such high selectivity also affords efficient reactions with few by-products, thereby making enzymes an environmentally friendly alternative to conventional chemical catalysts.

These attributes have resulted in myriad applications, especially in the food and pharmaceutical industries where high reaction selectivity on complex substrates is critical. Examples include the production of high-fructose corn syrup, by the action of xylose isomerase (Jensen & Rugh, 1987) which catalyzes the isomerization of D-glucose to D-fructose, and the preparation of semisynthetic penicillins catalyzed by penicillin amidase (Boesten et al., 1996). Selective catalysis is now also becoming a requirement for the pharmaceutical industry.

Biocatalytic processes differ from conventional chemical processes, owing mainly to enzyme kinetics, protein stability under technical conditions and catalyst features that derive from their role in the cell's physiology, such as growth, induction of enzyme activity or the use of metabolic pathways for multistep reactions. In the laboratory, new biocatalytic reactions often originate with new enzyme activities. For applications, a more rational approach is needed. The starting point will usually be a product, which can perhaps be produced by one of several possible biocatalytic reactions that convert suitable substrates to the desired product. Figure 1.1 illustrates the development of such biocatalytic processes (Schmid et al., 2001). One or more biocatalysts must be identified or developed, a process must be set up, and the resulting bioconversion will ultimately have to be economically feasible. The development of such a process requires the input of many different specialists. Limiting aspects of the biocatalytic process are improved in an iterative manner, gradually leading to an efficient industrial process. In setting priorities for improvements at each process step, a detailed understanding of the costs and improvement potential of each of the partial steps in a process is vital.

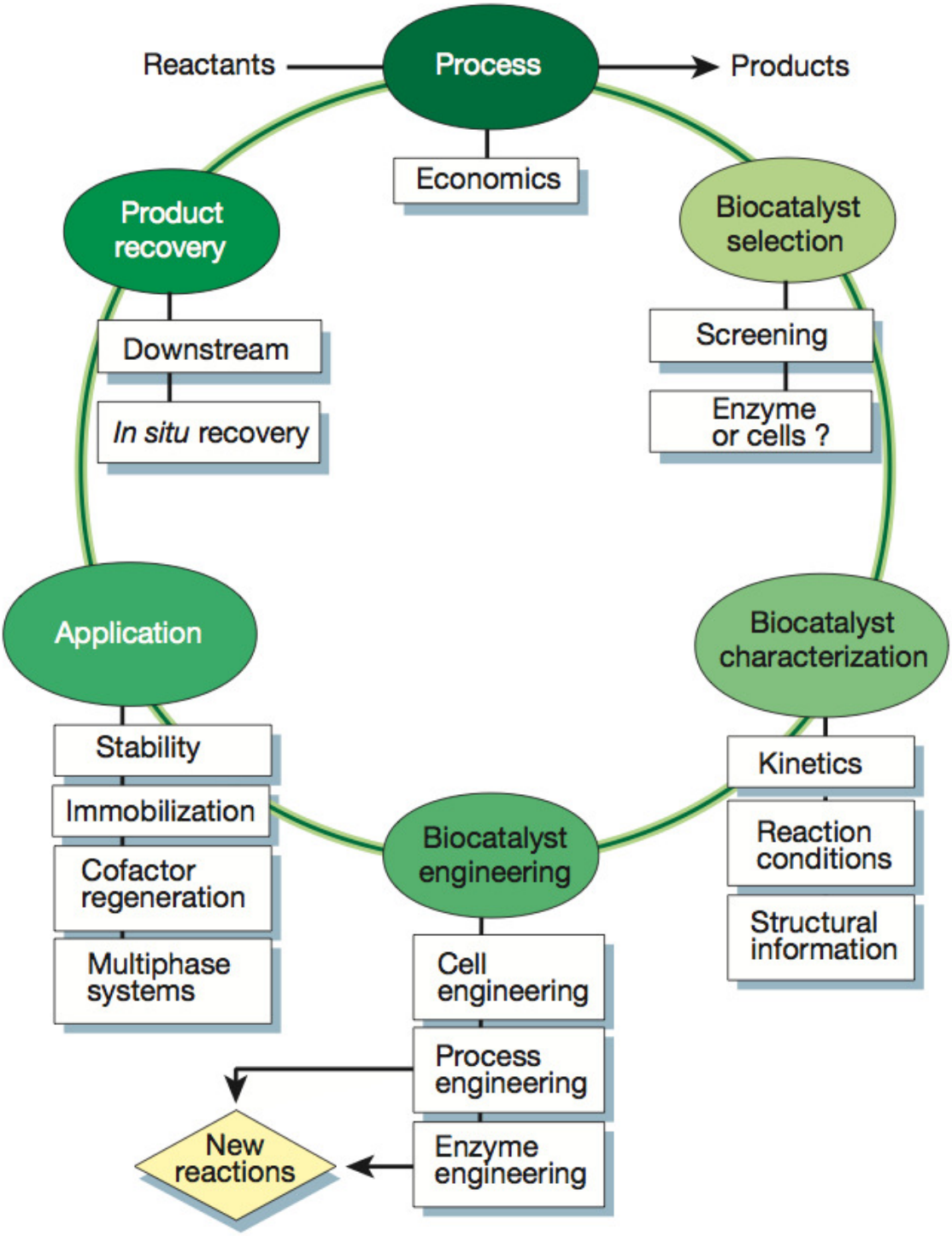

Figure 1.1. *The biocatalysis cycle.*

New processes can be based on the availability of an interesting new enzyme, or on the identification of desired products, after which a biocatalyst is then selected that permits conversion of available reactants. Such an enzyme might be

available commercially, or it might have been described in the literature. Alternatively, it will be necessary to screen for organisms or enzymes that carry out the desired reaction, or completely new enzyme activities, will be developed by protein design or directed evolution (Kuchner & Arnold, 1997).

1.1. Enzyme applications in the chemistry and pharma sectors

The industrial chemicals sector is difficult to penetrate for enzyme technology, as chemical manufacturing processes are well established and the current overall economic advantage of biotechnological processes is rather small (Bull et al., 1998). If new biocatalytic processes are to be accepted, they should bring decisive improvements, must be integrated with chemical and downstream processes, and must perform with high rates at high substrate and product concentrations. Nevertheless, enzyme-based processes are already quite prominent in the production of fine-chemicals and pharmaceuticals (Liese et al., 2001). As these product groups often include new chiral compounds, it is easier for biotechnology to compete with traditional organic chemistry methods, especially if a new process is more economical and raw materials and other resources are used more efficiently (Rogers et al., 2001). Among the pharmaceutical compounds, those related with sialic acids are relevant to glycobiotechnology.

Another important issue in the pharma sector is the large number of compounds that must be tested for biological activity to find a single promising lead. Enzymatic high-throughput screening has received much attention here, as it could add a level of complexity to the diversity of existing chemical libraries or could be used to produce libraries de novo (Rich et al., 2002). An example is the new screening methods for bioactive compounds (Mendez & Salas, 2001) related to aging, and more concrete, for compounds able to modulate sirtuin activity. These two areas need to improve enzymes efficiency and precision. However, naturally occurring enzymes often lack features necessary for commercial applications. Although protein biochemists continue to elucidate the relationships between the sequence, structure and function of proteins, the extensive knowledge that is necessary for the application of rational engineering approaches is available for only a tiny fraction of known enzymes (Figure 1.2). Directed evolution has proved to be useful for modifying enzymes in the absence of such knowledge.

Directed enzyme evolution generally begins with the creation of a library of mutated genes. Gene products that show improvement with respect to the desired property or set of properties are identified by selection or screening, and the gene(s) encoding those enzymes are subjected to further cycles of mutation and screening in order to accumulate beneficial mutations (Figure 1.2). This evolution can involve few or many generations, depending on how far one wish to progress and the effects of mutations observed in each generation.

The main requirements for successful directed evolution are (1) the functional expression of the enzyme in a suitable microbial host, (2) the availability of a screen (or selection) sensitive to the desired properties and (3) identifying a workable evolution strategy. The vast majority of possible evolutionary paths lead to poorer enzymes; the strategic challenge is to identify a path that will result in the improvement of the desired feature(s). The number of possible variants increases rapidly with the size of the enzyme and with the number of amino acids that are allowed to vary simultaneously. Even for a small protein, an impossibly large number of variants can be generated when multiple mutations are introduced. Because most mutations are deleterious (Suzuki et al., 1996) (Shafikhani et al., 1997), the chances of identifying improved enzymes in libraries containing large numbers of mutations are very small indeed. Therefore, the mutation rate must be tuned to the power of the screen or selection (Arnold, 1996). In the final analysis, a combination of rational and random methods of protein modification is likely to be the most productive approach to enzyme optimization (Figure 2.1).

Protein libraries are usually screened in microtiter plates using a range of selection parameters. Protein characterization and product analysis sort out desired and negative mutations. In vitro recombination by DNA shuffling, for example, can be used for further improvements. Both protein engineering approaches can be repeated or combined until biocatalysts with desired properties are generated.

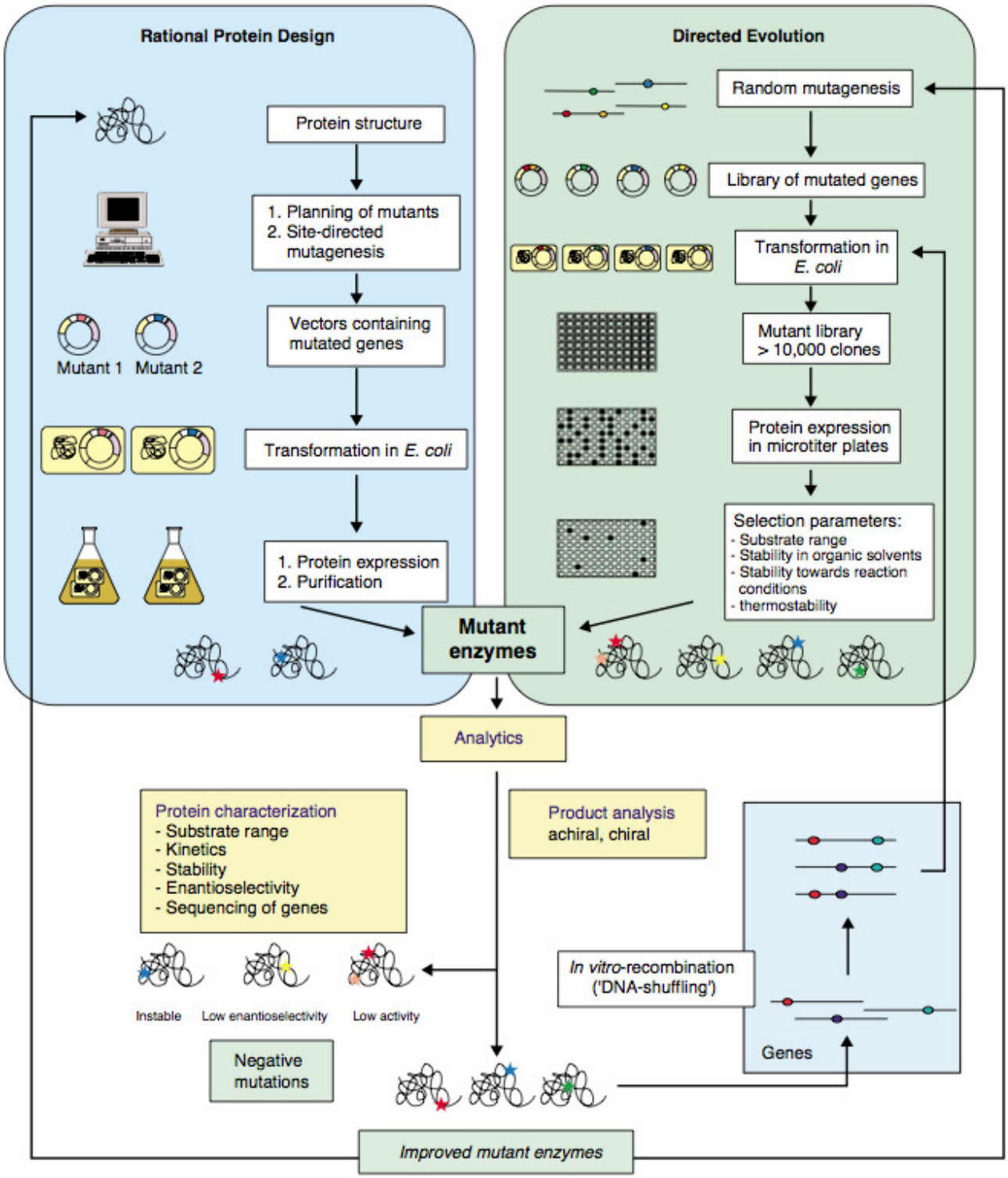

Figure 1.2. *Comparison of rational protein design and directed evolution.* During rational protein design, mutants are planned on the basis of their protein structure and then prepared by site-directed mutagenesis. After transformation in the host organism (i.e. *E. coli*), the variant is expressed, purified and analyzed for desired properties. Directed evolution starts with the preparation of mutant gene libraries by random mutagenesis, which are then expressed in the host organism, usually in microtiter plates. Selection of desired properties in then carried out.

2. SIALIC ACID

Sugars, which usually play an important role in the storage and transport of energy, also serve as starting materials in the biosynthesis of other organic compounds. Some sugars also play an important role as structural components of living organisms and in cellular recognition processes. Like this, oligosaccharides carry out functions essential for the maintenance of biological activities of cell, including morphological functions, transmissions of biological information and structural features by covalently binding with proteins (Varki, 1993). Among this, the sialic acid-related higher order sugars form a unique family and are usually displayed on the cell surface or are located in cell membranes.

Sialic acids are a family of α-keto acids with a nine-carbon backbone. They are all derivatives of *N*-acetylneuraminic acid (Neu5Ac) and 2-keto-3-deoxy-D-glycero-D-galacto-2-nonulosolic acid (KDN), and include pseudaminic acid, 2-keto-3-deoxy-D-*manno*-octulosonic acid (KDO), 3-deoxy-D-arabino-heptulosonate 7-phosphate (DAH 7-P) and legionaminic acid (Figure 1.3). More than 60 sialic acid forms have been found in nature including the most abundant Neu5Ac, nonhuman *N*-glycolylneuraminic acid (Neu5Gc), KDN, and their *O*-methyl, *O*-lactyl, *O*-sulfo, *O*-phospho-, and single or multiple *O*-acetyl derivatives (Angata & Varki, 2002) (Chen & Varki, 2010; Schauer, 2000).

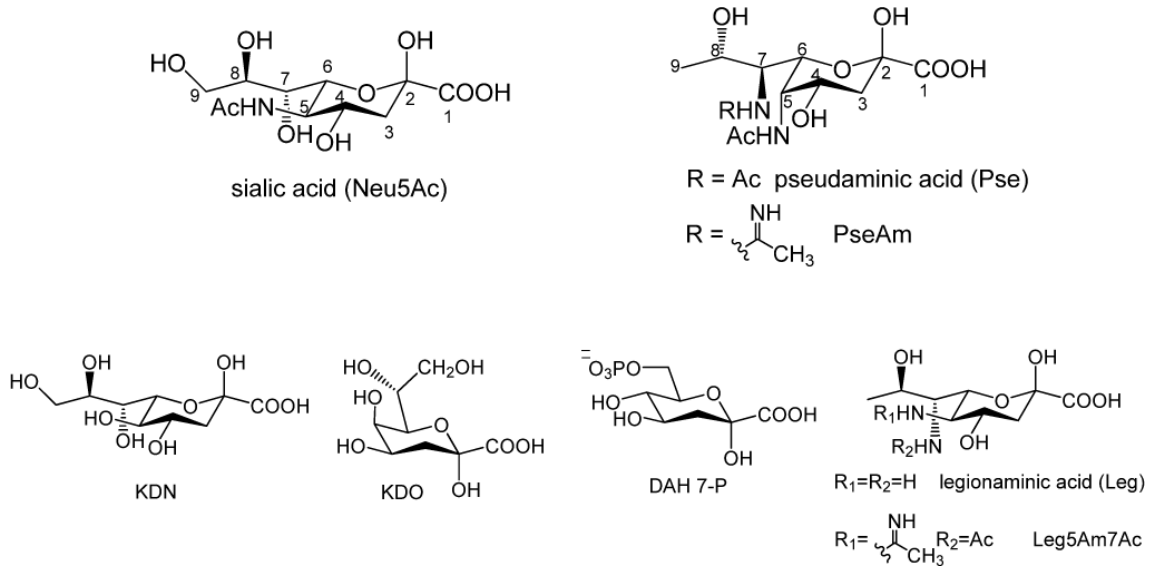

Figure 1.3. *Sialic acids and sialic acid-related molecules.*

2.1. The discovery of Sialic Acid

In the 1930's Klenk found a brain glycolipid showing an unusual purple color upon treatment with Bial's reagent. This compound, which became crystalline when subjected to methanolysis, contained a carboxylic group and a free aminoacid group and it was named methoxyneuraminic acid, because of its brain glycolipid origin. Latter in 1936, Blix isolated a crystalline substance from the glycoprotein bovine submaxillary mucin, which shared common characteristics with the compound discovered by Klenk. It appeared to have an *N*-acetyl group, and was identified as *N*-acetylneuramic acid (Blix, 1936; Blix, 1952). This could be converted into the neuraminic acid methylglycoside isolated by Klenk upon treatment with methanolic HCl at 105 ºC. Further studies fully elucidated the structure of neuraminic acid and its *N*-acetyl derivative (Figure 1.3) (Gottschalk, 1955; Kuhn, 1962). Then, "Sialic acid" was suggested as the group name for all *N*- and *O*- substituted neuraminic acid derivatives, and over the years, it has become in a large family of more than 60 members (Blix *et al*., 1957). However, the name "sialic acid", in its narrow sense, still refers to Neu5Ac.

2.2. Properties and biological roles

Sialic acids are commonly found as the terminal monosaccharides of the glycans presented in glycoconjugates (glycoproteins and glycolipids) on cell surfaces of vertebrates and higher invertebrates (Chen & Varki, 2010; Varki et al., 2011b). They are also components of lipooligosaccharides or capsular polysaccharides of some pathogenic bacteria including well-studied pathogens such as *Escherichia coli* K1, *Haemophilus influenzae*, *Haemophilus ducreyi*, *Pasteurella multocida*, *Neisseria gonorrhoeae*, *Neisseria meningitidis*, *Campylobacter jejuni*, and *Streptococcus agalactiae* (Almagro-Moreno & Boyd, 2009; Severi et al., 2007; Vimr et al., 2004)

They are all synthesized from the condensation of a four to six-carbon monosaccharide and phosphoenolypyruvate (PEP) and, unlike other monosaccharides, most of them are activated as cytidine 5'-monophosphate (CMP) nucleotides before being transferred onto cell surfaces.

Sialic acids play pivotal roles in many physiologically and pathologically important processes, including nervous system embryogenesis, cancer metastasis,

immunological regulation, bacterial and viral infection, etc. (Figure 1.4) (Angata & Varki, 2002; Chen & Varki, 2010; Li & Chen, 2012)

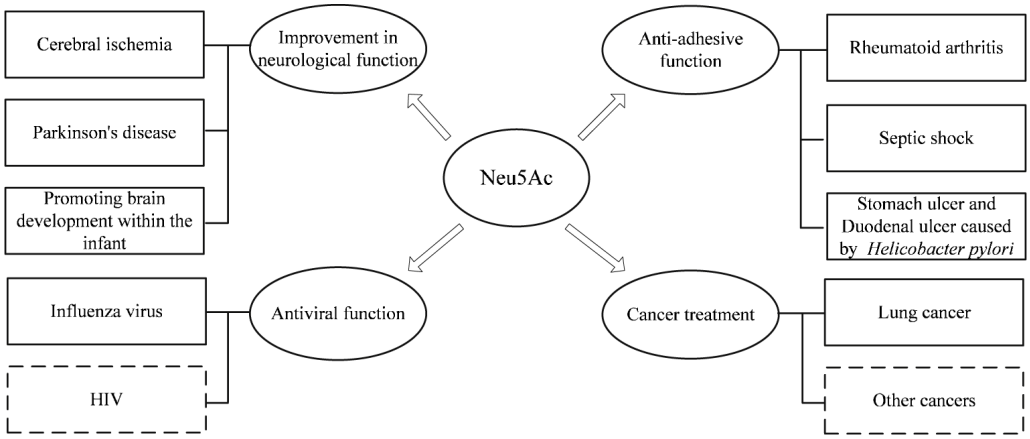

Figure 1.4. *Functions and applications of Neu5Ac*. The solid lines indicates the current uses of this compound, and the dashed lines represents potential uses.

In mammals, sialic acids are usually found as an α-glycoside, at the distal end of oligosaccharide chains, occupying the nonreductive terminal end, and in glycoconjugates, such as glycoproteins and glycolipids. Their outer most position and negative charge make them key determinants in regulating cellular processes, such as cell adhesion and recognition (Traving & Schauer, 1998).

Sialic acid is known to play a key role in the development and regeneration of the vertebrate embryonic nervous system. Neural cell adhesion molecules (NCAMs) are cell surface glycoproteins expressed in neurons, muscles and glia, and are important in cell-cell adhesion, neurite growth and learning. The adhesion properties of NCAMs are mainly due to homophilic binding. During the early stages of neural cell development, surface-displayed NCAMs are glycosylated with polysialic acid (PSA), a homopolymer of up to 200 α-(2→8)-linked sialic acids. The high surface charge and hydration brought about by sialylation inhibits the hemophilic binding of NCAMs. At later stages NCAMs are desialylated and regain their full adhesion function (Cunningham *et al*., 1983; Kleene & Schachner, 2004). Lectins are proteins that bind certain carbohydrates with high specificity. Endogenous and exogenous (from pathogens) sialic acid-binding lectins play critical roles in an animal's life cycle, from pathogen invasion to the immune response and the regulation of cell death (Angata & Varki, 2002; Varki, 1997). For

example, sialyloligosaccharides on a cell surface serve as receptor determinants for influenza virus and other pathogens, as well as for blood groups and tumor specific antibodies. Among these lectins, selectins are a family of three calcium-dependent lectins, and can be subcategorized into E-, L- and P-selectins. These cell adhesion proteins are expressed on the surface of cells such as activated endothelial cells, leukocytes or activated platelets and are found to be essential factors in leukocyte trafficking during inflammation and the immune response (Lasky, 1995; Vestweber & Blanks, 1999). The interactions of selectins with two tetrasaccharide-containing sialic acids, sialyl Lewis x (Le^x) and sialyl Lewis a (Le^a), are vital for transporting leukocytes from the flowing bloodstream to the site of inflammation (Lowe *et al*., 1990; Phillips *et al*., 1990). For example, Le^x binds to ELAM-1(Endothelium leukocyte adhesion molecule-1) and mediates inflammatory responses between leukocytes and injured tissues (Lowe *et al*., 1990; Phillips *et al*., 1990). Moreover, high amounts of sialyl Le^x and Le^a have been found on the surface of certain cancer cells, being responsible for the adhesion of cancer cells to endothelium. The interactions of P- and E-selectins with sialyl Le^x and Le^a has been shown to mediate tumor metastasis (Fukuda, 1996; Kim *et al*., 1998; Ugorski & Laskowska, 2002).

Pathogens such as viruses and bacteria also express sialic acid-binding lectins and use them to recognize and infect host cells. Among these lectins, influenza virus hemagglutinins are the most well known. Infection of the host cell by influenza virus is accomplished as follows. Viral sialic acid-recognizing lectins, refered as hemagglutinins because of their capability to agglutinate red blood cells, bind to Neu5Ac on the viral superficial layer at the end of the sugar chain of the host cell in order to infiltrate the cell. The infiltrating virus repeatedly proliferates in the cell. At the instant when the virus is to be freed from the cell, Neu5Ac on the superficial layer on the host cell is detached by neuraminidase located on the viral surface in order to liberate the virus itself and then the freed virus binds to other non-infected cells. Furthermore, virus can adapt to new hosts by producing hemagglutinins that bind to new types of sialic acids through cross-specific infections. Some bacteria also express soluble sialic acid-recognizing lectins that are called adhesins. Adhesins expressed by certain strains of bacteria usually

specifically recognize carbohydrate side chains on the cell surface of the target tissue that is to be infected or colonized.

Animals also have similar molecules, such as complement factor H, that act as defensive system to fight against invaders. This complement factor is an inhibitory regulator that binds to sialic acid on the cell surface and prevents cells from being attacked by the host's own complement pathway (Kazatchkine *et al*., 1979). Pathogenic cells not covered by sialic acids will be exposed to the attack by complement, which triggers proteolytic cascade, phagocytosis, inflammation and finally the response of the whole immune system. Several pathogenic bacteria strains are able to biosynthesize and display sialic acids on their cell surface to evade this immune response by mimicking the sialylated mammalian cells. *Escherichia coli* K1 and *Neisseria meningitidis* produce a capsule composed of α-(2→8)-linked polysialic acid (PSA). This, not only serves as a shield against harmful chemicals and phagocytosis, but also helps the pathogen to evade the host's immune system by mimicking the mammalian NCAM-containing cells. *Campylobacter jejuni* and *Neisseria meningitidis* also have sialic acid in lipooligosaccharides (LOS), which mimic human glycolipids (Vogel *et al*., 1996). PSA-capsule and LOS are considered important virulence factors in these bacterial pathogens (Preston *et al*., 1996; Vogel *et al*., 1996).

3. BIOTECHNOLOGICAL INTEREST OF SIALIC ACID

3.1. Antiviral precursor

Influeza, commonly known as the flu, is a highly infectious disease caused by RNA viruses of the family Orthomyxoviridae (the influenza viruses) that affects birds and mammals (Kilbourne, 2006; Oxford, 2000). In 1918, the Spanish Flu caused the death of 20,000,000 to 40,000,000 persons all over the world. Since then, three flu epidemics, in 1957 (Asian Flu), 1968 (Hong-Kong Flu) and 1977 (Russian Flu), have been recognized worldwide.

Neu5Ac is a precursor for the manufacture of many pharmaceutical drugs, including inhibitors against human influenza viruses, such as Relenza (Zanamivir) and Tamiflu (Oseltamivir), which have been commercialized and used for the infection of both influenza types A and B (such as the avian influenza virus H5N1)

(Kawai *et al*., 2009) although recent emerging drug resistant strains demand new anti-flu therapeutics (Mitrasinovic, 2010; Von Itzstein et al., 1993). They are potent inhibitors of influenza sialidases (Hayden *et al*., 1996; Von Itzstein *et al*., 1993), and were designed generated by protein crystal structure-assisted rational drug design based on the three dimensional structure of the influenza virus neuraminidase revealed by Colman *et al*. (Colman et al., 1983). Zanamivir (Figure 1.5, A), which inhibits influenza A and B neuraminidases with $IC_{30} \approx 5$ nM, prevents viral replication *in vitro* and *in vivo* and is marketed as a drug for the treatment of influenza (Hayden *et al*., 1996). It is prepared by replacing the hydroxyl group at the 4-position in the Neu5Ac derivative (NeuAc2en) with a guanidine group. Its derivative (Figure 1.5, B) is a selective inhibitor of influenza A sialidase, and has been prepared *via* a multi-step reaction sequence involving the oxidative cleavage of the side chain of sialic acid (Smith *et al*., 1998; Taylor *et al*., 1998).

Notably, a recent study on the oseltamivir (Tamiflu)-resistance mutation sequence suggested that zanamivir, with the optimal contacts with the oseltamivir-resistant neuraminidase mutants, might be preferred to oseltamivir in preventing widespread seasonal H1N1 (Soundararajan *et al*., 2009).

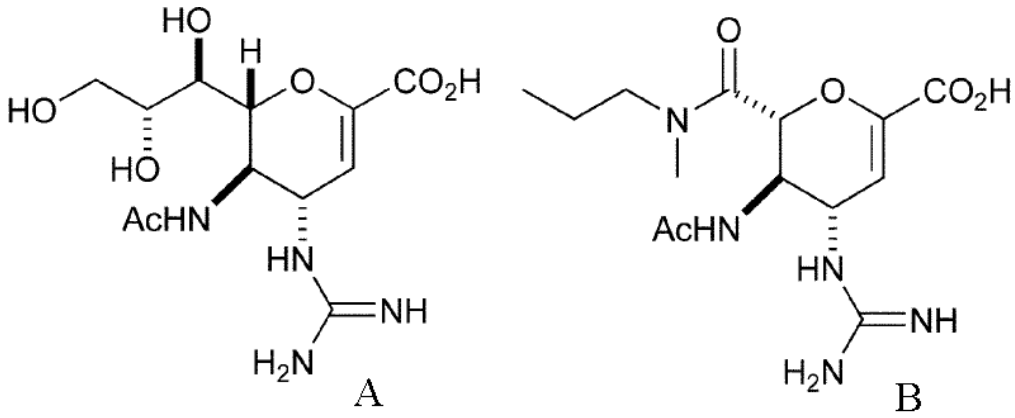

Figure 1.5. *Chemical structures of sialic acid derivatives*. Zanamivir (A) and its derivative (B), two anti-influenza virus drugs.

3.2. Supplement in infant food

The rapid growth and development of the newborn infant puts exceptional demands on the supply of nutrients. Any deficit has profound effects on somatic growth and organ structural and functional development, especially the brain. The rapid initial growth of the brain exceeds that of other of other body tissues. At 6th month gestation, it comprises 21 % of total body weight and 15 % at term (Friede, 1989). The brain weight more than doubles during the first 9 postnatal months to reach over 90 % of the adult weight by the 6th year. Once the time for the critical period of brain growth has passed, it cannot be restarted. The challenge is accentuated in the premature infants, particularly in relation to nutritional support for brain growth. Sialic acid is a promising new candidate that may support this brain growth.

Several studies have shown that children who where breast-fed as babies attain higher scores on intelligence test than those who were bottle-fed (Fergusson *et al*., 1982; Rodgers, 1978). Human breast milk is unique among milk of eutherian mammals, as it is rich source of more than 200 human milk oligosaccharides (HMO) (Tao et al., 2009), and about 100 different complex structures have been elucidated (Dai et al., 2000; Wang & Brand-Miller, 2003). The level of HMO ranges between 21 to 24 g/L in colostrums and 12 to 14 g/L in mature milk. In contrast, the level of milk oligosaccharides in cow's colostrums is 20 to 30-fold lower (0.7 to 1.2 g/L) than in human milk (Veh et al., 1981). Neutral oligosaccharides, many of which are fucosylated, and acidic oligosaccharides, nearly all of which are sialylated, constitute the respective core molecules of HMO. Sialic acid is present in HMO as Neu5Ac (Harduin-Lepers et al., 2001; Wang & Brand-Miller, 2003), attached to a penultimate galactose or *N*-acetyl glucosamine (GlcNAc) residue via an α2→3 or α2→6 glycosidic linkage. These sialyl residues are synthesized by a specific monosialyltranferase (Harduin-Lepers et al., 2001; Wang & Brand-Miller, 2003) (Wang, 2009; Wang et al., 2001).

Some of these natural oligosachcarides, including Neu5Ac, have been used as nutraceutical products in milks and food for infants to enhance the presumed usefulness of HMO, especially for the brain growth and development. However, there remains a paucity of information on the ideal carbohydrate structure to use and the efficacy of such supplementation (Harduin-Lepers et al., 2001; Wang & Brand-Miller, 2003).

3.3. Production of recombinant human glycoproteins with Neu5AC

All cells are covered with a dense and complex array of sugar chains. Sialic acids are typically present at the outer-most units of these chains. Cytidine monophosphate-*N*-acetylneuraminic acid hydroxylase (CMAH) converts the sialic acid *N*-acetylneuraminic acid (Neu5Ac) to *N*-glycolylneuraminic acid (Neu5Gc). In non-human mammals, Neu5Gc is recognized by a number of endogenous binding proteins, as well as by pathogenic organisms such as bacteria and viruses. Humans are unable to produce endogenous Neu5Gc because of an evolutionary inactivating mutation in their CMAH gene. Furthermore, Neu5Gc is known to be immunogenic in humans. Such immunogenicity is believed to play a role in the immune response observed in humans that come into contact with mammalian products, such as cosmetics, food, mammalian cells and cell products, as well as therapeutic agents derived from non-human mammals or exposed to non-human mammalian products. Attempts have been undertaken to try to diminish the Neu5Gc content of recombinantly produced human glycoproteins in cell lines by altering the cell lines using RNAi to suppress expression of the CMAH gene (Chenu et al., 2003).

The non-human sialic acid Neu5Gc contaminates both biotherapeutic products and the human body by becoming metabolically incorporated into cultured cells and into human tissues, respectively. In the first case the contamination arises from animal derived components in the culture medium and/or the animal cell lines used, and in the second case, from dietary intake from foods such as red meats. A recent study (Bork et al., 2009; Varki et al., 2011a) described how to eliminate or reduce the amount of Neu5Gc in human subject, biotherapeutics or cell lines (Figure 1.6). The method comprises flooding the system with the human sialic acid Neu5Ac. Both Neu5Ac and Neu5Gc compete for activation by the enzyme CMP-Sia Synthetase. Thus, an excess of Neu5Ac from any source provides a simple and effective method for reducing or eliminating the Neu5Gc burden by metabolically competing out the Neu5Gc, either as it enters the cells for the first time and/or when it recycles from breakdown of preexisting cellular molecules.

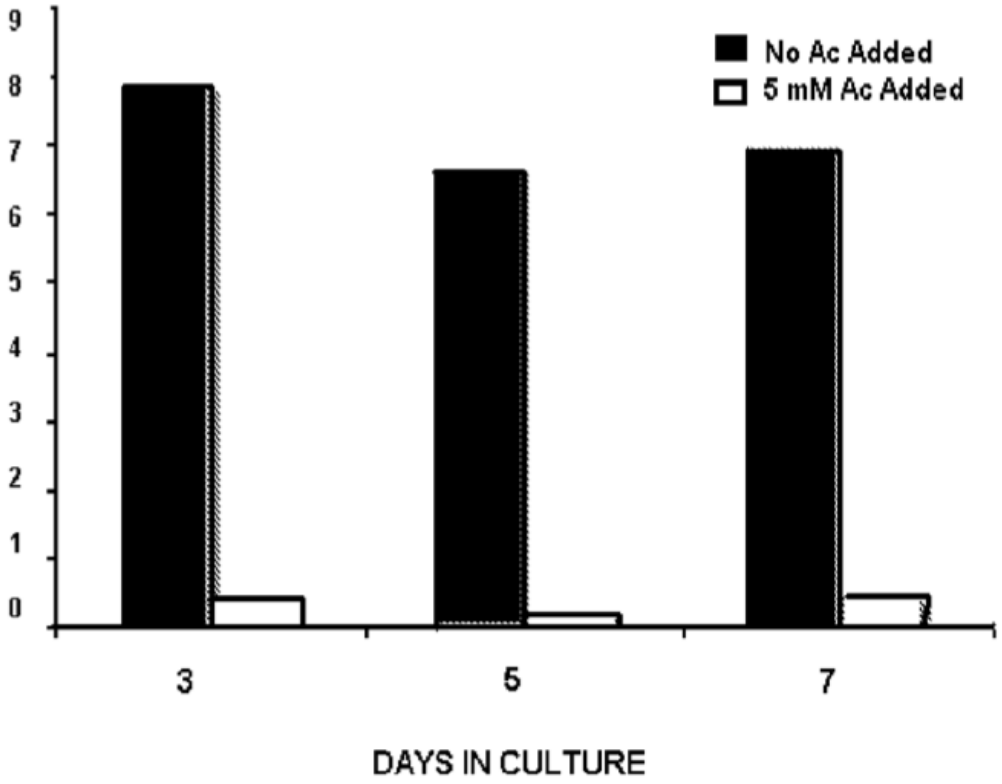

Figure 1.6. *Neu5Gc content in two cell lines with and without Neu5Ac addition.* Stably transfected CHO-KI cells expressing recombinant soluble Siglec 13-Fc protein were grown in the absence or presence of 5 mM Neu5Ac (Varki et al., 2011a).

In addition, this patented method comprises the culturing of a cell line with an effective amount or increasing amounts of Neu5Ac, and derivatives, analogues or precursors (ManNAc) of it thereof in a sufficient amount for a sufficient period of time to eliminate or substantially reduce Neu5Gc present in a cell or the cell line or a product produced by the cell or cell line.

3.4. Industrial production of Neu5Ac

The high price of Neu5Ac (50-100 \$ g^{-1}) caused by its conventional method of production has impeded its industrial application. Neu5Ac its traditionally prepared by extraction from natural sources, such as egg yolk, and by hydrolysis of colominic acid (a homopolymer of Neu5Ac) (Maru et al., 2002). These methods are often restricted to low yield and unsatisfactory stereoselectivity. As for chemical synthesis, the tedious protection and deprotection steps would be

unsuitable for large-scale production of Neu5Ac (Maru et al., 2002; Xu et al., 2007). An alternative approach for the preparation of sialic acid and its derivatives involve the use of enzyme-catalysed reaction, followed by the functional group manipulation. A biotechnological source of these enzymes could be bacteria. Thus, a comprehensive view of sialic acid metabolism will be relevant before selecting the appropriate enzyme.

4. SIALIC ACID METABOLISM IN BACTERIA

Most Neu5Ac aldolases come from pathogens or commensals of mammals, because of the ability of these species to utilize the carbon sources present in the mucus-rich surfaces of the mammalian bodies. The emergence of microbial sialic acid catabolism is hypothesized to be central to a variety to host-microbe interactions. On the assumption that this bacteria expressed an efficient transporter and degradative system for sialic acid dissimilation, Vimr and Troy (Vimr & Troy, 1985a; Vimr & Troy, 1985c) isolated mutants of *E. coli* K1 which failed to use sialic acid as sole carbon source. The genetic defects in two of these nan (for *N*-acyl-neuraminate) mutants were subsequently located in genes for sialate transport and the aldolase (*nanA*) (Vimr & Troy, 1985a) The *nanAT* genes were part of an operon that responded to apparent induction based on sialic acid availability. The results of genetic and physiological studies indicated that exogenous sialic acid is transported by a secondary transporter (Plumbridge & Vimr, 1999) of the major facilitator superfamily and degraded intracellularly by NanA to yield pyruvate and the amino sugar ManNAc (Vimr & Troy, 1985a; Vimr & Troy, 1985c). Upon completion of the *E. coli* K-12 genomic DNA sequencing project (Blattner et al., 1997), the *nan* operon was seen to potentially include two more open reading frames, which were subsequently suggested for phosphorylating ManNAc (*nanK*) (Plumbridge & Vimr, 1999; Ringenberg et al., 2003) and then for epimerizing the ManNAc-6-P generating GlcNAc-6-P (*nanE*) (Figure 1.7). Later biochemical analyses confirmed that NanK is an ATP-dependent kinase specific for ManNAc and that NanE is a reversible 2-epimerase (Ringenberg et al., 2003). Since then, a complete *nan* system was defined as one that minimally includes orthologues of genes encoding NanA, NanE and NanK.

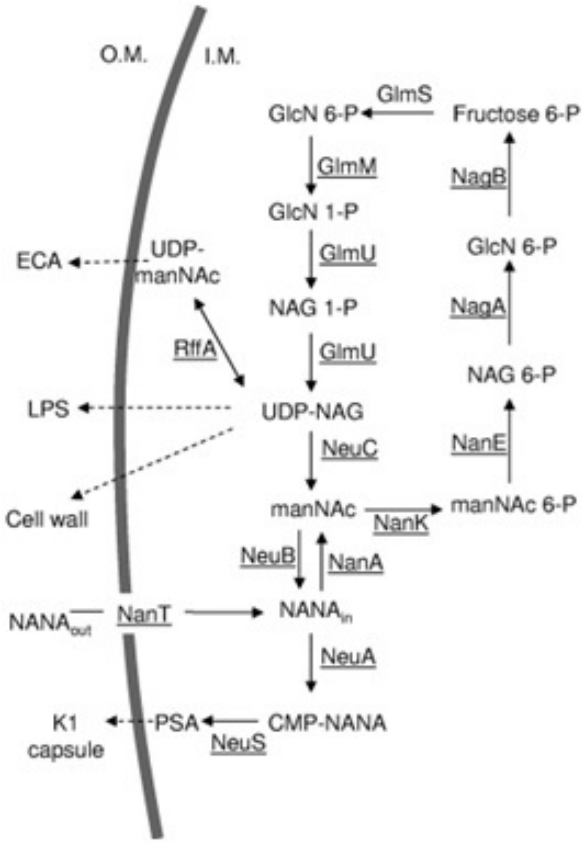

Figure 1.7. *Neu5Ac and amino sugar utilization pathways in* E. coli.

5. *N*-ACETYLNEURAMINATE LYASE

Sialic acid aldolase or *N*-acetylneuraminate lyase (NAL; EC 4.1.3.3) is a class I aldolase that catalyzes the cleaveage of Neu5Ac to form ManNAc and pyruvate via a Schiff bases intermediate (Figure 1.8) along with the reverse aldol condensation reaction. The equilibrium of this reaction favors Neu5Ac cleaveage. As said above, the enzyme plays an important role in the regulation of sialic acid metabolism in bacteria (Vimr & Troy, 1985b). Neu5Ac lyase has been found in pathogenic as well as nonpathogenic bacteria (Aisaka et al., 1991) and in mammalian tissues.

NAL has previously been cloned from *E. coli* (EcNAL) (Aisaka et al., 1986; Ohta et al., 1986; Ohta et al., 1985), *Clostridium perfringens* A99 (Traving et al., 1997), *Haemophilus influenzae* (Lilley et al., 1998), *Trichomas vaginalis* (Meysick et al., 1996) and *Pasteurella multocida* (Li et al., 2008). In addition, X-ray

structure of NAL and some mutants from *E. coli* and *H. influenza* have also been solved (Barbosa et al., 2000; Campeotto et al., 2010; Campeotto et al., 2009; Izard et al., 1994; Joerger et al., 2003; Lawrence et al., 1997b).

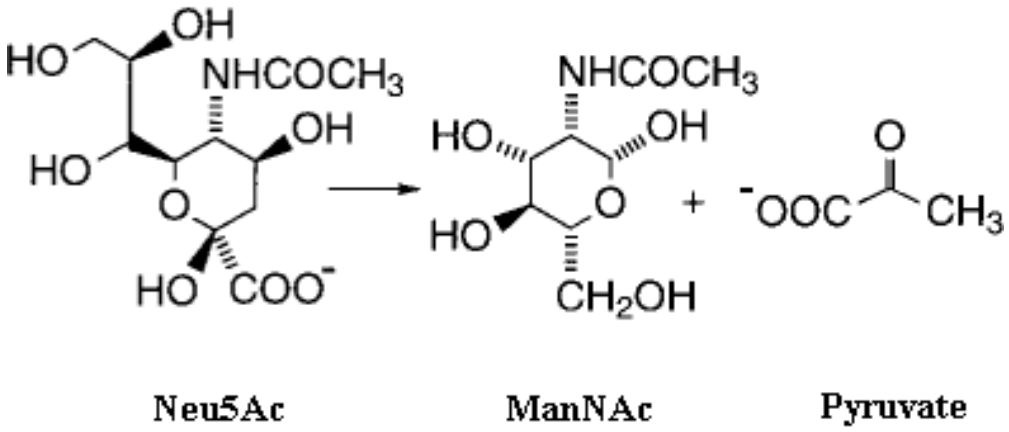

Figure 1.8. *Overall reaction catalyzed by NAL.* Neu5Ac is cleaved into ManNAc and Pyruvate *via* the formation of a Schiff base.

NAL is a homotetramer (Barbosa et al., 2000; Izard *et al.*, 1994), each monomer of which consisting on a $(\alpha/\beta)_8$ barrel elaborated at its C-terminus by three α-helices (Figure 1.9). NAL shares this structural framework with other members of the $(\alpha/\beta)_8$ subfamily enzymes (Lawrence et al., 1997a), such as dihydrodipicolinate synthase (DHDPS) and D-5-keto-4-deoxyglucarate dehydratase (KDGDH), although they catalyze different reactions. It has been proposed (Lawrence et al., 1997a) that these enzymes share a unifying step in their reaction pathway, namely the formation of a Schiff base between a strictly conserved lysine residue and C2 carbon of the common α-keto acid moiety of the substrate.

On the basis of X-ray structural analysis of covalent complexes of EcNAL (Izard et al., 1994) and *Haemophilus influenzae* (HiNAL) (Barbosa et al., 2000), the existence of a highly conserved structural motif associated with Schiff base formation has been proven. This results are similar to those obtained for *E. coli*

DHDPS (Blickling et al., 1997). In both, a covalent link is seen between the C2 carbon of pyruvate and the amine nitrogen of the strictly conserved lysine residue (Figure 1.10). In the complexes, the carboxylate moiety of the bound pyruvate is oriented to form hydrogen bonds with the backbone amides of residues Ser and Thr, as well as with the hydroxyl of Tyr (Figure 1.10). Ser and Thr form the respective second and third residues of a highly conserved GxxGE motif, the three-dimensional conformation of which can be described as two overlapping type I β-turns (Lawrence et al., 1997b)

Neu5Ac lyase also catalyzes the reverse aldol condensation reaction and has been used in this way to synthesize sialic acid and some of its derivatives from pyruvate and ManNAc (Huang et al., 2007; Yu & Chen, 2006; Yu et al., 2004) and with the availability of aldolase from recombinant sources (Aisaka et al., 1991; Lilley et al., 1998; Ohta et al., 1986), this has become the preferred route for production of large quantities of Neu5Ac.

However, a number of issues must be addressed in producing Neu5Ac using the aldolase:

1. ManNAc is expensive and must be synthesized from GlcNAc by epimerization at C2 however, GlcNAc dominates in the equilibrium mixture (GlcNAc:ManNAc ≈ 4:1) (Spivak & Roseman, 1959)
2. ManNAc and GlcNac have very similar chemical properties and hence, might be expected to be difficult to separate.
3. Although GlcNAc is not a substrate for the enzyme, it is an inhibitor (Kragl et al., 1991)
4. The K_M of the enzyme for ManNAc is high (Kragl et al., 1991).
5. The "normal" role of Neu5Ac aldolase is to cleave Neu5Ac and in dilute solution, the equilibrium lies over to pyruvate and ManNAc (k_{eq}, 28.71 mol^{-1} at 25 ºC) (Kragl et al., 1991). The usual solution to this problem is to push the equilibrium over to Neu5Ac using an excess (up to tenfold) of pyruvate, however, this necessitates the removal of large amounts of residual pyruvate.

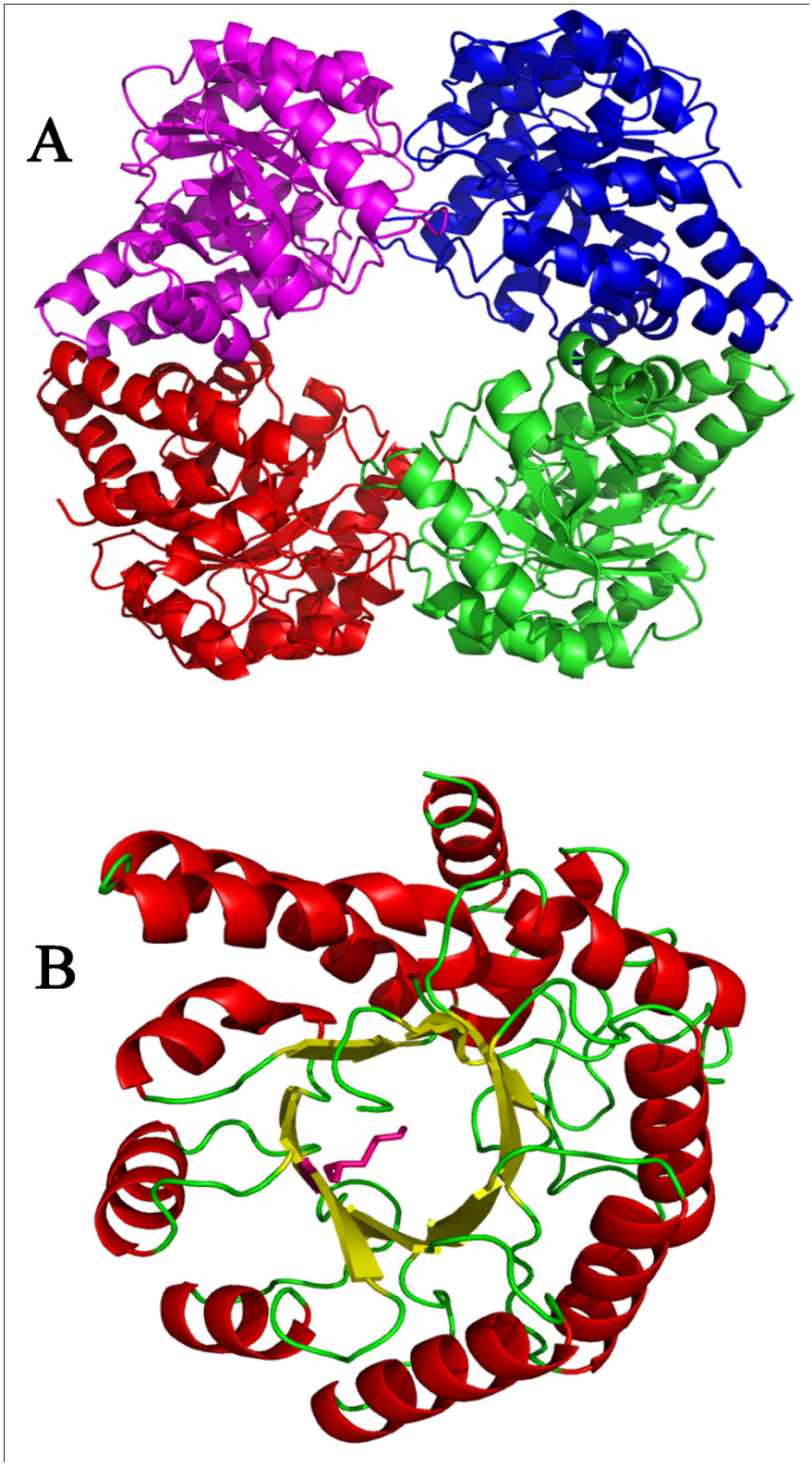

Figure 1.9. *3D view of EcNAL in the tetrameric form (A) and as a monomer (B).* In the monomer, the catalytic lysine residue is represented in pink [pdb code: 1NAL (Aisaka et al., 1991)].

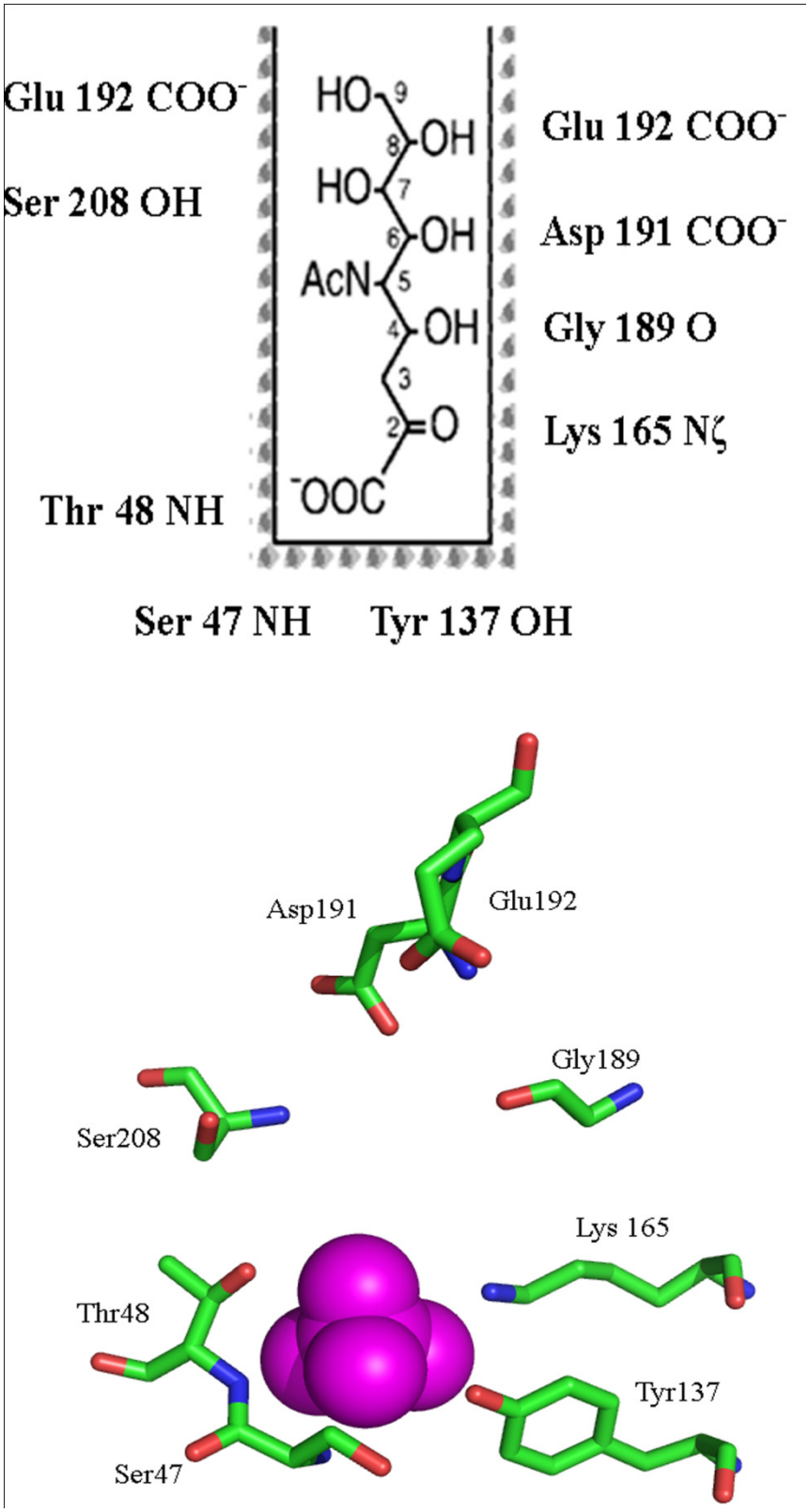

Figure 1.10. *Schematic (A) and 3D view (B) of the active site of EcNAL.* (A) Residues implicated in the catalytic mechanism and their interaction with Neu5Ac. (B) 3D view of the same residues as (A). Pyruvate is represented in magenta.

In 1997, Glaxo Wellcome Research reported an efficient process for production of Neu5Ac using NAL providing partial solutions to these issues (Mahmoudian et al., 1997). Two processes were described, which both could be operated at substantial scales. In the first process, the use of a large molar excess of pyruvate (five to seve*N*-fold) to drive the equilibrium to Neu5Ac was made feasible by development of a bisulfate complexation method for pyruvate removal from the reaction mixture. In the second process, the development of a method for enrichment of ManNAc in GlcNAc/ManNAc mixtures allowed ManNAc to be used at a very high concentration and this obviates the need to use a large molar excess of pyruvate. The GlcNAc residue recovered from the enrichment procedure could be recycled through the epimerization procedure. Under these circumstances, it was possible to develop a method for recovery of Neu5Ac from the reaction mixture by a simple crystallization.

6. SIRTUINS AND NICOTINAMIDASES

The silent information regulator 2 (Sir2) gene was first identified as a *Saccharomyces cerevisiae* mutant, and was subsequently shown to be involved in transcriptional silencing at telomeres (Gottschling et al., 1990) and ribosomal RNA gene (rDNA) clusters (Smith & Boeke, 1997) giving rise to the lengthening of life span in yeast (Lin et al., 2000). Sir2 is also required for the lengthening of life span due to calorie restriction in yeast (Lin et al., 2000). Since then, Sir2-like proteins, also known as sirtuins, have been found in all eukaryotes and in many archaea and prokaryotes (Avalos et al., 2002).

Sirtuins (SIRT) belong to the unique family of class III NAD^+-dependant protein deacetylases, which catalyze the deacetylation of acetylated lysine residues of key proteins, involved in a variety of cellular functions, including glucose homeostasis, life span extension, cell cycle regulation, apoptosis, DNA repair and neurodegeneration (Oberdoerffer & Sinclair, 2007). Humans have seven distinct sirtuin gene products (SIRT1-SIRT7). SIRT 1 is localized in the nucleus, and modulates gene expression by deacetylating proteins, including histone H4, p53 and BCL6 (Asaba et al., 2009). SIRT2 is localized in the cytoplasm, and has been implicated in the process of cell division, via deacetylation of α-tubulin (Inoue et

al., 2007). SIRT3 and SIRT4 are mitochondrial proteins, that are responsible of activation of mitochondrial functions (Shi et al., 2005), and insulin secretion (Argmann & Auwerx, 2006), respectively. SIRT5 is also localized in mitochondria, but the function of SIRT5 is not yet well understood (Michishita et al., 2008). SIRT6, which is located in the nucleus, has recently been reported to be a deacetylase of lysine 9 of histone H3, playing a role in regulation of telomere metabolism and function (Michishita et al., 2008). SIRT7 is also localized in the nucleus, and is involved in the activation of RNA polymerase I transcription, but its natural substrates have yet to be identified (Ford et al., 2006). More detailed interactions with known regulatory mammalian proteins are shown in figure 1.11 (Michan & Sinclair, 2007).

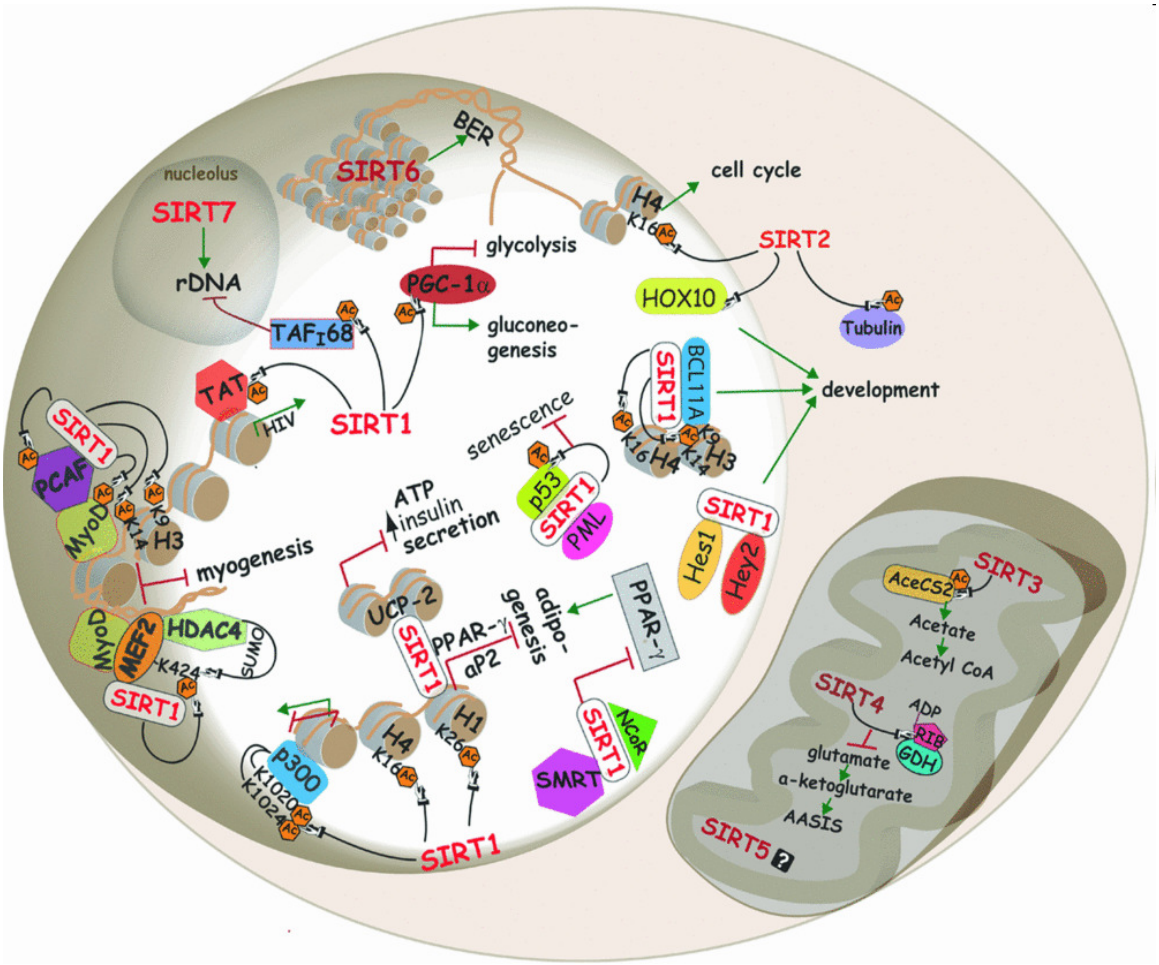

Figure 1.11. *SIRT proteins interactions with regulatory mammalian proteins.*

Although the functions of SIRTs have not been yet fully understood, as mentioned above, they have been suggested to be associated with various disease states, and their activation has been thought to provide protection from certain neurodegenerative disease and metabolic disorders, whereas their inhibition could delay the progression of cancer (Outeiro et al., 2007). Thus, there is an increasing interest in the discovery of small molecule modulators of sirtuins to develop novel therapeutic agents for Alzheimer's and Parkinson´s diseases, diabetes or cancer (Feng et al., 2009). The first known inhibitor of sirtuins was nicotinamide (NAM) (IC50 ~50 µM), which is one of the products obtained from the NAD^+ transformation, as shown in the following reaction (Figure 1.12):

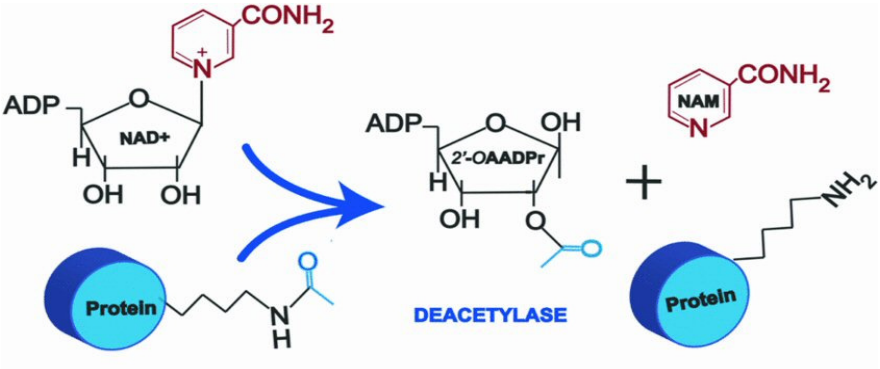

Figure 1.12. *Deacetylating sirtuin reaction producing nicotinamide as by-product.*

To date, several inhibitors have been described, including not only NAD derivatives (NADH), but also dihydrocoumarin (IC50 ~ 31-66 µM), naphthopyranone derivatives (IC50 ~60-100 µM), 2-hydroxy-naphthaldehyde derivatives (IC50 ~ 45 µM, for sirtinol), EX-527, HR73, AGK2 and acetylated lysine analogue derivatives (Asaba et al., 2009; Porcu & Chiarugi, 2005). On the other hand, several phenolic compounds have emerged as activators of sirtuins, especially human SIRT1 (hSIRT1). Among them, resveratrol with 13-fold activation is the most active among the *trans*-stilbene derivatives, chalcone derivatives and flavones derivatives (Porcu & Chiarugi, 2005). SRT1720, SRT218 and SRT1460 were recently described by Sirtris Pharmaceutical as hSIRT1 activators (Milne et al., 2007). They are structurally unrelated to resveratrol, and were reported to activate SIRT1 with potencies 1,000-fold greater than resveratrol (Milne et al., 2007). These compounds were identified via high throughput fluorescence polarization assay, which uses a quenched fluorophore (7-amino-4-

methylcoumarin = AMC) containing p53-derived tetrapeptide substrate (commercially known as "Fluor de Lys", Enzo Life Science). On deacetylation, the liberated ε-amino group of the lysine transforms the tetrapeptide into a trypsin substrate. Trypsin cleavage releases the fluorophore, resulting in an increase of fluorescence (Wegener et al., 2003). However, the activation of hSIRT1 by some of the above compounds in "Fluor de Lys" assay does not correlate with the activity measured using non fluorescent peptides or full length proteins, such as p53 (Borra et al., 2005; Pacholec et al., 2010), but rather the activation seems to be derived from the direct interaction of such compounds with flourophore-containing peptide substrate (Pacholec et al., 2010). Thus, there is a need for a more accurate assay to determine such potential modulators.

Additional sirtuins assays include those based on Caliper´s mobility shift assay technology (Liu et al., 2008), enzyme-linked immunosorbent assays (ELISAs) (Schlicker et al., 2008), a capillary electrophoresis assay (Fan et al., 2009), a bioluminescence assay (Liu et al., 2008), a radioactive assay (Pacholec et al., 2010) and an HPLC assay (Pacholec et al., 2010). Although each of the above methods has advantages and disadvantages, all of them are end-point assay. The only one continuous assay was recently developed by Denu´s group (Smith et al., 2009), in which, nicotinamide produced by SIRT enzymes is converted to nicotinic acid and ammonia by nicotinamidase. The ammonia is transferred to α-ketoglutarate via glutamate dehydrogenase, yielding glutamate and the oxidation of NAD(P)H to $NAD(P)^+$, which is measured spectrophotometrically at 340 nm (Figure 1.13).

The main drawback of this method is the cost of the enzymes used, except for the last dehydrogenase, which is freely available from SIGMA. In addition, the expression of sirtuins is extremely low. As an example, the best expression of human SIRT1 protein achieved from *Escherichia coli* codon optimized cDNA was 3-5 mg of purified protein per liter culture. This value is far from the 200 mg/L usually obtained in overexpressed proteins in *E. coli,* as example one of the enzymes used in our lab, such is glycine oxidase (Martinez-Martinez et al., 2007). In addition, nicotinamidase is also not commercially available, and only few studies have been carried out in pathogenic microorganisms, such as *Salmonella* enterica (Garrity et al., 2007), *Acinetobacter baumanii* (Fyfe et al., 2009), and *Mycobacterium tuberculosis* (Cheng et al., 2000).

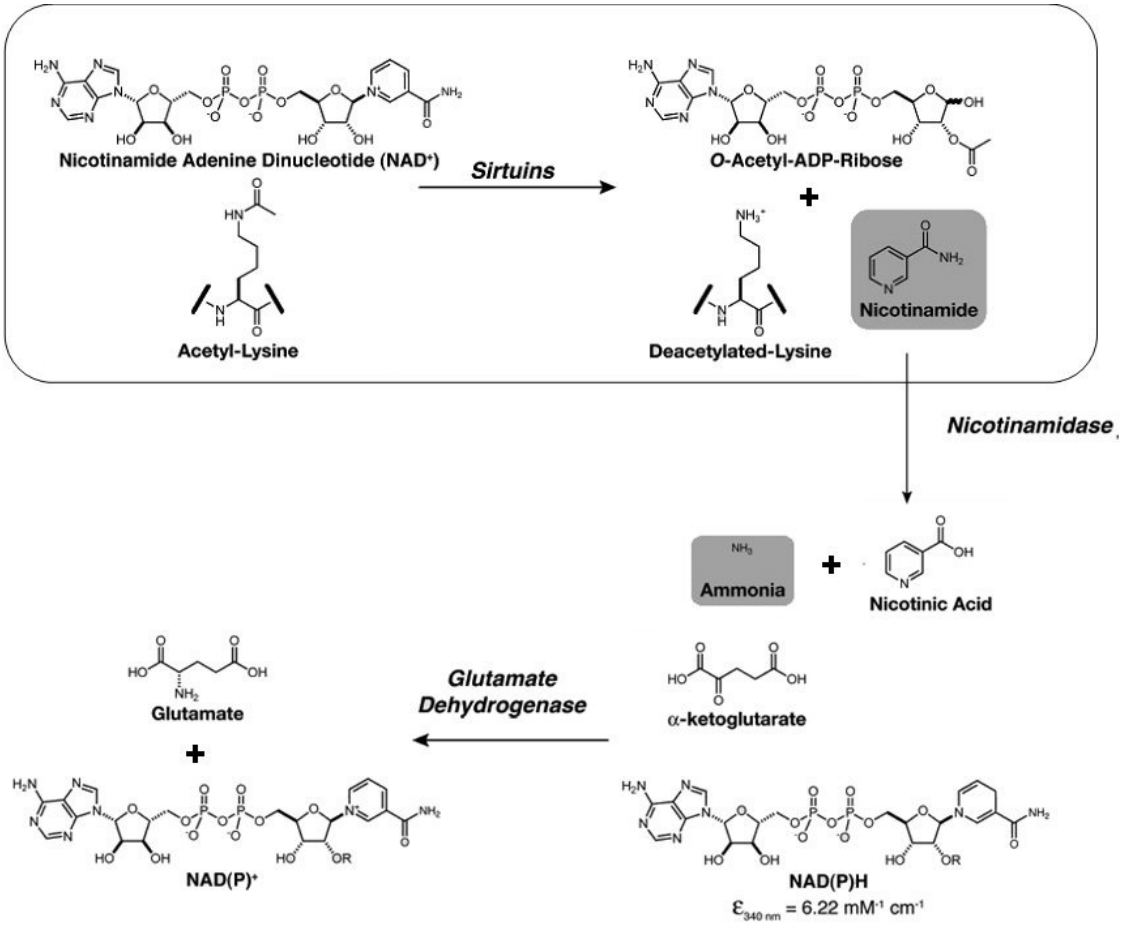

Figure 1.13. *Continuos spectrophotometric assay for detection of sirtuin activity.*

In archeans, nicotinamidase has only been studied in *Pyrococcus horikoshii* (Du et al., 2001). In the yeast, in *S. cerevisiae*, where deletion of the corresponding gene (Pnc1), correlates with a decrease in transcriptional silencing, whereas overexpression of Pncl, correlates with an extension of replicative life span (Hu et al., 2007). This activity has a fortuitous medical benefit, since the *M. tuberculosis* enzyme, also converts the nicotinamide analogue pro-drug pyrazimamide into the bacteriostatic pyrazinoic acid, hence the alternative name, pyrazinamidase, also found in the bibliography. Pyrazinoic acid inhibits mycolic acid biosynthesis and affects membrane energetic of the pathogen.

Surprisingly, nicotinamidase is absent in vertebrates (including humans), and both enzymes, sirtuins and nicotinamidases, are only present in prokaryotes and yeast (Imai, 2010). In these organisms, these two enzymes belong to the salvage NAD^+ biosynthetic pathway (Figure 1.14), which begins with the

breakdown of NAD^+ into nicotinamide (NAM) and *O*-acetyl-ADP-ribose, that is catalyzed by sirtuins, and continues with the deamination of NAM to nicotinic acid (NA), calalyzed by nicotinamidase (PncA).

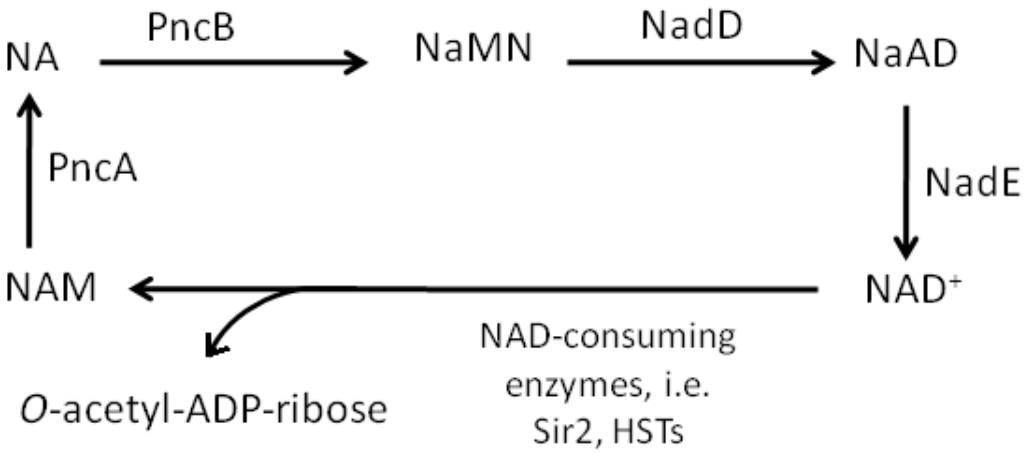

Figure 1.14. *NAD^+ salvage pathway.*

Nicotinic acid phosphoribosyltransferase (PncB) converts NA to nicotinic acid mononucleotide (NMN), which is eventually converted to NAD^+ through the sequential reactions of nicotinamide/nicotinic acid mononucleotide adenyl-transferase (NadD) and NAD synthetase (NadE). Importantly, it has been demonstrated that nicotinamidase gene is a master regulator, translating nutritional and environmental stimuli to the regulation of aging in yeast (Anderson et al., 2003).

From the above, it is clear that the study of the enzyme nicotinamidase is not only interesting as a tool for screening modulators of sirtuins, but also, and not least, a challenge to understand the high regulation between environmental stimuli, sirtuins and NAD^+ biosynthesis, in order to develop effective scientifically-sound nutraceuticals and/or anti-aging pharmaceutical drugs (Imai, 2010).

7. PYRIDINE NUCLEOTIDE CYCLE AND NAD^+ METABOLISM IN BACTERIA

Nicotinamide adenine dinucleotide (NAD^+) and NAD-phosphate ($NADP^+$) are compounds of immeasurable importance in cellular metabolism. They function in numerous anabolic and catabolic reactions and are widely distributed throughout biological systems. NAD^+ and $NADP^+$ are known to participate in over 300 enzymatically catalyzed oxidation-reduction reactions. In addition, a number of reactions have been discovered in which NAD^+ serves as a substrate. For example, certain prokaryotes, such as *E. coli,* utilize NAD^+ as a substrate for deoxyribonucleic acid ligase, an essential for deoxyribonucleic acid synthesis, repair and recombination (Olivera & Lehman, 1967; Park et al., 1989) and such in the above described case of sirtuins (Smith et al., 2009). Reduced pyridine nucleotide coenzymes also play an important role in the regulation of amphibolic pathways, such as the citric acid cycle and the oxidative pentose pathway (Sanwal, 1970). Thus, there is a growing awareness of the extent to which cells are dependent upon NAD^+ and an increased emphasis on the need for more extensive research into the synthesis, recycling and regulation of NAD^+ metabolism (Foster & Moat, 1980).

The pyridine nucleotide cycle (PNC) is a network of biochemical transformations that allow cells to recycle the byproducts of endogenous NAD^+ consumption back to the coenzyme, and to salvage the available pyridine bases, nucleosides and nucleotides as NAD^+ precursors. The importance of NAD^+ regeneration through recycling pathways is emphasized by the occurrence of an intense non redox NAD^+ consumption as suggested by the rapid turnover of the coenzyme pool within the cell (Park et al., 1989). In bacteria, the pyridine by-products of the NAD^+ consuming enzymes, nicotinamide mononucleotide (NMN) and nicotinamide (NAM), can be recycled back to NAD^+ through the PNC depicted on Figure 1.15 (Galeazzi et al., 2011). Briefly, NAM can be converted to NAD^+ through two different routes. The most commonly occurring pathway is initiated by NAM deamidation to nicotinic acid (NA), followed by conversion to Nicotinic acid mononucleotide (NaMN), NaMN adenylation to nicotinic acid adenine dinucleotide (NaAD), and NaAD amidation to NAD. The last three reactions comprise the so-called Preiss-Handler pathway (Preiss & Handler, 1958a; Preiss & Handler, 1958b). The second NAM recycling route is a relatively rare, non

deamidated pathway, whereby NAM is directly phosphoribosylated to NMN and NMN is then adenylated to NAD^+. NMN can be recycled back to NAD^+ through two pathways shown to be functional in *E. coli* and *Salmonella typhimurium* (Foster & Baskowsky-Foster, 1980): the predominant route, PNC IV, proceeds via NMN deamidation to NaMN, which is then converted to NAD^+ by entering the Preiss-Handler pathway; the alternative route, PNC VI, comprises NMN hydrolysis to NAM followed by NAM conversion to NAD^+ through the deamidated pathway. The same routes described for pyridine recycling can be used by the cell to salvage exogenous pyridines, i.e. NA and NAM. Nicotinamide riboside (NmR) and NMN can also be exogenous NAD precursors, the latter being converted to NmR prior to uptake (Grose et al., 2005). Different combinations of the various PNCs among the NAD^+ biosynthetic machinery may be found in the sequenced bacterial genomes, depending on the bacterial species. Indeed salvage and recycling pathways appear to be a subject of substantial variations even between closely related species. While most of the enzymes involved in such routes have been characterized, some of them, like NMN deamidase (EC 3.5.1.42), were not assigned to any gene until 2011 (Galeazzi et al., 2011). The existence of an enzyme endowed with NMN deamidase activity is supported by experimental evidence dating back to the early '70s (Foster & Brestel, 1982; Friedmann & Garstki, 1973; Kinney et al., 1979). In *S. typhimurium* and *E. coli* it was suggested to be involved in NMN recycling through PNC IV (Foster & Baskowsky-Foster, 1980; Hillyard et al., 1981) and to prevent inhibition of bacterial NAD^+-dependent DNA ligase by accumulated NMN, a well-known ligase inhibitor (Olivera & Lehman, 1967; Park et al., 1989). In addition, physiological studies in *S. typhimurium* suggested that NMN deamidase might play a key role in salvaging of NmR via NMN; in fact NMN would be deamidated to NaMN and thus enter the Preiss-Handler pathway rather than being directly adenylated to NAD (Grose et al., 2005).

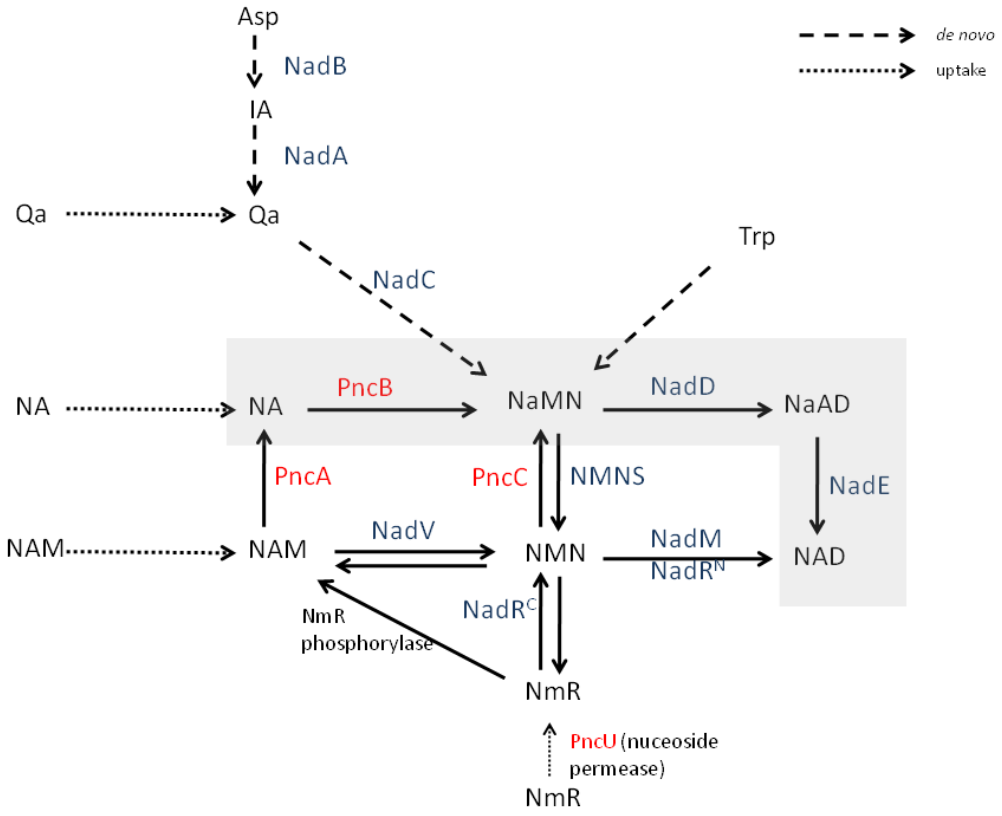

Figure 1.15. *Pyridine nucleotide cycle and NAD+ biosynthetic routes*. The routes known to be functional across diverse bacterial species are shown by solid lines. Preiss-Handler pathway is shadowed. Dotted and dashed lines relate to uptake and *de novo* NaMN synthesis, respectively. Enzymes are indicated as the acronyms used to identify the corresponding gene locus.

Moreover, the product of the NMN deamidase-catalyzed reaction, e.g. NaMN, is used as the preferred phosphoribosyl donor by the enzyme CobT, that catalyzes a late step in adenosylcobalamin biosynthesis (Maggio-Hall & Escalante-Semerena, 2003), thus conferring to NMN deamidase a role in the regulation of vitamin B12 biosynthesis.

The main drawback for characterizing this enzyme is that the enzymatic described until now are based both in complex chromatographic methods (Cheng & Roth, 1995; Foster, 1981; Kinney et al., 1979; Liu et al., 1982), HPLC assays relying on direct quantization of NaMN (Galeazzi et al., 2011) or expensive spectrophotometric assays using 3 coupled non-commercially available enzymes (Galeazzi et al., 2011). A direct spectrophotometric method for nicotinamide mononucleotide deamidase measurement would increase the knowledge of these PNC related enzymes.

The aim of this thesis was to study these three pharma-related enzymes (Neu5Ac aldolases, nicotinamidases and nicotinamide mononucleotide deamidases) in microorganisms by using cloning, overexpression and kinetic characterization of selected microbial enzymes, not only obtained by the classical molecular biology techniques, but also by directed evolution (*in vitro* molecular evolution). The development of high-throughput assays for measuring Neu5Ac aldolases and nicotinamidases as well as a novel spectrophotometric method for NMN deamidase detection was pursued.

II. OBJECTIVES

The main objective of the present PhD Thesis was the characterization of nicotin deamidases and aldolases, which are enzymes of biotechnological interest, using enzyme-coupled assays. This main objective could be divided in the following partial objectives:

1. Cloning and biochemical characterization of *N*-acetylneuraminic acid aldolase from *Lactobacillus plantarum* WCFS1, in comparison with the *N*-acetylneuraminic acid aldolase from *Escherichia coli* K-12 MG1655.
2. Cloning and characterization of an L-lactate dehydrogenase from *Bacillus halodurans* C-125, and development of an enzyme-coupled assay for high-throughput screening of *N*-acetylneuraminic acid aldolase libraries generated by directed evolution techniques.
3. Cloning and Characterization of a nicotinamidase from *Oceanobacillus iheyensis* HTE831.
4. Cloning and characterization of a glutamate dehydrogenase from *Bacillus halodurans* C-125, and development of a coupled-enzyme assay for high-throughput screening of nicotinamidases or sirtuins.
5. Cloning of a nicotinamide mononucleotide deamidase from *Oceanobacillus iheyensis* HTE831, and its characterization by a novel coupled-assay method using *Bacillus halodurans* C-125 glutamate dehydrogenase.

III. Materials and Methods

1. GENOMIC DNA

Genomic DNAs to obtain the different enzymes used in this thesis were from:

1. *Lactobacillus plantarum* strain WCFS1. It was used as the source of an *N*-acetylneuraminic acid aldolase. It was purchased from the NCIMB collection (#8826). The strain was cultivated in Man's Rogosa and Sharpe (MRS)-Agar medium (10 g/L tryptone, 5 g/L yeast extract, 10 g/L NaCl) and when colonies were obtained, it was cultivated in MRS liquid medium overnight. Genomic DNA was obtained using DNeasy tissue and blood extraction kit (Qiagen, USA).

2. *Escherichia coli* K12 strain MG1655. It was purchased from the Coli Genetic Stock Center (CGST, USA) and provided the source of *N*-acetylneuraminic acid aldolase gene. The strain was cultivated in Luria Bertani (LB)-Agar medium (10 g/L tryptone, 5 g/L yeast extract, 10 g/L NaCl) and when colonies were obtained, it was cultivated in LB liquid medium overnight. Genomic DNA was obtained using DNeasy tissue and blood extraction kit (Qiagen, USA).

3. *Bacillus halodurans* strain C-125. Its genomic DNA was a kindly provided by Professor Hideto Takami, from Japan Agency from Marine-earth Science and Technology (JAMSTEC, Japan) and was used as the source of Lactate dehydrogenase and Glutamate dehydrogenase gene.

4. *Oceanobacillus iheyensis* strain HTE831. Its genomic DNA was a gift from Professor Hideto Takami, from Japan Agency from Marine-earth Science and Technology (JAMSTEC, Japan) and was used as the source of Nicotinamidase and Nicotinamide mononucleotide amidase gene.

2. REACTIVES AND COMERCIAL STRAINS

Enzymes substrates (nicotinamide, nicotinic acid, pyrazinamide, methyl-nicotinate, ethylnicotinate, α-ketoglutarate, fructose1,6-diphosphate), divalent ions ($CaCl_2$, $FeSO_4$, $MnCl_2$, $MgCl_2$, $NiSO_4$ and $ZnSO_4$), EDTA, EGTA, IPTG, glycerol, hydroxiectoine, trifluoroacetic acid, antibiotics (kanamycin and chloramphenicol), protein inhibitors (nicotinaldehyde, 5-br-nicotinaldehyde), detergents (sodium lauroyl sarcosinate), fluorophores (Sypro Orange®), enzymes (rabbit muscle L-lactate dehydrogenase), molecular mass standard for gel filtration chromatography, bovin serum albumin (BSA) for protein quantification and ethidium bromide were

purchased from Sigma-Aldrich (Madrid, Spain). Deep Purple total protein stain was from GE Lifescience (Uppsala, Sweden). Ammonium sulfate and inorganic buffers were obtained from Fluka. Neu5Ac, sodium pyruvate and cofactors (NADPH, NADH) were from Carbosynth (UK). Nicotinamide mononucleotide was from Santa Cruz biotechnology (Heidelberg, Germany). 5-Methylnicotinamide was from Alfa Aesar (USA). Electrophoresis and protein quantification (Bradford) reactives were from Biorad (Hercules, USA). HPLC disolvents were from Análisis Vínicos (Tomelloso, Spain). Purified water was obtained through a MilliQ system (Millipore, Bedford, USA). Culture media were acquired from Pronadisa (Condalab, Madrid, Spain).

Restriction enzymes, antartic phosphatase (CIP), deoxyribonucleotides (DNTPs) and *Taq* polymerase were obtained from New England Biolabs (Berverly, MA, USA). *Pfu* Ultra II polymerase and T_4 DNA ligase were purchased from Agilent technologies (CA, USA). The oligonucleotides specifically designed for each cloned gene were obtained from Isogen Life Sciences (Darmstad, Germany). Cloning strain DH5α was from Invitrogen (Frederick, USA). Expression vectors, *Escherichia coli* strains for protein expression and 3C/LIC cloning kit used were obtained from Novagen, EMDmillipore (USA) (Table 3.1 and 3.2).

Table 3.1. E. coli *strains used in this work.*

Strain	Company	Utility
DH5α	Invitrogen	Cloning
Novablue Giga	Novagen	Cloning
BL21 (DE3) pLysS	Novagen	Expression
Rosetta 2 (DE3)	Novagen	Expression

Table 3.2: *Cloning vectors used in this work.*

Plasmid	Company	Resistance	Tag	Utility
pET52 3C/LIC	Novagen	Amp^R	*N*-ter His_{10}	Expression
pET28a	Novagen	Kan^R	*N*-ter His_6	Expression
pET24b	Novagen	Kan^R	*C*-ter His_6	Expression
pGEX-KG	Amersham	Amp^R	*N*-ter GST	Expression
pTYB21	NEB	Amp^R	*N*-ter CBD	Expression

Molecular biology kits used in the purification of DNA (genomic, plasmid and PCR fragments) were purchased from Qiagen (Valencia USA). DNA recovery gel kit was obtained from Zymo (Irvine, USA). DNA quantification and purity were spectrophotometrically determined in a TrayCell (Hellma, Müllheim, Germany), through a spectrum between 220 and 300 nm.

3. BIOINFORMATIC TOOLS

Gene sequences were obtained from National Center for Biotechnology Information (NCBI: http://www.ncbi.nlm.nih.gov/). Sequence alignment and identification of protein similarities were made by BLAST (Basic Local Alignment Search Tool) (Altschul et al., 1990). The sequences were aligned using ClustalW2 (Thompson et al., 1994) and ESPript (Gouet et al., 1999). Protein sequences were 3D modelled with Geno3D (Combet et al., 2002), and their topological drawing obtained with TOPS (Michalopoulos et al., 2004). Molecular visualizations were performed with PyMOL (http://pymol.org) (Schrodinger, 2010).

Hydrogen bonds, and salt bridges, defined as an ion pair with an interatomic distance of less than 4 Å between two oppositely charged residues (Asp, Glu, Arg, and Lys), were calculated through the Whatif web interface (http://swift.cmbi.ru.nl/servers/html/) (Hooft *et al*., 1996). The solvent accessible surfaces were calculated by Getarea (http://curie.utmb.edu/) (Negi *et al*., 2006).

Tree-building method used was Neighbor Joining (NJ) as implemented in MEGA 4, (Huson & Bryant, 2006; Tamura et al., 2007). The Bootstrap values for NJ trees were obtained after 1000 generations. MEGA 4 tree viewer was used to visualize the trees and calculate confidence values (Karlin, 2001).

4. MICROBIOLOGIC METHODS

4.1 Culture media, growing and conservation of strains

L. plantarum was grown at 30 ºC in solid or liquid Man's Rogosa and Sharpe (MRS) broth.

Man's Rogosa and Sharpe (MRS):	Peptone	10 g/L
	Meat extract	10 g/L
	Yeast extract	5 g/L
	D-glucose	20 g/L
	K_2HPO_4	2 g/L
	Sodium acetate	5 g/L
	Triammonium citrate	2 g/L
	$MgSO_4.7H_2O$	0.2 g/L
	$MnSO_4.4H_20$	0.05 g/L

The ingredients were dissolved in distilled water and the pH was adjusted at 6.2 to 6.6 and then medium was sterilized at 121°C for 15 minutes, under 15Ib pressure.

E. coli was grown at 37 ºC with agitation in solid or liquid Luria-Bertani medium (LB) (Pronadisa, Condalab, Spain). For high yield protein expression Terrific Broth (TB) (Pronadisa, Condalab, Spain) was used, supplemented with the necessary antibiotics, kanamycin (50 µg/mL) and chloramphenicol (34 µg/mL). For the induction of T7 RNA polymerase promoter, isopropyl-β-D-thiogalactoside

(IPTG) was added to the cultures, in a final concentration of 0.5 mM. The composition of media was as follow:

Luria-Bertani (LB):	Tryptone	10 g/L
	Yeast extract	5 g/L
	NaCl	10 g/L
Terrific Broth (TB):	Tryptone	12 g/L
	Yeast extract	24 g/L
	Potassium monophosphate	2.3 g/L
	Potassium diphosphate	12.5 g/L
	Glycerol (v/v)	4 ml/L

The dehydrated media were dissolved in distilled water and autoclaved at 121 ºC during 20 minutes, and then conserved at 4 ºC, until use. Once the culture was inoculated, its growth was followed spectrophotometrically (UV-2401PC, Shizamdzu Corporation, Japan), by measuring optical density at 600 nm (OD_{600}). When *E. coli* cells were stored for long periods, glycerol stocks (16 %) were stored at -80 ºC (UltraLow MDFU3086, Sanyo Electric, Japan)

4.2 Transformation

E. coli competent cells (Novablue and BL21) were transformed by the Heat-shock method as described in 3C/LIC cloning kit users protocol (TB453 Rev B0107).

E. coli competent cells (DH5α and Rosetta) were transformed by the electroporation method (Dower *et al.*, 1988), with an electroporator BioRad (Hercules, USA). After transformation cells were recovered at 37 ºC in SOC medium (0.5 % yeast extract, 2% tryptone, 10 mM NaCl, 2.5 mM KCl, 10 mM $MgCl_2$, 10 mM $MgSO_4$ and 20 mM glucose) for 1 hour, before platting in the corresponding Petri dishes, containing the appropriate antibiotic.

5. PCR AMPLIFICATION AND CLONING OF DNA FRAGMENTS

In general terms, all the methods used for cloning are described in the book of Sambrock *et al* (Sambrook, 1989). The amplification of DNA fragments was made by PCR reaction using a thermocycler TGradient Biometra (MJ Research, USA)c. For each PCR reaction, specific oligonucleotides were used (100 µM), which were complementary to 5' and 3' ends of the target gene. Then, this PCR product was cloned, using Ligase Independent Cloning (LIC) system for *L. plantarum* and *E.* coli Neu5Ac aldolase or from restriction enzymes for the rest of enzymes. Amplified fragments were cloned in a pET vector (T7 RNA polimerase promoter), which is inducible by IPTG. PCR conditions were as follow unless otherwise is indicated:

Table 3.3. *PCR standard conditions*

Step	Temperature (ºC)	Time
1	95	1 minute
2	95	30 seconds
3	54	45 seconds
4	72	1 minute/Kb
5	Repeat steps 2-4 (x29)	
6	72	10 minutes

5.1 Cloning of recombinant LpNAL of Lactobacillus plantarum *WCFS1*

L. plantarum Neu5Ac aldolase gene (*nanA*) (Uniprot entry number P59407), was amplified by PCR using *Pfu* Ultra II, and the following oligonucleotides: 5'-*CAGGGACCCGGT*ATGAGTAAAAAACTATTGTATGCAGCCCAAATG-3'and reverse primer 5'-*GGCACCAGAGCGTT*GTTTTTGAAGTATTTTTCGTAAATC GCCG-3' (LIC extensions sites are italicized). The resulting PCR product was purified and treated with LIC-qualified T4 DNA polymerase (+dATP), annealed to the C-terminal 10x His-Tag pET52 3C/LIC vector and transformed into competent *E. coli* Novablue Giga competent cells. Ampicillin resistant clones were confirmed by colony PCR and analytic digestion. A selected clone, denoted as pET52-*LpNAL*,

was transformed into *E. coli* BL21 (DE3)*pLys* competent cells (Novagen) and the correct sequence was checked by DNA sequencing.

For using as template in the error-prone PCR library creation, LpNAL gene was subcloned into pET28a vector, providing N-terminal 6x histidine tag. *nanA* gene was PCR amplified from vector pET52-*LpNAL* using the following oligonucleotides containing restriction enzyme sites (italics) for *EcoRI* in the 5' and *XhoI* in the 3': GCCC*GAATTC*ATGAGTAAAAAACTATTATATG CAGCAC (forward primer) and GCCC*CTCGAG*TCATTAGTTCTTGAAG TATTTTTCGTA (reverse primer). The PCR product was digested with the same restriction enzymes, purified by QIAquick PCR purification kit (Qiagen) and inserted into the expression vector pET28a downstream of the T7 RNA polymerase promoter, which had been previously digested with the same restriction enzymes. This produced the recombinant plasmid named pET28a-*LpNAL.* Plasmids were transferred to *E. coli* DH5α. Kanamycin resistant clones were confirmed by colony PCR and analytic digestion. The positive clones were transformed in *E. coli* Rosetta 2 (DE3), and the correct sequence was checked by DNA sequencing.

5.2 Cloning of recombinant EcNAL from Escherichia coli *K-12 strain MG1655.*

PCR amplification of the gene *nanA* (Uniprot entry number: P0A6L4) was obtained using genomic DNA of *Escherichia coli* K-12 strain MG1655, and the following oligonucleotides containing LIC extension sites (italics): 5´*CAGGGACCCGGT*ATGGCAACCAATTTACGTGGCGTA and 3'*GGCACCAG AGCGTT*CCCGCGTTCTTGCATCAACTGCT. The resulting PCR product was purified and treated with LIC-qualified T4 DNA polymerase (+dATP), annealed to the C-terminal 10x His-Tag pET52 3C/LIC vector and transformed into competent *E. coli* Novablue Giga competent cells. Ampicillin resistant clones were confirmed by colony PCR and analytic digestion. A selected clone, denoted as pET52-*EcNAL*, was transformed into *E. coli* BL21 (DE3)*pLys* competent cells (Novagen) and the correct sequence was checked by DNA sequencing.

5.3 Cloning of recombinant BhLDH from Bacillus halodurans *C-125.*

Genomic DNA from *Bacillus halodurans* C-125 was used as the source of L-lactate dehydrogenase gene (*lctE)*, denoted as Q9K5Z8 (Uniprot). PCR amplification of this gene was obtained using *Pfu* Ultra II and the following oligonucleotides containing restriction enzyme sites (italics) for *NheI* in the 5' and *XhoI* in the 3': CCGGC*GCTAGC*ATGGCTATTACTAAAGGAAACAAAATTG (forward primer) and CGCC*CTCGAG*CTACGACCAAATGGCTGCTT (reverse primer). The PCR product was digested with the same restriction enzymes, purified by QIAquick PCR purification kit (Qiagen), and inserted into the expression vector pET28a downstream of the T7 RNA polymerase promoter, which had been previously digested with the same restriction enzymes. This produced the recombinant plasmid named pET28a-BhLDH, which encodes for an additional 36 amino acid *N*-terminal sequence containing a six histidine tag. Plasmids were transferred to *E. coli* DH5α electrocompetent cells (Novagen) and plated onto LB-kanamycin overnight. The obtained clones were checked by colony PCR, analytical digestion and sequencing. Then, a positive clone was transformed in *E. coli* Rosetta 2 (DE3) for protein expression.

5.4 Cloning of recombinant OiNIC from Oceanobacillus iheyensis *HTE831.*

Genomic DNA from *Oceanobacillus iheyensis* HTE831 was used as the source of nicotinamidase gen (Uniprot entry number: Q8ESQ6). The 552 bp gene was amplified by PCR using forward primer 5'CGCGGC*CATATG*AAAAAAA AGGCATTATTAAATATCGATTATA-3' and reverse primer 5'-CGCC*GAATTC*CTATCTTACCTCTGCACCAAT-3' (restriction enzymes cleavage sites are italicized). The resulting PCR product was purified and digested with *NdeI* and *EcoRI* restriction enzymes, ligated to the digested Intein-tag pTYB21 vector (New England Biolabs) which carries a chitin binding domain, and transformed into competent *E. coli* DH5α competent cells. A selected clone harboring the correct sequence, denoted as pTYB21-OiNic was transformed into *E. coli* Rosetta 2 (DE3) competent cells (Novagen). *OiNic* was also cloned into pET28a vector using the same primers and cloning and expression *E. coli* strains

with the purpose of high-yield overexpression of the protein. The recombinant vector was called pET28a-OiNIC.

5.5 Cloning of recombinant BhGDH from Bacillus halodurans *C-125.*

Genomic DNA from *Bacillus halodurans* C-125 was used as the source of NADP-dependent glutamate dehydrogenase (*gudB)* (Uniprot entry number: Q9KB34). PCR amplification of this gene was obtained using *Pfu* Ultra II and the following oligonucleotides containing restriction enzyme sites (italics) for *NdeI* in the 5' and *EcoRI* in the 3': GGCGG*CATATG*ACAACATTGGTAAGAGAGAAA CAAAC (forward primer) and CGGC*GAATTC*CTAGACGACCCCGTGGGAAAT (reverse primer). The PCR product was digested with the same restriction enzymes, purified by QIAquick PCR purification kit (Qiagen), and inserted into the expression vector pET28a downstream of the T7 RNA polymerase promoter, which had been previously digested with the same restriction enzymes. This produced the recombinant plasmid named pET28a-BhGDH, which encodes for an additional 36 amino acid *N*-terminal sequence containing a six histidine tag. Plasmids were transferred to *E. coli* DH5α electrocompetent cells (Novagen) and plated onto LB-kanamycin overnight. The obtained clones were checked by colony PCR, analytical digestion and sequencing. Then, a positive clone was transformed in *E. coli* Rosetta 2 (DE3) for protein expression.

5.6 Cloning of recombinant OiPncC from Oceanobacillus iheyensis *HTE831.*

The annotated *cinA* gene from *O. iheyensis* HTE831, (Uniprot entry number: Q8EQR8), was PCR amplified with KapaHIFI polymerase (Kapa Biosystems) using the following oligonucleotides containing restriction enzyme sites for *BamHI* and *XhoI* (italics), cleavage site for Human rhinovirus 3C protease, commonly referred to as PreScission (underlined) and 6 histidine sequence (bold): 5'GCGC*GGATCC*CTCGAGGTTCTGTTTCAAGGACCTATGAAAAATTATCA AGCTGAAATAGTA (forward primer) and GCC*CTCGAG*TTA**GTGGT GGTGGTGGTGGTG**TGGACCCTGGAACAGACTTCCAGGCTTTTACTTTT TAAATA. Amplification fragments were inserted downstream of the IPTG inducible promoter of pGEX-KG expression vector, which provides GST-tagged recombinant protein. Resulting plasmid pGEX-OiPncC, was used to transform *E.*

coli DH5α electrocompetent cells (Novagen) and plated onto Ampicillin-LB overnight. The obtained clones were checked by colony PCR, analytical digestion and sequencing. Then, a positive clone was transformed in *E. coli* Rosetta 2 (DE3) for protein expression.

OiPncC was re-cloned into pET24b due to solubility problems of the pGEX-OiNIC resulting protein. Primers used for PCR amplification from *O. iheyensis* genomic DNA included *NdeI* and *XhoI* restriction sites (italics) and were: 5' GCGG*GCTAGC*ATGAAAAATTATCAAGCTGAAATAGTAG (forward primer) and 3' GCCG*CTCGAG*GCTTTTACTTTTTAAATATTGATATATTA GTTC (reverse primer). The PCR product was digested with the same restriction enzymes, purified by QIAquick PCR purification kit (Qiagen), and inserted into the expression vector pET24b downstream of the T7 RNA polymerase promoter, which had been previously digested with the same restriction enzymes. This produced the recombinant plasmid named pET24b-OiPncC, which encodes for a *C*-terminal sequence containing a six histidine tag. Plasmids were transferred to *E. coli* DH5α electrocompetent cells (Novagen) and plated onto LB-kanamycin overnight. The obtained clones were checked by colony PCR, analytical digestion and sequencing. Then, a positive clone was transformed in *E. coli* Rosetta 2 (DE3) for protein expression.

5.7 Site directed mutagenesis of OiNIC.

Seven single mutants, (T12Q, Q96K, Q96A, K104A, C133A, F68W, E65H), and two double-mutants (C133A-F68W, C133A-E65H) were constructed using the method of overlap extension PCR (Ho *et al*., 1989) (Figure 3.1). Primers used for amplification are listed in Table 3.4. pET28a-OiNIC doubled stranded plasmid DNA was extracted from *E. coli* DH5α and used as the template for the mutagenesis PCR. The 18 cycles used with high-fidelity Pfu Ultra II (Stratagene) were: 30 s at 95 ºC (denaturation), 60 s at 55 ºC (annealing) and 380 s at 68 ºC (polymerization). PCR products were digested with *Dpn*I to ensure complete removal of the parental plasmid, and transformed in *E. coli* DH5α electrocompetent cells. All ligations were confirmed by sequencing of the whole ligated PCR fragment.

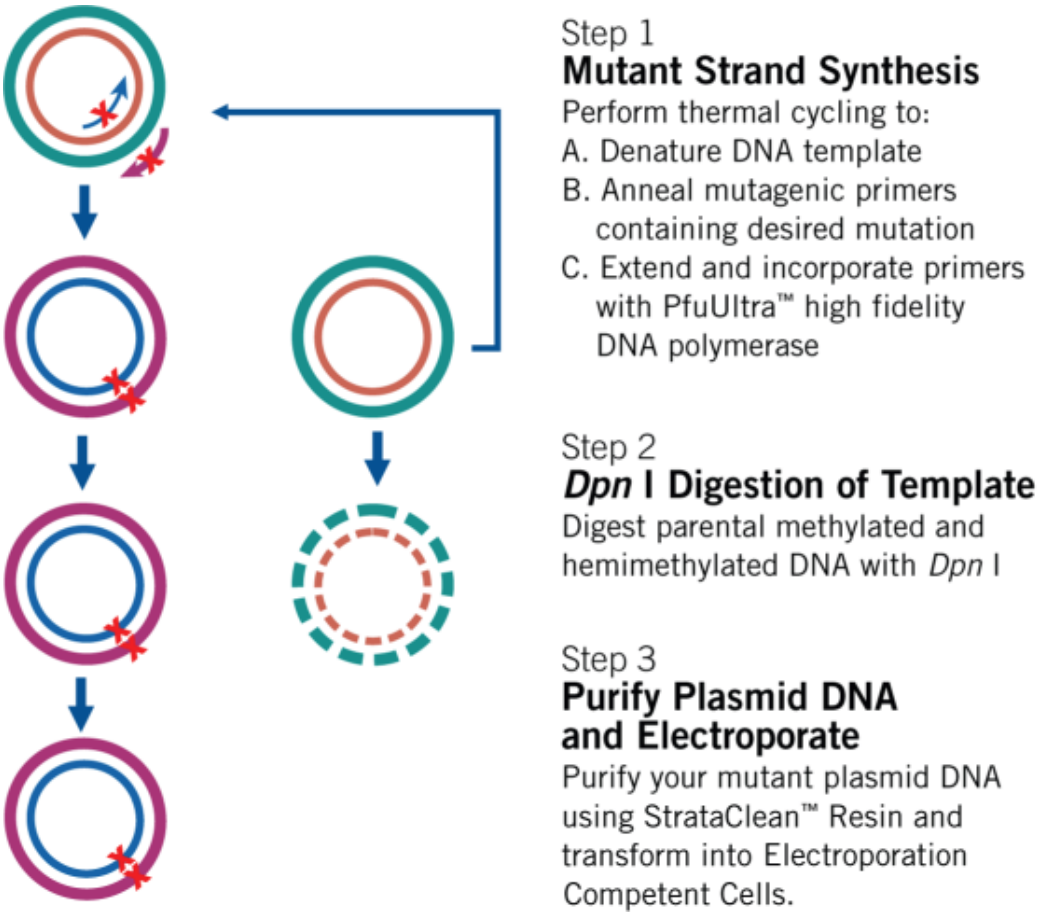

Figure 3.1. *Description of the technique used for site directed mutagenesis.*

Table 3.4. *Sequences of oligonucleotides used for site-directed mutagenesis of OiNIC*

OiNIC Mutant	**Primers**
T12Q	5' GGCATTATTAAATATCGATTATCAAATTGATTTTGTAGCAGAAGATGG 3' CCATCTTCTGCTACAAAATCAATTTGATAATCGATATTTAATAATGCC
Q96K	5'CACTTTATCAACGTATAAAAGAAAAGGAAAATGTCTATTACTTTGATAA 3' TTATCAAAGTAATAGACATTTTCCTTTTCTTTTATACGTTGATAAAGTG
Q96A	5' CACTTTATCAACGTATAAAAGAAGCGGAAAATGTCTATTACTTTGATAA 3' TTATCAAAGTAATAGACATTTTCCGC TTCTTTTATACGTTGATAAAGTG
K104A	5' AGGAAAATGTCTATTACTTTGATGCAACAAGATATAGTGCATTTGCTGG 3' CCAGCAAATGCACTATATTTGTTGCATCAAAGTAATAGACATTTTCCTG
C133A	5' GAAGTTCATCTTGTTGGAGTTGCTACTGATATATGTGTTTTACATAC 3' GTATGTAAAACACATATATCAGTAGCAACTCCAACAAGATGAACTTC
F68W	5' GTATCATCCCGAACAACAACTATGGCCTCCCCATAATATAGTTGGAAC 3' GTTCCAACTATATTATGGGGAGGCCATAGTTGTTGTTCGGGATGATAC
E65H	5' AACCTGACGATGAGTATCATCCCCACCAACAACTATTTCCTCCCCATAA 3'TATGGGGAGGAAATAGTTGTTGGTGGGGATGATACTCATCGTCAGGTTG
C133A-F68W (template C133A)	5' GTATCATCCCGAACAACAACTATGGCCTCCCCATAATATAGTTGGAAC 3' GTTCCAACTATATTATGGGGAGGCCATAGTTGTTGTTCGGGATGATAC
C133A-E65H (template C133A)	5' AACCTGACGATGAGTATCATCCCCACCAACAACTATTTCCTCCCCATAA 3'TATGGGGAGGAAATAGTTGTTGGTGGGGATGATACTCATCGTCAGGTTG

5.8 LpNAL error-prone library construction

Mutagenic PCR was carried out under standard error-prone conditions. Forward and reverse primers for LpNAL were used to amplify and mutate the template gene, which had been previously cloned into vector pET28a by ligation and transformation into *E. coli*. 50 nM each of the primers were used and the reaction conditions were: 10 ng template, 1X Error prone Mutagenic buffer, 1X error prone dNTP mix, 0.2 mM $MnCl_2$ and 5 U *Taq* polymerase (NEB), in a final volume of 100 µl. The PCR reaction was carried out for 25 cycles of 94 ºC, 30 s; 54 ºC, 45 s; 72 ºC, 60 s, and then 1 cycle of 72 ºC for 10 min. The library fragment was agarose gel-purified and digested with *EcoR*I and *Xho*I. The resulting PCR products were ligated to pET28a, which had been previously

digested and gel-purified. Plasmids were transferred into high efficiency *E. coli* DH5α electrocompetent cells. A small amount of transformed cells was platted on LB-agar in order to check transformation efficiency, measured as cfu/µg. The rest of the transformation was used to inoculate a 10 mL Kan-LB culture, and was grown overnight. If transformation efficiency was above 10^6 cfu/µg and < 10% background was observed, library vectors were obtained from o/n grown culture and transformed into *E. coli* Rosetta 2 (DE3) electrocompetent cells. The mutation rate was checked by DNA sequencing of a representative number of clones. Resulting library was called *EpLpNAL3.*

10X Error prone mutagenic buffer: 70 mM $MgCl_2$, 500 mM KCl, 100 mM Tris pH 8.3 and 0.1% (wt/vol) gelatin.
10X Error prone dNTP mix: 2 mM dGTP, 2 mM dATP, 10 mM dCTP and 10 mM dTTP.

6. PROTEIN PURIFICATION

E. coli cells harboring the recombinant plasmid were grown for 4 hours at 37º C in 400 mL of LB Amp-Chlor (LpNAL and EcNAL) or Kan-Chlor (BhLDH, OiNIC, OiPncC) before being transferred to a 5-L fermentor (Sartorius), containing 4 L of Terrific Broth, supplemented with the latter antibiotics. This culture was allowed to grow for 3h at 37 ºC, and then, induced by adding 0.4-1 mM isopropyl-β-D-thiogalactoside (IPTG) for 12 hours at 30 ºC with constant stirring and oxygenation. The culture was diafiltered through a 500-kDa membrane (GE Lifesciences, Uppsala, Sweden), and cleaned with 50 mM of the appropriate buffer. Cells were disrupted using a homogenizer (MiniZetaII, Netzsch) and the cell debris was harvested by centrifugation. The recovered supernatant was treated with 3 U/mL DNase I (Sigma) to remove nucleic acids, and then centrifuged for 20 min at 6,000 x *g*.

The purification was usually performed in two steps, starting with tangential ultrafiltration with a 50-kDa cutoff membrane (for OiNIC and OiPncC) or 100 kDa cutoff membrane (for EcNAL, LpNAL, BhLDH, BhGDH,) on a QuixStand system (GE Lifesciences). After centrifugation at 40,000*g,* the resulting supernatant was

purified by Ni^{2+}-chelating affinity chromatography (ÄKTA Prime Plus, GE Lifesciences) onto a HiPrep IMAC 16/10 FF 20 mL column (GE Lifesciences). The bound enzyme was eluted with a linear imidazol gradient up to 250 mM in the appropriate buffer at a flow rate of 10 mL/min. The fractions containing the desired activity were pooled, desalted, concentrated and stored at -80 ºC.

7. PROTEIN METHODOLOGY

7.1 Protein quantification

Protein concentration determination was carried out using Bradford method (Bradford, 1976), using bovine serum albumin as standard for the calibration curve.

7.2 SDS-Polyacrylamide gel electrophoresis (SDS-PAGE)

For the electrophoretic resolution of proteins, SDS-polyacrylamide gel electrophoresis (SDS-PAGE) method was performed in the presence of the anionic detergent sodium dodecyl sulfate (SDS), as described by Laemmli *et al* (Laemmli, 1970). Gel of 1.5 mm thick was prepared as follows: 12% (w/v) acrylamide-bis-acrylamide in 375 mM Tris-HCl pH 8.8, 0.1 % (w/v) SDS, 0.05 % (w/v) ammonium persulfate and 0.07 % (v/v) TEMED, being the two last components necessary to start the polymerization reaction. A comb was introduced in the 4% stacking gel [4 % (w/v) acrylamide-bisacrylamide in 125 mM Tris-HCl pH 6.8, 0.1 % (w/v) SDS, 0.05 % ammonium persulfate and 0.07 % (v/v) TEMED] to obtain a wells to load the samples.

Each sample (15 µL) was mixed with 5 µL of 4X loading buffer, whose composition was: 15 % (v/v) glycerol, 3 % (w/v) SDS, 0.015 % (w/v) bromophenol blue and 7.5 % (v/v) β-mercaptoethanol in 100 mM Tris-HCl buffer pH 6.8. Then, the samples were heated at 100 ºC for 4 minutes before loading them in the staking gel.

Electrophoresis was carried out in a Mini Protean III system (Biorad, Hercules, USA) at 200 V for 45 minutes using 25 mM Tris-HCl, 200 mM glycine, 0.1 % SDS (w/v) pH 8.3 as a running buffer. Proteins were stained with Brilliant Blue Coomasie (Sigma, Madrid, Spain) for 30 minutes, and then, the gel was destained using a solution containing 30 % methanol and 10 % acetic acid. For determining the molecular mass of the protein under denaturing conditions, molecular weight

standard P7708S (NEB, Beverly MA, USA) was used which included the following proteins (MBP-β-galactosidase, MW 175 kDa; MBP-paramyosin, MW 80 kDa; MBP-CBD, MW 58 kDa; CBD-*Mxe* Intein-2CBD, MW 46 kDa; CBD-*Mxe* Intein, MW 30 kDa; CBD-BmFKBP13, MW 25 kDa, lysozyme 17 kDa; aprotinin, MW 7 kDa.

7.3 Molecular mass determination

Monomeric molecular mass determination of the proteins were carried out under denaturing conditions, as described above, and by liquid chromatography-mass spectrometry with electrospray ionization, using an HP-1100 (Agilent Technologies), according to previously published methods (Pearcy & Lee, 2001; Williams *et al*., 2001). This procedure is based on the previous separation of the sample in a HPLC HP-1100 (Agilent technologies, USA), which is coupled to a mass spectrometer ESI Trap (*Trap XCT Plus*, Agilent technologies, USA). Analysis by LC/MSD Ion Trap software (version 3.2) was used to calculate with an accuracy of about 1 Da. This analysis was performed in the Servicio de Proteómica of Centro de Ayuda a la Investigación y Desarrollo (CAID) of the University of Murcia.

Gel filtration (Superdex 200 10/300 GL, GE Lifesciences, Uppsala, Sweden) was used to confirm the homogeneity, and the molecular weight of the native purified enzyme. The column was equilibrated with 50 mM Tris-HCl buffer pH 7.5, containing 0.15 M NaCl, and previously calibrated using standard proteins of know molecular weight (Figure 3.2). The chromatography was performed in an ÄKTA purifier FPLC (GE Lifesciences, Uppsala, Sweden) at a flow rate of 0.5 mL/min.

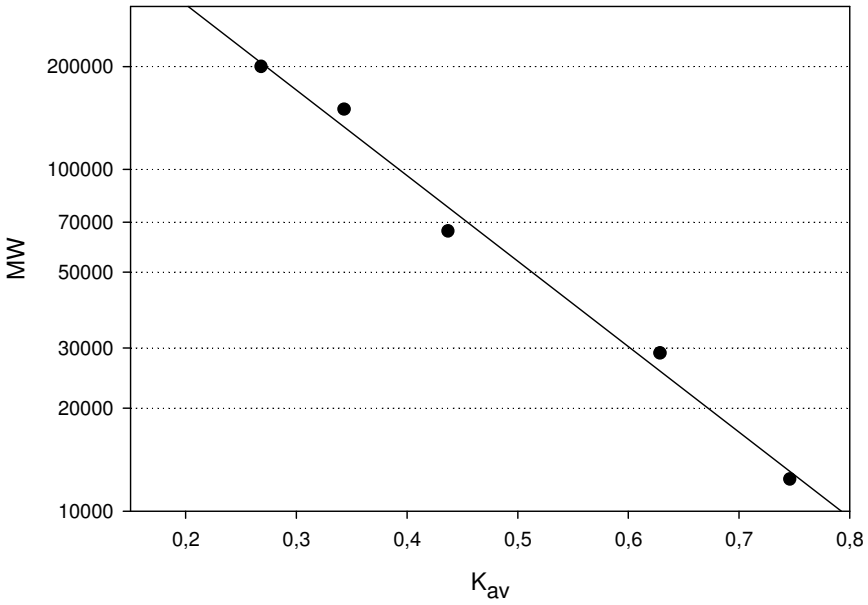

Figure 3.2. *Standard calibration curve for determining molecular mass using gel filtration.* K_{av}=(Ve-Vo)/(Vt-Vo); where K_{av} is the phase distribution coefficient, Ve is the elution volume, Vo is the death volume (calculated with blue dextran) and Vt is the total volume of the column. Proteins used were: Blue Dextran, 2000 kDa; β-amilase, 200 kDa; Alcohol dehydrogenase, 150 kDa; Albumin bovine serum, 66 kDa; Carbonic anhydrase, 29 kDa and Cytochrome C 12.4 kDa.

7.4 Protein cross-linking with Dimethylsuberimidate (DMS)

Cross-linking of OiNIC using dimethylsuberimidate (DMS) was carried out in order to confirm the quaternary structure of the enzyme. DMS induces formation of covalent bonds between the natural protomers of proteins. Protein incubated with DMS, when loaded on a SDS-PAGE, reveals a spot corresponding to the molecular weight of the native protein. DMS was dissolved at 34 mg/ml concentration with 250 mM triethanolamine buffer pH 8.5 right before adding to the reaction. In a final volume of 11 µl, reactives were added in the following order: protein to a final concentration of 0.3 mg/ml, 1 µl DMS (final concentration 3.1 mg/ml) and triethanolamine buffer. Final pH of the reaction was around pH 8.3. A control reaction without DMS was prepared. Reactions were incubated at 25 ºC in a water bath during 3 hours. Reactions were then stopped by adding 1X loading buffer, and reactions were loaded and resolved in a 12% SDS-PAGE.

7.5 Protein unfolding: determination of melting temperature

Melting curves to determine protein unfolding were obtained with the fluorescent dye SYPRO Orange (Molecular Probes, Paisley, UK). SYPRO Orange is a hydrophobic, environmentally sensitive fluorophore, that is quenched in aqueous solutions, but which binds to exposed hydrophobic surfaces of an unfolding protein, leading to a sharp increase in fluorescence emission as a function of temperature. Thermally induced unfolding is an irreversible process that follows a typical two-state model with a sharp transition between the folded and unfolded states, where T_m is defined as the midpoint of the protein-unfolding transition temperature. The T_m values obtained with this method correlate well with those obtained by other biophysical methods, such as circular dichroism (CD) or differential scanning calorimetry (DSC) (Schneider & Giffhorn, 1991). The assay was carried out in Milli-Q water or buffer containing 10X SYPRO Orange (emission at 530 nm and excitation at 490 nm), using a real time-PCR machine (model 7500, Applied Biosystems). The time/temperature control of the PCR machine was adapted from Malawski *et al.*(Malawski et al., 2006) , and consisted of 70 steps of 1 min each, raising the temperature by 1 °C steps, from 20 to 100 °C. Independent experiments were conducted with a minimum of three replicates per condition. This technique was used not only to determine the thermal protein stability, but also its pH stability.

For OiPncC, no melting curves were obtained using Sypro orange® under any of the conditions tested. For the T_m calculation of this enzyme, Deep Purple Total protein stain (GE Healthcare) was used. Deep Purple is based on a small naturally occurring fluorescent compound that reversibly binds to lysine, arginine and histidine residues (Coghlan et al., 2005) in proteins and peptides and it has been developed as an ultra-sensitive fluorescent stain for the detection of proteins in-gel and blots following electrophoretic separation (Mackintosh et al., 2003). No protocol was described for the determination of T_m using this fluorescent dye. We adapted the Sypro orange® thermofluor assay to Deep Purple protein stain for the first time. The same rtPCR conditions above described for Sypro orange® were used with OiPncC, with 1:10 diluted Deep Purple stain.

7.6 Determination of OiNIC metal ion content.

The metal ion content (Fe^{2+}, Zn^{2+} and Mn^{2+}) of the wild type enzyme OiNIC was determined using ICP-OES (Inductively Coupled Plasma-Optical Emission Spectrometer) model Optima 2000 DV, Perkin-Elmer, MA, USA) (Fyfe et al., 2009; Zhang et al., 2008). For the analysis of the protein at a 6 mg/ml concentration, a range of calibration standards were prepared using single element 100 mg/L stock solutions, diluted with 30 mM Tris/HCl buffer pH 7.3 at three different concentrations: 0.1, 1 and 10 mg/L. This analysis was performed in the Servicio de Instrumentación of Sevicio de Apoyo a la Investigación of the University of Murcia.

7.7 Purification of expressed proteins from E. coli *inclusion bodies.*

This method was used for *E. coli* cultures that resulted in the accumulation of protein in insoluble "inclusion bodies". The protein could be refolded by this procedure to produce functional proteins. Bacteria cultures were centrifuged and cell pellet was frozen. This bacterial pellet was re-suspended in lysis buffer (see below) and sonicated with bursts of 30 seconds making sure that the temperature did not increase locally. Sonicated extract was centrifuged (20 minutes, 6500*g*) and supernatant recovered and conserved. Cell pellet was re-suspended in Inclusion Body Buffer 1 (see below) and stirred for 15-30 minutes on bench. Centrifugation (20 minutes, 6500*g*) was carried out to recover the supernatant. Cell pellet re-suspended in Inclusion Body Buffer 2 (see below) and stirred for 15-30 minutes on bench. Centrifugation was carried out and last step was repeated 3 times always conserving the resulting supernatant.

The supernatants must be loaded on a SDS-PAGE to check protein extraction from inclusion bodies. Those extracts can be buffer exchanged for following purification of the extracted proteins.

Lysis buffer: Tris pH 8.0	50 mM	
EDTA	1 mM	
Sucrose	25 %	
Inclusion Body Buffer 1: Tris pH 8.0		20 mM
EGTA		2 mM
NaCl		0.2 M
Sodium deoxycolate		1%
Inclusion Body Buffer 2: Tris pH 8.0		10 mM
EGTA		1 mM
Sodium deoxycolate		0.25 %

8. SPECTROPHOTOMETRIC ASSAYS

8.1 Enzyme assay for LpNAL and EcNAL

Aldolase cleavage was determined spectrophotometrically by measuring the decrease in absorbance at 340 nm corresponding to the oxidation of NADH produced by lactate dehydrogenase (LDH) when pyruvate appeared as a consequence of the hydrolysis of Neu5Ac into such compound and ManNAc by LpNAL or EcNAL (Aisaka et al., 1991). The standard reaction medium (1 mL) for the above assay, which was carried out in a Shimadzu UV-2401 PC Spectrophotometer, contained 150 μM NADH, 0.5 U LDH, 10 mM Neu5Ac and 1.5 μg of purified LpNAL or EcNAL in 20 mM phosphate buffer pH 7.0. A control assay without Neu5Ac was also carried out to determine the presence of any other NADH-consuming enzymes. One unit of activity was defined as the amount of enzyme required to cleave 1 μmol of Neu5Ac or consuming 1 μmol of NADH in 1 min at pH 7.0 and 37 ºC. Kinetic parameters were obtained after three repeated experiments.

8.2 *Enzyme assay for BhLDH*

In the 'standard' assay, lactate dehydrogenase activity was measured spectrophotometrically at 37 ºC in a mixture that contained 30 mM of sodium pyruvate, 0.3 mM of NADH, and 50 mM of sodium phosphate buffer pH 6.0 for BhLDH or 50 mM Tris/HCl Buffer pH 8.0 for the commercial rabbit-muscle LDH (RmLDH). 2 or 4 mM fructose-1,6-biphosphate (FBP) was added in the reaction to determine if BhLDH was activated by FBP. The reaction was initiated by adding enzyme and the rate of absorbance decrease at 360 nm was measured ($\varepsilon_{360\ nm}$=4320 M^{-1} cm^{-1}). This wavelength (360 nm) was used instead of 340 nm, in order to ensure the correct measurement of the activity when adding 0.3 mM NADH to the reaction, which at 340 nm would raise the absorbance to 2. The standard reaction medium (1 mL) for the above assay was carried out in a Shimadzu UV-2401 PC Spectrophotometer. A control assay without pyruvate was also carried out to determine the presence of any other NADH-consuming enzymes. One unit of enzyme was defined as the amount which oxidizes 1 µmol of NADH/min. Kinetic parameters were obtained after three repeated experiments.

8.3 Enzyme assay for OiNIC and OiNIC mutants

Nicotinamidase spectrophotometric method measured the decrease in absorbance at 360 nm corresponding to the oxidation of NADPH produced by glutamate dehydrogenase (GDH) when NH_3, along with α-ketoglutarate, appeared as a consequence of the hydrolysis of nicotinamide into NH_3 and nicotinic acid by OiNIC. The standard reaction medium (1 mL) for the above assay, which was carried out in a Shimadzu UV-2401 PC Spectrophotometer, contained 300 µM NADPH, 9.7 µg BhGDH, 1 mM NAM, 10 mM α-ketoglutarate and 1.3 µg of purified OiNIC in 100 mM phosphate buffer pH 7.3. A control assay without NAM was also carried out to determine the presence of any other NADPH-consuming enzymes. One unit of activity is defined as the amount of enzyme consuming 1 µmol of NADPH in 1 min at pH 7.3 and 37 ºC. Kinetic parameters were obtained after three repeated experiments. Kinetic parameters where also measured for NAM analogues pyrazimamide (PZA) and 5-methylnicotinamide.

8.4 *Enzyme assay for BhGDH*

In the 'standard' assay, glutamate dehydrogenase activity was measured spectrophotometrically at 37 ºC in a mixture that contained 10 mM α-ketoglutarate, 100 mM NH_4Cl, 0.3 mM of NADPH, and 50 mM of sodium phosphate buffer pH 7.5. The reaction was initiated by adding 0.13 μg enzyme and the rate of absorbance decrease at 360 nm was measured ($\varepsilon_{360\ nm}$=4320 M^{-1} cm^{-1}). The standard reaction medium (1 mL) for the above assay was carried out in a Shimadzu UV-2401 PC Spectrophotometer. A control assay without α-ketoglutarate was also carried out to determine the presence of any other NADPH-consuming enzymes. One unit of enzyme was defined as the amount which oxidizes 1 μmol of NADPH/min. Kinetic parameters were obtained after three repeated experiments.

8.5 Enzyme assay for OiPncC

NH_3 resultant of nicotinamide mononucleotide deamidation by the enzyme OiPncC was converted, along with α-ketoglutarate, in glutamate with the concomitant oxidation of NADPH by the action of the coupling enzyme glutamate dehydrogenase. NADPH consumption could be followed spectrophotometrically at 360 nm ($\varepsilon_{360\ nm}$=4320 M^{-1} cm^{-1}). The standard reaction medium (200 μL) for the above assay, which was carried out in a Synergy HT 96-well plate reader (Biotek), contained 300 μM NADPH, 9.7 μg BhGDH, 0.5 mM NMN, 10 mM α-ketoglutarate and 15 μg of purified OiPncC in 50 mM phosphate buffer pH 7.5.A control assay without α-ketoglutarate was also carried out to determine the presence of any other NADPH-consuming enzymes. One unit of activity is defined as the amount of enzyme consuming 1 μmol of NADPH in 1 min at pH 7.3 and 37 ºC

8.6 Development of screening assay in 96-well plate and EpLpNAL3 library screening.

Libraries transformed in *E. coli* Rosetta 2 (DE3) were platted on 20x20 LB-agar plates supplemented with kanamycin and chloramphenicol (Chlor) and incubated overnight at 37 ºC. Dilutions of the transformation to be platted were required to get around 2000 colonies per plate, which ensures a big number of separate colonies. Individual colonies were picked in 96-well microtiter plates containing 100 mL of Kan-Chlor liquid LB, using a QPix2^{XT} robotic colony picker (Genetix, New Milton, UK). Six wells in column 9 in each plate were inoculated with parental transformed cells as a control (100 % activity), and two wells in the same column were not inoculated (to check for the possibility of cross-contamination). Plates were allowed to grow overnight at 37 ºC, with vigorous shaking (175 rpm) rpm (Certomat BS1 shaker, B. Braun International, Sartorius group, Germany). Cultures in stationary phase were then replicated onto 96 deep-well plates containing 250 µl fresh Kan-Chlor Terrific Broth, using the robotic colony picker. Plates were incubated during 16 hours at 30 ºC, with vigorous shaking (185 rpm) until cultures reached and OD_{600} of around 1-1.2. At this point 50 µl TB broth with IPTG were added to each well, to a final IPTG concentration of 1 mM. Cultures were induced at 30 ºC during 6 hours, 200 rpm shaking. After induction, cultures were centrifuged at 2700*g* for 20 minutes at 4 ºC and Supernatants were removed. Cell pellets were o/n frozen at -20 ºC.

Disruption of the cultures was achieved by resuspending cell pellets in 300 µl of 20 mM sodium phosphate buffer pH 8.0 with 1 mg/mL lysozime. After 1 hour incubation at 37 ºC, cell debris was pelleted by centrifugation and supernatants were used for the library screening reaction (Wada et al., 2003). All of these steps were carried out automatically by a StarPlus robotic liquid handling workstation (Hamilton, Bonaduz, Switzerland).

For the screening of wild type LpNAL and EpLpNAL libraries plates, 30 µL of enzymatic extract from each well was used to monitor Neu5Ac cleavage in an assay solution containing 50mM sodium phosphate at pH 7.0 or 50 mM glycine/NaOH pH 9.5, 0.2 mM NADH, 2 mM Neu5Ac and 8.5 µg pure BhLDH or 0.5 U/mL commercial RmLDH. The decrease in absorbance at 340 nm ($\varepsilon_{340\ nm}$=6300 M^{-1} cm^{-1}) was monitored continuously for 20 min with mild shaking

in a synergy HT spectophotometer plate reader (Biotek). The activity of each mutant was reflected by the rate of decrease in absorbance at 340 nm (Wang & Lee, 2005). The mean of the Abs/min and the coefficient of variation (CV) of each 96-well plate were calculated in order to estimate the heterogeneity and the reproducibility of the method.

For the validation screening of OiNIC using glutamate dehydrogenases, 30 µL of enzymatic extract from each well was used to monitor nicotinamide deamidation in an assay solution containing 50 mM sodium phosphate at pH 7.3, 0.2 mM NADPH, 1 mM pyrazinamide, 10 mM α-ketoglutarate and 1.3 µg pure BhGDH The decrease in absorbance at 340 nm ($\varepsilon_{340\ nm}$=6300 M^{-1} cm^{-1}) was monitored continuously for 20 min with mild shaking in a synergy HT spectophotometer plate reader (Biotek). The activity of each mutant was reflected by the rate of decrease in absorbance at 340 nm (Wang & Lee, 2005). The mean of the Abs/min and the coefficient of variation (CV) of each 96-well plate were calculated in order to estimate the heterogeneity and the reproducibility of the method.

Data quality and reproducibility from the replicate microplate assays were estimated using the Z' factor calculated from the following equation:

$Z' = 1 - [3 * (SD_{positive} + SD_{negative})/(\text{Average Rate}_{positive} - \text{Average Rate}_{negative})]$

Thus, Z' factors were calculated using the average rate values and corresponding standard deviation (SD) values measured for replicate positive and negative controls included on each microwell plate. Typical Z' factors observed during our screening of compound library plates ranged from 0.65 to 0.75.

9. HPLC ASSAYS

9.1 Enzyme assay for OiNIC

This hydrolytic activity was also measured from the increase of area of the Nicotinic acid peak, using an HPLC (GE healthcare), a reverse-phase C_{-18} 250 mm x 4.6 mm column (Phenomenex), and a mobile phase (20 mM ammonium acetate, pH 6.9) running at 1 mL/min. In these conditions, the retention time (R_T) for NAM and NA were 19.9 and 7 min, respectively. One unit of activity was defined as the amount of enzyme required to cleave 1 µmol of NAM releasing 1

μmol of NA in 1 min. The standard reaction medium for the HPLC reaction followed the above HPLC conditions and consisted of 1 mM NAM and 0.67 μg purified OiNIC in 100 mM phosphate buffer pH 7.3. Reactions were stopped by addition of TFA to a final pH of 3.0.

9.2 Enzyme assay for OiPncC

OiPncC activity was measured from the decrease of area of the Nicotinamide mononucleotide (NMN) peak, using an HPLC (GE healthcare), and the same reverse-phase $C\text{-}_{18}$ 250 mm x 4.6 mm column, (Phenomenex), and mobile phase (20 mM ammonium acetate, pH 6.9) as described for OiNIC, running at 1 ml/min. In these conditions, the retention time (R_T) for NMN and Nicotinic acid mononucleotide (NaMN) were 3.2 and 2.9 min, respectively. One unit of activity was defined as the amount of enzyme required to cleave 1 μmol of NMN releasing 1 μmol of NaMN in 1 min. The standard reaction medium for the HPLC reaction followed the above HPLC conditions and consisted of 0.5 mM NMN and 30 μg purified OiPncC in 50 mM phosphate buffer pH 7.5. Reactions were stopped by addition of TFA to a final pH of 3.0.

10. STABILITY ASSAYS

10.1 Temperature effect

The thermostability of the enzyme was examined using the standard assay for each enzyme after incubation of the enzyme from 4 ºC to 65 ºC for different periods of time (from 5 minutes to 24 hours, depending on the enzyme stability). When a stabilizer was tested, it was added to the enzyme during the incubation period at the appropriate final concentration.

10.2 pH effect

The optimum pH of the purified enzyme was studied from pH 4.0 to 11.0 in its corresponding reaction medium and using the following 50 mM buffers: sodium acetate (pH 4.0 to 5.5), sodium phosphate (pH 6.0 to 8.0), Tris-HCl (pH 8.0 to 9.0) and glycine (pH 9.0 to 11.0). In the pH stability study, the residual

enzyme activity for the reaction was measured after different periods of time (from 5 minutes to 72 hours, depending on the enzyme stability) of incubation at 37 ºC in its corresponding standard reaction medium and in the same buffers as described above.

10.3 Effect of inhibitors

Nicotinaldehyde was characterized as an inhibitor versus nicotinamide. Reactions were performed using the GDH-coupled assay described above. Inhibition reactions contained 10 mM α-ketoglutarate, 300 µM NADPH, 1 mM NAM, 9.7 µg BhGDH, 1.3 µg of purified OiNIC and varying concentrations of inhibitors in 100 mM phosphate buffer pH 7.3. Rates were plotted and fitted to Morrison´s quadratic equation (Murphy, 2004), which accounts for tight binding, using Graphpad Prism 5, and in all cases inhibitors were found to have intrinsic K_i of < 5 µM:

$$V_{inh}=V_0 * \frac{1-(([E]_t+[I]_t+ ki^{app})-(([E]_t +[I]_t + ki^{app})^2-4*[E]_t *[I]_t)^{0.5})}{2*[E]_t}$$

where V_{inh} is the inhibited rate for a given concentration of inhibitor, V_0 is the uninhibited rate, $[E]_T$ is the total enzyme concentration, $[I]_T$ is the total inhibitor concentration, and K_i^{app} is the apparent inhibition constant. k_i, the intrinsic binding constant for binding of the inhibitor to the enzyme, can be calculated from K_i^{app} by the relation:

$$k_i^{app} = k_i*(1+([S]/K_M))$$

where [S] is the substrate concentration and K_M is the Michaelis constant for binding of the substrate to the enzyme, both in the same units as $[I]_T$.

The above described GDH-coupled assay was also used for the analysis of competitive inhibition. Reactions containing 300 µM NADPH, 10 mM α-ketoglutarate, 9.7 µg BhGDH, 1.3 µg of purified OiNIC and different concentrations of NAM (0.25, 0.5, 1, 2.5, 5 mM) in 100 mM phosphate buffer pH 7.3, with inhibitor concentrations 0, 2 or 4 times the estimated K_i. Double reciprocal plots of 1/v versus 1/ [nicotinamide] at different fixed concentrations of

inhibitor were plotted. Intersection of the lines in the 1/v axis indicates competitive inhibition.

IV. Molecular characterization of the *N*-acetylneuraminate lyase from *Lactobacillus plantarum* WCFS1

1. INTRODUCTION

Sialic acid aldolase or *N*-acetylneuraminate lyase (NAL, EC 4.1.3.3) is a class I aldolase that catalyzes the cleavage of *N*-acetylneuraminic acid (sialic acid, Neu5Ac) to pyruvate and *N*-acetyl-D-mannosamine, with an equilibrium that favors Neu5Ac cleavage. The enzyme plays an important role in the regulation of sialic acid metabolism in bacteria (Schauer, 1982; Traving et al., 1997; Vimr & Troy, 1985). Neu5Ac lyase has been found in pathogenic as well as non-pathogenic bacteria (Aisaka et al., 1991), and in mammalian tissues. Neu5Ac lyase also catalyzes the reverse aldol condensation reaction and has been used in this way to synthesize sialic acid and some of its derivatives from pyruvate and *N*-acetyl-D-mannosamine (Huang et al., 2007; Wong & Whitesides, 1994; Yu & Chen, 2006; Yu et al., 2004). Interest in this aspect of the enzyme's activity has increased with growing appreciation of the role of sialic acid in controlling biomolecular interactions, particularly at the cell surface.

N-acetylneuraminate lyase has previously been cloned from *E. coli* (Aisaka & Uwajima, 1986; Ohta et al., 1986; Ohta et al., 1985), *Clostridium perfringens* A99 (Traving et al., 1997), *Haemophilus influenzae (Lilley et al., 1998)*, *Trichomonas vaginalis (Meysick et al., 1996)* and *Pasteurella multocida* (Li et al., 2008). In addition, X-ray structures of NAL and some mutants from *E. coli* and *H. influenzae* have also been solved (Barbosa et al., 2000; Campeotto et al., 2010; Campeotto et al., 2009; Izard et al., 1994; Joerger et al., 2003; Lawrence et al., 1997). All the *N*-acetylneuraminate lyases cloned up to the present moment come from human pathogens, because of the ability of these species to utilize the carbon sources present in the mucus-rich surfaces of the human body. *Lactobacillus plantarum* is a Gram positive lactic acid bacterium, commensal of the human gastro-intestinal tract, which has a long history of safe use in many fermented sausages and fermented lactic products. *Lactobacillus* has also been used as a probiotic supplement or as an approved food additive that enjoys Generally Recognized as Safe (GRAS) status (Title 21 of the Code of Federal Regulations (21 CFR) and the FDA Office of Premarket Approval lists microorganisms). These characteristics make the *Lactobacillus plantarum* genome ideal for obtaining new recombinant enzymes, such as *N*-acetylneuraminate lyase, which can be safely used in industrial production processes.

Based on the above, this chapter describes the cloning, overexpression and a detailed characterization of a novel *N*-acetylneuraminate lyase (*nanA*) from *Lactobacillus plantarum* WCFS1 (LpNAL), and compared it with that of *Escherichia coli* K-12 Substr. MG1655 (EcNAL) in the same cloning system. The results obtained showed that LpNAL reaches a higher expression level and showed similar catalytic efficiency to EcNAL and to the best NALs previously described. In addition, both enzymes were remarkably thermostable, finding improved stability in the presence of additives. The detailed study of their topology and phylogeny also revealed the presence of four different bacterial NAL groups, and several subgroups.

2. RESULTS AND DISCUSSION

2.1. Amino acid sequence comparison.

The deduced amino acid sequence of the *L. plantarum N*-acetylneuraminate lyase (LpNAL) showed significant identity with those of other bacterial species in the database. Sequence alignment indicates that LpNAL has 60%, 54%, 51% and 38 % amino acid sequence identity with the *N*-acetylneuraminate lyase from *Clostridium perfringens, Trichomonas vaginalis, Haemophilus influenzae* and *E. coli* K-12 (GenBank accessions: Q9S4K9, AAB42182, P44539 and AAC76257) respectively. LpNAL is more closely related to *Haemophilus influenzae* NAL (PDB code: 1F5Z) than to the other crystallized NAL from *E. coli* (PDB code: 1NAL).

In addition, sequence alignment (Figure 4.1) revealed that LpNAL contained conserved residues forming the characteristic active site of the NAL subfamily (Figure 4.1, filled triangles), the catalytic lysine at position 163 (K163), a tyrosine at position 135 (Y135), and the conserved specific substrate (Neu5Ac) binding motif, which includes the GxxGE motif and a group of amino acids (D189, E190 and S206) involved in the carbohydrate-moiety binding. The GxxGE motif, situated between positions 45 to 49 (LpNAL numbering), is involved in the binding of the carboxylate group of the α-keto moiety of the subtrate, and xx are usually S and/or T, respectively. These two last amino acids, together with Y135 and a water

molecule, are involved in the hydrogen-bond network with pyruvate (Barbosa et al., 2000; Lawrence et al., 1997).

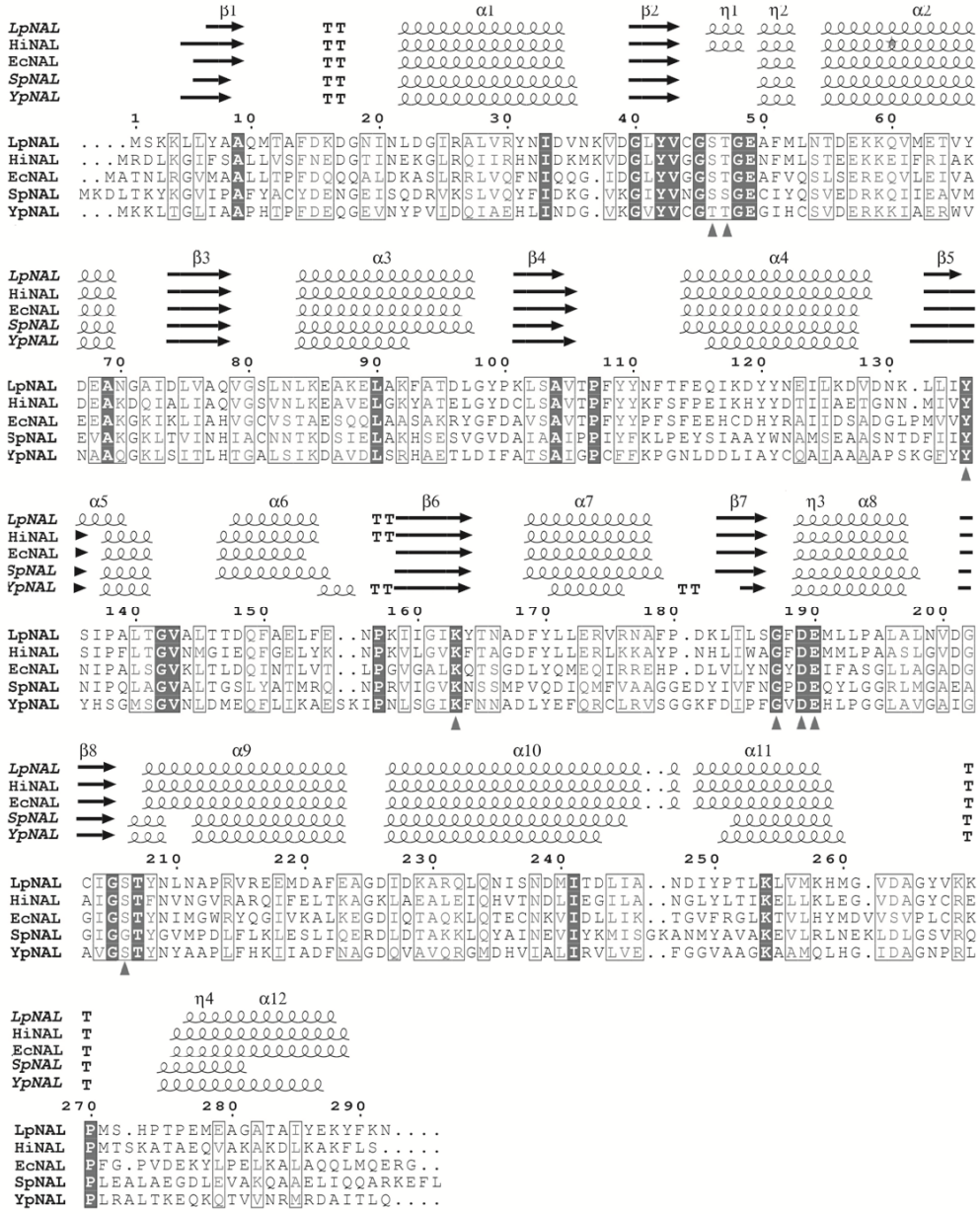

Figure 4.1. *Multiple sequence alignment for L. plantarum WCFS1 (LpNAL) and related N-acetylneuraminate lyases*. ESPript outputs (Gouet et al., 1999) obtained with the sequences from the SWISSPROT databank and aligned with CLUSTAL-W (Thompson et al., 1994). Sequences are grouped according to similarity. The enzyme showed 51% sequence identity with NAL from *H. Influenzae* (GI 162960935)kS, 37% with NAL from *E. coli* K-12 Substr. MG1655 (GI 49175990), 29 % with *S. pneumoniae* (GI 169832377) and 31 % with *Yersinia pestis* (GI 16120353). Residues strictly conserved across NAL enzymes have a dark background. Symbols above blocks of sequences represent the secondary structure, springs represent helices and arrows represent β-strands. The residues forming the active site are indicated by small black triangles.

2.2. Enzymes cloning, expression and purification.

The *nanA* gene from *Escherichia coli* K-12 Substr. MG1655 was inserted into the pET52 3C/LIC vector, a vector which provides His_{10}-tagged recombinant protein, through a Ligation-Independent Cloning system (see Materials and Methods). The DNA sequence of the cloned gene showed no mutations compared to the *nanA* gene sequence reported for *Escherichia coli* K-12 Substr. MG1655 (GenBank accession no. NC_000913.2). The recombinant vector named pEcNAL was used to transform *E. coli* BL21 (DE3) pLysS electrocompetent cells. The clone with the highest expression rate was induced with 0.5 mM IPTG in a 5 L-fermenter at 30 ºC for 6 h with vigorous stirring and oxygenation. The *nanA* gene from *Lactobacillus plantarum* WCFS1 was cloned into pET52-3C/LIC vector as described above, and transformed into BL21 (DE3) pLysS electrocompetent cells. The clone with the highest expression rate was induced with 1 mM IPTG in a 5 L-fermenter at 30ºC for 12 h instead of 6 h, with vigorous stirring and oxygenation, reaching a greater cell culture density. In both cases, the enzymes were almost totally expressed in soluble form under these conditions (Figure 4.2, lane 1 and Figure 4.3, lane 1).

Both, EcNAL and LpNAL, were purified from *E. coli* cells by a three-step procedure consisting of a 100-kDa ultrafiltration and 65 ºC heat-shock steps followed by Ni^{2+} chelating affinity chromatography in a HisTrap FF column. After these three steps (Figures 4.2 and 4.3), the enzymes were pure, as shown in SDS-PAGE (Figure 4.2, line 3 and Figure, 4.3 line 3), with a 11.8-fold purification and a 46% recovery for LpNAL (Table 4.1) and a 2.7-fold purification and 20.1 % recovery for EcNAL (Table 4.2).

In the LpNAL purification, up to 215 mg of Ni^{2+}-column-purified LpNAL could be obtained from 1 L of *E. coli* BL21(DE3)pLys culture, which is 2.6-fold higher than the expression level achieved by the cloned EcNAL (82 mg L^{-1} cell culture) and 2.2-fold higher than the best expression level reported for NAL (94 mg L^{-1} cell culture). LpNAL showed specific activity of 7.65 U/mg for the hydrolysis of Neu5Ac at 37 ºC and pH 7.0 (Table 4.1).

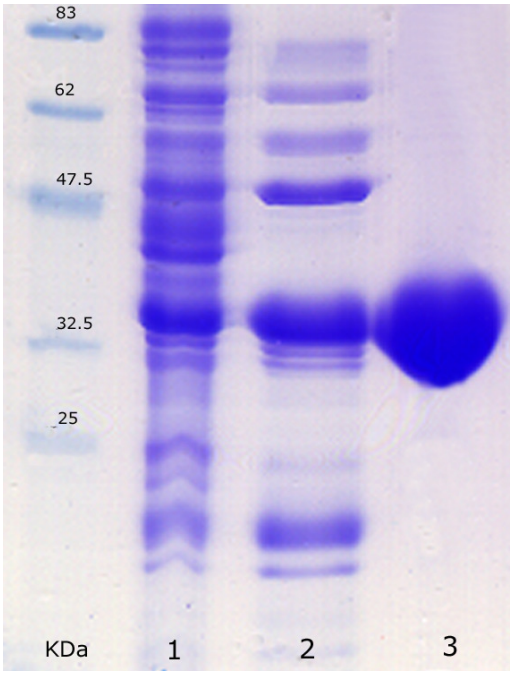

Figure 4.2. *SDS-PAGE of the LpNAL gene product obtained after 12 hours IPTG induction*. Each lane contained 20 µg of protein. Lane M: molecular weight standards (New England Biolabs: P7708S). Lane 1: cell extract after 100 kDa tangential ultrafiltration. Lane 2: cell extract after heat-shock step . Lane 3: LpNAL after HisTrap column, purified protein is about 37 kDa.

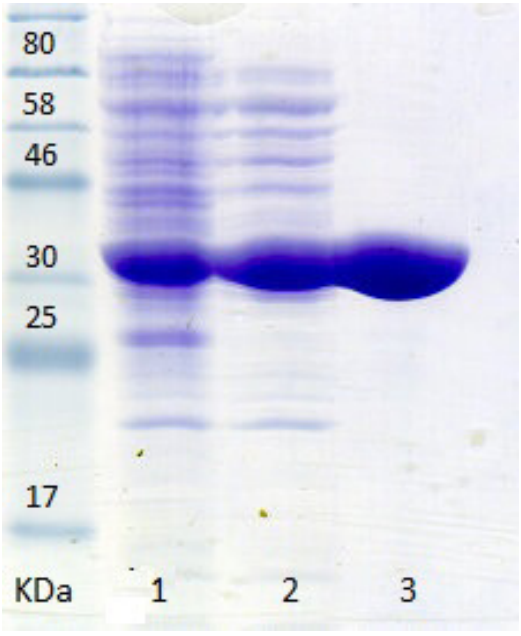

Figure 4.3. *SDS-PAGE of the EcNAL gene product obtained after 6 hours IPTG induction*. Each lane contained 15 µg of protein. Lane M: molecular weight standards (New England Biolabs: P7708S). Lane 1: cell extract after 100 kDa tangential ultrafiltration. Lane 2: cell extract after heat-shock step. Lane 3: EcNAL after HisTrap column, purified protein is about 37 kDa.

Table 4.1. *Purification of the recombinant LpNAL expressed in Rosetta 2(DE3)pLysS*

Purification Step	Volume (mL)	Total Activity[¶] (U)	Total protein (mg)	Specific activity (U/mg)	Purification (*x*-fold)	Yield (%)
Crude extract[†]	5060	14248	21962	0.65	1	100
100 kDa Tangential Ultrafiltration	540	13388	7744	1.73	2.6	93.9
Heat-shock	516	11548	3480	3.32	5.1	81
His-trap affinity chromatography	283.5	6592	861	7.65	11.8	46.3

[¶]The activity was assayed in the standard spectrophotometric reaction medium.

[†]Crude extract represents the volume obtained after lysis and centrifugation of cell debris, corresponding to a 4 L culture broth, after 12 hours induction. See Material and Methods for details.

Table 4.2. *Purification of the recombinant EcNAL expressed in Rosetta 2(DE3)pLysS*

Purification Step	Volume (mL)	Total Activity[¶] (U)	Total protein (mg)	Specific activity (U/mg)	Purification (*x*-fold)	Yield (%)
Crude extract[†]	2335	45254	8450	5.35	1	100
100 kDa Tangential Ultrafiltration	312	35063	8205	4.28	0.8	77.5
Heat-shock	303	18651	2350	7.94	1.5	41.2
His-trap affinity chromatography	38	9114	647	14.08	2.6	20.1

[¶]The activity was assayed in the standard spectrophotometric reaction medium

[†]Crude extract represents the volume obtained after lysis and centrifugation of cell debris, corresponding to a 4 L culture broth after 6 hours induction. See Material and Methods for details.

The molecular weight of purified LpNAL protein was determined by gel filtration (132 kDa), 12 % SDS-PAGE (about 36 kDa, Figure 4.2, lane 4) and by

HPLC/ESI/ion trap (37.31 kDa), confirming the homotetrameric nature of the novel LpNAL protein. As it had been described in the bibliography, EcNAL protein was also a homotetramer, showing a molecular weight of 146 kDa by gel filtration, about 37 KDa by SDS-PAGE (Figure 4.3, lane 3), and 37.17 kDa when determined by HPLC/ESI/Ion trap.

2.3. Biochemical characterization of recombinant EcNAL and LpNAL.

The optimum pH for the hydrolysis of Neu5Ac for EcNAL and LpNAL was assayed in a broad pH range (Figure 4.4), using discrete (sodium acetate, sodium phosphate, glycine) and continuous (Citric-HEPES-CHES) buffers. The activity of both enzymes was pH-dependent, being active over a broad pH range, from pH 6.0 to 8.0 in the hydrolytic direction. The optimum pH of both enzymes was around pH 7-7.3, which is similar to values described for other NALs, such as those from *E.coli* K-12 and C600 (Aisaka et al., 1991; Ferrero et al., 1996), the native and the recombinant NAL from *C. perfringens* (Kruger et al., 2001; Nees et al., 1976) and the recombinant NAL from *P. multocida* (Li et al., 2008). However, there exist some differences in the shape of the pH curve depending on the buffers used, suggesting that some buffers are more adequate for hydrolytic activity than others. Continuous buffer Citric-HEPES-CHES lowers LpNAL and EcNAL activity at acid pHs with respect to acetate and sodium phosphate buffer, but not at basic pHs. This result led to the conclusion that the activity of both recombinant NALs were not only pH-dependent but also buffer dependent.

The optimal temperature of LpNAL and EcNAL could not be fully characterized by the spectrophotometric method due to its effect on the coupled enzyme used in the assay (L-Lactate dehydrogenase), whose activity drops quickly above 45 ºC (Figure 4.5, dotted line open tringle). Thus, LpNAL and EcNAL activity rises from 10 ºC to 45 ºC (Figure 4.5, filled circle and square, respectively). To further study the behavior of NALs in relation to temperature, thermostability studies were carried out.

LpNAL showed a remarkable thermal stability compared to other described NALs (Aisaka et al., 1991), and maintained 80 % of cleavage activity after 48

hours at 60 ºC (Figure 4.6 A). At higher temperatures (70 ºC), activity decreased to less than 15 % in 5 hours.

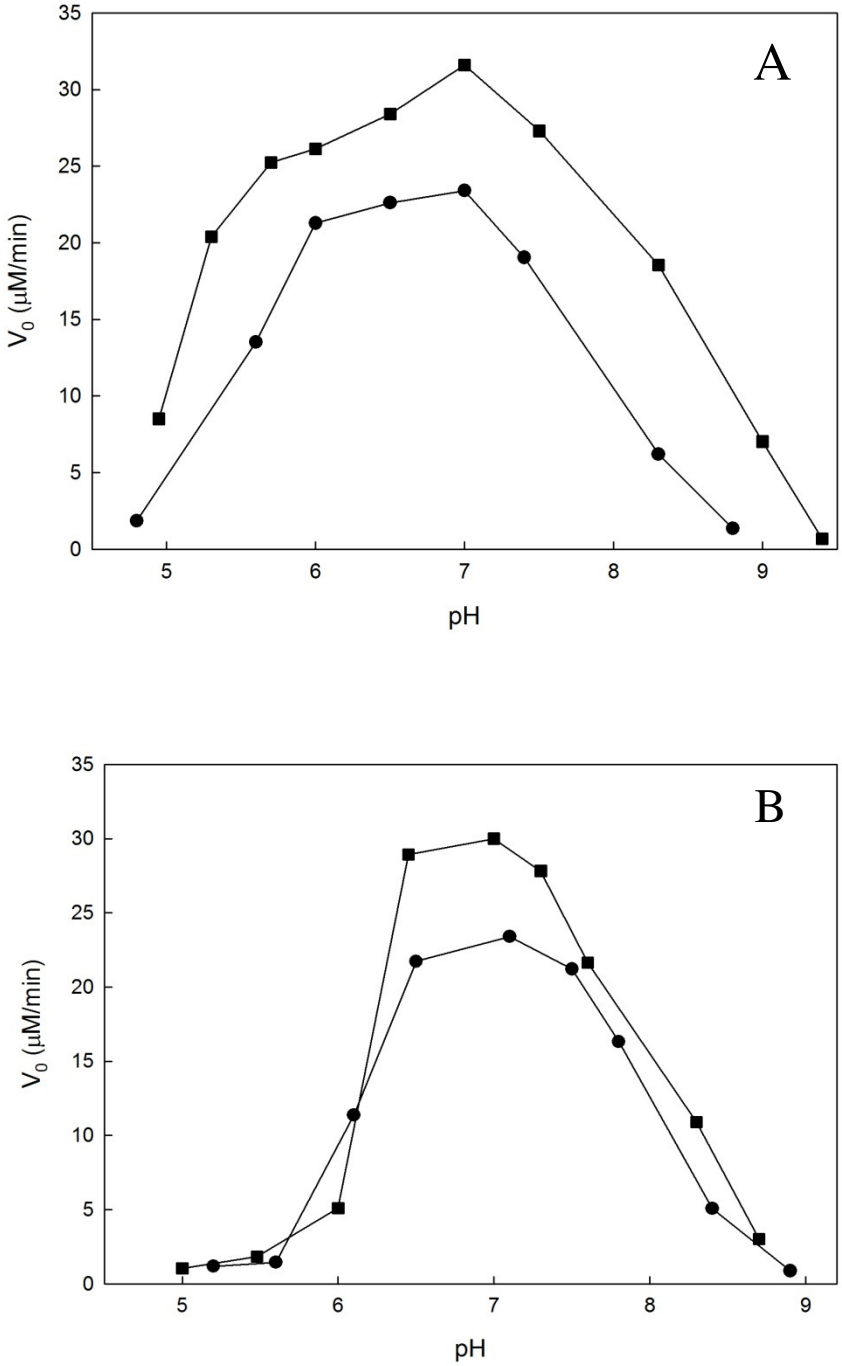

Figure 4.4. *Effect of pH on LpNAL (●) and EcNAL (■) activity.* A) Optimum pH with discrete buffers. Assay conditions at 37 ºC were 1.5 µg enzyme, 10 mM Neu5Ac, 0.5 U/ml LDH, 150 µM NADH. Buffers used: 100 mM sodium acetate (pH 4.5-5.7), 100 mM sodium phosphate (6-7.5), 100 mM glycine-NaOH (8.0-9.5). B) Optimum pH with continuous Citric-HEPES-CHES buffers. Assay conditions at 37 ºC were 1.5 µg enzyme, 10 mM Neu5Ac, 0.5 U/mL LDH, 150 µM NADH.

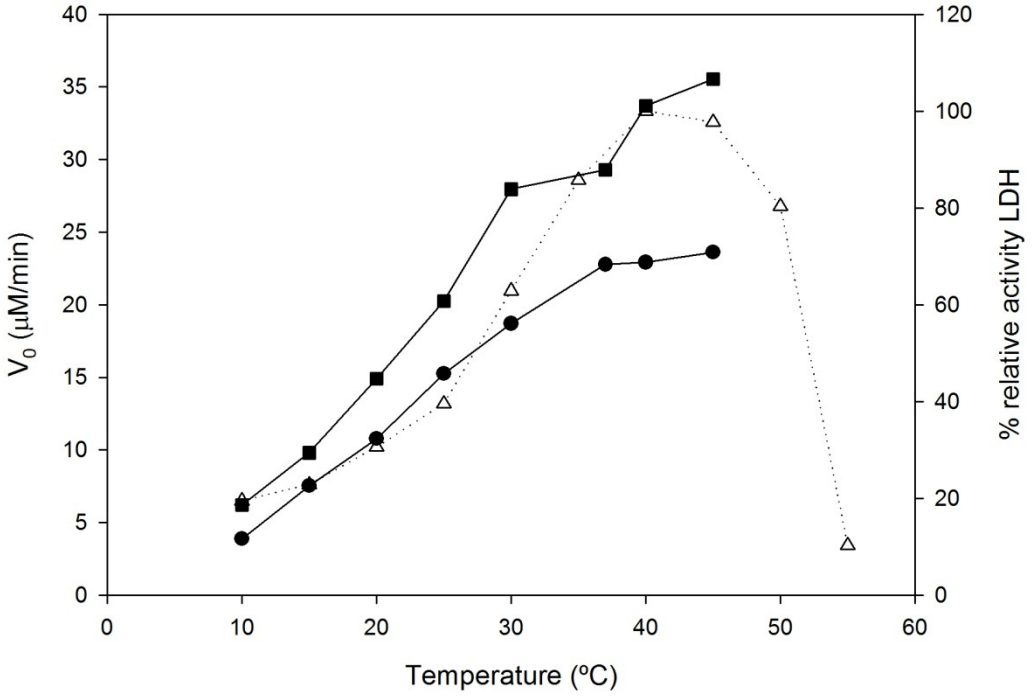

Figure 4.5. *Temperature profile of LpNAL* (●)*, EcNAL* (■) *and LDH* (Δ). Assay conditions at 37 ºC were 1.5 µg enzyme, 10 mM Neu5Ac, 0,5 U/mL LDH, 150 µM NADH in sodium phosphate 100 mM pH 7.3.

Recombinant EcNAL also showed good thermostability, maintaining 33% of cleavage activity after 48 h at 60 ºC, and 60% activity after 5 and 2 hours at 70 and 80 ºC, respectively (Figure 4.6 B). This inactivation of LpNAL and EcNAL at high temperatures was minimized up to 8-fold by the use of protein stabilizers, such as ammonium sulfate (Figure 4.7 A, open triangles) and hydroxy-ectoine (Figure 4.7 B filled circles). The use of stabilizers increased from 4 to more than 8 hours the half-life of LpNAL at 70 ºC (Figure 4.7 A). Ammonium sulfate produces the same effect in EcNAL increasing half-life at 80 ºC from 1 to 3-4 hours.

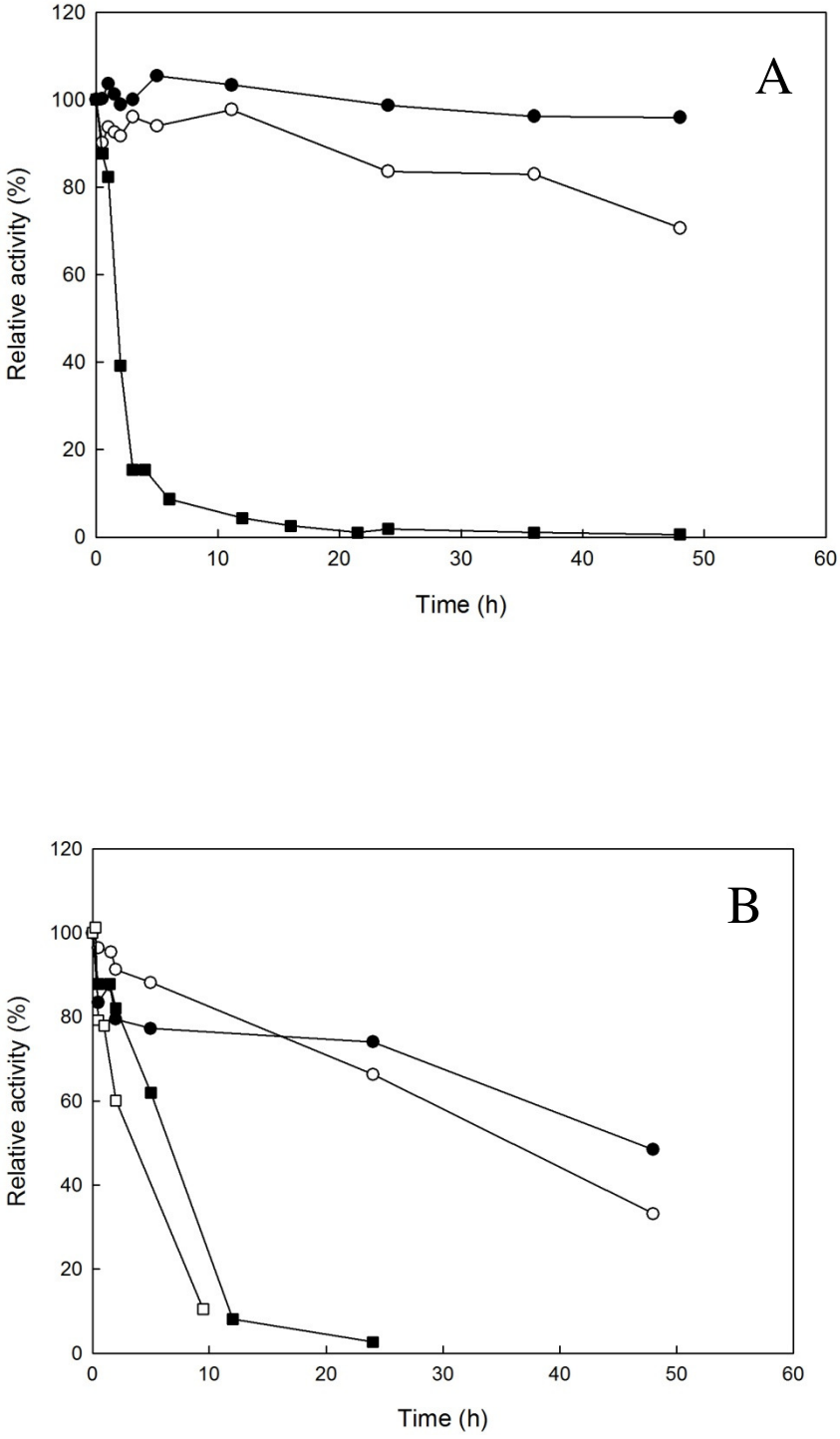

Figure 4.6. *Thermostability assays.* A) LpNAL. B) EcNAL. Aliquots of enzyme incubated at different temperatures [50 ºC (●), 60 ºC (○), 70 ºC (■) and 80 ºC (□)], were removed and relative activity was measured using the enzyme-coupled spectrophotometric assay at different times. Assay conditions at 37 º C were 2.5 µg enzyme, 10 mM Neu5Ac, 0.5 U/mL LDH, 150 µM NADH, in 20 mM sodium phosphate pH 7.0.

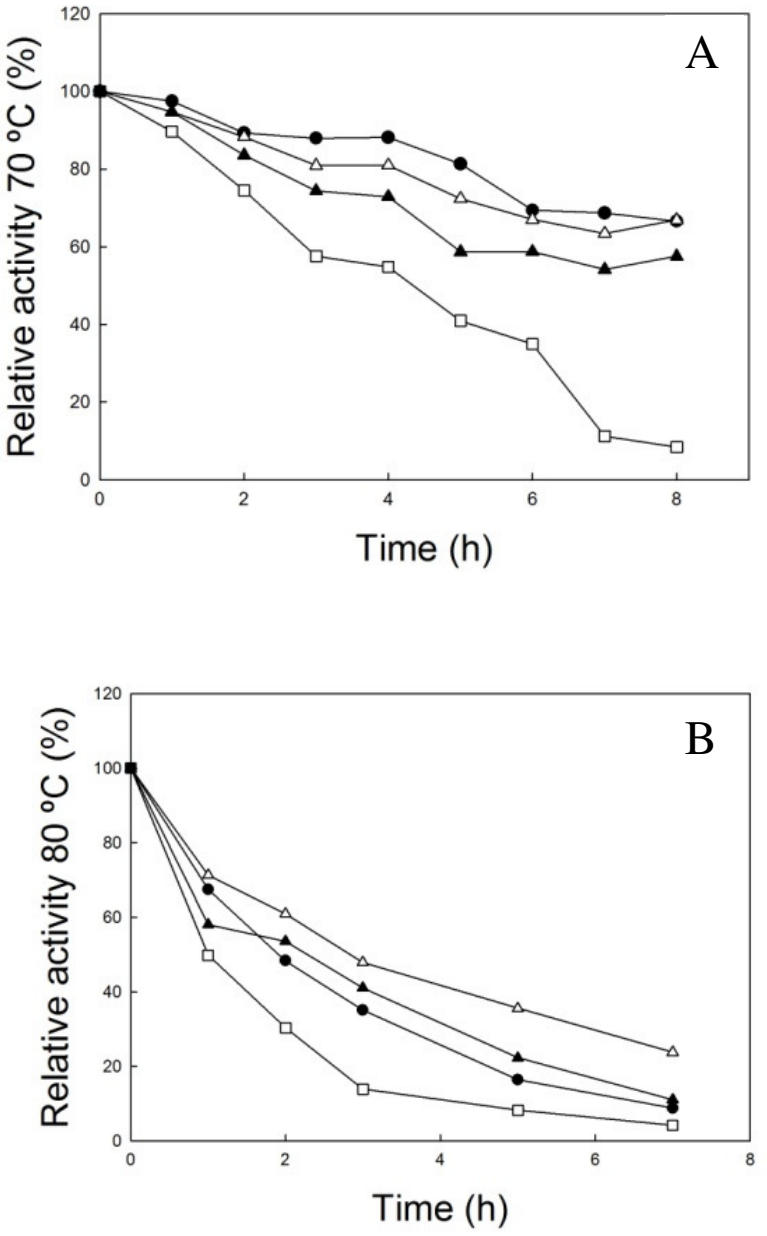

Figure 4.7. *Effect of additives on the relative activity of LpNAL incubated at 70 ºC (A) and EcNAL incubated at 80 ºC (B).* 20 mM Phosphate buffer without any of the following additives (□), and in the same buffer with the following additives: 1 M hydroxy-ectoine (●), 0.4 M ammonium sulfate (▲) and 1 M ammonium sulfate (Δ), Aliquots were removed every hour and measured spectrophotometrically using the enzyme-coupled assay at 37 º C.

This thermal stability was further confirmed by a thermal melt assay (see Materials and Methods section). EcNAL showed a melting temperature (T_m) value of 86.4±0.1 ºC in MilliQ® water (Figure 4.8 B, open circles), 16.4 ºC above the T_m obtained for LpNAL in the same conditions (71.0±0.1 ºC) (Figure 4.8 A, open circles). The presence of a buffered solution (100 mM sodium phosphate pH 7.0) stabilized LpNAL, raising the T_m value up to 76.5±0.2 ºC (Figure 4.8 A, open squares). However, this effect is not evident in EcNAL, where the T_m in a buffered solution (100 mM sodium phosphate pH 7.0) (86.1±0.1 ºC) was very similar to the T_m calculated in MilliQ® water (Figure 4.8 B, open squares). The use of the above mentioned protein stabilizers (1M hydroxy-ectoine and 0.4 M and 1 M ammonium sulfate) increased T_m in both enzymes. While hydroxy-ectoine raised in T_m of LpNAL from up to 78.9±0.1 ºC (Figure 4.8 A, filled circles), EcNAL was more stable in ammonium sulfate than in hydroxy-ectoine, rising in the T_m up to 91.23 ºC (Figure 4.8 B, open triangles). These results corroborate the data obtained by the thermostability assay, in which LpNAL incubated at 70 ºC during 8 hours maintained more relative activity in the presence of 1 M hydroxyl-ectoine (Figure 4.7 A, filled circles), whereas the best relative activity for EcNAL was obtained with 1 M ammonium sulfate. (Figure 4.8 B, open triangles).

Thermal melt curves were also used to understand the pH profile described above (Figure 4.4). Melting curves were calculated for LpNAL and EcNAL in different buffer and pH conditions ranging from pH 5.0 to 11.0, and the ΔT_m at each condition was plotted with respect to Milli Q water (Figure 4.9). The effect observed was more evident in LpNAL, where, as previously described buffered solutions tend to stabilize LpNAL, which showed high thermal stability from pH 6.0 to 10.0 with the T_m raising to ~74-76.5 ºC, this is, increasing up to 5 ºC compared with T_m in Milli Q water (Figure 4.9, A). Conversely, thermal stability decreased in buffered solutions below pH 5.5 or above pH 10.0, for instance, T_m at pH 10.5 was 64±0.1 ºC, falling 7 ºC compared with T_m of Milli® Q water (Figure 4.9 A). In the case of EcNAL, calculated T_m in Milli Q water was very similar from pH 6.0 to pH 8.0, but decreased dramatically at pHs below 5.5 and above 9.5, up to 9 ºC in glycine buffer pH 11.0 and 19 ºC in citric-HEPES-CHES buffer pH 5.0 (Figure 4.9 B). These results agreed with the pH-profile previously described in Figure 4.6.

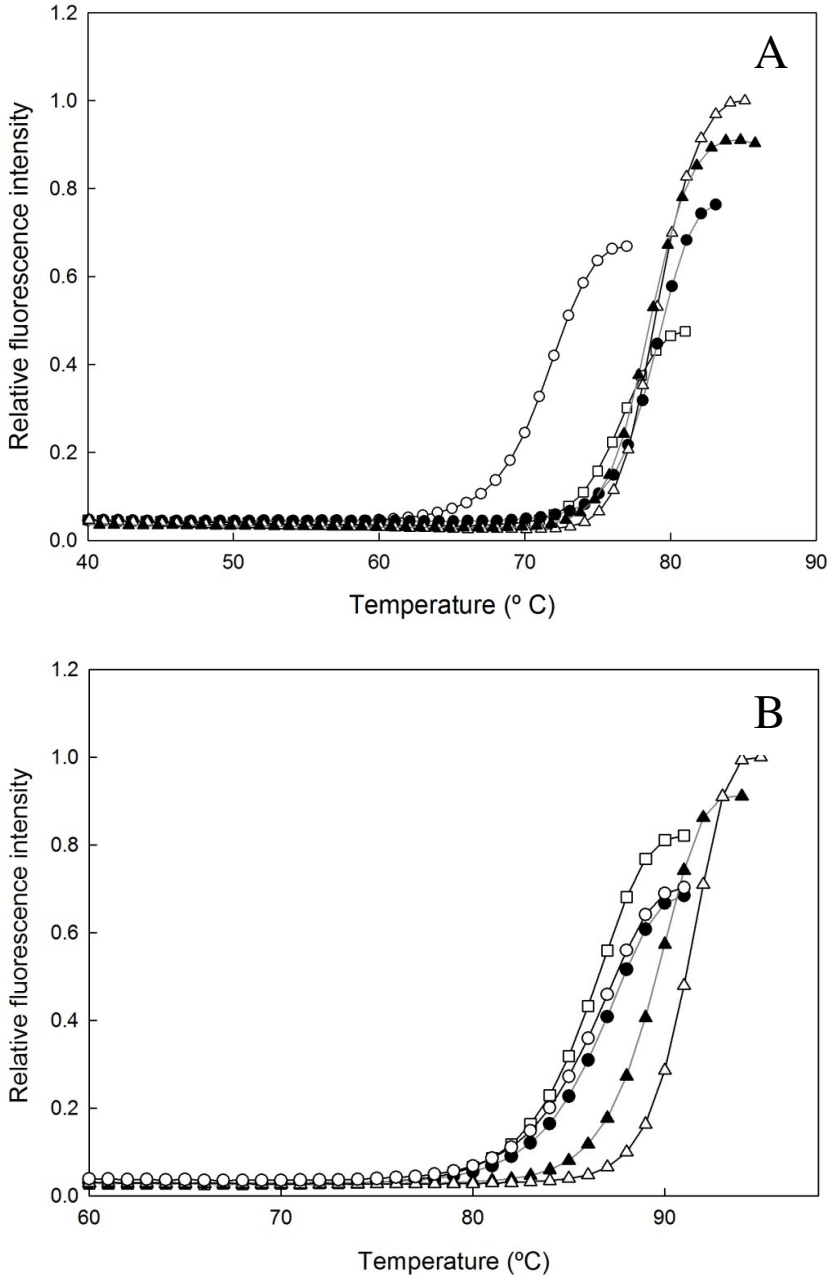

Figure 4.8. *Study of thermal stability of LpNAL (A) and EcNAL (B).* Melting temperature curves of purified enzyme (1 µg) were obtained in Milli Q® water (○), in 100 mM sodium phosphate buffer pH 7.0 (□) and in the presence of additives such as 1 M hydroxy-ectoine (●), 0.4 M ammonium sulfate (▲) and 1 M ammonium sulfate (Δ), in the above buffer. Assays were performed in a real time PCR apparatus with 10X Sypro Orange.

NAL stability towards pH was not only pH-dependent but also buffer-dependent (Figure 4.9), since different buffers, discrete buffers (Figure 4.9, black bars) or continuous buffers (Citric-HEPES-CHES; Figure 4.9, grey bars), had different stabilizing effects on the enzyme. This results have not been described for NAL, and the T_m values obtained are summarized in Table 4.3

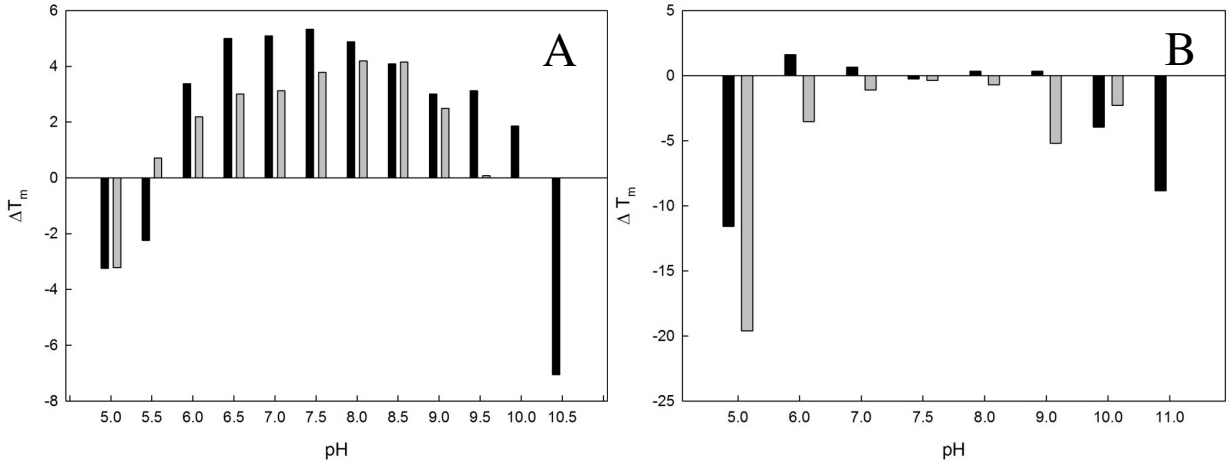

Figure 4.9. *Effect of different pHs on melting temperatures of LpNAL (A) and EcNAL (B).* The differences in *Tm* were calculated by subtracting the value obtained in MilliQ® water. Black bars: 100 mM discrete buffers (sodium acetate for pHs 5.0- 5.5, sodium phosphate for pHs 6.0-7.5, TRIS-HCl for pHs 8.0-9.0, glycine for pHs 9.5-10.0, CAPS for pH 10.5); grey bars: 100 mM continuous buffers (Citric-HEPES-CHES).

2.4. Kinetic parameters

The K_M for Neu5Ac cleavage in LpNAL (1.8 ± 0.1 mM) was lower than the K_M for the recombinant EcNAL (2.8±0.2 mM) and lower than the reported values for *E. coli* NAL (2.5± 0.3 mM) and for *P. multocida* (4.9 ± 0.7 mM) (Table 4.4) (Li et al., 2008). In addition, reported K_M for *C. perfringens* (2.8-3.2 mM) (Kruger et al., 2001; Schauer et al., 1999) was also higher than that for the LpNAL enzyme. This LpNAL value, together with the k_{cat}/K_M value obtained (5.6 mM^{-1} s^{-1}), point to a similar catalytic efficiency for LpNAL toward hydrolysis, compared with other NALs reported previously for the same substrate (from 3 to 4 mM^{-1} s^{-1}) (Li et al., 2008).

Table 4.3. *Melting temperatures for EcNAL and LpNAL in different conditions.*

pH	Buffer composition	*Tm* EcNAL (ºC)	*Tm* LpNAL (ºC)
Milli Q water		86.4	71.5
5.0	Acetate	75.3	68.2
5.5	Acetate	—	69.3
6.0	Sodium phosphate	88.0	74.9
7.0	Sodium phosphate	87.0	76.6
7.5	Sodium phosphate	86.2	76.8
8.0	Sodium phosphate	82.8	76.0
8.0	TRIS-HCl	86.7	76.4
8.5	TRIS-HCl	—	75.6
9.0	TRIS-HCl	86.6	74.5
9.0	Glycine	86.7	73.8
9.5	Glycine	—	74.6
10.0	Glycine	82.4	73.4
10.0	CAPS	—	69.4
10.5	CAPS	—	64.4
11.0	Glycine	77.5	
5.0	Citric-HEPES-CHES	69.4	68.3
5.5	Citric-HEPES-CHES	—	72.2
6.0	Citric-HEPES-CHES	82.8	73.7
6.5	Citric-HEPES-CHES	—	74.5
7.0	Citric-HEPES-CHES	85.3	74.6
7.5	Citric-HEPES-CHES	86.0	75.3
8.0	Citric-HEPES-CHES	85.7	75.7
8.5	Citric-HEPES-CHES	—	75.6
9.0	Citric-HEPES-CHES	81.2	74.0
10.0	Citric-HEPES-CHES	84.1	71.6
Protein stabilizers	0.4 M $(NH_4)_2SO_4$	89.5	78.4
	1 M $(NH_4)_2SO_4$	91.2	79.1
	1M Hydroxy-ectoin	86.5	78.9

As expected, recombinant EcNAL has a similar K_M value for Neu5Ac than the reported EcNAL (Li et al., 2008), however, its calculated k_{cat}/K_M is slightly higher, probably due to the cloning in a different vector.

Table 4.4. *Kinetic parameters of recombinant LpNAL, EcNAL and other previously described NALs.*

Enzymes	LpNAL[§]	EcNAL[§]	EcNAL[¶]	PmNAL[¶]	CpNAL[¥]
K_M (mM)	1.8±0.1	2.8±0.3	2.5±0.3	4.9±0.7	3.2
k_{cat} (s^{-1})	10.18	17.00	10.0	14.7	
k_{cat}/K_M (mM^{-1} s^{-1})	5.6	5.8	4	3	

[§]The activity was assayed by spectrophotometric method described in Material and Methods.

[¶]Data taken from (Li et al., 2008).

[¥]Data taken from (Kruger et al., 2001)

2.5. Structural and topological analysis.

The 3D structure of crystallized *H. influenzae* NAL (HiNAL) (PDB code: 1F5Z, 51 % identity) (Barbosa et al., 2000) was selected as a template by Geno 3D (Combet et al., 2002) to create an LpNAL model (Figure 4.10). The modeled enzyme shows the typical $(\beta/\alpha)_8$-barrel (Figure 4.10 B), as is usual in the NAL subfamily, which includes NAL, dihydrodipicolinate synthethase (DHDPS), D-5-keto-4-deoxyglucarate dehydratase (KDGDH), trans-o-hydroxybenzylidene-pyruvate hydratase-aldolase (HBPHA) and other related enzymes (Barbosa et al., 2000). These enzymes share a common structural framework, but catalyze different reactions in separate biochemical pathways. Within the subfamily, NAL catalyses the aldol cleavage of Neu5Ac to form ManNAc and pyruvate via a Schiff base intermediate, as mentioned above.

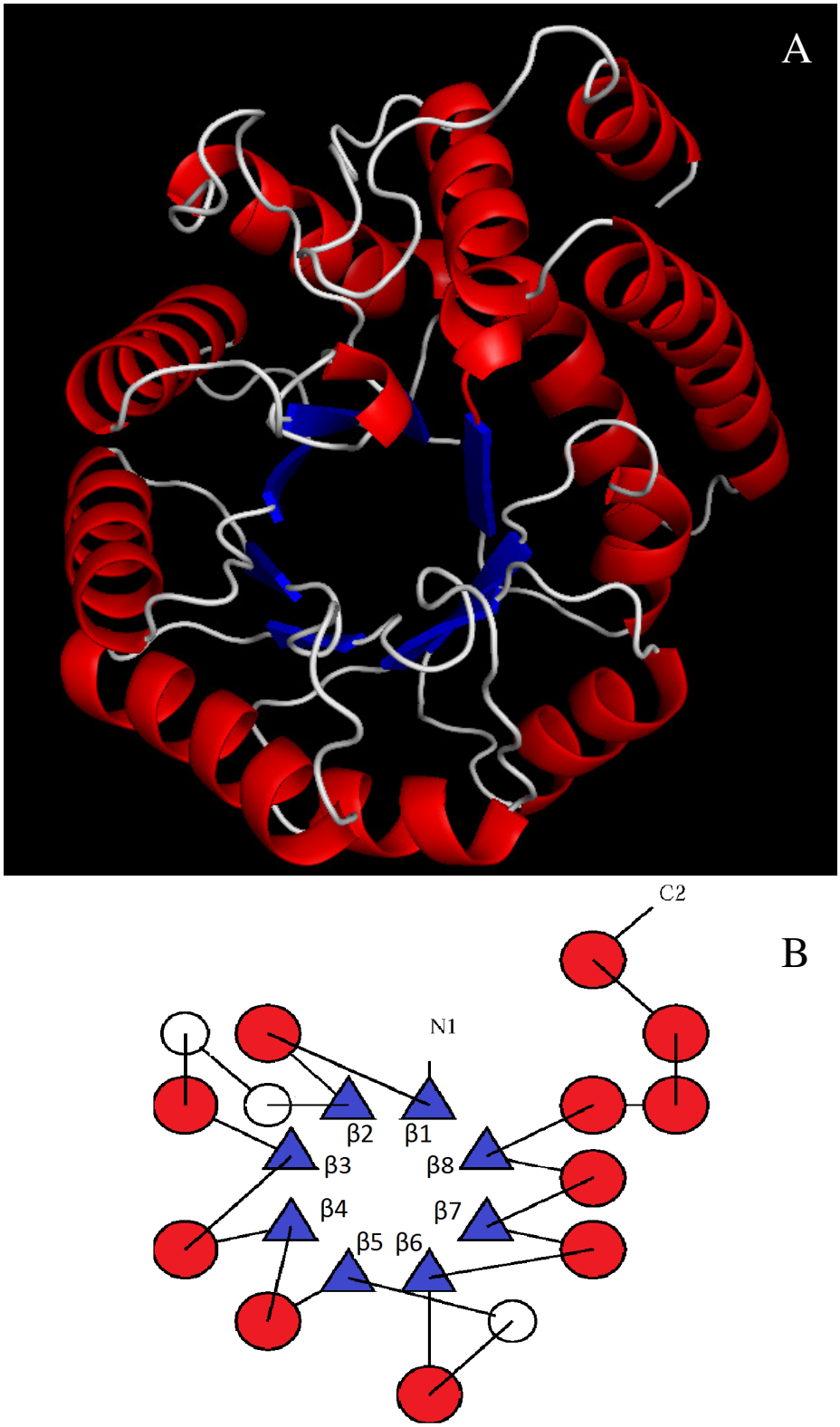

Figure 4.10. *Schematic representation of LpNAL ternary structures.* (A) 3D modeled structure of the monomeric LpNAL. (B) Topology diagram of LpNAL. Circles represent α-helices, and β-strands are represented by triangles. White circles represent small or 3_{10} helices in the structures. The diagrams were made using TOPS program (Michalopoulos et al., 2004).

The fact that Geno 3D chooses HiNAL (PDB code: 1F5Z) (Barbosa et al., 2000) as template instead of EcNAL (PDB code: 1NAL) (Izard et al., 1994) was also due to its higher sequence identity (Figure 4.1), probably indicating a different phylogenetic origin. To test this hypothesis a phylogenetic analysis was carried out including other putative NAL sequences found in the databases (Figure 4.11). Distribution of the putative NAL protein sequence is curiously limited among bacteria. Interestingly, apart from a few aquatic bacteria (*Photobacterium profundum, Pseudoalteromonas haloplanktis, Shewanella pealeana, Psychromonas and Vibrio sp.*), the NAL gene is only present in commensal or pathogenic bacteria, related with human (Almagro-Moreno & Boyd, 2009). Based on this analysis, four structural groups of NALs were clear (Figure 4.11).

The first group, included enzymes from Gram-negative genera, *Haemophilus*, *Actinobacillus*, *Pasteurella,* as well as Gram-positive genera, *Lactobacillus, Clostridium, Staphylococcus* and *Mycoplasma,* and also Fusobacteria (Figure 4.11; see also Figure 4.13). Group 2 (Figure 4.11) includes NAL sequences from *E. coli, Shigella spp., Salmonella enterica,* which all are human gastrointestinal pathogens and have high sequence identities (~ 90-100 %) (Figure 4.14). *Streptococcus* genera, some species of *Lactobacillus* (*L. sakei*), *Clostridium* (*C. bolteae, C. hylemonae),* and other human gut commensal such as *Ruminococcus gnavus* or *Dorea formicigenerans* make up group 3 Fusobacteria (Figure 4.11; see also Figure 4.15). Finally, group 4 is formed by NAL proteins with low sequence identity from members of the family Vibrionaceae, Shewanelaceae, Psychromonadaceae, Pseudoalteromonaceae and some species of genera *Bacteroides, Parabacteroides* and *Capnocytophaga* Fusobacteria (Figure 4.11; see also Figure 4.16, 4.17 and 4.19). These four groups agree with the phylogenetic analysis of NAL sequences (Almagro-Moreno & Boyd, 2009), which divided NALs into four lineages (named I, II, III and IV), which corresponds to the groups 1 to 4 described in this thesis. However, taking into account this analysis, it was not possible to clearly understand the heterogeneity of group 4. In order to clarify this, the phylogenetic relationships between the NAL sequences used above and the active center residues (Figure 4.11, top left. See also Figure 4.12) were also analysed. Three blocks of the active center were considered, the carboxylate-binding zone (sequence GxxGE), the sugar-binding zone (sequence GxDE) and the

aldol-cleavage zone (sequences KxT/Sx and xxG/ST). Groups 1 and 2 are closely related in the active center sequence, with just small changes (1 or 2) in the sequence.

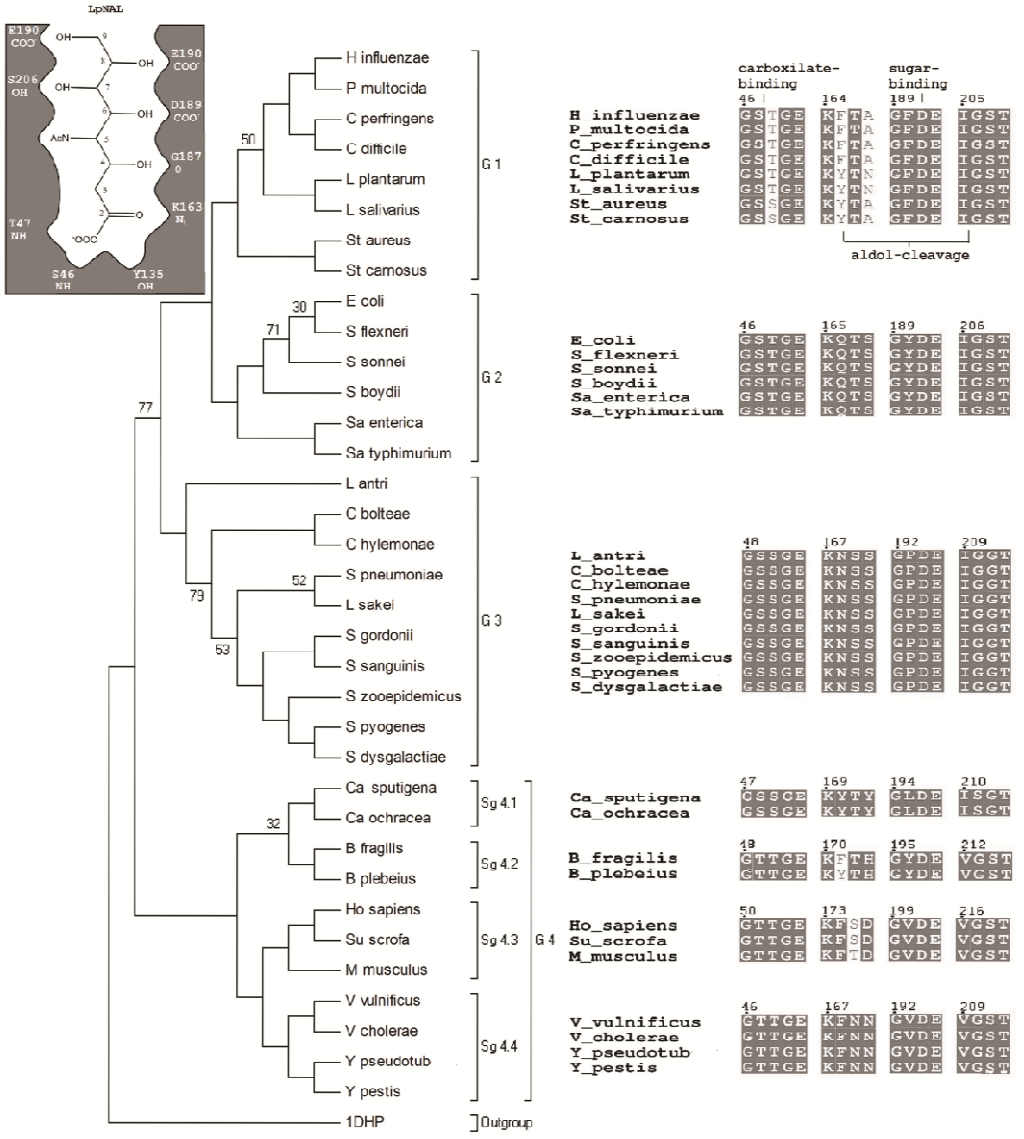

Figure 4.11. *Phylogenetic analysis of the bacterial NAL subfamily***.** Bacterial NALs used in this study (see text for details) are phylogenetically divided into 4 groups. *E. coli* Dihydrodipicolinate synthethase (PDB code: 1DHP) was used as outgroup. Only bootstrap values below 95 are shown. The phylogenetic tree was constructed by Mega 4.0 (Tamura et al., 2007). Details of ESPript alignments outputs (Gouet et al., 1999) are shown on the right side of the figure. An adapted drawing of the NAL active site (Barbosa et al., 2000) is shown in the upper left corner of the figure in order to clarify the meaning of the blocks (LpNAL numbering). H: *Haemophilus*, P: *Pasteurella*, C: *Clostridium*, L: *Lactobacillus*, St: *Staphylococcus*, E: *Escherichia*, S: *Shigella*, Sa: *Salmonella*, S: *Streptococcus*, S. pseudotub: *Streptococcus pseudotuberculosis*, Ca: *Capnocytophaga*, B: *Bacteroides*, Ho: *Homo,* Su: *Sus,* M: *Mus,* V: *Vibrio*, Y: *Yersinia*, G: group, Sg: subgroup.

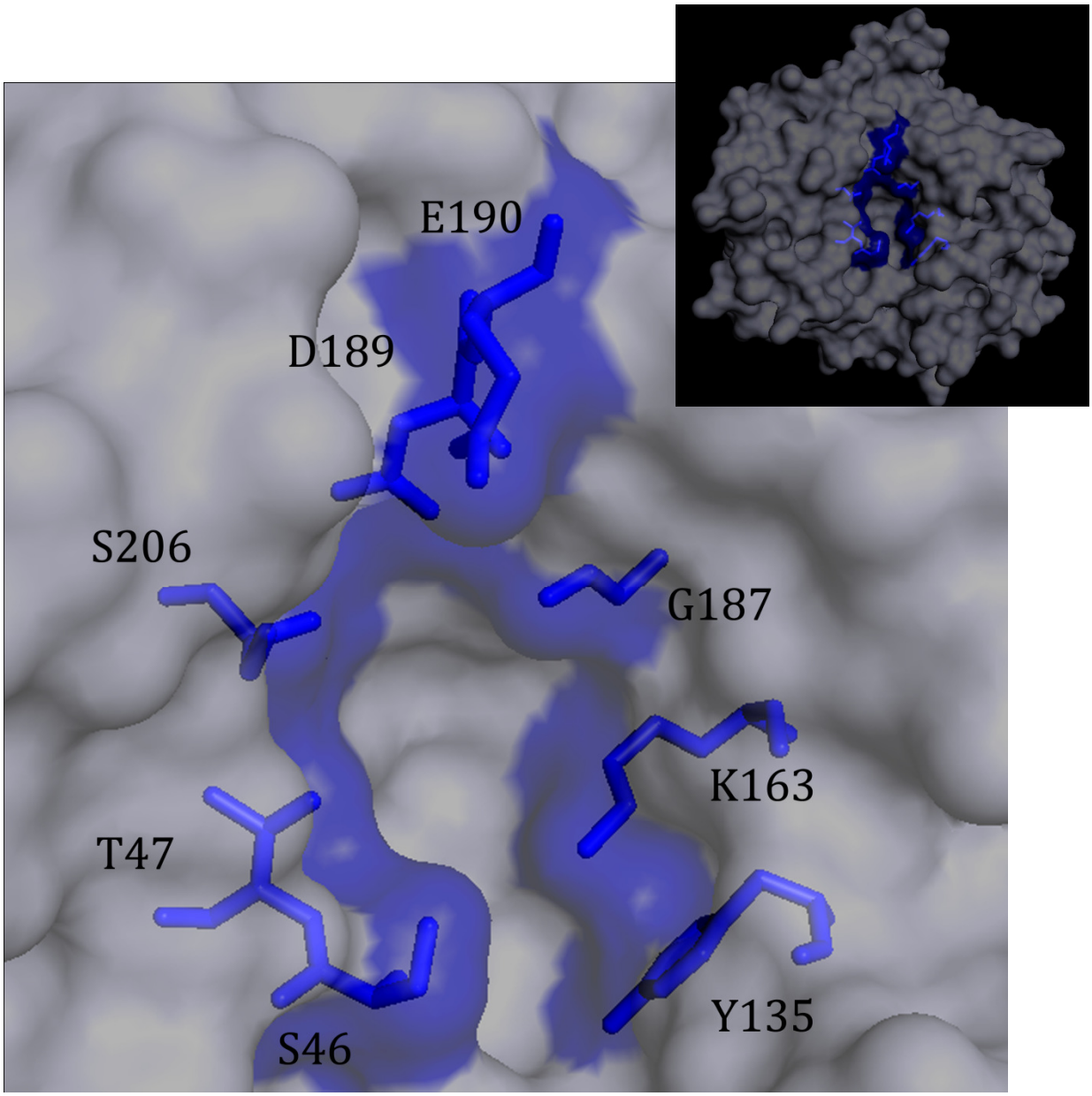

Figure 4.12. *Detail of the active center of LpNAL.* Residues responsible for the binding of Neu5Ac are coloured in blue with LpNAL numbering. Figures were rendered using PyMOL (Schrodinger, 2010).

However, although related to group 1 and 2, group 3 has its own fully conserved active center signature (GSSGE/KNSS/GFDE/IGGT) (Figure 4.11, right; see also Figure 4.15). Finally, in group 4, the diversity is more evident in the active center sequence, in which four clear subgroups could be described: subgroup 4.1, which includes *Capnocytophaga* sp. (Figure 4.16); subgroup 4.2, which includes *Bacteroides* sp. (Figure 4.17); subgroup 4.4 (Figure 4.19), which includes *Vibrio* sp. and *Yersinia* sp. When animal NAL sequences were considered (Figure 4.18), they clustered together within group 4, forming subgroup 4.3, but not a different clade (Almagro-Moreno & Boyd, 2009). Subgroup 4.4 is closely related to human NAL, as revealed by the similarities between both active center sequences (GTTGE/KFxx/GVDE/VGST), indicating lateral gene transfer between bacteria and humans. This was previously described for human NAL (Andersson et al., 2001), but no direction of the transfer was assigned. This new phylogenetic and sequence analysis supports the hypothesis of transfer of NAL from group 4 bacteria to mammals.

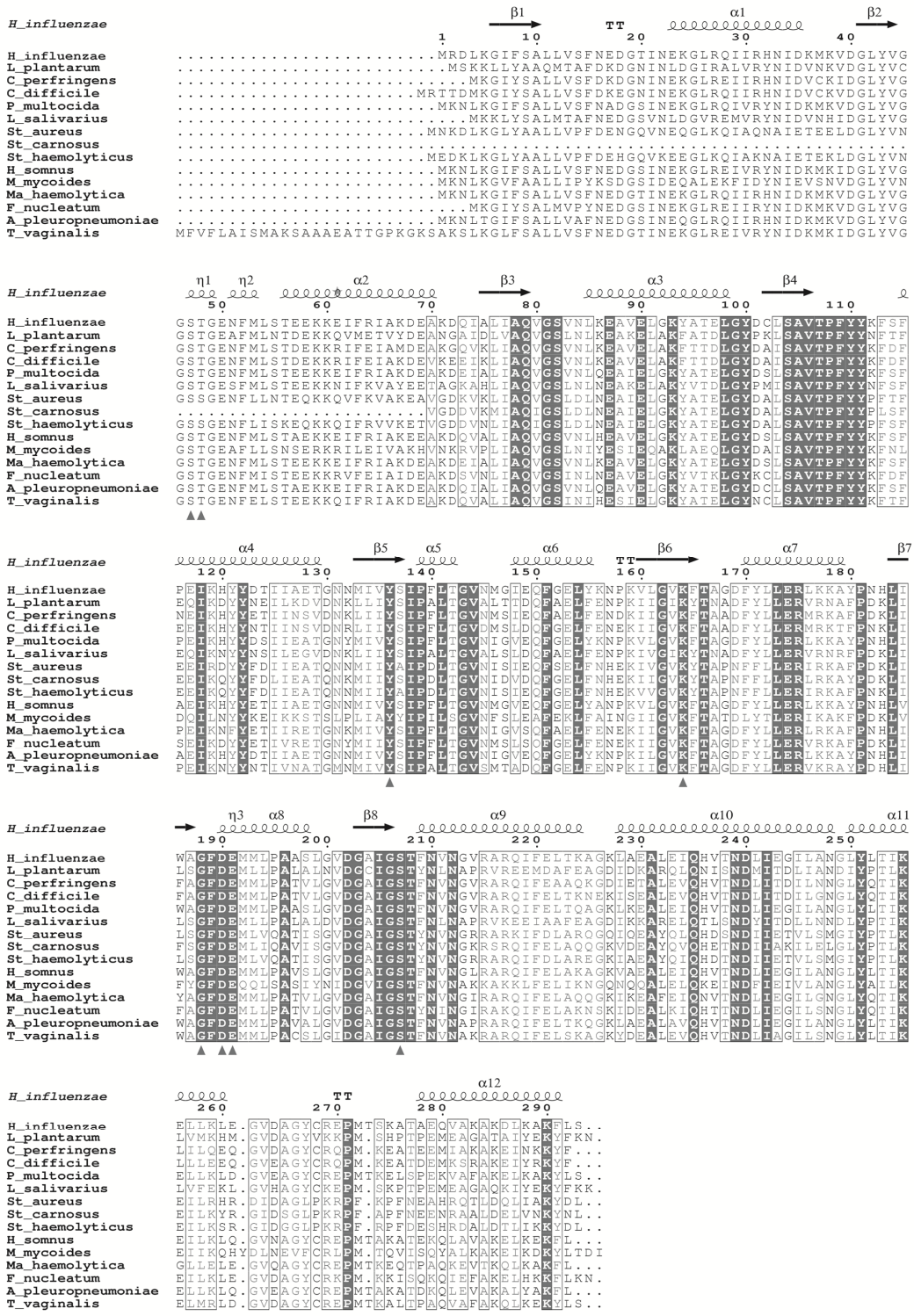

Figure 4.13. *Multiple sequence alignment for NALs belonging to group 1.* The sequences from the SWISSPROT databank were aligned with CLUSTAL-W (Thompson et al., 1994) and with ESPript (Gouet et al., 1999). Residues strictly conserved across Group 1 NAL enzymes have a dark grey background. Symbols above blocks of sequences represent the secondary structure of *Haemophilus influenzae*, corresponding to a crystallized structure (PDB: 1F5Z). Springs represent helices and arrows represent β-strands. The residues forming the active site are indicated by small triangles. H: *Haemophilus,* P: *Pasteurella,* C: *Clostridium,* L: *Lactobacillus,* St: *Staphylococcus,* M: *Mycoplasma,* Ma: *Mannheimia,* F: *Fusobacterium,* A: *Actinobacillus,* T: *Trichomonas.*

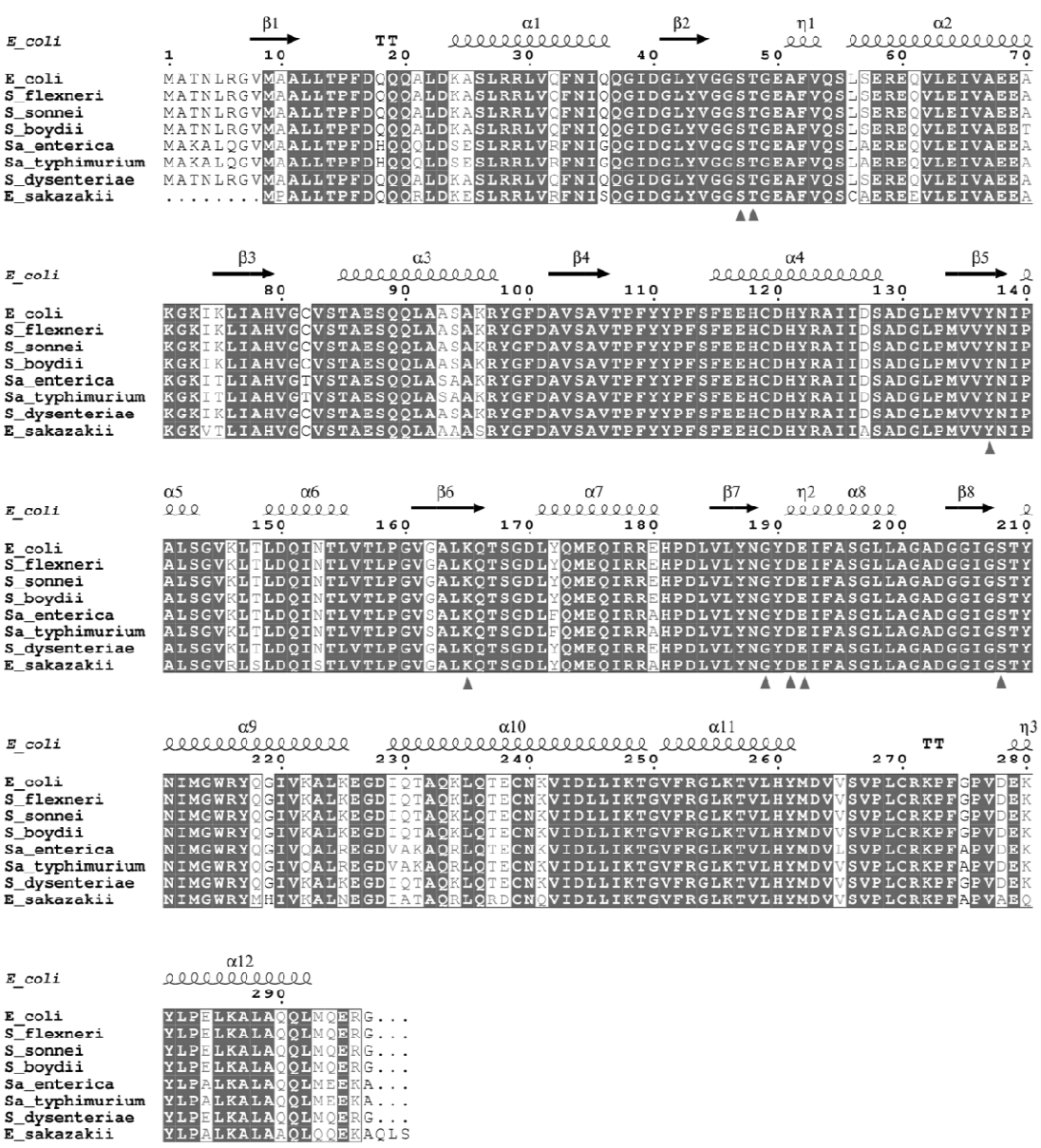

Figure 4.14. *Multiple sequence alignment for NALs belonging to group 2*. The sequences from the SWISSPROT databank were aligned with CLUSTAL-W (Thompson et al., 1994)and with ESPript (Gouet et al., 1999). Residues strictly conserved across Group 2 NAL enzymes have a dark grey background. Symbols above blocks of sequences represent the secondary structure of *Escherichia coli*, corresponding to a crystallized structure (PDB: 1NAL). Springs represent helices and arrows represent β-strands. The residues forming the active site are indicated by small triangles. E: *Escherichia*, S: *Shigella*, Sa: *Salmonella,* E: *Enterobacter.*

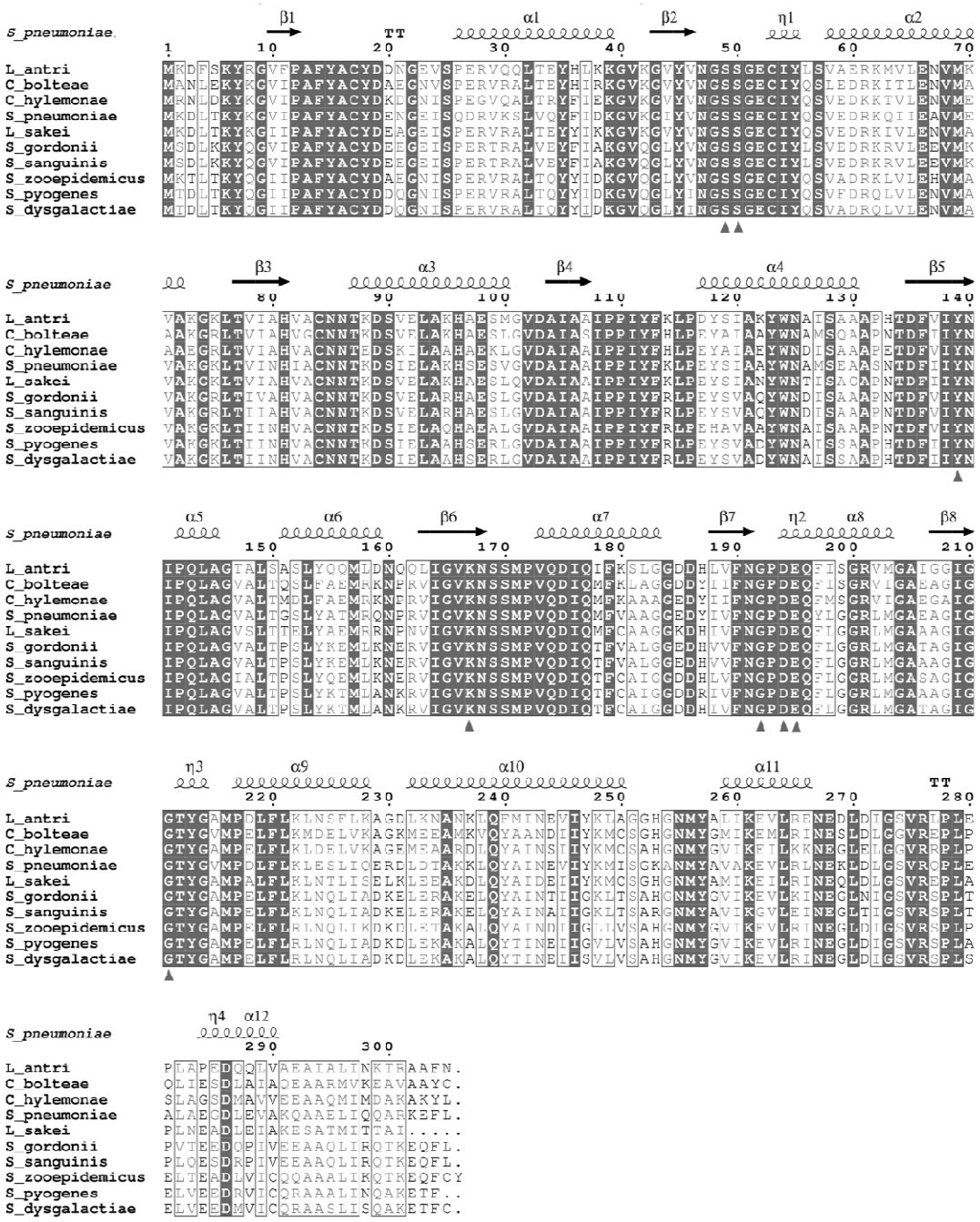

Figure 4.15. *Multiple sequence alignment for NALs belonging to group 3*. The sequences from the SWISSPROT databank were aligned with CLUSTAL-W (Thompson et al., 1994) and with ESPript (Gouet et al., 1999). Residues strictly conserved across Group 3 NAL enzymes have dark grey background. Symbols are the same as Figure 4.14. L: *Lactobacillus,* C: *Clostridium*, S: *Streptococcus.*

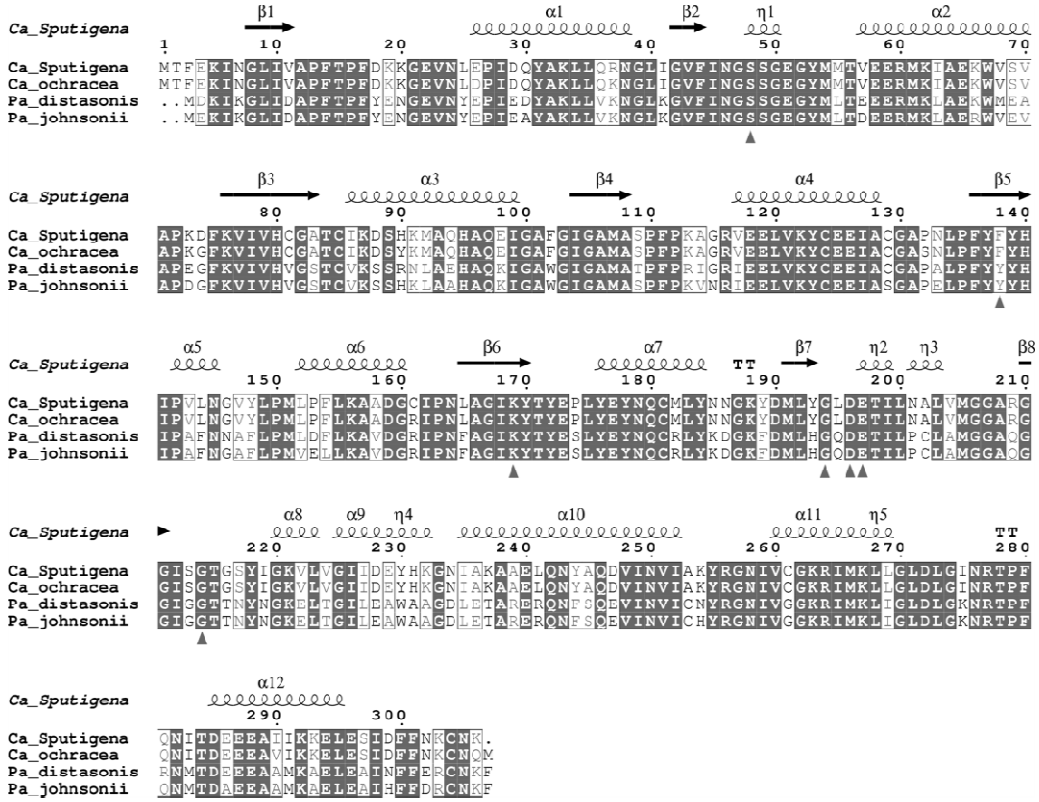

Figure 4.16. *Multiple sequence alignment for NALs belonging to subgroup 4.1.* The sequences from the SWISSPROT databank were aligned with CLUSTAL-W (Thompson et al., 1994) and with ESPript (Gouet et al., 1999). Residues strictly conserved across subgroup 4.1 NAL enzymes have dark grey background. Symbols are the same as Figure 4.14. C: *Capnocytophaga.*

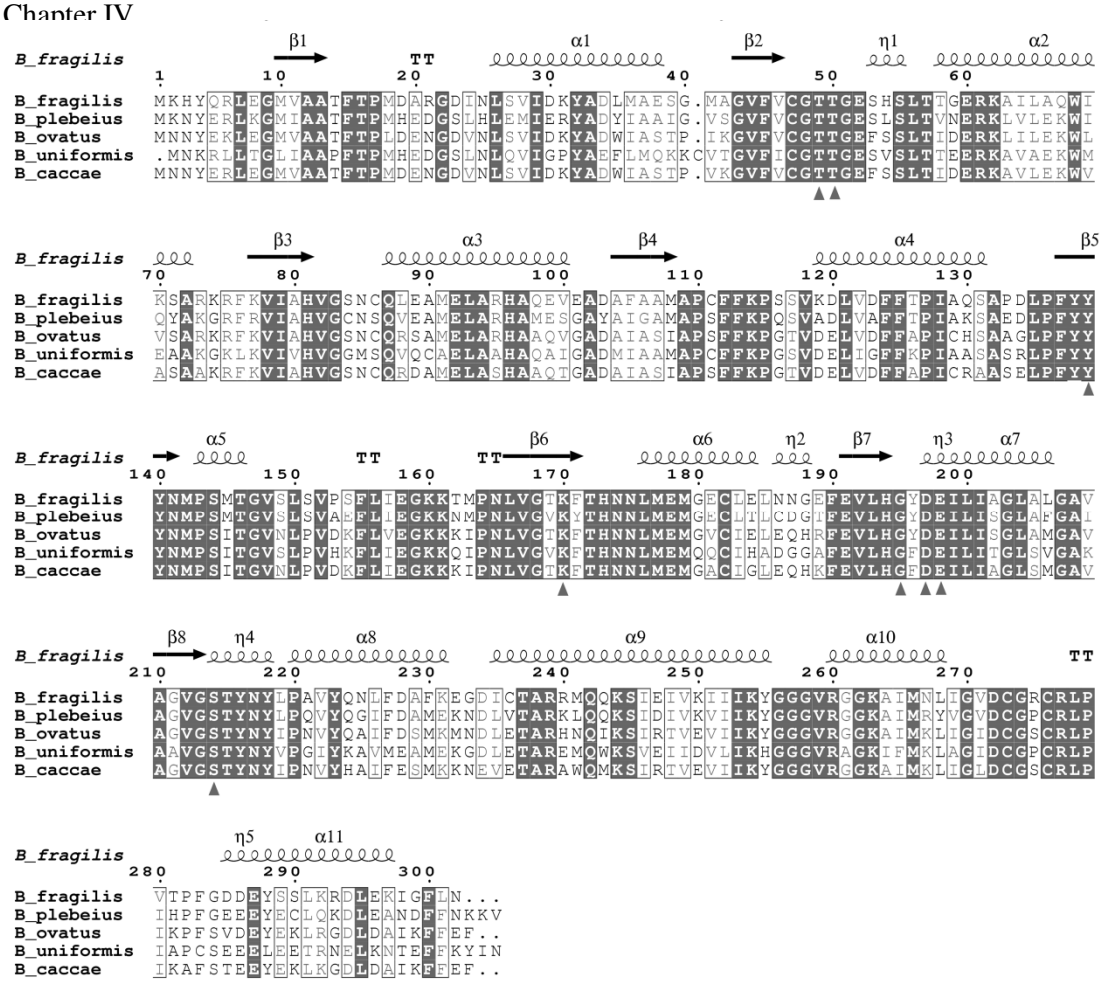

Figure 4.17. *Multiple sequence alignment for NALs belonging to subgroup 4.2.* The sequences from the SWISSPROT databank were aligned with CLUSTAL-W (Thompson et al., 1994) and with ESPript (Gouet et al., 1999). Sequences are grouped according to similarity. Residues strictly conserved across subgroup 4.2 NAL enzymes have dark grey background. Symbols are the same as Figure 4.14. B: *Bacteroides.*

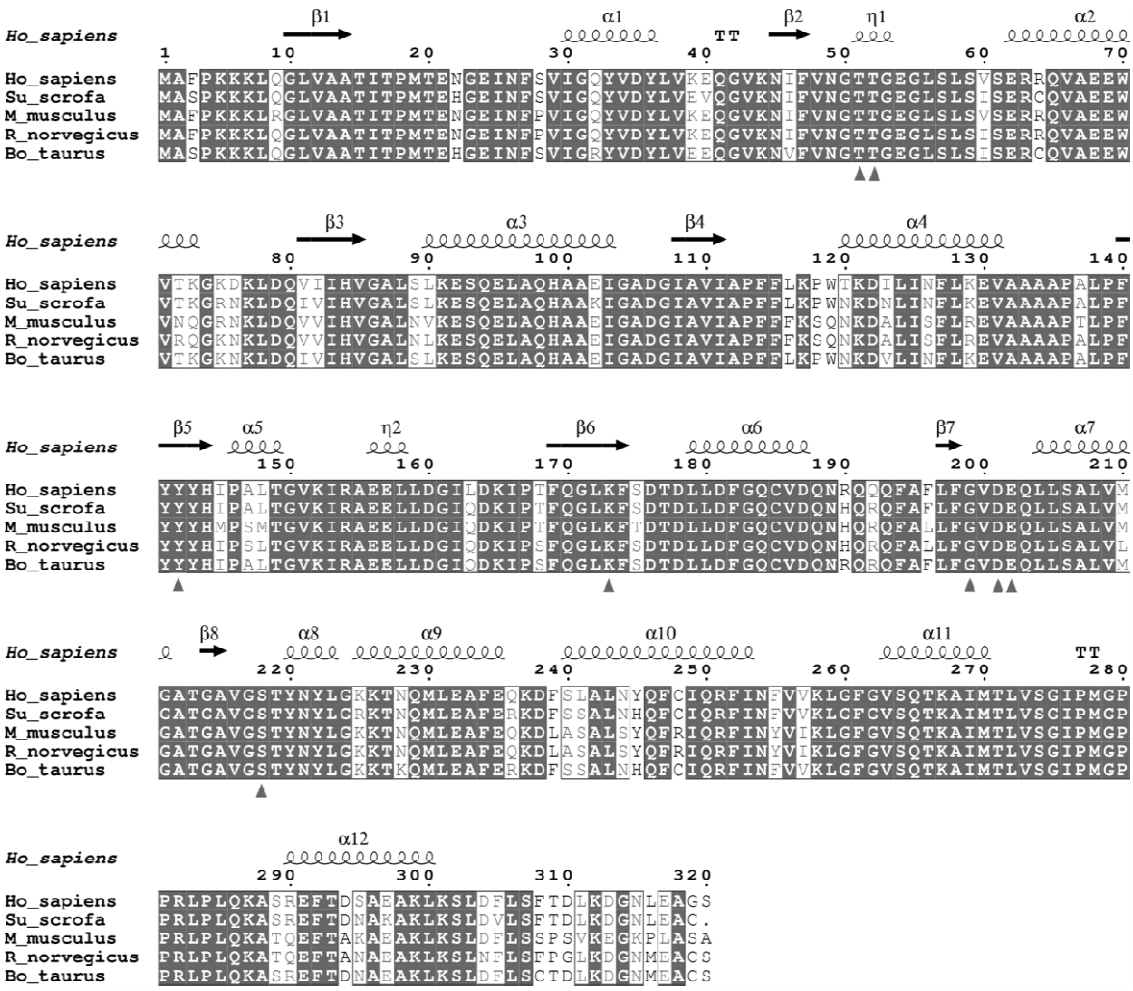

Figure 4.18. *Multiple sequence alignment for NALs belonging to subgroup 4.3.* The sequences from the SWISSPROT databank were aligned with CLUSTAL-W (Thompson et al., 1994) and with ESPript (Gouet et al., 1999). Residues strictly conserved across subgroup 4.3 NAL enzymes have dark grey background. Symbols are the same as Figure 4.143. Ho: *Homo,* Su: *Sus,* Mu: *Mus,* R: *Rattus,* Bo: *Bos.*

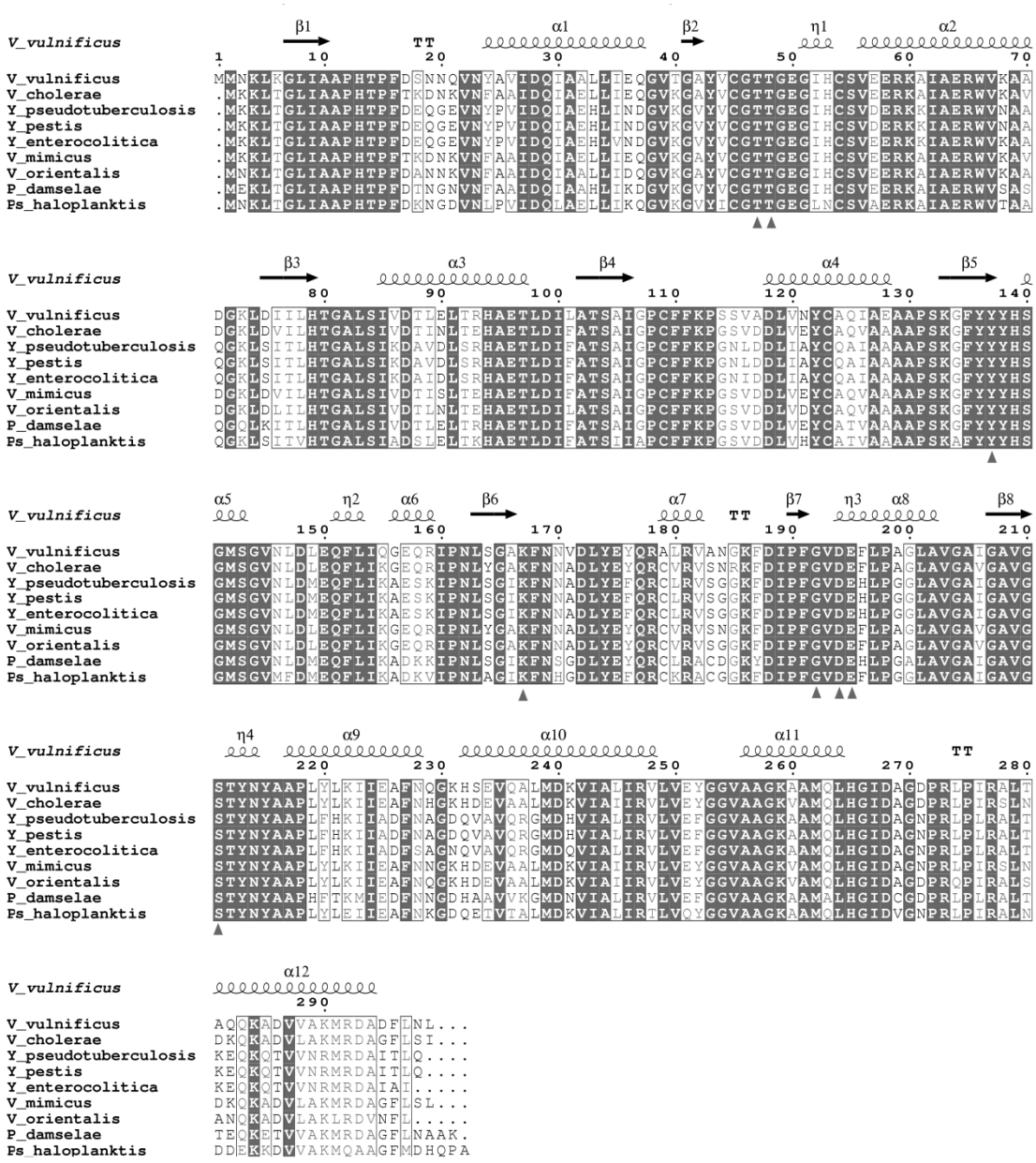

Figure 4.19. *Multiple sequence alignment for NALs belonging to subgroup 4.4.* The sequences from the SWISSPROT databank were aligned with CLUSTAL-W (Thompson et al., 1994) and with ESPript (Gouet et al., 1999). Residues strictly conserved across subgroup 4.4 NAL enzymes have dark grey background. Symbols are the same as Figure 4.14. V: *Vibrio,* Y: *Yersinia,* P: *Photobacterium,* Ps: *Pseudoalteromonas*

3. CONCLUSION

In conclusion, the *N*-acetylneuraminate lyases from *Lactobacillus plantarum* WCFS1 and *Escherichia coli* K-12 MG1655 were cloned in *E. coli*, over-expressed and purified to obtain stables 132 kDa and 146 kDa homotetrameric proteins, respectively. Both enzymes were able to cleave Neu5Ac with a similar catalytic efficiency to the best previously described NALs. These enzymes show good stability and activity under alkaline pH conditions and a wide range of temperatures (up to 70 ºC). In addition to these biotechnologically useful characteristics, the phylogenetic analysis of LpNAL, and other related bacterial NAL from the databases, led to a new classification of bacterial NALs into four groups and three subgroups (4.1, 4.2 and 4.4), as has been carried out for other enzymes, such us lipases/esterases (Arpigny & Jaeger, 1999). Among these groups, subgroup 4.4 was related with some mammalian NALs (subgroup 4.3), including human.

V. High-yield production of a new L-lactate dehydrogenase from *Bacillus halodurans* C-125 as a tool for screening directed evolution libraries.

VI. Characterization of a novel *Oceanobacillus iheyensis* HTE831 nicotinamidase.

1. INTRODUCTION

The previous experience achieved during the characterization of LpNAL and the couple enzyme BhLDH that allows the rapid and cost-effective characterization of the former, even in high-throughput detection systems, lead us to the study of other enzymes with great biotechnological interest, such as nicotinamidases. The nicotinamidases catalyze the deamination of nicotinamide (NAM) to produce ammonia and nicotinic acid (NA) (Scheme 6.1). For measuring those enzymes, a coupled detection method based on a dehydrogenase, glutamate dehydrogenase, of similar characteristic as BhLDH for LpNAL, is used.

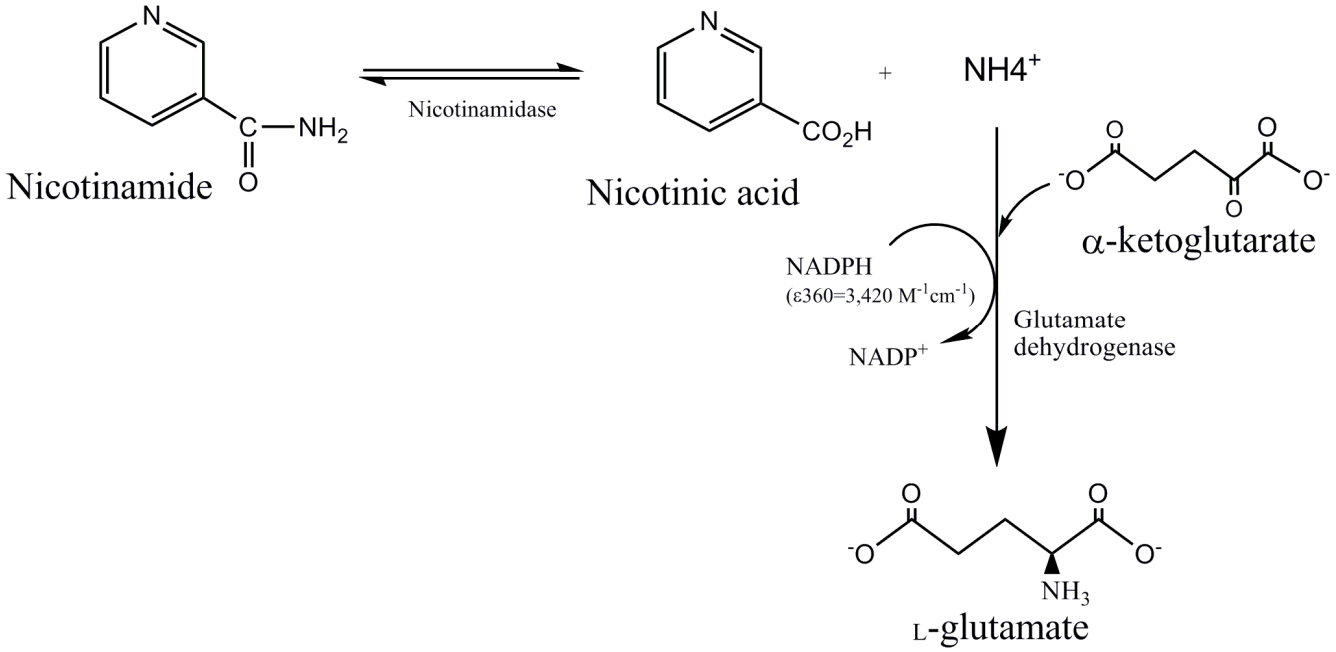

Scheme 6.1. *Coupled reaction for continuous monitoring of nicotinamidase activity.*

In vivo, nicotinic acid is converted back to NAD^+ in a series of reactions catalyzed by other enzymes in the NAD^+ salvage pathways, where nicotinamidases are key enzymes in many organisms, including bacteria (French et al., 2010b), mycobacteria (Boshoff & Mizrahi, 1998; Zhang et al., 2008), yeast (Ghislain et al., 2002; Hu et al., 2007; Joshi & Handler, 1962; Scorpio & Zhang, 1996), protozoa (Zerez et al., 1990) plants (Wang & Pichersky, 2007) and even invertebrates, such as *Drosophila melanogaster* (Balan et al., 2008) or *Caenorhabditis elegans* (van der Horst et al., 2007). Maintenance of NAD+ concentrations is important for cell and organism viability. Most prokaryotes, unicellular eukaryotes and invertebrates

recycle NAM to NAD^+ through a nicotinamidase that converts NAM to Nicotinic acid. However, mammalian genomes do not encode nicotinamidases, and use nicotinamide phosphoribosyltransferase to convert NAM to nicotinamide mononucleotide (NMN) which is later adenilated back to NAD^+. Mammals are also capable to use nicotinic acid to make NAD via the Preiss-Handler pathway (Vrablik et al., 2009). Recent works indicates the importance of the nicotinamidase activity for the viability and proliferation of organisms that are pathogenic to humans (Gazanion et al., 2011; Purser et al., 2003; Vrablik et al., 2009). This fact, together with the absence of nicotinamidase in human NAD^+ biosynthetic pathways, has increased the interest in this enzyme as a possible drug target, suggesting that small molecule inhibitors of nicotinamidases could serve as antimicrobial agents (Sauve, 2008).

In addition, nicotinamide is the product of multiple NAD^+-consuming enzymes (Gallo et al., 2004), such as sirtuins, NAD-dependent deacetylases that are widely distributed in biology (Sauve et al., 2006). Increased sirtuin activity increases life span as described in various organisms such as *D. melanogaster* (Balan et al., 2008), *C. elegans* (van der Horst et al., 2007) and *Sacharomyces cerevisiae* (Anderson et al., 2003). Local accumulation of NAM results in negative feed-back inhibition of sirtuins (Bitterman et al., 2002; Landry et al., 2000). Nicotinamidases have received considerable attention as increasers of life span in response to low calorie stress (Anderson et al., 2003) and oxidative stress (Balan et al., 2008) through depletion of intracellular nicotinamide concentration, thereby increasing sirtuin activity. These data suggests that these enzymes are central to phylogenetic conserved adaptative response to environmental stresses.

The growing interest in the study of modulators (activators and inhibitors) of sirtuins requires the utilization of a method to measure sirtuin activity. A continuous spectophotometrical assay couples the activity of sirtuins (Smith et al., 2009), which produces nicotinamide as a co-product, with a nicotinamidase and a glutamate dehydrogenase, which converts the ammonia produced by the nicotinamidase reaction and α-ketoglutarate in glutamate, with oxidation of NADPH, whose decrease in absorbance could be followed spectrophotometrically at 340 nm (Scheme 6.2).

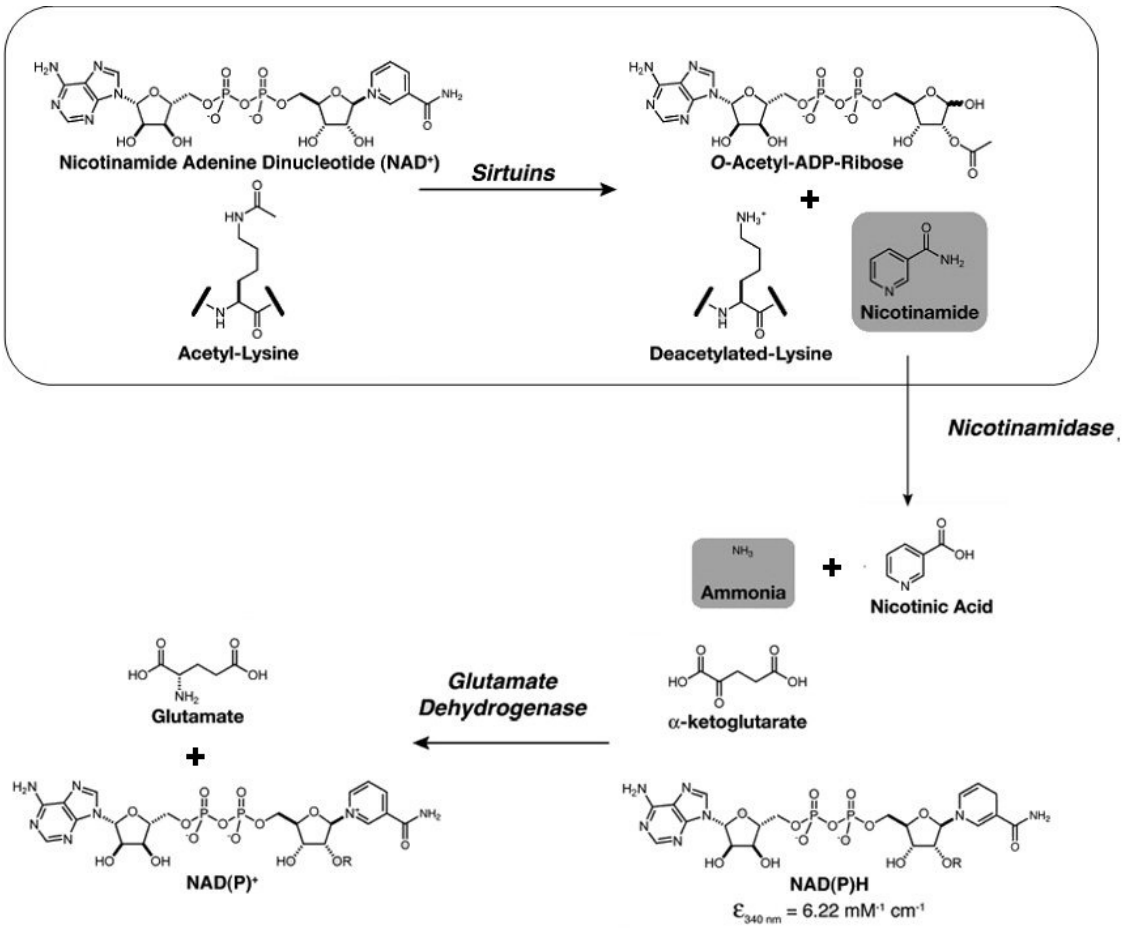

Scheme 6.2. *Coupled reaction for continuous monitoring of sirtuin activity*

The second coupled enzyme of this method, glutamate dehydrogenase can be purchased from different commercial sources. However, there is not a commercial nicotinamidase available. This suggests that an efficient nicotinamidase overexpression and purification method would be of mayor interest in the development of sirtuin activity detection kits.

Of additional interest, nicotinamidase from *Mycobacterium pneumoniae* (PncA) is active towards the pro-drug pyrazinamide (PZA), an analogue of nicotinamide, which is an important front-line tuberculosis drug. Mutations in this enzyme are associated with resistance to pirazinamide (Scorpio & Zhang, 1996). Interestingly, in the databases, enzymes are usually classified as nicotinamidases, as the *S. cerevisiae* Pnc1 (Hu et al., 2007) or *Streptococcus pneumoniae* SpNIC (French et al., 2010a), bifunctional pyrazinamidase/nicotinamidases as *Pyrococcus horikoshii* PH999 (Du et al., 2001) and *Acinetobacter baumanii* AbPncA (Fyfe et

al., 2009) or pyrazinamidases (*M. tuberculosis* PncA (Petrella et al., 2011), depending on their ability to catalyze more efficiently nicotinamide or pyrazinamide. However, no study has been carried out to determine which residues are implied in the binding and catalysis of one or another substrate.

This chapter describes the cloning, overexpression and a detailed characterization of the nicotinamidase gene from the extremophile microorganism *Oceanobacillus iheyensis* HTE 831(*OiNic*), isolated at a 1050 m depth in the Iheya Ridge, Japan. OiNIC was found to be a good catalyst (k_{cat} 10.6 s^{-1} for NAM and 2.6 s^{-1} for PZA), and stable from acid to neutral pHs. The enzyme was active over a range of nicotinamide analogues, including the pro-drug pyrazinamide. The generation of 7 mutants and one double mutant was carried out to increase the knowledge of the residues involved in the catalysis and in the binding of the metal ion and the substrate. Finally, OiNIC showed a strong inhibition by nicotinaldehydes, with K_i values below 5 μM.

2. RESULTS

2.1. Amino acid sequence comparison.

The deduced amino acid sequence of the *O. iheyensis* nicotinamidase (OiNIC) showed significant identity with those of other species in the database. Sequence alignment indicates that OiNIC has an elevated sequence identity with isochorismatase hydrolases; a subfamily within the cystein-hydrolases superfamily that encloses the nicotinamidases/pyrazinamidases as well; from *Geobacillus sp.* and other *Bacillus* species (74 %, GenBank accessions: ACS24337 and EEL50819). OiNIC shows 53 % sequence identity with the crystallized nicotinamidase from the firmicute *Streptococcus pneumoniae* (PDB codes: 3O90, 3O91, 3O92, 3O93, 3O94). Less sequence identity was found between OiNIC and other crystallized nicotinamidases such as the one from the Gamma-proteobacteria *Acinetobacter baumanii* (32%, PDB code: 2WT9, 2WTA), the Actinobacteria *Mycobacterium tuberculosis* (34%, PDB code: 3PL1), the Archaea *Pyrococcus horikoshii* (31%, PDB codes: I1LW, I1MS), the yeast *Sacharomyces cerevisiae*

(25%, PDB code: 2HOR) and the recently crystallized eukaryotic nicotinamidase from *Leishmania infantum* (31 %, PDB code: 3R2J).

In addition, sequence alignment revealed that OiNIC contained conserved residues forming the characteristic catalytic triad of the cystein-hydrolases family (Figure 6.1, up filled triangles), a catalytic cysteine at position 137 (C137), an aspartate at position 10 (D10), and a lysine at position 104 (K104) (Du et al., 2001; French et al., 2010b; Hu et al., 2007; Zhang et al., 2008).

Another conserved feature of the active centre is the presence of a cis-peptide bond (Figure 6.1, down filled triangles), whose sequence differs between species (V132 and C133 in the case of OiNIC), but which is invariably preceded by a conserved glycine (G131) (Du et al., 2001). The second residue implicated in the formation of the *cis*-peptide bond in pyrazinamidases, such as *Mycobacterium tuberculosis* NIC (PDB: 3PL1) is commonly the alanine 133 (see Figure 6.1, position 133 in 3pl1). However, it differs in the firmicutes species studied and in OiNIC (see Figure 6.1, position 133) (French et al., 2010b). This residue which forms the cavity of the active center could play a role in the binding of NAM or PZA. The conserved specific metal ion binding motif usually includes one aspartate and two histidines, D54, H56, and H72 (OiNIC numbering) (Figure 6.1, stars). Depending on the metal ion and on the structural conformation of the protein, a fourth residue could be implicated in the metal ion binding, which remains unclear (Du et al., 2001; Petrella et al., 2011; Zhang et al., 2008). Structure alignment of OiNIC with *S. Pneumoniae* nicotinamidase (SpNIC) and other nicotinamidases suggests that this fourth residue could be a glutamate (E65, OiNIC numbering) in nicotinamidases and a serine or an histidine in pyrazinamidases (French et al., 2010a). Other residues are also involved in the formation of the hydrophobic cavity where nicotinamide and the ion metal bind, like T12, F15, D14, L22, F68, Y107, S108 and T141 (OiNIC numbering) (Du et al., 2001).

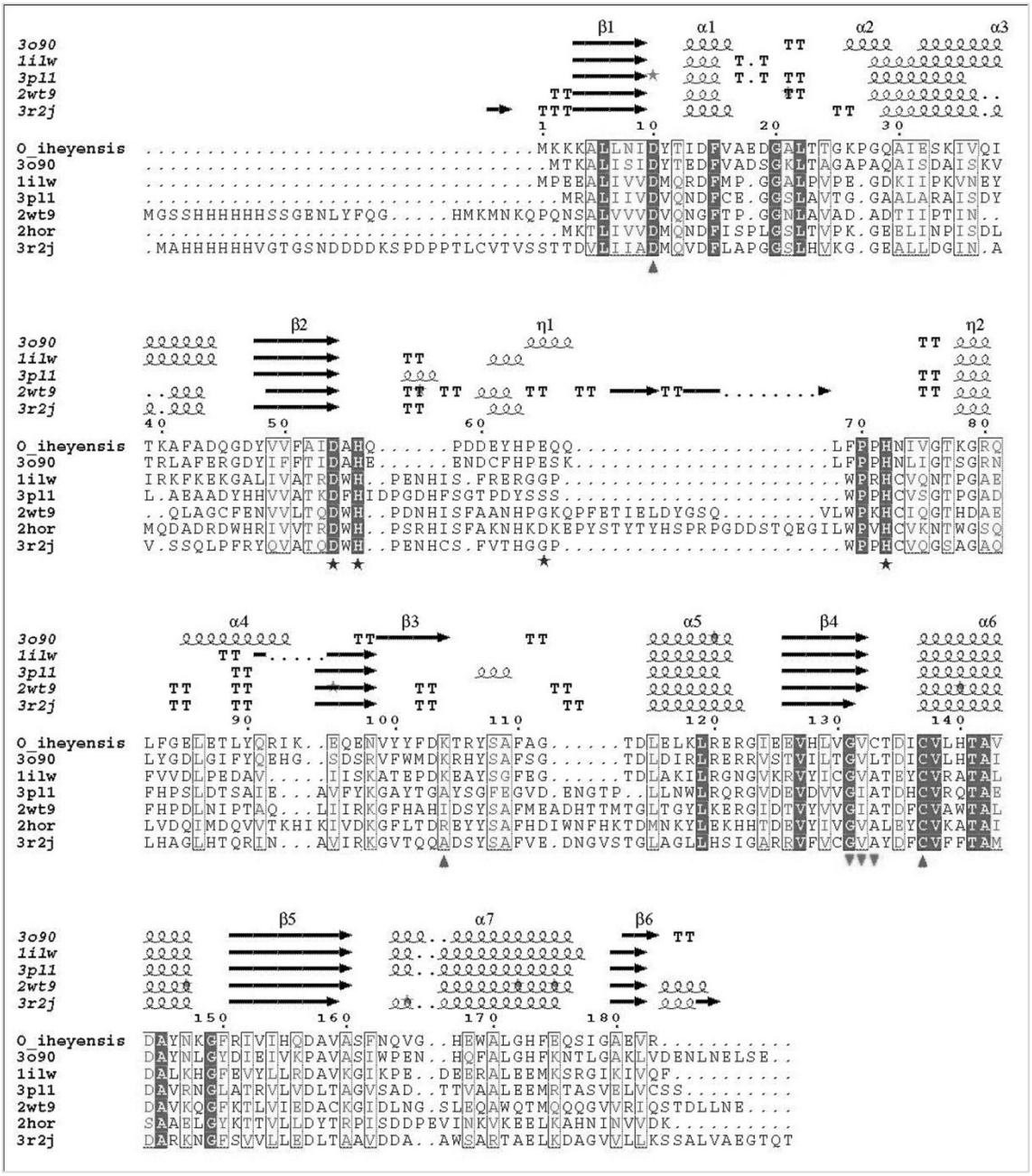

Figure 6.1. *Multiple sequence alignment for O. Iheyensis nicotinamidase (OiNIC) and related nicotinamidases*. ESPript outputs (Gouet et al., 1999) obtained with the sequences from the SWISSPROT databank and aligned with CLUSTAL-W (Thompson et al., 1994). Sequences are grouped according to similarity. The enzyme showed 54% sequence identity with nicotinamidase from *S. pneumoniae* (PDB: 3O90), 31% with *P. horikoshii* nicotinamidase (PDB:I1LW), 34% with *M. tuberculosis* nicotinamidase (PDB: 3PL1), 32 % with *A. baumanii* nicotinamidase (PDB:2WT9), 25% with *S. Cerevisiae* nicotinamidase (PDB: 2HOR) and 31 % with *Leishmania infantum* nicotinamidase (PDB: 2R3J). Residues strictly conserved across nicotinamidase enzymes have a dark background. Symbols above blocks of sequences represent the secondary structure, springs represent helices and arrows represent β-strands. The residues forming the active site are indicated by up filled triangles. Residues implicated in the coordination of the metal ion are indicated by stars and residues forming the cis-peptide bond are indicated by down filled triangles.

Those residues delimiting the active site are usually conserved among species, except in the case of F68 and T12, conserved in nicotinamidases from firmicutes, such as *S. Pneumoniae* NIC and OiNIC, but not in the pyrazinamidases crystallized, where they are a tryptophan and a glutamine, respectively. This suggests that these residues could modify the substrate specificity of nicotinamidases to be more or less active over the pro-drug pyrazinamide (Table 6.10029.

Table 6.1. *Residues involved in nicotinamidase activity.* [¶]

Residues	OiNIC	SpNIC	AbPncA	PncA	PH999
Catalytic triad	C137	C136	C159	C138	C133
	D10	D8	D16	D8	D10
	K104	K103	K114	K96	K94
Metal binding	D54	D53	D54	D49	D52
	H56	H55	H56	H51	H54
	H72	H71	H89	H71	H71
	E65	E64	S62	H57	S60
cis-peptide bond	G131	G130	G153	G132	G127
	V132	V131	I154	I133	A129
	C133	L132	A155	A134	V128
Active site forming residues	F68	F68	W86	W68	W68
	I136	I135	F158	H137	Y131
	Y107	Y106	Y123	Y103	Y103
	F15	F14	F21	F13	F15
	L22	L21	L27	L19	L21
	T105	R104	G115	G97	A95
Hidrogen bonds between main and lateral chains	T12	T11	Q18	Q10	Q12
	D14	D13	G20, D96?	D12	D14
	S108	R104	S124	S104	S104
	T141	T140	T163	T142	T137

[¶]OiNIC: *O. iheyensis* nicotinamidase; SpNIC: *Streptococcus pneumoniae* nicotinamidase; AbPncA: *Acinetobacter baumanii* nicotinamidase; PncA: *Mycobacterium tuberculosis* nicotinamidase; PH999: *Pyrococcus horikoshii* nicotinamidase.

2.2. Cloning, overexpression and purification of OiNIC

The gene encoding the nicotinaminidase enzyme from *Oceanobacillus iheyensis* HTE831 was cloned into pTYB21 vector, which provides an intein-tagged recombinant protein, as described in Materials and Methods. The DNA sequence of the cloned gene showed no mutations compared to the *OiNic* gene sequence reported for *O. iheyensis* genomic strain HTE831 (Uniprot entry: Q8ESQ6). The recombinant clone with the highest expression was induced with 0.4 mM IPTG in 1 L TB-medium at 20 ºC for 12 h with vigorous shaking.

OiNIC was purified from *E. coli* cells by a two steps of affinity chromatography as described in Materials and Methods. After these steps, the enzyme was pure, as shown in SDS-PAGE (Figure 6.2, lane 2). The molecular weight of purified protein was determined by gel filtration (40.9 kDa) and by HPLC/ESI/ion trap (21.10 kDa), confirming the dimeric nature of OiNIC. To further confirm this dimeric association of OiNIC monomers, a cross-linking experiment with dimethylsuberimidate (DMS) was carried out as explained in Materials and Methods (Figure 6.2). After 8 hours incubation with dimethylsuberimidate (DMS) at room temperature, OiNIC dimer (42 kDa) became evident in SDS-PAGE (Figure 6.2, lane 1).

2.3. Biochemical characterization of recombinant OiNIC.

The enzyme activity was both pH- and temperature-dependent (Figure 6.3). The optimal pH of OiNIC was found to be around to pH 6.0-6.5. The enzyme activity decreased rapidly below pH 5.0 and above pH 8.0 (Figure 6.3 A). Optimum pH and temperature could not be measured by the spectrophotometric assay due to the distortion caused by the coupling enzyme glutamate dehydrogenase (GDH). GDH activity falls quickly below pH 7.0, showing reduced activity at OiNIC optimum pH (pH 6-6.5) (Figure 6.3 A), and therefore, modifying the real pH curve. To solve this, HPLC method was used to measure this data (see Materials and Methods).

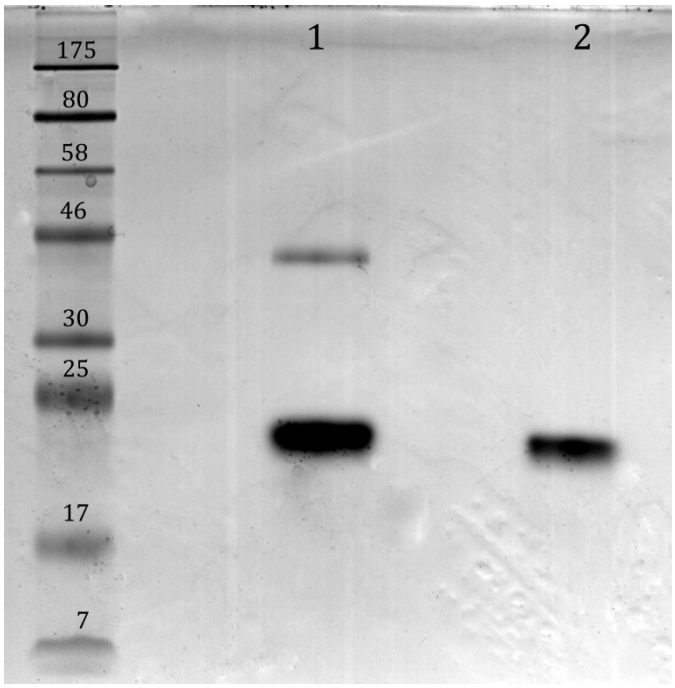

Figure 6.2. *SDS-PAGE of the pure OiNIC and enzyme cross-linked with dimethylsuberimidate.* M: molecular weight standards (New England Biolabs: P7708S). Lane 1: Purified OiNIC with 3 mg/mL DMS. Lane 2: Purified OiNIC without DMS. Protein monomer is about 21 kDa, protein dimer is about 42 kDa. The incubation with dimethylsuberimidate shows the formation of the dimeric form of the enzyme.

OiNIC enzyme exhibited its maximum activity at a temperature close to 45 ºC. Below 25 ºC or above 55 ºC, the enzyme lost its activity rapidly (Figure 6.3 B). These results are consistent with the few data on the bibliography, where optimum temperatures range from 30 to 40 ºC (Pardee et al., 1971; Yan & Sloan, 1987; Zhang et al., 2008). However, and for the purpose of comparison (French et al., 2010b; Zhang et al., 2008), stability and kinetic experiments were carried out at pH 7.3 and 37 ºC.

Interestingly, OiNIC was very stable at pH 6.0 and 7.0, where it maintained after 20 hours of incubation 40 % and 30 % residual activity, respectively (Figure 6.3, C). This stability profile is a remarkable feature compared with other nicotinamidases. Thermostability of OiNIC was also studied both, spectrophotometrically by incubating the enzyme at different temperatures, and by thermal shift assays (TSA) as described in Materials and Methods.

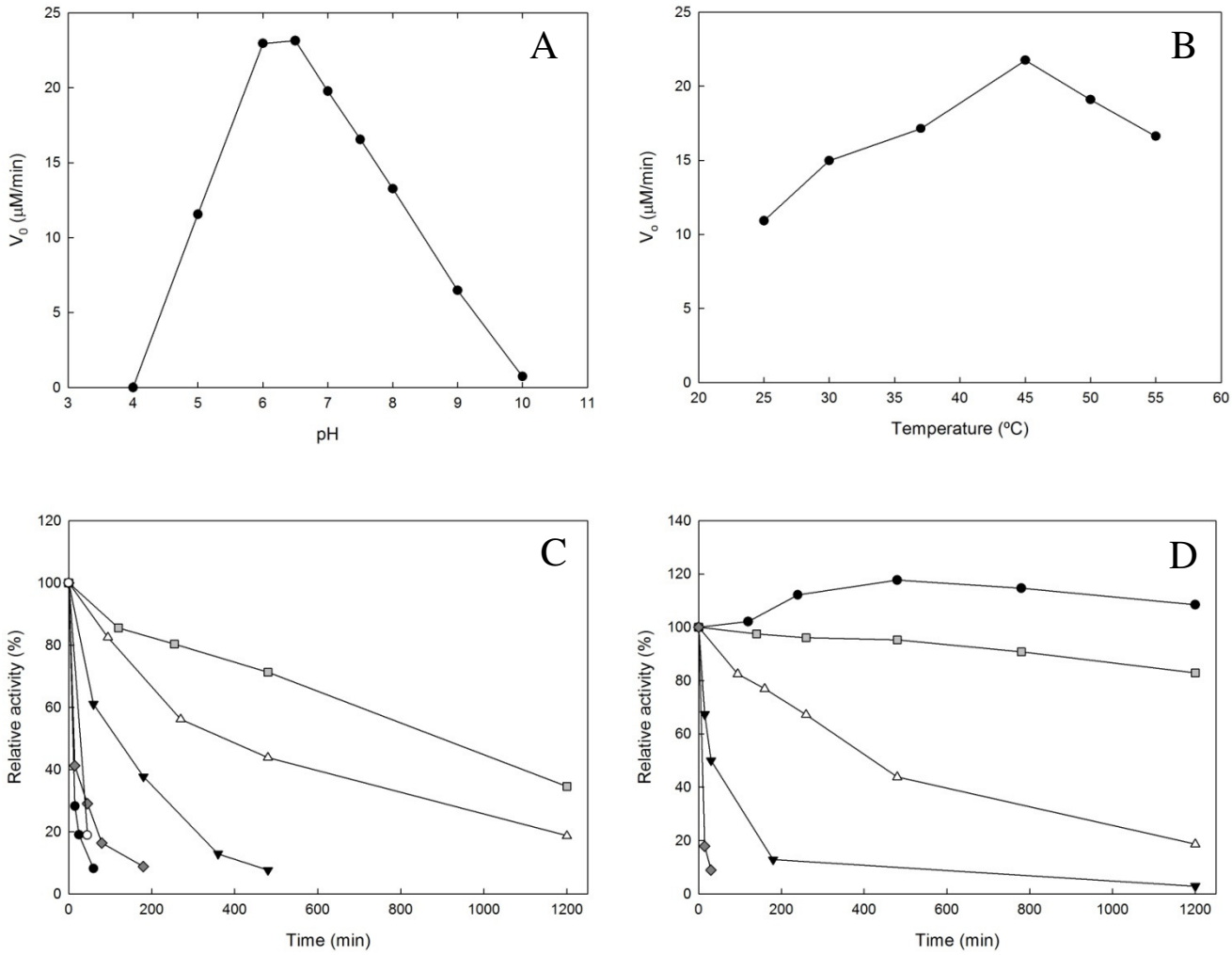

Figure 6.3. *Effect of pH and temperature on OiNIC activity and stability*. A) pH profile for OiNIC determined by HPLC. Assay conditions at 37 ºC were 1 mM nicotinamide, 0.67 µg of OiNIC. The buffers (100 mM) used were sodium acetate pH 4.0-6.0, sodium phosphate pH 7.0-8.0, TRIS-HCl pH 9.0 and glycine pH 10.0. B) Temperature profile. Assay conditions were the same as above at pH 7.3. C) pH stability. OiNIC was incubated at 37 ºC at pH 5 (●), pH 6 (■), pH 7.3 (Δ), pH 8 (▼), pH 9 (♦) and pH 10(○). Buffer composition was the same as above. Residual activity was spectrophotometrically measured under the standard reaction at 37 ºC, consisting of 0.3 mM NADPH, 10 mM α-ketoglutarate, 9.7 µg BhGDH, 1 mM NAM, 1.3 µg de OiNIC in 100 mM sodium phosphate pH 7.3. D) Temperature stability. OiNIC was incubated at 5 (●), 20 (■), 37 (Δ), 45 (▼) and 55 ºC (♦) in 100 mM sodium phosphate buffer pH 7.3. Residual activity was measured spectrophotometrically using the standard reaction media.

OiNIC was stable at 4 ºC and 20 ºC for 20 hours (Figure 6.3 D), even showing a slight increase in relative activity (over relative 100%), when the enzyme was incubated at 4 ºC (Figure 6.3, filled circles). The enzyme maintained 50 % activity after 1 hour at 45 ºC (Figure 6.3 D, open triangles), but dropped quickly when incubated at 55 ºC (Figure 6.3 D, filled triangles). These data were also similar to that found in TSA carried out in MilliQ® water (Figure 6.4, A, filled circles) and in 100 mM buffered solutions at different pH (Figure 6.4, A). T_m was ~51.71±0.2 ºC in MilliQ® water, increasing about 2 ºC in buffered solutions at pHs 7.3 and 8.0. (53.3±0.2 ºC and 52.9±0.2 ºC, respectively). But falling 7 ºC above pH 9.0 (T_m 47.9±0.2 ºC). At acid side, T_m was similar to MilliQ water at pH 6.0 (52.2±0.1 ºC), but dropped to 44.7±0.1 ºC at pH 5.0. In general OiNIC was about 10 ºC more thermostable than the *Mycobacterium tuberculosis* nicotinamidase (PncA), whose T_m was 43 ºC (Zhang et al., 2008).

Protein melting assay was also used to study the binding of different molecules to OiNIC structure (Figure 6.4, B). The addition of a competitive inhibitor, nicotinaldehyde, to enzyme produced a T_m increase of about 6 ºC (T_m: 59.7±0.1 ºC), indicating a possible strong binding to OiNIC. The protein stabilizer, ammonium sulphate, also increased the T_m up to 61.34±0.1 ºC. These results indicate that this technique could be very useful for the high-throughput discovery of novel therapeutic inhibitors or analogues of the enzyme using chemical libraries

2.4. Kinetic parameters and substrate specificity.

The substrate specificity of OiNIC was studied towards nicotinamide and some of its derivatives (Table 6.2), which include pyrazinamide, 5-methylnicotinamide and two nicotinate esters (methylnicotinate and ethylnicotinate). Substitutions at the 5-position were well-tolerated, showing 38 % of NAM specific activity, almost 3-fold more than shown for pyrazinamide. However, nicotinate esters were not as good substrates representing only 0.5 % (ethylnicotinate) and 1.8 % (methylnicotinate) activity. This substrate specificity was similar to that of other nicotinamidases (French et al., 2010b).

The kinetic parameters of *O. iheyensis* nicotinamidase were determined for all the above compounds (Table 6.2). The K_M values were 0.26±0.1 mM for NAM and 0.81±0.1 mM for PZA. These values are in the range described in the bibliography, which varies from 0.0002 mM to 0.65 mM for NAM (French et al., 2010b; Hu et al., 2007; Tanigawa et al., 1980) and from 0.056 to 0.63 mM for pyrazinamide (Boshoff & Mizrahi, 1998; Hu et al., 2007). However, the values obtained in OiNIC for K_M was closer to that previously described for non-pathogenic nicotinamidases, whereas the K_M for PZA was slightly higher than that described in the bibliography (0.1-0.4 mM), suggesting that this enzyme is more a nicotinamidase than a pyrazinamidase. However, its k_{cat} for PZA (2.6 s^{-1}) was more than 50 times greater than the k_{cat} for PZA of the nicotinamidase/pyrazinamidase from *Acinetobacter Baumanii* (Fyfe et al., 2009).

The catalytic efficiency of OiNIC towards NAM was 43.48 mM^{-1} s^{-1}, which is 2-fold higher compared to *Caenorhabditis elegans* CePNC1 (French et al., 2010b), but lower than that described for *S. pneumoniae* NIC, *M. tuberculosis* NIC and *S. cerevisiae* NIC (French et al., 2010b). On the PZA side, the catalytic efficiency of OiNIC (3.20 mM^{-1} s^{-1}) was 6-fold higher than that of *Acinetobacter baumanii* (Fyfe et al., 2009), but 3-fold lower than that of *M. tuberculosis* (French et al., 2010b). these data indicated that the catalytic efficiencies of OiNIC are in the average of nicotinamidases, which could be in accordance with the versatility of *Oceanobacillus iheyensis*, which is a non-pathogenic microorganism.

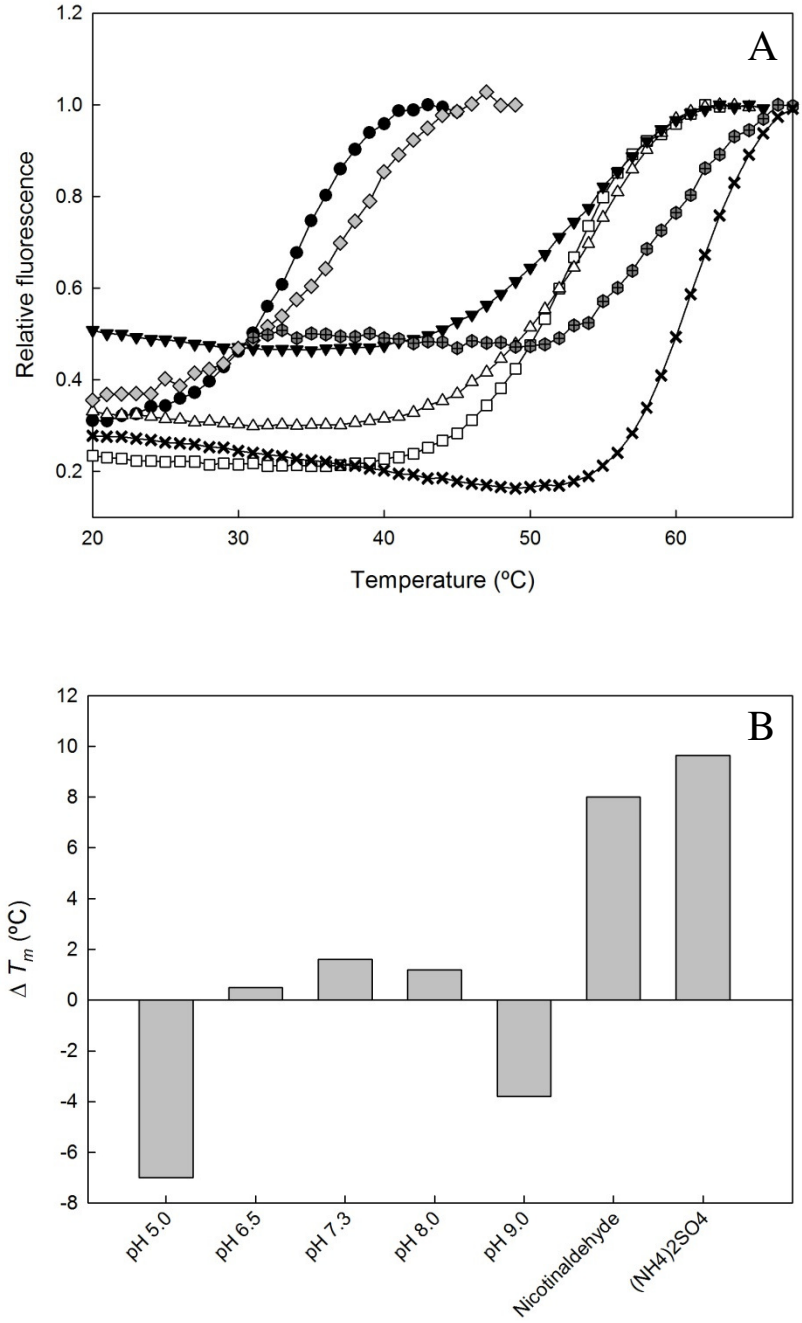

Figure 6.4. *Stability of OiNIC under in various conditions monitored in the presence of fluorescent probe SYPRO Orange.* A) Melting temperature curves of purified enzyme (1 µg) were obtained in 100 mM sodium acetate pH 5.0 (●),100 mM sodium phosphate pH 6.5 (□), pH 7.3 (Δ), pH 8.0 (▼), 100 mM TRIS-HCl pH 9 (♦) , 1 mM nicotinaldehyde ( ) and 1 M ammonium sulphate (**x**) prepared in 100 mM sodium phosphate pH 7.3. Melting temperatures were 51.7 ºC in mQ, 44.7 ºC at pH 5.0, 52.2 ºC at pH 6.5, 53.3 ºC at pH 7.3, 52.9 ºC at pH 8.0, 47.9 ºC at pH 9.0, 59.7 ºC with 1 mM Nicotinaldehyde and 61.3 ºC with 1 M Ammonium sulphate. B) Differences in Δ*Tm* were calculated subtracting MilliQ *Tm* value, to the *Tm* values obtained for the enzyme in the different conditions used above.

In order to study critical amino acids that participate in substrate specificity and activity, seven mutants were generated by site-directed mutagenesis (table 6.2) on two residues involved in the catalysis of nicotinamide (K104 and Q96), on one residue involved in metal binding (E65), on one residue forming hydrogen bonds between main and lateral chains (T12), on one residue participating in the *cis*-peptide bond formation (C133), and on one residue forming the surface of the active site (E65). Specific activity and kinetic parameters of the mutants were determined for NAM and NAM analogues (Table 6.2). Mutant T12Q affecting the residue that makes hydrogen bonds between lateral main chains expressed as insoluble inclusion bodies. This was also the case of mutant K104A that affects a catalytic residue. Although these two mutants were solubilized using the protocol described in Materials and Methods, they only showed 1.58 % and 1.45 %, respectively, of the specific activity shown by the unmodified enzyme towards its natural substrate NAM. Two changes were generated at position 96 (Q96K and Q96A), since this aligns with the catalytic lysines of the crystallized nicotinamidases from (Du et al., 2001; French et al., 2010a; Fyfe et al., 2009; Gazanion et al., 2011; Kruger et al., 2001; Petrella et al., 2011). However, this mutation in OiNIC reduced, but not abolished the activity over NAM. Q96K showed a 37.3% of specific activity, while Q96A maintained full activity, probably because alanine modifies less the conformation of vicinity of the active site. Both mutants (Q96K and Q96A) also showed a lower K_M for methylnicotinate than the wild-type. Mutant Q96A also showed a remarkably higher k_{cat} and k_{cat}/K_M for 5-methylnicotinamide (15,9 s^{-1} and 29.04 $mM^{-1}s^{-1}$, respectively) and for methylnicotinate (1.17 $mM^{-1}s^{-1}$) (Table 6.2). This residue modifies in some way the active center broadening the specificity of the enzyme but it is not an essential residue for catalysis.

Surprisingly mutation at cysteine 133, which forms part of the conserved *cis*-peptide bond, does not affect the specific activity of the protein, maintaining 75 % of the activity. In addition, this mutation also changes a bit the specificity of OiNIC, making this mutant more active towards pyrazinamide than the WT enzyme. Mutants C133A shows a lower K_M for PZA (0.36 mM vs. 0.81mM of WT) and ethylnicotinate (0.34 mM vs. 1.02 mM of WT). It also shows greater k_{cat} and k_{cat}/K_M value than wild-type for PZA, 5-methylnicotinamide, methylnicotinate

and ethylnicotinate (Table 6.2). This residue may be involved in the binding of nicotinamide or pyrazinamide in the active site, since this mutation rises 2.9-fold the catalytic efficiency of OiNIC towards PZA.

Mutation F68W also affects the active site cavity and improved the binding of pyrazinamide, increasing the affinity of OiNIC for PZA (K_M 0.5 mM) compared to wild-type, improving a 2.5-fold the k_{cat}/K_M (7.9 $mM^{-1}s^{-1}$). This mutations also reduces 2-fold the K_M for the natural substrate NAM to 0.17 mM. Based on the above, doubled mutant (C133A/F68W) combining the two latter mutations was constructed in order to obtain more activity towards PZA. However, both changes did not improved the catalytic efficiency compared with single mutants, since bothe mutants gave rise a higher k_{cat} for PZA (5.21 s^{-1}), but also a higher K_M (0.83 mM)

Finally, mutation at position E65H, which affects a residue involved in the ion metal binding, produced a dramatic loss in the catalytic efficiency for PZA (0.7 $mM^{-1}s^{-1}$), without changing its K_M (0.82 mM). However, this mutant showed the lowest K_M for NAM among the enzymes shown in Table 6.2.

Table 6.2. *Parameters of wild type OiNIC and mutants*.

	Specific activity (U/mg)	K_M	k_{cat}	k_{cat}/K_M
Wild-type				
NAM[b]	23.3[a]/25 [b]	0.26	11.65	43.48
PZA[a]	3.62	0.81	2.60	3.20
5-methyl-NAM[a]	9.01	0.68	5.10	7.50
Methylnicotinate[b]	0.45	1.03	0.32	0.31
Ethylnicotinate[b]	0.13	1.02	0.10	0.10
T12Q				
NAM[a]	0.37	N.D.	N.D.	N.D.
Q96K				
NAM[b]	8.70	0.57	2.37	4.15
PZA[a]	0.46	1.15	0.45	0.39
5-methyl-NAM[a]	3.96	0.62	2.16	3.40
Methylnicotinate[b]	0.31	0.44	0.17	0.38
Ethylnicotinate[b]	0.06	1.11	0.05	0.05
Q96A				
NAM[b]	24.8	0.36	16.05	44.59
PZA[a]	1.80	1.20	1.61	1.34
5-methyl-NAM[a]	28.0	0.55	15.90	29.04
Methylnicotinate[b]	1.16	0.56	0.60	1.17
Ethylnicotinate[b]	0.22	1.43	0.19	0.13
K104A				
NAM[a]	0.36	N.D.	N.D.	N.D.
C133A				
NAM[b]	17.50	0.40	13.60	34
PZA[a]	6.39	0.36	3.31	9.19
5-methyl-NAM[a]	11.74	0.64	7.09	11.07
Methylnicotinate[b]	1.40	0.89	1.02	1.14
Ethylnicotinate[b]	0.34	0.34	0.14	0.41
F68W				
NAM[a]	19.97	0.17	8.79	52.01
PZA[a]	7.50	0.50	3.94	7.9
E65H				
NAM[a]	13.50	0.13	5.63	42.65
PZA[a]	*0.70*	*0.82*	*0.43*	*0.52*
C133A/F68W				
NAM[a]	22.90	0.19	9.82	52.8
PZA[a]	7.43	0.83	5.21	6.28

[a]Reactions were conducted following the standard spectrophotometric method. 10 mM α-ketoglutarate, 300 µM NADPH, 9.7 µg BhGDH, nicotinamide analogue, 100 mM sodium phosphate buffer pH 7.3, 37 ºC. [b]Reactions were analyzed by HPLC. Conditions: 100 mM sodium phosphate buffer pH 7.3, 37 ºC, various concentrations nicotinamide analogue.

2.5. Metal binding

As it has been extensively described in the bibliography, nicotinamidases accommodate a metal ion in the active center cavity that actively participates in the orientation of the substrate in the active site and in the conversion of NAM to NA. However, different nicotinamidases present different metal ions. While *Pyrococcus horikoshii, Streptococcus pneumoniae,* and *Acinetobacter baumanii* nicotinamidases bind a Zn^{2+} ion (Du et al., 2001; French et al., 2010b; Fyfe et al., 2009), *Mycobacterium tuberculosis* nicotinamidase contains Mn^{2+}/Fe^{2+} or Fe^{2+} in its structure (Petrella et al., 2011; Zhang et al., 2008). Inductively Coupled Plasma-Optical Emission Spectrometry (ICP-OES) confirmed the presence of Zn^{2+} in the active center of OiNIC. The enzyme contained 44.95 ±0.06 μM of Zn^{2+} in 266 μM protein, while it only contained 3.438 ± 0.001 μM of Fe^{2+} and 0.892 ±0.001 μM Mn^{2+}. However, the mutant E65H showed a 2-fold increase in Fe^{2+} concentration. This could be due to the presence of a histidine, as in the case of *M. tuberculosis*, which binds Fe^{2+}:Mn^{2+}. Duplicated ICP-OES experiment of this mutant shows a higher concentration of Fe^{2+} in the sample compared to the WT, representing 2.6% of the protein, 2-fold higher than the 1.3% of Fe^{2+} found in the WT samples. Moreover, Zn^{2+} concentration slightly decreases from 16% to 12% in comparison with the concentration in the WT protein sample. In addition when this mutant E65H was incubated with Fe^{2+} for 1 hour and extensively washed in order to remove unbound Fe^{2+}, a dramatic increase in the presence of Fe^{2+}in the protein, was found (73.5±0.05 μM of Fe^{2+} in 83.3 μM protein), and the Zn^{2+} content was reduced to 9.9 ± 0.001 μM. This results together with the kinetic characterization of this mutant, confirmed E65 as the fourth residue involved in the metal binding together with D54, H56 and H72 in OiNIC.

2.6. Inhibition by nicotinaldehydes.

Nicotinaldehydes have been reported as good competitive inhibitors for several nicotinamidases (French et al., 2010b). Thus, OiNIC was tested with nicotinaldehyde and 5-Br-nicotinaldehyde. Doubled-reciprocal plots confirmed competitive nature of the inhibition with nicotinamide in both cases (Figure 6.5, A and B). The K_i values for inhibition of nicotinaminidase were calculated using

Morrison quadratic equation (Graphpad prism 5) (see Materials and Methods), and in both cases, were lower than 5 μM (k_i for nicotinaldehyde was 3.4 μM and k_i for 5-Br-nicotinaldehyde was 4.4 μM. (Figure 6.5, C). These k_i values were similar to that of *S. Cerevisiae* Pnc1 (1.4 μM and 4 μM, respectively) but higher that that corresponding to the enzymes from *Plasmodium falciparum, S. Pneumoniae* and *Clostridium burgdorferi* with k_i in the nM range (French et al., 2010b).

2.7. Structural and phylogenetic analysis

The 3D structure of crystallized *S. pneumoniae* nicotinamidase (PDB code: 3O90, 53 % identity) (French et al., 2010a) was selected as a template by Geno 3D (Combet et al., 2002) to create a OiNIC model (Figure 6.6). The enzyme folds as a typical α/β protein with five-stranded β-sheets flanked by three helices on one side and four helices on the opposite side. This structure is characteristic of the Isochorismatase-like hydrolases superfamily that includes nicotinamidases /pyrazinamidases, *N*-carbamoylsarcosin amido hydrolases, YecD proteins, YcaC proteins, and PhzD proteins. These enzymes share a common structural fold, but catalyse different reactions in separate biochemical pathways. The active site of the modelled OiNIC dimer was located in a solvent-accessible pocket formed primarily by three loop regions containing residues 11-22 (between β1 and α1), residues 104-112 ((between β3 and α5), and residues 133-137 (between β4 and α6) (OiNIC numbering). The conserved catalytic triad of model was located at positions 10 (D10), 137 (C137), and 104 (K104). The involvement of the latter, K104, was demonstrated not only by the mutants described (K104 and Q96A), where the mutant lacking the lysine losses its activity completely while Q96A mutant maintains 97% activity, but also by the modelled enzyme.

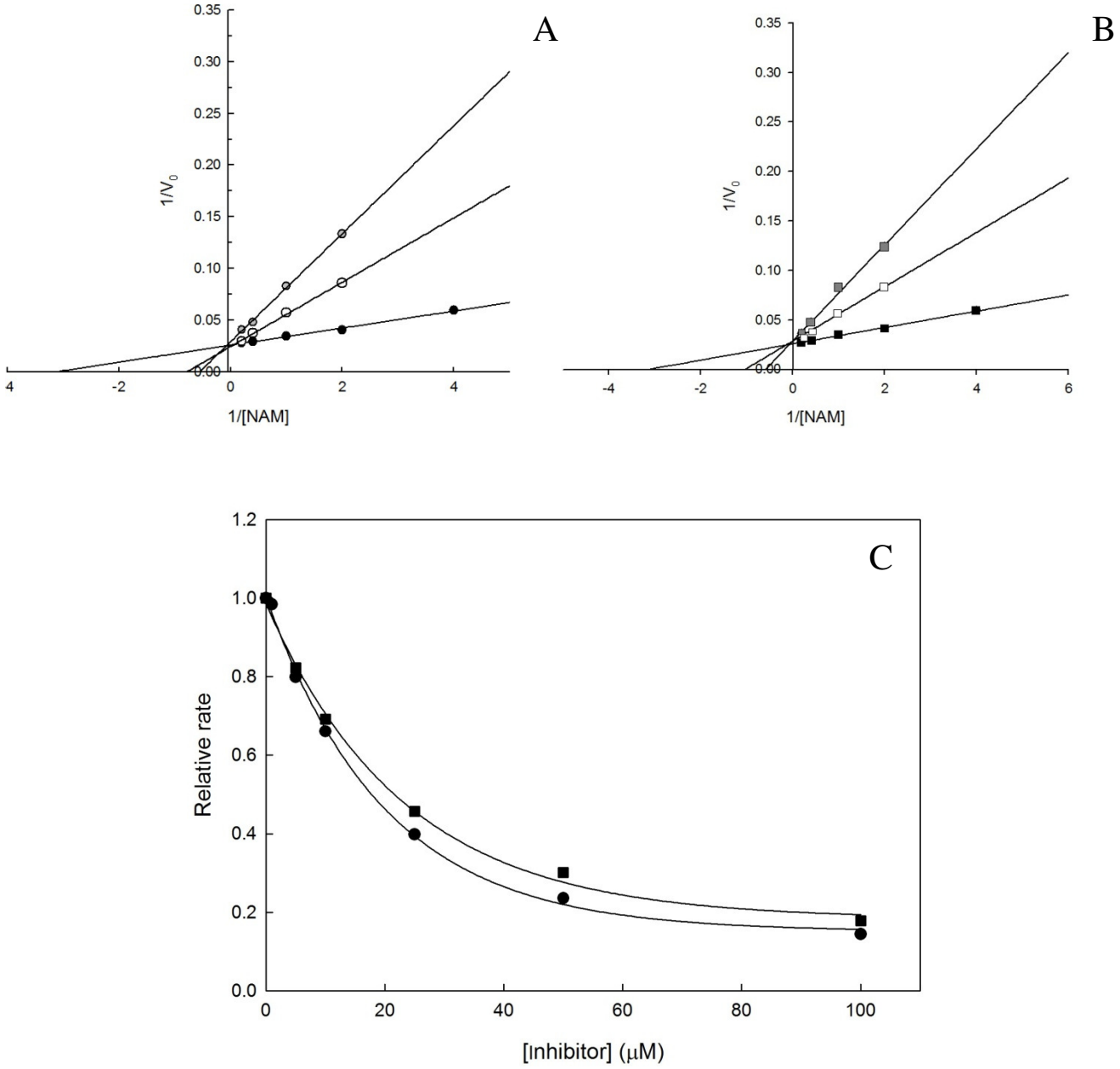

Figure 6.5. *Inhibición of OiNIC by nicotinaldehydes*. The Lineweaver-Burke plots for competitive inhibition by nicotinaldehyde (A) and 5-Br-nicotinaldehyde (B). Inhibition reactions were performed in 1 mL volume containing 100 mM sodium phosphate pH 7.3, 0.3 mM NADPH, 10 mM α-ketoglutarate, 9.7 μg BhGDH, 1.3 μg of OiNIC, and increasing concentrations of NAM in presence of 0 μM (filled symbol), 10 μM (open symbol) and 20 μM (grey symbol) of corresponding inhibitor at 37 ºC. C) Inhibition curves of the OiNIC by nicotinaldehyde (●) and 5-Br-nicotinaldehyde (■). The reactions at 37 ºC were carried out in the presence of 1 mM NAM and different concentrations of the inhibitor 100 mM sodium phosphate pH 7.3, 0.3 mM NADPH, 10 mM α-ketoglutarate, 9.7 μg BhGDH and 1.3 μg of OiNIC. Morrisons equation was used for fitting plotted data and for obtaining the K_i value as described in Materials and Methods.

The 3D-structure of OiNIC, clearly shows that Q96 is not in an appropriate position to interact with the substrate, while K104 is only 4.9 Å from NAM and in the correct orientation. This has been further confirmed by the study of K104A and Q96A mutants. The structural model also confirmed that D54, H56 and H72 are the residues implicated in binding the putative Zn^{2+} metal ion of the active site cavity, along with E65, which is structurally close enough to bind the metal ion.

A phylogenetic analysis was carried out with all putative bacterial nicotinamidase sequences found in the Uniprot database. Due to the huge amount of nicotinamidases among the bacterial kingdom, the sequences were processed to include just one strain from each species. With the information provided by the phylogenetic tree created with MEGA 4.0 (Tamura et al., 2007), it was possible to determine that nicotinamidases were clustered following the bacterial phylogenetic classification, where Gram+ bacteria (firmicutes and actinobacteria) were clustered together apart from Gram- bacteria (Proteobacteria, Spirochaeta, Aquifex, etc...). In addition, inside Gram+ bacteria, three clusters separated the phylum Firmicutes class Bacilli, from Firmicutes class Clostridia and from phylum Actinobacterias. Within the Gram– bacteria, phylum proteobacteria was separated in its normal clades: alpha, beta, delta, epsilon and gamma- proteobacterias (Figure 6.7). A few exceptions are observed, with some Gram- species belonging to phyla proteobacteria, bacteroidetes and aquificae, clustering closer to Gram + than to the general Gram- clade.

Since *Oceanobacillus iheyensis* belongs to the phylum firmicutes, a closer study of the sequences of firmicutes nicotinamidases was carried out and compared with that of 16S rRNA sequences (Figure 6.8 and 6.9). Once more, both phylogenetic trees were very similar, showing an overall evolution of the nicotinamidases in parallel with the evolution of bacterial species. However, a few evidences of horizontal gene transfer events seem to be clear. The cluster comprising the nicotinamidases of the genus *Lactobacillus*, clustered together with the nicotinamidases of the class Bacillales (*Bacillus, Oceanobacillus, Geobacillus*) instead of with the nicotinamidases from *Streptococcus*.

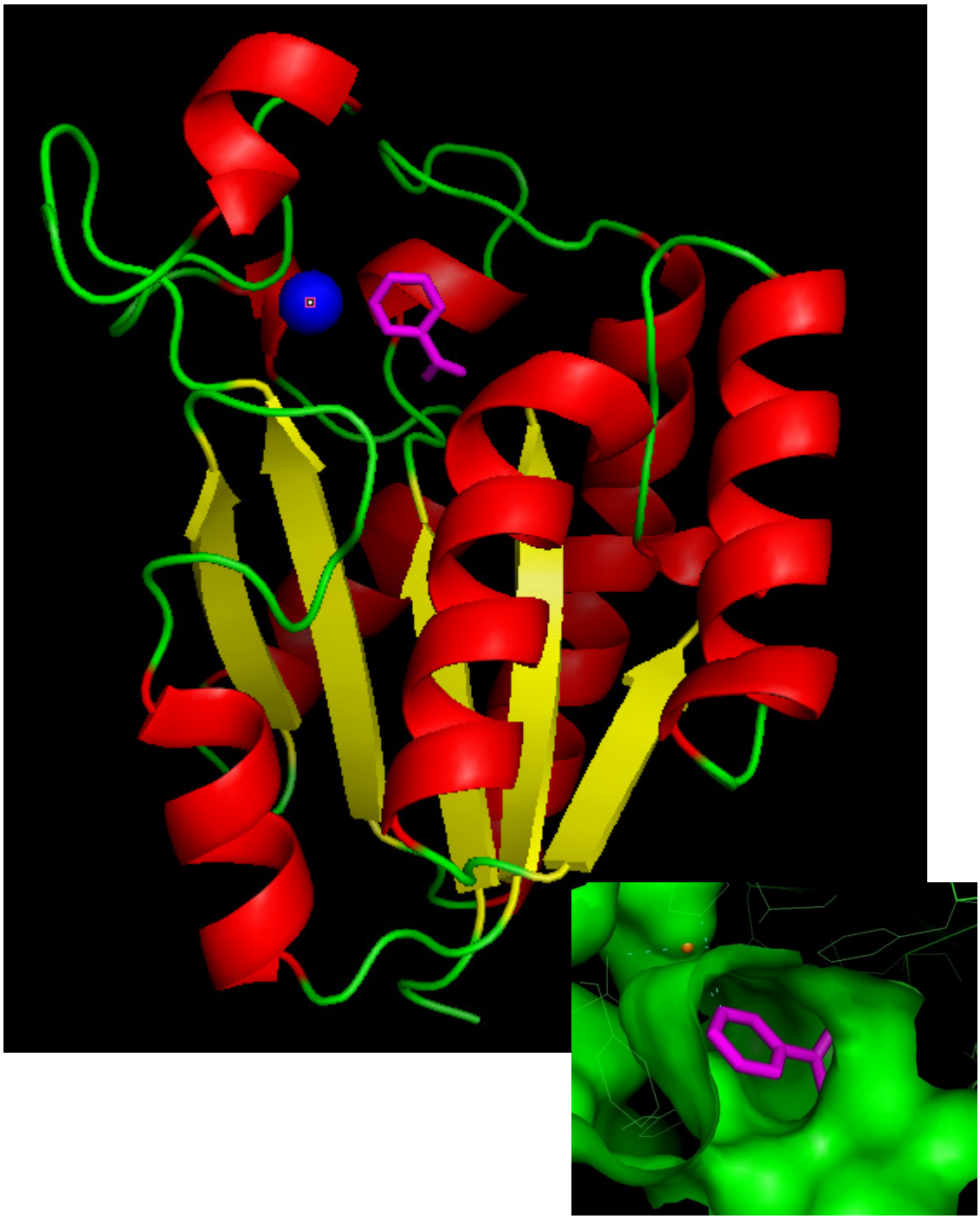

Figure 6.6. *3D modeled structure of the monomeric OiNIC* with a Zn^{2+} atom and a nicotinamide represented inside the cavity of the active site. Detail of the hydrophobic cavity with the substrate nicotinamide.

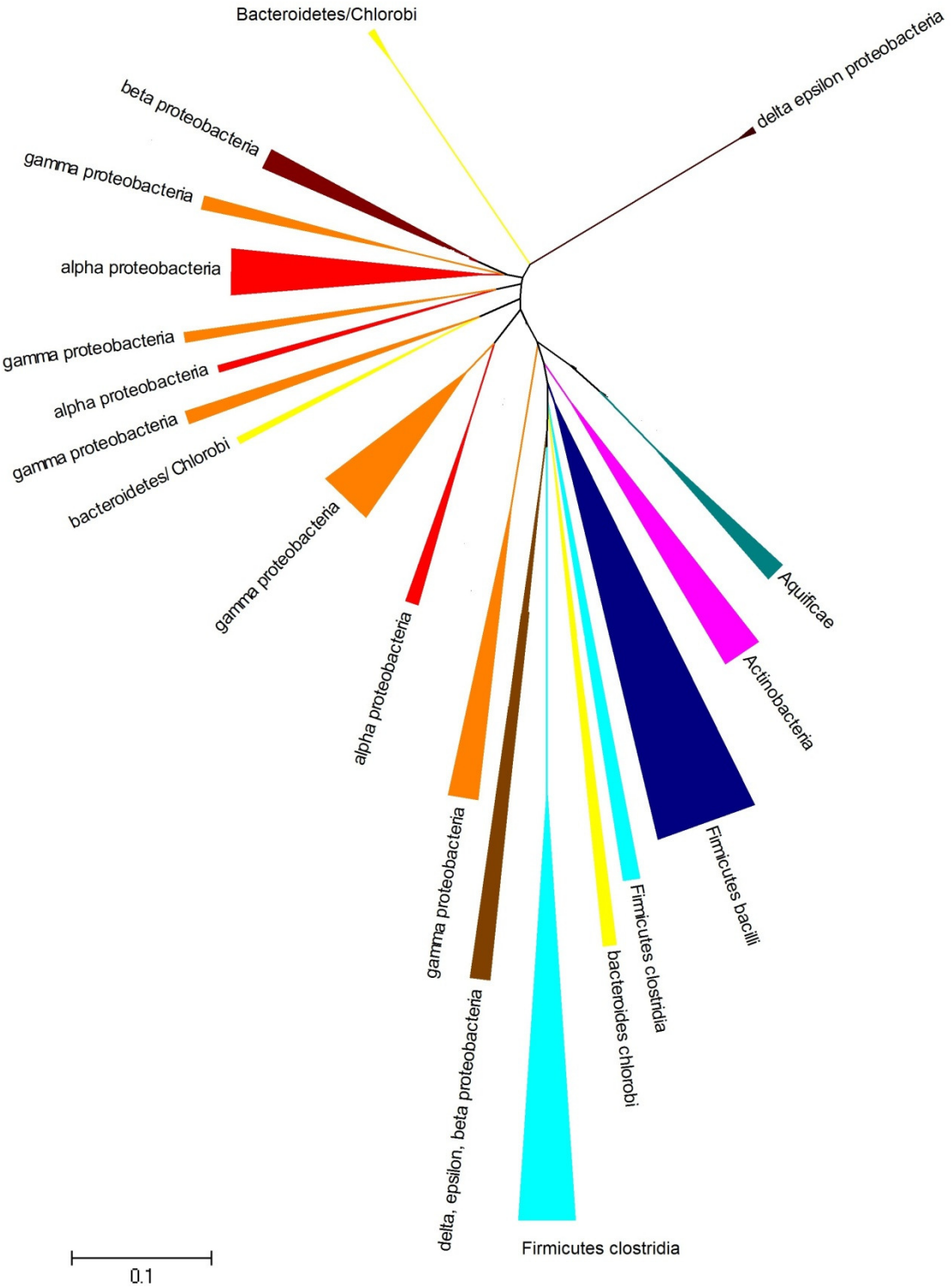

Figure 6.7. *phylogenetic distribution of bacterial nicotinamidases.*

Curiously, OiNIC clustered together with nicotinamidases from *Geobacillus kaustophilus* and *G. thermodenitrificans,* which appear as a separate clade in 16S rRNA tree. In the side of the phylogenetic tree that groups firmicutes of the class Clostridia, two separate clusters of *Clostridium* nicotinamidases showed a divergent evolution of the nicotinamidase gene (Figure 6.7 and 6.8).

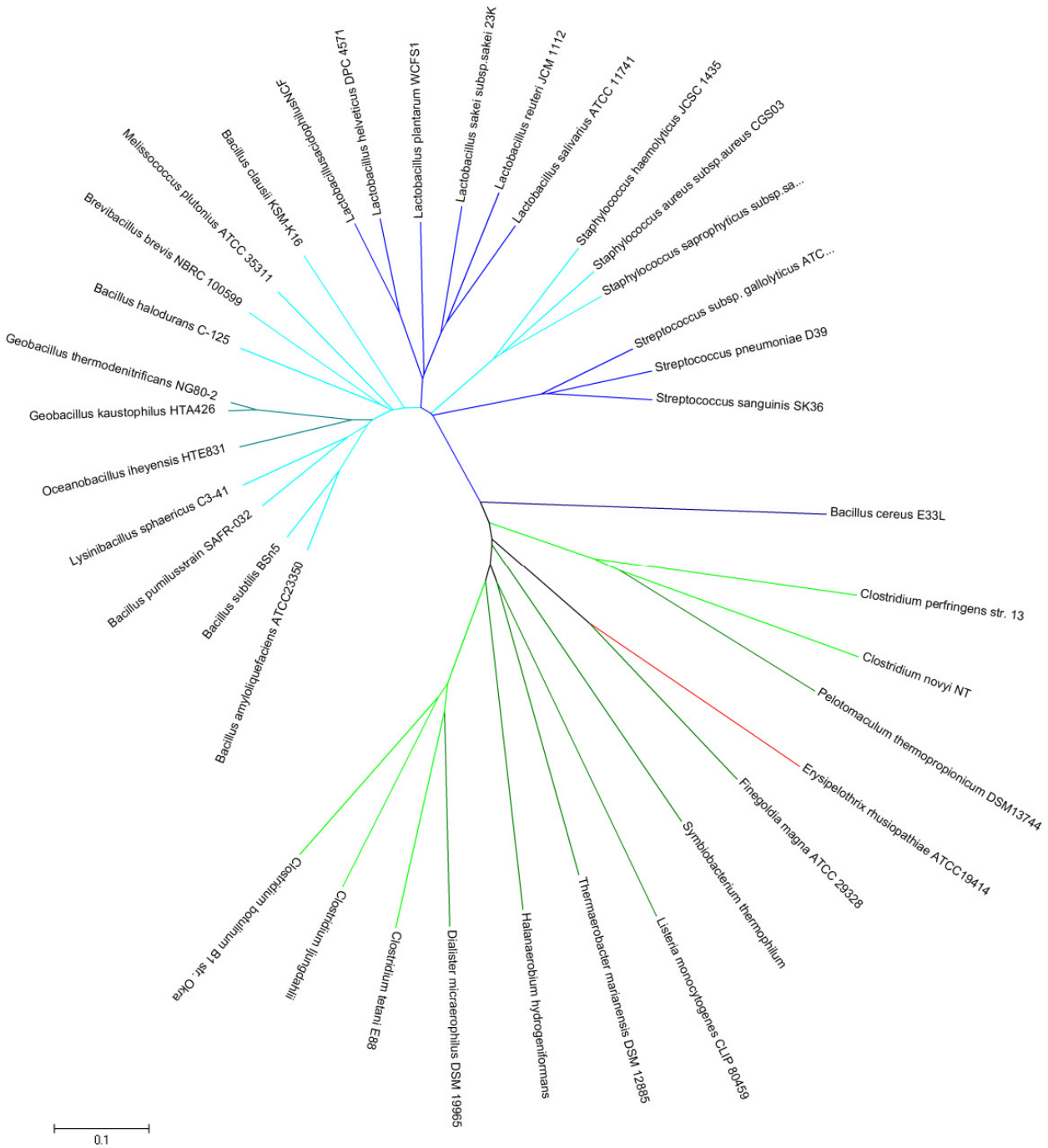

Figure 6.8. *phylogenetic distribution of nicotinamidases from phylum firmicutes*

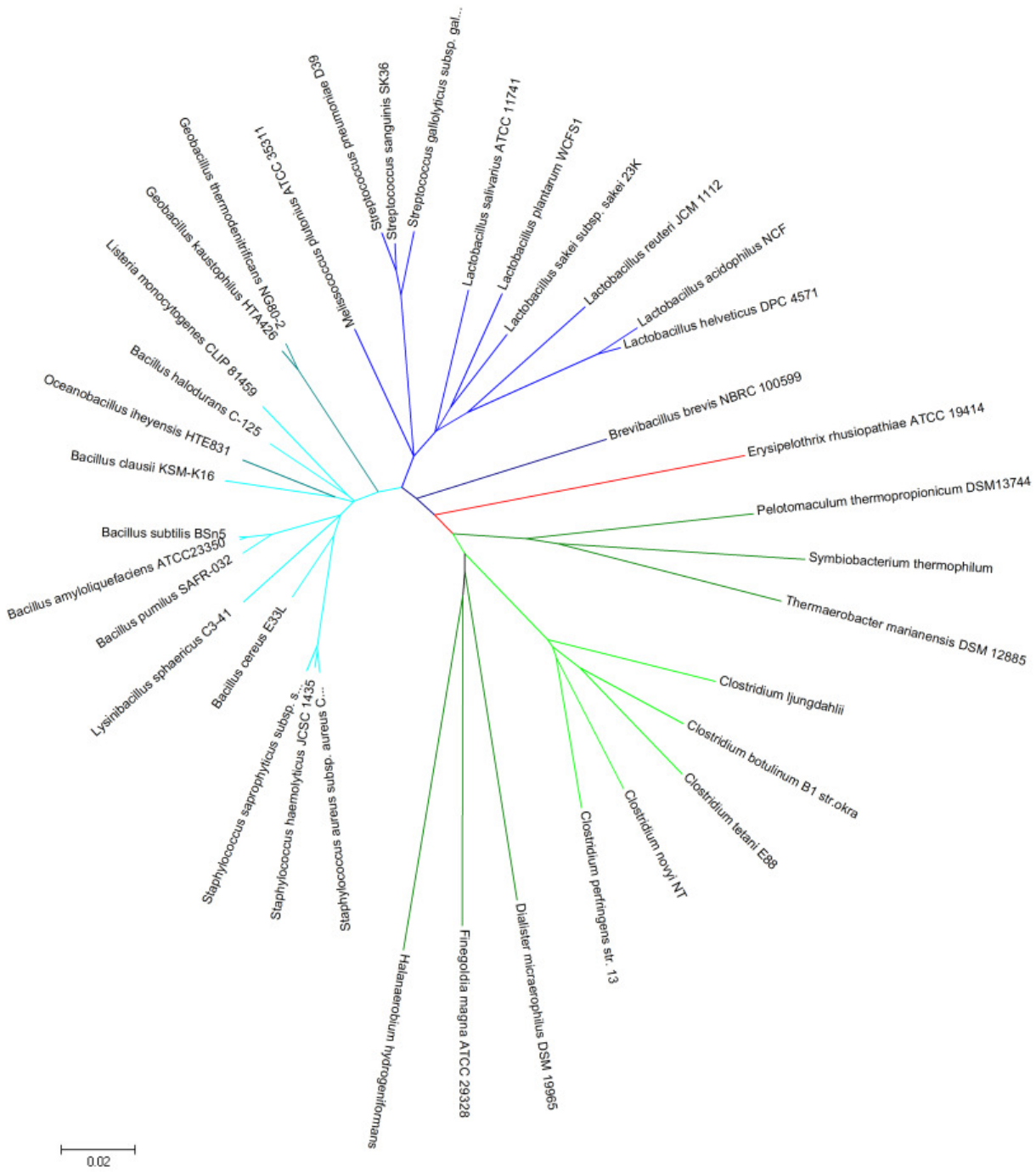

Figure 6.9. *16S rRNA phylogenetic distribution of the selected species.*

3. CONCLUSION

Nicotinamidases have gained biotechnological interest in the last years due to its great importance as possible therapeutic targets, its relation with the treatment of tuberculosis and especially due to its participation as modulators of sirtuin activity. In addition, they are also interesting tools for finding new sirtuin modulators, when used in a enzyme-coupled assay with glutamate dehydrogenase. However, little is known about these interesting enzymes. This chapter has been focused on the characterization of a novel nicotinamidases from *O. Iheyensis* HTE831. OiNIC has been cloned, overexpressed, purified and biochemically characterized. The enzyme, which binds Zn^{2+} in the active site, had broad substrate specificity, being active over several nicotinamide analogues and over the pro-drug pyrazinamide, although not as much as pyrazinamidases from *M. tuberculosis.* Inhibition studies demonstrate that OiNIC was strongly inhibited by nicotinaldehydes. The creation of several mutants of selected residues helped in the understanding of structure and function of nicotinamidases, confirming K104 as part of the catalytic triad, E65 as metal binding residue and C133 and F68 as residues involved in the substrate specificity of OiNIC, by modifying the shape and volume of active center. Changes of those residues to A133 and W68 respectively, generates mutants with increased pyrazinamidase activity. Finally OiNIC was modelled to further study the structural characteristic of the active site and phylogenetic analysis were carried out in order to improve our understanding on the evolution of these enzymes, whose classification remains unclear.

VII. Characterization of a new Glutamate dehydrogenase from *Bacillus halodurans* C-125 as a tool for High-Throughput screening of nicotinamidases

Contenido inhibido autorizado por Comisión General de Doctorado de fecha 15 de Febrero de 2013

VIII. Development of a new coupled assay for the characterization of a novel nicotinamide mononucleotide deamidase from *Oceanobacillus iheyensis* HTE-831

Contenido inhibido autorizado por Comisión General de Doctorado de fecha 15 de Febrero de 2013

IX. General discussion

The enzymes studied in this Thesis are all considered biotechnologically relevant. Enzyme-based processes are already quite prominent in the production of fine-chemicals and pharmaceuticals (Schmid et al., 2001). As these products often include new and/or chiral compounds, it is easier for biotechnology to compete with traditional organic chemistry methods, especially if a new process is more economical and raw materials and other resources are used more efficiently (van Beilen & Li, 2002). Among the pharmaceutical compounds, those related with sialic acids are relevant to glycobiotechnology. *N*-acetylneuraminate lyase (NAL) catalyzes the reverse aldol condensation reaction and has been used in this way to synthesize sialic acid and some of its derivatives from pyruvate and *N*-acetyl-D-mannosamine (Huang et al., 2007; Wong & Whitesides, 1994; Yu et al., 2004). These derivatives include the anti-influenza virus agent named Zanamivir, which can be used in treating and preventing the infection of both influenza types A and B (such as the avian influenza virus H5N1) (Kawai et al., 2009). New compounds are now under development. Interest in this aspect of the enzyme's activity based on the role of sialic acid in controlling biomolecular interactions, particularly at the cell surface is related to cancer and immunological diseases (Angata & Varki, 2002; Chen & Varki, 2010; Li & Chen, 2012). Thus, a cheap source of sialic acid is needed to fulfill future demand for pharma compounds. Improvements in NAL to reduce costs and to increase yield are needed. A compulsory step to reach this goal is a simple and efficient screening method, as that using Lactate dehydrogenase.

Another relevant enzymes used in this thesis are nicotinamidases, which are involved in maintaining the NAD homeostasis in the bacterial cells. This fact makes them possible therapeutic targets due to the absence of nicotinamidases in human genome. The importance of these enzymes also relies, on their relation with the treatment of tuberculosis. These nicotinamidases are also important in controlling sirtuin activity, by avoiding its inhibition by nicotinamide. In addition, the recent development of a continuous spectrophotometric method to measure sirtuins with nicotinamidases and glutamate dehydrogenase has opened a new simple screening method for finding new modulators for sirtuins in order to treat cancer, obesity, Alzheimer and Parkinson. Another enzyme involved in the bacterial NAD metabolism, forming part, as well as nicotinamidases, in the Pyridine Nucleotide Cycles are Nicotinamide mononucleotide deamidases (OiPncC). NMN is a by-product of NAD-consuming enzymes such as DNA ligase (Foster & Moat, 1980; Hillyard et al., 1981). The lack of those enzymes in human genomes (Vrablik et al., 2009) points out PncCs as possible drug targets.

1. *Molecular characterization of the N-acetylneuraminate lyase from* Lactobacillus plantarum *WCFS1.*

This chapter described the cloning, overexpression and a detailed characterization of a novel *N*-acetylneuraminate lyase (*nanA*) from *Lactobacillus plantarum* WCFS1 (LpNAL), and compared it with that of *Escherichia coli* K-12 Substr. MG1655 (EcNAL) in the same cloning system. The results obtained showed that LpNAL reaches a higher expression level Up to 215 mg of Ni^{2+}-column-purified LpNAL could be obtained from 1 L of *E. coli* BL21(DE3)pLys culture, which is 2.6-fold higher than the expression level achieved by the cloned EcNAL (82 mg L^{-1} cell culture) and 2.2-fold higher than the best expression level reported for NAL (94 mg L^{-1} cell culture) (Table 4.1). The enzyme showed good catalytic efficiency, being its K_M for Neu5Ac cleavage (1.8 ± 0.1 mM), lower than the K_M for the recombinant EcNAL (2.8±0.2 mM) and lower than the reported values for *E. coli* NAL (2.5± 0.3 mM) and for *P. multocida* (4.9 ± 0.7 mM) (Li et al., 2008). Both enzymes have optimum pH around 7.0 (Figure 4.4), showing an activity-dependence of the buffer composition. In addition, both enzymes were remarkably thermostable, finding improved stability in the presence of additives (T_m for LpNAL in MilliQ® water 71.5 ºC, T_m for LpNAL in presence of 1 M ammonium sulphate, 78.9 ºC) (Figure 4.7). The detailed study of LpNAL and EcNAL topology and phylogeny (Figures 4.10-4.12), along with that of other neu5Ac aldolases from the database, led to a new classification of bacterial NALs into four groups. The first group, to which LpNAL belongs, included enzymes from Gram-negative genera, *Haemophilus*, *Actinobacillus*, *Pasteurella,* as well as Gram-positive genera, *Lactobacillus, Clostridium, Staphylococcus* and *Mycoplasma,* and also Fusobacteria. Group 2 includes NAL sequences from *E. coli, Shigella spp., Salmonella enterica,* which all are human gastrointestinal pathogens and have high sequence identities (~ 90-100 %). *Streptococcus* genera, some species of *Lactobacillus* (*L. sakei*), *Clostridium* (*C. bolteae, C. hylemonae),* and other human gut commensal such as *Ruminococcus gnavus* or *Dorea formicigenerans* make up group 3. Finally, group 4 is formed by NAL proteins with low sequence identity from members of the family Vibrionaceae, Shewanelaceae, Psychromonadaceae, Pseudoalteromonaceae and some species of genera *Bacteroides, Parabacteroides* and *Capnocytophaga*. This group has been

divided into three subgroups formed by bacteria (4.1, 4.2, and 4.4). Subgroup 4.4 is related with some mammalian NALs (subgroup 4.3), including human, indicating lateral gene transfer from bacteria from group 4 to mammals.

This LpNAL with remarkable features was used as template for further directed evolution libraries.

2. *High-yield production of a new L-lactate dehydrogenase from* Bacillus halodurans *C-125 as a tool for screening directed evolution libraries.*

3. *Characterization and classification of a novel* Oceanobacillus iheyensis *HTE831 nicotinamidase.*

Nicotinamidases are also relevant enzymes in pharma and biotechnology to develop new antibacterial and to find new modulators of sirtuins. Therefore, is this chapter aimed to cope the cloning, overexpression and a detailed characterization of the nicotinamidase gene (*OiNic*) of the extremophile microorganism *Oceanobacillus iheyensis* HTE 831. The nicotinamidases catalyze the deamination of nicotinamide to produce ammonia and nicotinic acid, The latter compound is converted back to NAD^+ in a series of reactions catalyzed by other enzymes in the NAD^+ salvage pathways where nicotinamidases play an important role in many organisms, ranging from bacteria (French et al., 2010), and mycobacteria (Boshoff & Mizrahi, 1998; Zhang et al., 2008), to yeast (Ghislain et al., 2002; Hu et al., 2007; Joshi & Handler, 1962; Scorpio & Zhang, 1996), protozoa (Zerez et al., 1990) and even plants (Wang & Pichersky, 2007) and invertebrates, such as *Drosophila melanogaster* (Balan et al., 2008) or *Caenorhabditis elegans* (van der Horst et al., 2007). OiNIC was found to be a good catalyst (k_{cat} 10.6 s^{-1} for NAM and 2.6 s^{-1} for PZA, Table 6.2) and stable from acid to neutral pHs. The enzyme, which binds Zn^{2+} in the active center, was active towards different nicotinamide analogues, including the pro-drug pyrazinamide, used in the tuberculosis treatment. Mutants of selected residues were designed to find critical amino acids for catalysis and metal binding. The results found K104 as part of the catalytic triad, E65 as metal binding residue and C133 and F68 as residues involved in the substrate specificity of OiNIC, by modifying the shape and volume of active center. In fact, mutants C133A and F68W, showed increased pyrazinamidase activity compared to

the wild-type (Table 6.2). Finally OiNIC was modelled to further study the structural characteristic of the active site and phylogenetic analysis were carried out in order to improve our understanding on the evolution of these enzymes.

4. *Characterization of a new Glutamate dehydrogenase from* Bacillus halodurans *C-125 as a tool for High-Throughput screening of nicotinamidases.*

5. *Development of a new coupled assay for the measure and characterization of a novel nicotinamide mononucleotide deamidase from* Oceanobacillus iheyensis *HTE-831*

X. CONCLUSIONS

From the results presented in this Thesis, the following conclusions could be obtained:

1. The *N*-acetylneuraminate lyases (NALs) from *Lactobacillus plantarum* WCFS1 and *Escherichia coli* K-12 MG1655 were successfully cloned in *E. coli*. They were over-expressed and purified to obtain stables 132 kDa and 146 kDa homotetrameric proteins, respectively. Both enzymes were able to cleave Neu5Ac with a similar catalytic efficiency to the best previously described NALs. These enzymes show good stability and activity under alkaline pH conditions and a wide range of temperatures (up to 70 ºC). In addition to these biotechnologically useful characteristics, the phylogenetic analysis of LpNAL, and other related bacterial NAL from the databases, led to a new classification of bacterial NALs into four groups and three subgroups (4.1, 4.2 and 4.4). Among these groups, subgroup 4.4 was related with some mammalian NALs (subgroup 4.3), including human. This new phylogenetic analysis supports for the first time the hypothesis of a gene transfer of NAL from group 4 bacteria to mammals.

2. Chapter V conclusion.

3. A novel nicotinamidase from *O. Iheyensis* HTE831 (OiNIC) was cloned, overexpressed and biochemically characterized. The metalloenzyme bound Zn^{2+} in the active site and had a broad substrate specificity, being active towards several nicotinamide analogues, including the pro-drug pyrazinamide, but with 10-fold less activity compared to nicotinamide. OiNIC was also strongly inhibited by nicotinaldehydes, with k_i values in the μM range. Several mutants were carried out to understand the structure-function relationship of nicotinamidases, confirming that Lys104 was part of the catalytic triad, Glu65 was involved in metal binding, and C133 and F68 were modulating the substrate specificity of OiNIC, by affecting the shape and volume of active center. Thus, mutants Cys133Ala and Phe68Trp showed higher pyrazinamidase activity than parental enzyme. Finally, its phylogenetic analysis showed OiNIC more closely related to *Geobacillus* species than to *Bacillus* species, as expected from the 16S rRNA tree, indicating an evolutive divergence of this nicotinamidase.

4. Chapter VII conclusion.

5. Chapter VIII conclusion.

XI. Spanish Version

XI. Resumen en Castellano

INTRODUCCIÓN

1. BIOTECNOLOGÍA DE ENZIMAS

Las enzimas son biocatalizadores de notables capacidades capaces de aceptar un amplio rango de moléculas complejas como substrato y de forma muy selectiva, catalizando reacciones con selectividad quiral (-enantio) y posicional (-regio). Los biocatalizadores pueden, por tanto, usarse en biotransformaciones sin necesidad de las complejas etapas de bloqueo y desbloqueo, comunes en la síntesis orgánica regio y enantioselectiva. Esta elevada selectividad también permite reacciones eficientes con pocos co-productos, convirtiendo a las enzimas en una alternativa a la catálisis química convencional de una forma respetuosa con el medio ambiente. Estos atributos de las enzimas encuentran diversas aplicaciones especialmente en la industria alimentaria y farmacéutica, en las que se requiere elevada selectividad de las reacciones con sustratos complejos.

El desarrollo de un proceso biocatalítico (Figura 1.1) implica diversas etapas, en las que se debe identificar un biocatalizador en primer lugar, establecer un proceso industrial y finalmente la bioconversión resultante de ese proceso debe ser viable económicamente. Los procesos basados en el uso de enzimas están siendo utilizados en la producción de compuestos químicos y farmacéuticos. Dentro de la producción de compuestos farmacéuticos, aquellos relacionados con el ácido siálico tienen gran relevancia en el campo de la glicobiotecnología. Otro factor de interés en el sector farmacéutico, es el elevado número de compuestos que deben ser testados en busca de actividad biológica para encontrar un solo compuesto prometedor. Respecto a esto, los ensayos enzimáticos de cribado masivo han atraído mucha atención, ya que permiten aumentar la complejidad y diversidad de librerías de compuestos químicos pre-existentes o la producción de librerías *de novo*. Un ejemplo es el cribado de compuestos bioactivos relacionados con el envejecimiento y más concretamente, de compuestos capaces de modular la actividad de sirtuinas.

La mejora en la eficiencia y precisión de la enzimas utilizadas en este tipo de ensayos se persiguen mediante ingeniería racional o mediante técnicas de evolución dirigida. Esta última comienza generalmente con la creación de una librería de genes mutados. Las proteínas producto de estos genes que muestren

mejoras respecto a la propiedad deseada, se identifican por selección y cribado (Figura 1.2). Las librerías de proteínas se criban generalmente en placas de 96 pocillos, utilizando parámetros de selección. Este y otros métodos de generación de nuevas variedades proteicas mejoradas se deben repetir o combinar hasta la generación de un biocatalizador con las propiedades deseadas.

2. ÁCIDO SIÁLICO

El ácido siálico y sus derivados forman una familia de oligosacáridos que llevan a cabo funciones esenciales para el mantenimiento de las actividades celulares. Estos oligosacáridos se encuentran normalmente desplegados en la superficie de la membrana celular, y participan en funciones tales como el reconocimiento celular o la transmisión de señales. Químicamente, estos compuestos son 2-keto-3-deoxi ácidos polihidroxilados con más de seis carbonos. Todos son derivados del ácido *N*-acetilneuramínico (Neu5Ac) y del ácido 2-ceto-3-deoxi-D-glicero-D-galacto-2-nonulosólico (KDN). Se conocen más de 60 derivados de estos dos compuestos que presentan distintas modificaciones en distintos carbonos (Figura 1.3).

El Neu5Ac fue descubierto por Klenk en los años 30 y fue nombrado de esta forma debido a fue aislado de glicoproteínas de células de cerebro. Posteriores investigaciones dilucidaron su estructura (Figura 1.3) y el nombre "ácido siálico" fue propuesto como nombre para el grupo de todos los *O*- y *N*- derivados del Neu5Ac. Sin embargo, en sentido estricto el nombre "ácido siálico" se sigue refiriendo al Neu5Ac. El ácido siálico se sintetiza mediante la condensación de un monosacárido de 4 a 6 carbonos y el PEP, y a diferencia de otros monosacáridos su forma activada para ser transferido a la célula es CMP-Neu5Ac.

Sus principales funciones *in vivo* son:

1. Dotar de carga negativa a los glucoconjugados presentes en las membranas celulares.
2. Determinar la estructura macromolecular de ciertas glicoproteínas.
3. Transferencia de información entre células.
4. Reconocimiento específico de glucoconjugados y de células basado, en bio-activos específicos.

En mamíferos, se pueden encontrar en el extremo distal de la cadena de oligosacáridos de glicoproteínas y glicolípidos, y su carga negativa los hace determinantes en la regulación de ciertos procesos, tales como la adhesión celular y el reconocimiento entre células. Entre los procesos biológicos que desempeñan en mamíferos cabe destacar su implicación en el desarrollo neural durante la embriogénesis y los primeros meses de vida, su participación en la respuesta inmune a patógenos (lectinas, selectinas y Factor H) y en la inflamación, y también se ha demostrado su implicación en ciertos tipos de cáncer, y su mediación en la metástasis (ver Figura 1.4). Del mismo modo, ciertos patógenos como *Haemophilus influenzae* utilizan el ácido siálico para mimetizar células humanas, y así, poder colonizar e infectarlas.

3. INTERÉS BIOTECNOLÓGICO DEL ÁCIDO SIÁLICO.

El principal interés biotecnológico del Neu5Ac es su uso como precursor de ciertos antivirales para el tratamiento de la gripe estacionaria, la gripe aviar (H5N1) o el reciente brote de la variante H1N1. Basándose en la estructura tridimensional de la neuraminidasa de *H. influenzae*, se diseñó el antiviral Zanamivir. Este fármaco es inhibidor del virus influenza A y B, con una IC50 ≈ 5 nM. Además se ha sintetizado un derivado de este compuesto que es inhibidor selectivo de la sialidasa de la variante A del virus de la influenza. Debido a la aparición de ciertas cepas resistentes a las concentraciones no tóxicas de Tamiflu (oseltamivir) el tratamiento con Zanamivir, solo o en combinación con Tamiflu, está siendo utilizado para el tratamiento y la prevención de brotes de gripe estacionales tales como el ocurrido en 2009 con la variante H1N1.

Una de las principales funciones del ácido siálico es su implicación en el desarrollo neural. El sistema nervioso, y en concreto el cerebro, es uno de los sistemas que más rápido se desarrolla durante el periodo embrionario y en los primeros años de vida (el cerebro supone el 15% del peso total del cuerpo), por ello es extraordinariamente importante que durante este desarrollo, especialmente en las primeras etapas, no se produzca ningún déficit en las necesidades nutritivas. En diversos estudios se han comprobado los efectos beneficiosos de la leche materna. Esta leche se caracteriza por su alto contenido en oligosacáridos comparado con otras leches de origen animal. La mayoría de estos oligosacáridos se encuentran unidos a Neu5Ac o derivados, por lo que éste se ha estado utilizando como

nutracéutico en leche, y preparados alimenticios para niños, aunque aún no se conoce exactamente la composición ideal de oligosacáridos para que dicha suplementación sea efectiva.

Como ya se ha mencionado anteriormente, los ácidos siálicos se encuentran presentes en todas las células, formando parte de las últimas fracciones de las cadenas de azúcares que recubren estas. La enzima citidina monofosfato *N*-acetilneuramínico hidroxilasa (CMAH) convierte neu5Ac en ácido *N*-glicolilneuramínico (Neu5Ac). Este compuesto es reconocido por varias proteínas endógenas, así como virus y bacterias, en mamíferos no humanos. Sin embargo, debido a una mutación en CMAH, los humanos no pueden sintetizar neu5Gc endógeno, siendo este inmunogénico en humanos. Se ha descrito que neu5Gc puede ser el responsable de la respuesta inmune generada cuando se entra en contacto con productos de mamíferos no humanos, como cosméticos, líneas celulares, alimentos o agentes terapéuticos. Un método para reducir los niveles de neu5Gc en estos productos, basado en la utilización de neu5Ac se ha descrito recientemente (Figura 1.6). El método se basa en la inundación del sistema con neu5Ac, o análogos, derivados o precursores de este. El neu5Ac en exceso compite con neu5Gc por su activación por la enzima CMP-Sia sintetasa, reduciendo de este modo los niveles de neu5Gc incorporados en las cadenas de azúcares que revisten las células.

El principal inconveniente de la producción biotecnológica de Neu5Ac hasta la fecha ha sido su elevado precio en el mercado (50-100 $ g-1). Este elevado precio es debido a su método convencional de preparación a partir de fuentes naturales como la leche, el huevo o el ácido colomínico. Se han planteado alternativas para abaratar este proceso, entre las cuales se encuentra la síntesis enzimática para lo cual se necesita una fuente que pueda proveer las enzimas implicadas en la síntesis en grandes cantidades. Las enzimas bacterianas implicadas en la síntesis y degradación del Neu5Ac podrían ser una buena opción, pero para ello, es necesario previamente un estudio detallado de cómo funciona el metabolismo del ácido siálico entre las bacterias.

4. METABOLISMO DEL ÁCIDO SIÁLICO EN BACTERIAS.

Debido a que los ácidos siálicos predominan en animales complejos, sobre todo en mamíferos, es lógico pensar que existan microorganismos capaces de

realizar su metabolismo íntimamente asociados a ellos, bien sea como comensales o como patógenos. Diferentes estudios, en los que se han aislado mutantes de *E. coli* K1 incapaces de metabolizar el ácido siálico, han demostrado la presencia de un operón para el metabolismo del Neu5Ac inducible según su disponibilidad. Este operón cuenta con 4 genes: *nanT*, *nanA*, *nanE* y *nanK* y *nanA* fueron los primeros en descubrirse, y su función está relacionada con el transporte del Neu5Ac al interior de la célula (*nanT*) y con la degración del mismo a *N*-acetil manosamina (ManNAc) y piruvato (*nanA*; Neu5Ac aldolasa, NAL). Posteriormente se comprobó que *nanK* es una kinasa dependiente de ATP para ManNAc y que *nanE* epimeriza ésta ManNAc-6P generando GlcNAc-6P. Desde entonces se ha considerado un sistema *nan* completo, aquel que mínimamente incluya estos cuatro genes.

5. *N*-ACETILNEURAMINIDATO LIASA

Neu5ac aldolasa, ácido siálico aldolasa o *N*-acetilneuraminidato liasa (NAL, EC 4.1.3.3) es una aldolasa de tipo I, que cataliza la ruptura del Neu5Ac para formar ManNAc y piruvato mediante la formación de una base de Schiff. El equilibrio de la reacción favorece la formación de ManNAc, y está considerada como una enzima clave en la regulación del metabolismo del ácido siálico. Esta enzima también cataliza la reacción contraria, por lo que el interés en esta reacción ha ido creciendo, debido a su uso potencial en la síntesis de Neu5Ac y sus derivados. Así NAL ha sido clonada de varios microorganismos, incluyendo patógenos (*E. coli* o *H. influenzae*) y no patógenos (*Lactobacillus plantarum* WCFS1) y su estructura tridimensional ha sido resuelta. NAL es un homotetrámero cuyos monómeros consisten en un barril (α/β)8, con tres α-hélices en el C-terminal. Su mecanismo de acción consiste en la formación de una base de Schiff en la que interviene un residuo lisina altamente conservado. Esta lisina interactúa sobre el C2 del piruvato, que a su vez forma puentes de hidrógeno con residuos serina y treonina, también altamente conservados (Figura 1.8).

Como se ha mencionado antes, NAL también cataliza la reacción de condensación entre ManNAc y piruvato para dar Neu5Ac, y ha sido utilizada para la producción de Neu5Ac. La posibilidad de obtener esta enzima de forma recombinante ha hecho que esta sea la ruta preferida para la síntesis de Neu5Ac, a

gran escala. Sin embargo, existen ciertos inconvenientes a la hora de llevar a cabo su aplicación industrial:

1. ManNAc es un sustrato muy caro y debe ser sintetizado desde GlcNAc por epimerización. Sin embargo, el equilibrio está desplazado hacia la producción de GlcNac (4:1).
2. ManNAc y GlcNAc tienen propiedades químicas muy parecidas, por lo que son difíciles de separar.
3. Aunque GlcNAc no es sustrato de la enzima, sí que es un inhibidor.
4. La K_M para ManNAc es alta.
5. El papel normal de la enzima es el contrario, por lo que el equilibrio está desplazado hacia la hidrólisis en ManNAc y el piruvato. Este problema se ha intentado solventar llevando el equilibrio hacia Neu5Ac usando un exceso de piruvato en la reacción hasta 10 veces más.

Algunos procesos han ofrecido soluciones parciales a estos inconvenientes. Así, en 1997, Glaxo publicó un método eficaz para la producción de Neu5Ac a partir de ManNAc y piruvato usando NAL. Entre las modificaciones propuestas estaba la producción química de ManNAc a partir de GlcNAc a pH alcalino. A pesar de que estos procesos son eficientes en la producción de Neu5Ac, sigue existiendo el inconveniente de que usar ManNAc es económicamente inviable debido a su elevado precio.

6. SIRTUINAS Y NICOTINAMIDASAS

Las sirtuinas (SIRT) pertenecen a la clase III de desacetilasas dependientes de NAD^+, que catalizan la desacetilación de residuos acetilados de proteínas clave, involucradas en una gran variedad de funciones celulares, incluyendo la homeostasis de la glucosa, extensión de vida media, regulación del ciclo celular, apoptosis, reparación del DNA y neurodegeneración. En humanos se han descrito siete productos de genes de sirtuinas distintos, localizados en distintos compartimentos celulares e implicados en distintos procesos (Figura 1.11). Se han descrito así mismo varios inhibidores de sirtuinas, así como activadores de estas. La nicotinamida (NAM) es uno de los inhibidores de sirtuinas, siendo un coproducto de la propia reacción de desacetilación de éstas a partir de NAD.

La asociación de sirtuinas con ciertas enfermedades, donde se ha descrito que su activación puede proteger en cierta medida de enfermedades neurodegenerativas y desórdenes metabólicos, ha aumentado el interés en el descubrimiento de pequeñas moléculas moduladoras de sirtuinas, para el desarrollo nuevos agentes terapéuticos frente a Alzheimer, Parkinson, diabetes o cáncer.

Varios ensayos se han descrito para determinar la actividad de sirtuinas, la mayoría de ellos de elevada complejidad y siendo todos ensayos a punto final. El único método continuo fue desarrollado recientemente por el grupo de Denu, en el cual la NAM producida por las enzimas SIRT se convierte en ácido nicotínico y amonio, por acción de una nicotinamidasa. El amonio es transferido a α-cetoglutarato a través de una glutamato deshidrogenasa, rindiendo L-glutamato y oxidación de NADPH a $NADP^+$, que se detecta espectrofotométricamente a 340 nm. El mayor inconveniente de este método es el coste de las enzimas utilizadas.

La enzima nicotinamidasa no ha sido muy estudiada, existiendo hasta el momento únicamente algunos datos de enzimas provenientes de bacterias patógenas como *Salmonella, Acinetobacter* y *Mycobacterium*. También se ha descrito en arqueas (*Pyrococcus horikoshii*) y en levaduras y organismos superiores como *Saccharomyces cerevisiae* y *Drosophila melanobaster*, en los que se ha demostrado que su sobreexpresión se correlaciona con una extensión de la vida media, fenómeno ligado a la activación de sirtuinas mediante el consumo de nicotinamida, inhibidor de éstas.

La nicotinamidasa presenta otro beneficio fortuito, ya que la enzima de *Mycobacterium tuberculosis* convierte el pro-fármaco análogo de nicotinamida, pirazinamida, en ácido pirazinóico, que muestra características bactericidas y se utiliza en el tratamiento de la tuberculosis.

Sorprendentemente esta enzima no se encuentra en vertebrados. En los microorganismos la enzima forma parte del ciclo de reciclado de NAD^+, en el que también participan las sirtuinas. Inhibidores de esta enzima podrían utilizarse como diana terapéutica en microorganismos patógenos que no presentan síntesis *de novo* de NAD^+, dependiendo en exclusiva de las rutas de reciclado para la síntesis del cofactor.

Por todo lo anterior, parece claro que el estudio de nicotinamidasas es de interés no sólo como herramienta para la medida de sirtuinas, sino también para aumentar el conocimiento sobre la regulación entre estímulos ambientales, sirtuinas y

biosíntesis de NAD^+ para el desarrollo de nutracéticos o fármacos anti-edad eficientes.

7. CICLO DE LA PIRIDINA NUCLEÓTIDO Y METABOLISMO DE NAD^+ EN BACTERIAS.

NAD^+ y $NADP^+$ son compuestos de incalculable importancia en el metabolismo celular, participando en numerosas reacciones anabólicas y catabólicas. Además NAD^+ sirve de sustrato para muchas enzimas como es el caso de DNA ligasa o sirtuinas. Por tanto existe un elevado interés en el estudio de la síntesis, reciclado y regulación de NAD^+.

El ciclo de la piridina nucleótido (PNC) es un conjunto de reacciones para el reciclado de productos del consumo endógeno de NAD^+, para la formación de nuevo del coenzima y para el reciclado de bases piridínicas como precursores de NAD^+. En bacterias, los productos resultantes de las enzimas que consumen NAD^+, NAM y nicotinamida mononucleótido (NMN), se reciclan de nuevo a NAD^+ a través del PNC (Figura 1.15). Se han descrito dos PNCs, el primero (PNC VI) convierte NAM en ácido nicotínico (NA) que es transformado a ácido nicotínico mononucleótido (NaMN), que entra en la ruta de Preiss-Handler para ser transformado en NAD^+. El segundo ciclo (PNC IV) parte de NMN, sustrato que es desaminado por NMN desaminasa a NaMN que se incorpora a la misma ruta de Preiss-Handler.

La enzima NMN desaminasa, no se ha estudiado en detalle, habiéndose caracterizado únicamente dos de estas enzimas recombinantes de *E. coli* y *Shewanella oneidensis*. Esta enzima presenta un elevado interés ya que participa en el reciclado de NAD^+ a través de PNC IV en ciertas bacterias, algunas de las cuales son patógenas de humanos y dependen únicamente de esta ruta para la biosíntesis de NAD^+, convirtiendo a sus inhibidores en posibles dianas terapéuticas. Además su activación previene la inhibición de la ligasa bacteriana dependiente de NAD^+, por la acumulación de NMN, un potente inhibidor de ésta.

El principal inconveniente en la caracterización de esta enzima es la ausencia de un método continuo de medida sencillo, habiéndose descrito hasta el momento únicamente tediosos métodos cromatográficos y basados en HPLC.

El objetivo de esta tesis ha sido el estudio de tres de estas enzimas (Neu5Ac aldolasa, nicotinamidasa y nicotinamida mononucleótido desaminasa) de interés

biotecnológico y farmacológico en microorganismos, mediante su clonación, sobreexpresión y caracterización cinética, no sólo mediante técnicas de biología molecular convencionales, sino también mediante evolución dirigida. Se persiguió asimismo el desarrollo de ensayos masivos para la medida de nicotinamidasas y aldolasas, así como el desarrollo de un nuevo método espectrofotométrico para la detección de NMN desaminasa.

MATERIALES Y MÉTODOS

1. DNA GENÓMICO

El DNA genómico usado para esta tesis fue obtenido de:

1. *Lactobacillus plantarum* cepa WCFS1. Dicho microorganismo fue utilizado para la obtención de una potencial ácido *N*-acetilneuramínico aldolasa. Se adquirió de la colección NCIMB (Nº 8826). El microorganismo fue cultivado en medio YMRS.

2. *Escherichia coli* K12 strain MG1655. Se adquirió del Coli Genetic Stock Center (CGST, USA) y fue utilizado para la obtención de *N*-acetilneuramínico aldolasa .El microorganismo se cultivó en medio LB.

3. *Bacillus halodurans* cepa C-125. Su DNA genómico fue donado también por el Profesor Hideto Takami, de la Japan Agency from Marine-Earth Science and Technology (JAMSTEC, Japan) y sirvió para la obtención de los genes de L-lactato deshidrogenasa y L-glutamato deshidrogenasa.

4. *Oceanobacillus iheyensis* cepa HTE831. Su DNA genómico fue donado gentilmente por el Profesor Hideto Takami, de la Japan Agency from Marine-Earth Science and Technology (JAMSTEC, Japan) y sirvió para la obtención de los genes de Nicotinamidasa y nicotinamida mononucleótido desaminasa.

2. REACTIVOS Y CEPAS COMERCIALES

Los sustratos para las enzimas, los inhibidores, los iones divalentes, EDTA, EGTA, IPTG, antibióticos, detergentes, fluoróforos, las enzimas, los estándares de peso molecular y el bromuro de etidio se compraron a Sigma Aldrich (Madrid, España). El fluoróforo Deep Purple se compró en GE Lifescience (Uppsala,

Sweden). El sulfato amónico y las sales para los tampones fueron de Fluka. Los sustratos, Neu5Ac y piruvato sódico, y los cofactores se adquirieron en Carbosynth (UK). Nicotinamida mononucleótido fue comprado a Santa Cruz Biotechnology (Heidelberg, Germany). 5-Methilnicotinamida se compró a Alfa Aesar (USA). Los reactivos para la electroforesis y la cuantificación de proteínas (Bradford) fueron comprados a Biorad (Hercules, EEUU). Los disolventes orgánicos para el HPLC de Analisis Vínicos (Tomelloso, España) y el sistema de agua MilliQ® fue de Millipore (Bedford, EEUU). Los medios de cultivo se adquirieron a Pronadisa (Madrid, España). Los reactivos para biología molecular fueron comprados a NEB (Bervely, EEUU) a excepción de la Pfu polimerasa y la T_4 DNA ligase que se adquirieron de Agilent Technologies (CA, USA). Los oligos específicos para las PCR se pidieron a Isogen (Darmstad, Alemania), y las cepas de clonación y vectores de expresión usados fueron de Novagen (Tablas 3.1 y 3.2) a excepción de la cepa DH5α que fue de Invitrogen (Frederick, USA). Los kits de extracción y purificación de ácidos nucléicos fueron suministrados por Qiagen (Valencia, EEUU) y Zymo (Irvine, USA).

3. HERRAMIENTAS BIOINFORMÁTICAS

Las secuencias de los genes fueron obtenidas de la página del National Center for Biotechnology Information (NCBI, http://www.ncbi.nlm.nih.gov/), bien de Uniprot (http://www.uniprot.org/) y su alineamiento e identificación se llevó a cabo usando BLAST y ClustalW2. El modelo 3D de las proteínas se consiguió utilizando Geno3D y su visualización mediante PyMol o DINO. La interfaz Whatif y Getarea fueron utilizadas para el cálculo de las propiedades estructurales de las proteínas. En la realización de los arboles filogenéticos MEGA 5.0 para la visualización y construcción de los árboles.

4. MÉTODOS MICROBIOLÓGICOS

Como norma general, *E. coli* se cultivó a 37 ºC con agitación en medio LB. En caso de ser necesario el cultivo se suplementó con el antibiótico necesario para la selección de vectores. Para la sobreexpresión de proteínas los microorganismos se cultivaron en medio TB con los antibióticos necesarios. La inducción del cultivo se

realizó añadiendo IPTG a la concentración adecuada y posterior incubación a una temperatura de 30 ºC o inferior. *E. coli* se transformó por electroporación usando el método descrito por Dower *et al* (1988), utilizando un electroporador Biorad, salvo en el caso de *E. coli* NovaBlue y BL21 (DE3)pLys que se transformaron mediante choque térmico (heat-shock). Tras la recuperación en medio SOC durante 1 hora, las células se sembraron en placa de agar con antibiótico para la selección del vector.

5. AMPLIFICACIÓN POR PCR Y CLONACIÓN DE FRAGMENTOS DE DNA.

Los métodos de clonación usados fueron básicamente los descritos por Sambrock *et al* (1989). Las condiciones estándares de PCR son las indicadas en la Tabla 3.3. Tras la PCR y la digestión con enzimas de restricción (del vector y del inserto), el producto fue clonado en un vector pET (pET28a o pET24b), inducible por IPTG. La mutagénesis dirigida se realizó siguiendo el método descrito por Ho et al (1989), utilizando Pfu Ultra II. Los plásmidos usados están indicados en la Tabla 3.4. La creación de bibliotecas de PCR propensa a errores para el gen de Neu5Ac aldolasa de *L. plantarum* se realizó usando 10 ng de DNA molde, 1x Error prone Mutagenic buffer, 1x error prone dNTP mix, 0.2 mM $MnCl_2$ y 5 U de *Taq* polymerasa (New England Biolabs). Los fragmentos amplificados se clonaron en pET28a y se transformaron en *E. coli* DH5α.

6. PURIFICACIÓN DE PROTEÍNAS

La producción de proteína se llevó a cabo en un fermentador de 5 L, con 4 L de medio TB, el cual se indujo con IPTG a 30 ºC durante 12 horas. El cultivo obtenido se diafiltró en el buffer apropiado, y se concentró a través de una columna de 500-kDa, como paso previo a su ruptura en un rompedor celular (MiniZetaII, Netzsch). El extracto crudo obtenido se trató con DNasa I, y se concentró por ultrafiltración a través de una membrana de 50- ó 100-kDa (GE Lifesciences, Uppsala, Suecia). Después de ultracentrifugar a 40,000g, la proteína fue purificada mediante cromatografía de afinidad, aprovechando la presencia de colas de histidina en las enzimas, introducidas por los vectores pET. La enzima obtenida se desaló y se guardó con glicerol al 10 % en un ultracongelador (-80 ºC).

7. METODOLOGÍA DE PROTEÍNAS

La cuantificación se realizó utilizando el método descrito por Bradford (1976). La resolución electroforética de proteínas se llevó a cabo realizando una SDS-PAGE, utilizando un gel concentrador al 4 % y un separador al 12 % de acrilamida:bisacrilamida. La electroforesis se realizó en un sistema Miniprotean III (Biorad, Hercules, EEUU), y las proteínas se tiñeron usando Azul Brillante de Coomasie (Sigma, Madrid, España). El marcador de peso molecular utilizado se compró a NEB (P7708S). La determinación del peso molecular de la enzima nativa se llevó a cabo mediante cromatografía por filtración en gel usando una columna Superdex 200 10/30 GL (GE Lifesciences). Este método además se utilizo para confirmar la homogeneidad de la proteína purificada. Para la determinación del peso molecular bajo condiciones desnaturalizantes se utilizó la técnica HPLC acoplada a un espectrómetro de masas (HP/1100 LC/MSD Ion Trap System, Agilent technologies), la cual permite un cálculo exacto con una precisión de 1 Da. El estudio de las subunidades de OiNIC se realizó mediante la técnica de entrecruzado (cross-linking) con dimetil-suberimidato. Las curvas de fusión (melting) para la determinación de la desnaturalización de proteínas se realizaron con la sonda SYPRO orange (Molecular Probes, Paisley, Reino Unido) o Deep Purple (GE lifescience, Uppsala, Sweden). La desnaturalización se indujo incrementando la temperatura en un gradiente lineal de 20 a 100 ºC utilizando un aparato de RT-PCR (modelo 7500, Applied Biosystems), y la gráfica del incremento de fluorescencia obtenida se utilizó para el cálculo de la Tm. La determinación del contenido de iones metálicos de OiNIC se realizó utilizando un aparato de ICP-OES (Inductively Coupled Plasma-Optical Emission Spectrometer) modelo Optima 2000 DV, Perkin-Elmer, (MA, USA).

8. ENSAYOS ESPECTROFOTOMÉTRICOS

El ensayo de actividad de Neu5Ac aldolasa consistió en la medida del descenso de absorbancia a 340 nm, cuando el piruvato producido por la hidrólisis de Neu5Ac se convierte en lactato, por la acción de la enzima acoplada lactato deshidrogenasa, con consumo de NADH a 37 ºC. El ensayo estándar contenía NADH a 150 μM, 0.5 U de LDH, Neu5Ac 10 mM y 1.5 μg de LpNAL o EcNAL

en tampón fosfato sódico 20 mM pH 7. Con esta misma metodología, se adaptó el método a una medida en placa de 96 pocillos para el cribado (screening) a gran escala de bibliotecas de PCR propensa a errores (Error prone PCR). El cultivo de células en placa de 96 pocillos y la dispensación de líquidos para el procesado del extracto crudo y la medida de actividad se realizaron usando sistemas robóticos (QPix2^{XT} y Hamilton Star Plus). El método de medida en placa de 96 pocillos fue validado calculando el valor Coeficiente de Variación (CV=(desviación estándar/media)x100 %)).

La reacción catalizada por lactato deshidrogenasa se determinó añadiendo a la reacción a 37 ºC, NADH a 0.3 mM y piruvato sódico a 30 mM en tampón fosfato sódico 50 mM pH 6.0 para BhLDH o tampón TRIS-HCl 50 mM pH 8.0 para la lactato deshidrogenasa comercial. El ensayo determina el consumo de NADH producido por lactato deshidrogenasa mediante el seguimiento del descenso en la absorbancia a 360 nm.

El método espectrofotométrico para la medida de nicotinamidasa sigue el descenso en la absorbancia a 360 nm correspondiente a la oxidación de NADPH producida por la enzima glutamato deshidrogenasa cuando el NH_3 producido como consecuencia de la desaminación de nicotinamida, junto con α-cetoglutarato eran transformados en L-glutamato. La reacción estándar contenía NADPH a 0.3 mM, NAM a 1 mM, α-cetoglutarato a 10 mM, 9.7 μg de BhGDH y 1.3 μg de OiNIC pura en tampón fosfato sódico 100 mM pH 7.3. Con esta misma metodología, se adaptó el método a una medida en placa de 96 pocillos para el *screening* a gran escala. El cultivo de células en placa de 96 pocillos y la dispensación de líquidos para el procesado del extracto crudo y la medida de actividad se realizaron usando sistemas robóticos (QPix2^{XT} y Hamilton Star Plus). El método de medida en placa de 96 pocillos fue validado calculando su valor de C.V.

El ensayo estándar de glutamato deshidrogenasa a 37 ºC contenía α-cetoglutarato a 10 mM, NH_4Cl 100 mM, NADPH a 0.3 mM y 0.13 μg de enzima en tampón fosfato sódico 50 mM pH 7.5. El ensayo espectrofotométrico determina la oxidación de NADPH por la enzima, que se corresponde con el descenso en la absorbancia a 360 nm.

Finalmente, se utilizó el NH_3 producido en la reacción de desaminación por nicotinamida mononucleotido desaminasa, en otra reacción acoplada con BhGDH que junto con α-cetoglutarato produce L-glutamato, con oxidación de NADPH, cuyo consumo puede ser determinado por el descenso de absorbancia a 360 nm. La reacción estándar contenía NADPH 300 μM, NMN 0.5 mM, α-cetoglutarato a 10 mM, 9.7 μg BhGDH y 15 μg de OiPncC pura en tampón fosfato potásico 50 mM pH 7.5.

9. ENSAYOS EN HPLC

La aparición de ácido nicotínico por nicotinamidasa y la desaparición de nicotinamida mononucleótido por nicotinamida mononucleótido desaminasa se midió mediante HPLC (GE healthcare), utilizando una columna de fase reversa C_{18} (250 mm x 4.6 mm; Phenomenex) y una fase móvil (20 mM acetato amónico, pH 6.9) a un flujo de 1 mL/min. La reacción estándar para nicotinamidase consistió en NAM 1 mM y 0.67 μg de OiNIC pura en tampón fosfato potásico 100 mM pH 7.3. Las reacciones se detuvieron mediante la adición de ácido trifluoro acético (TFA) hasta un pH final de 3.0. El ensayo estándar para nicotinamida mononucleotido desaminasa contenía NMN a 0.5 mM y 30 μg de OiPncC pura en tampón fosfato potásico 50 mM pH 7.5.

10. ENSAYOS DE ESTABILIDAD

El efecto de la temperatura y el pH se ensayó incubando la enzima durante periodos de tiempo determinados a diferentes temperaturas y pHs, y posteriormente, midiendo en condiciones estándar. De la misma forma se comprobó también, el efecto de los inhibidores.

RESULTADOS Y DISCUSIÓN

CAPITULO IV. Caracterización molecular de *N*-acetilneuraminidato liasa de *Lactobacillus plantarum* WCFS1.

La enzima Neu5Ac aldolasa (EC 4.1.3.3), también conocida como *N*-acetilneuraminidato liasa (NAL) o ácido siálico aldolasa, cataliza la ruptura de

ácido *N*-acetilneuramínico (ácido D-siálico, Neu5Ac) hasta piruvato y *N*-acetil-D-manosamina (ManNAc). *In vitro* la enzima puede realizar también la reacción inversa de condensación aldólica produciendo la síntesis de ácido *N*-acetilneuramínico (Neu5Ac) y algunos de sus derivados, a partir de piruvato y *N*-acetil-D-manosamina. Neu5Ac es un componente importante de oligosacáridos, glicoproteínas y glicolípidos. Participa en diversas funciones biológicas, en las que actúa en el reconocimiento de microorganismos, virus, toxinas y hormonas. Además participa en la regulación del sistema inmune. Esto la convierte en una molécula de interés para la producción de nuevos tipos de terapéuticos, como inhibidores de la neuraminidasa (Zinamavir ó "Relenza®", GlaxoSminthKline), efectivos como antivirales contra la gripe aviar o aviárica. Los métodos convencionales de producción de Neu5Ac de fuentes naturales no son adecuados para el escalado a nivel industrial del proceso, siendo el proceso enzimático catalizado por Neu5Ac aldolasa una alternativa biotecnológica a optimizar.

Basado en lo anterior, el gen de Neu5Ac aldolasa de *L. plantarum* WCFS1 (LpNAL) ha sido clonado, sobreexpresado con alto rendimiento en *E. coli* BL21 (DE3)pLys y purificado en tres pasos para obtener una proteína pura tetramérica de 146 kDa. La actividad enzimática de esta enzima fue comparada con la de Neu5Ac aldolasa recombinante de *E. coli* K12 cepa MG1655 (EcNAL). La enzima purificada mostró K_M (1.8 mM) ligeramente inferior a otras NALs descritas y a la NAL de *E. coli* recombinante (2.5 mM). Su eficiencia catalítica (k_{cat}/K_M) fue similar a la de otras Neu5Ac aldolasas previamente descritas (5.6 $mM^{-1}s^{-1}$) (Tabla 4.2). Su óptimo de pH fue 7.0 (Figura 4.4), y mostró temperatura óptima por encima de 45 ºC (Figura 4.5). Tanto LpNAL como EcNAL resultaron ser muy termoestables, siendo el sulfato amónico el mejor estabilizante entre los estudiados, ya que produce un aumento en la temperatura de *melting* (fusión) de la proteína de cerca de 8 ºC (de 71.5 ºC a 79.1) (Figuras 4.6, 4.7 and 4.8).

Se realizó el análisis estructural de LpNAL, realizando su modelado molecular tomando como molde la estructura de la cristalizada NAL de *Haemophilus influenzae* (PDB code: 1F5Z) (Figura 4.10). Se realizó el estudio de las zonas conservadas en las secuencias de estas NALs disponibles en las bases de datos, lo que condujo a la clasificación de las NALs bacterianas en 4 grupos filogenéticos (Figura 4.11). El grupo 1 incluyó NALs de bacterias con mayor homología con *H.*

influenzae NAL, como es el caso de LpNAL. El grupo 2 mostró NALs de patógenos gastrointestinales como *E. coli, Shigella* o *Salmonella enterica.* El género *Streptococcus,* junto con algunos *Lactobacillus, Clostridium* y otros comensales intestinales conformaron el grupo 3. Finalmente el grupo 4 fue el más diverso de todos, dando lugar a 3 subgrupos distintos (4.1, 4.2 y 4.4). El subgrupo 4.4, formado por NALs de *Vibrio* y *Yersinia* se demostró muy relacionado con NALs de mamíferos, incluyendo la versión humana. El estudio filogenético indicó una transferencia horizontal de este gen desde bacterias del grupo 4.4 a mamíferos.

CAPITULO V. Obtención de una nueva L-Lactato deshidrogenasa de *Bacillus halodurans* C-125 como herramienta para el screening de bibliotecas de evolución dirigida.

CAPITULO VI. Caracterización de una nueva nicotinamidasa de *Oceanobacillus iheyansis* HTE831.

El trabajo y la experiencia previa adquirida durante la caracterización de LpNAL y su enzima acoplada BhGDH, que facilita la caracterización barata y rápida de la primera, incluso en sistemas de detección de alto rendimiento, nos condujo al estudio de otras enzimas con un gran interés biotecnológico, como son las nicotinamidasas. Estas enzimas catalizan la desaminación de nicotinamida (NAM) para producir amonio y ácido nicotínico (NA). Estas enzimas se miden espectrofotométricamente mediante una reacción acoplada basada en el uso de glutamato deshidrogenasa, que utiliza el amonio producido en la reacción junto con α-cetoglurtarato, para su conversión en L-glutamato, con oxidación de NADPH que puede ser medido espectrofotométricamente a 360 nm (Esquema 6.1).

Las nicotinamidasas son enzimas claves en el metabolismo de NAD^+, participando en el reciclado de este y siendo la única vía de obtención de NAD^+ para muchas bacterias patógenas, que no tienen las enzimas implicadas en la síntesis *de novo* de NAD^+ desde aspartato o triptófano. Debido a la ausencia de nicotinamidasas en el genoma humano, estas enzimas son potenciales dianas terapeúticas en el tratamiento de enfermedades producidas por estos patógenos. Asimismo, NAM es un producto de varias enzimas que consumen NAD^+, como es el caso de las

sirtuinas, desacetilasas dependientes de NAD^+ ampliamente distribuidas en la naturaleza. La importancia de estas últimas enzimas radica en el control que éstas realizan sobre varios procesos celulares relacionas con el aumento de vida media, homeostasis de glucosa, alargamiento de telómeros, respuesta a estrés ambiental, etc… Las nicotinamidasas actúan como activadores de sirtuinas mediante la conversión de NAM (que es inhibidora de sirtuina) a ácido nicotínico (NA). Desde el punto de vista biotecnológico pueden ser además usadas como enzimas acopladas para cribar librarías de potenciales moduladores de sirtuinas para su uso terapéutico.

En este capítulo se describe la clonación, sobreexpresión y caracterización detallada de la nicotinamidasa de *O. iheyensis* (OiNIC). Tras su purificación a homogeneidad, esta enzima resultó ser una proteína dimérica (Figura 6.2) con un pH óptimo entre 6.0-6.5 y una temperatura óptima de 45 ºC (Figura 6.3). La enzima fue relativamente estable entre pH 6.0-7.3 y a 45 ºC (Figura 6.3). Esta enzima contiene iones metálicos en su centro activo, obteniendo mediante ICP-OES que dicho ión es Zn^{2+}. Los parámetros cinéticos de esta enzima se calcularon para su sustrato natural nicotinamida, sobre el pro-fármaco utilizado en el tratamiento de la tuberculosis, pirazinamida (PZA), y sobre otros análogos de NAM (Tabla 6.2). OiNIC mostró mayor eficiencia catalítica (k_{cat}/ K_M) y menor K_M para NAM con respecto a los otros análogos estudiados (0.26 mM y 43.48 mM^{-1} s^{-1}, respectivamente). Por tanto se trata de una enzima que puede ser más bien considerada como nicotinamidasa que como pirazinamidasa. Se realizó un estudio más detallado de los amino ácidos implicados en la unión del ión metálico, para ello se generaron 7 mutantes de OiNIC: en el residuo catalítico (K104A), en un residuos implicados en la unión a metal (E65H), en un residuo que participa en la formación de un enlace cis-peptídico (C133A), en un residuo implicado en la formación de puentes de hidrógeno entre cadenas centrales y laterales (T12Q) y residuos que modifican la superficie y volumen del centro activo (Q96K, Q96A, F68W). Se calcularon los parámetros cinéticos para todos estos mutantes (Tabla 6.2), y se comprobó que K104 y T12Q son residuos esenciales para la actividad catalítica de OiNIC, ya que pierden totalmente su actividad. E65 se confirmó como el cuarto residuo implicado en la unión del ión metálico a la proteína, y los mutantes en Q96, C133 y F68 modifican y en algunos casos, mejoran, la

especificidad de sustrato de OiNIC. En particular, las mutaciones C133A y F68W generan una nicotinamidasa con mayor afinidad y eficiencia catalítica por PZA, posiblemente porque son capaces de acomodar mejor este substrato en el centro activo. La generación de un doble mutante C133A/F68W también mostró mayor eficiencia catalítica sobre PZA, pero en ningún caso mejor que los mutantes puntuales por separado (Tabla 6.2).

Se llevaron a cabo también ensayos de inhibición de OiNIC por nicotinaldehídos, mostrando una fuerte inhibión competitiva con valores de k_i inferiores a 5 μM (Figura 6.5). Por último, se realizó un estudio estructural y filogenético de las nicotinamidasas del phylum firmicutes, al que pertenece *O. iheyensis* en comparación con un árbol filogenético de las secuencias de rRNA 16S de las mismas enzimas (Figuras 6.7-6.8), observándose algunos fenómenos de transferencia horizontal de genes.

CAPITULO VII. Caracterización de una nueva glutamato deshidrogenasa de *Bacillus halodurans* C-125 como herramienta para el screening masivo de nicotinamidasas.

CAPITULO VIII. Desarrollo de un nuevo ensayo acoplado para la medida y caracterización de una nueva nicotinamida monoucleótido desaminasa de *Oceanobacillus iheyensis* HTE831.

XII. REFERENCES

Aisaka, K., Igarashi, A., Yamaguchi, K., & Uwajima, T. (1991). Purification, crystallization and characterization of *N*-acetylneuraminate lyase from *Escherichia coli*. *Biochem J, 276 (Pt 2)*, 541-546.

Aisaka, K., & Uwajima, T. (1986). Cloning and constitutive expression of the *N*-acetylneuraminate lyase gene of *Escherichia coli*. *Appl Environ Microbiol, 51*(3), 562-565.

Almagro-Moreno, S., & Boyd, E. F. (2009). Insights into the evolution of sialic acid catabolism among bacteria. *BMC Evol Biol, 9*, 118.

Altschul, S. F., Gish, W., Miller, W., Myers, E. W., & Lipman, D. J. (1990). Basic local alignment search tool. *J Mol Biol, 215*(3), 403-410.

Angata, T., & Varki, A. (2002). Chemical diversity in the sialic scids and related α-keto acids: an evolutionary perspective. *Chemical Reviews*, *102*(2), 439-470.

Anderson, R. M., Bitterman, K. J., Wood, J. G., Medvedik, O., & Sinclair, D. A. (2003). Nicotinamide and PNC1 govern lifespan extension by calorie restriction in Saccharomyces cerevisiae. *Nature, 423*(6936), 181-185.

Andersson, J. O., Doolittle, W. F., & Nesbo, C. L. (2001). Genomics. Are there bugs in our genome? *Science, 292*(5523), 1848-1850.

OECD (2001). The Application of Biotechnology to Industrial Sustainability. Paris, France.

Arai, K., Hishida, A., Ishiyama, M., Kamata, T., Uchikoba, H., Fushinobu, S., Matsuzawa, H., & Taguchi, H. (2002). An absolute requirement of fructose 1,6-bisphosphate for the *Lactobacillus casei* L-lactate dehydrogenase activity induced by a single amino acid substitution. *Protein Eng, 15*(1), 35-41.

Arai, K., Ishimitsu, T., Fushinobu, S., Uchikoba, H., Matsuzawa, H., & Taguchi, H. (2010). Active and inactive state structures of unliganded *Lactobacillus casei* allosteric L-lactate dehydrogenase. *Proteins, 78*(3), 681-694.

Argmann, C., & Auwerx, J. (2006). Insulin secretion: SIRT4 gets in on the act. *Cell, 126*(5), 837-839.

Arnold, F. A. (1996). Directed evolution: creation biocatalysts for the future. *Chem. Eng. Sci., 51*, 5091-5102.

Arpigny, J. L., & Jaeger, K. E. (1999). Bacterial lipolytic enzymes: classification and properties. *Biochem J, 343 Pt 1*, 177-183.

Asaba, T., Suzuki, T., Ueda, R., Tsumoto, H., Nakagawa, H., & Miyata, N. (2009). Inhibition of human sirtuins by in situ generation of an acetylated lysine-ADP-ribose conjugate. *J Am Chem Soc, 131*(20), 6989-6996.

Avalos, J. L., Celic, I., Muhammad, S., Cosgrove, M. S., Boeke, J. D., & Wolberger, C. (2002). Structure of a Sir2 enzyme bound to an acetylated p53 peptide. *Mol Cell, 10*(3), 523-535.

Baker, P. J., Britton, K. L., Engel, P. C., Farrants, G. W., Lilley, K. S., Rice, D. W., & Stillman, T. J. (1992). Subunit assembly and active site location in the structure of glutamate dehydrogenase. *Proteins, 12*(1), 75-86.

Balan, V., Miller, G. S., Kaplun, L., Balan, K., Chong, Z. Z., Li, F., Kaplun, A., VanBerkum, M. F., Arking, R., Freeman, D. C., Maiese, K., & Tzivion, G. (2008). Life span extension and neuronal cell protection by *Drosophila* nicotinamidase. *J Biol Chem, 283*(41), 27810-27819.

Barbosa, J. A., Smith, B. J., DeGori, R., Ooi, H. C., Marcuccio, S. M., Campi, E. M., Jackson, W. R., Brossmer, R., Sommer, M., & Lawrence, M. C. (2000). Active site modulation in the *N*-acetylneuraminate lyase sub-family as revealed by the structure of the inhibitor-complexed *Haemophilus influenzae* enzyme. *J Mol Biol, 303*(3), 405-421.

Bhuiya, M. W., Sakuraba, H., & Ohshima, T. (2002). Temperature dependence of kinetic parameters for hyperthermophilic glutamate dehydrogenase from *Aeropyrum pernix* K1. *Biosci Biotechnol Biochem, 66*(4), 873-876.

Binay, B., & Karaguler, N. G. (2007). Attempting to remove the substrate inhibition of L-lactate dehydrogenase from *Bacillus stearothermophilus* by site-directed mutagenesis. *Appl Biochem Biotechnol, 141*(2-3), 265-272.

Bitterman, K. J., Anderson, R. M., Cohen, H. Y., Latorre-Esteves, M., & Sinclair, D. A. (2002). Inhibition of silencing and accelerated aging by nicotinamide, a putative negative regulator of yeast sir2 and human SIRT1. *J Biol Chem, 277*(47), 45099-45107.

Blattner, F.R., Plunkett, G., Bloch, C.A., Perna, N.T., Burland, V., Riley, M., Collado-Vides, J., Glasner, J.D., Rode, C.K., Mayhew, G.F., Gregor, J., Davis, N.W., Kirkpatrick, H.A., Goeden, M.A., Rose, D.J., Mau, B., & Shao, Y. (1997). The Complete Genome Sequence of *Escherichia coli* K-12. *Science*, *277*(5331), 1453-1462

Blayer, S., Woodley, J. M., Dawson, M. J., & Lilly, M. D. (1999). Alkaline biocatalysis for the direct synthesis of *N*-acetyl-D-neuraminic acid (Neu5Ac) from *N*-acetyl-D-glucosamine (GlcNAc). *Biotechnol Bioeng, 66*(2), 131-136.

Blickling, S., Renner, C., Laber, B., Pohlenz, H.-D., Holak, T.A., & Huber, R. (1997). Reaction Mechanism of *Escherichia coli* Dihydrodipicolinate Synthase Investigated by X-ray Crystallography and NMR Spectroscopy. *Biochemistry*, *36*(1), 24-33.

Blix, F.G., Gottschalk, A., & Klenk, E. (1957). Proposed nomenclature in the field of neuraminic and sialic acids. *Nature*, *179*(4569), 1088.

Blix, G. (1936). Über die Kohlenhydratgruppen des Submaxillarismucins. Hoppe-Syler's Z. *Physiol. Chem.*, *240*, 43-45.

Blix, G., Svennerholm, L., & Werner, I. (1952). The isolation of chondrosamine from gangliosides and from submaxillary mucin. *Acta Chem. Acand.*, *6*, 358-356.

Boesten, W. H. J., Moody, H. M., & Roos, E. C. (1996). Process for the recovery of ampicillin from enzymatic acylation of 6-aminopenicillanic acid. In Chemferm (Ed.), vol. WO. 9630376). The Netherlands.

Bork, K., Horstkorte, R., & Weidemann, W. (2009). Increasing the sialylation of therapeutic glycoproteins: the potential of the sialic acid biosynthetic pathway. *J Pharm Sci, 98*(10), 3499-3508.

Borra, M. T., Smith, B. C., & Denu, J. M. (2005). Mechanism of human SIRT1 activation by resveratrol. *J Biol Chem, 280*(17), 17187-17195.

Boshoff, H. I., & Mizrahi, V. (1998). Purification, gene cloning, targeted knockout, overexpression, and biochemical characterization of the major pyrazinamidase from *Mycobacterium smegmatis*. *J Bacteriol, 180*(22), 5809-5814.

Bradford, M.M. 1976. A rapid and sensitive method for the quantitation of microgram quantities of protein utilizing the principle of protein-dye binding. *Anal Biochem*, **72**, 248-54.

Britton, K. L., Yip, K. S., Sedelnikova, S. E., Stillman, T. J., Adams, M. W., Ma, K., Maeder, D. L., Robb, F. T., Tolliday, N., Vetriani, C., Rice, D. W., & Baker, P. J. (1999). Structure determination of the glutamate dehydrogenase from the hyperthermophile *Thermococcus litoralis* and its comparison with that from *Pyrococcus furiosus*. *J Mol Biol, 293*(5), 1121-1132.

Buckel, W. (1980). Analysis of the fermentation pathways of clostridia using double labelled glutamade. *Arch Microbiol, 127*(2), 167-169.

Bull, A. T., Bunch, A. W., & Robinson, G. K. (1998). Biotechnology for Clean Industrial Products and Processes.

Camardella, L., Di Fraia, R., Antignani, A., Ciardiello, M. A., di Prisco, G., Coleman, J. K., Buchon, L., Guespin, J., & Russell, N. J. (2002). The Antarctic *Psychrobacter sp*. TAD1 has two cold-active glutamate dehydrogenases with different cofactor specificities. Characterisation of the NAD^+-dependent enzyme. *Comp Biochem Physiol A Mol Integr Physiol, 131*(3), 559-567.

Campeotto, I., Bolt, A. H., Harman, T. A., Dennis, C., Trinh, C. H., Phillips, S. E., Nelson, A., Pearson, A. R., & Berry, A. (2010). Structural insights into substrate specificity in variants of *N*-acetylneuraminic Acid lyase produced by directed evolution. *J Mol Biol, 404*(1), 56-69.

Campeotto, I., Carr, S. B., Trinh, C. H., Nelson, A. S., Berry, A., Phillips, S. E., & Pearson, A. R. (2009). Structure of an *Escherichia coli N*-acetyl-D-neuraminic acid lyase mutant, E192N, in complex with pyruvate at 1.45 Angstrom resolution. *Acta Crystallogr Sect F Struct Biol Cryst Commun, 65*(Pt 11), 1088-1090.

Chaikuad, A., Fairweather, V., Conners, R., Joseph-Horne, T., Turgut-Balik, D., & Brady, R.L. (2005). Structure of lactate dehydrogenase from *Plasmodium vivax*: complexes with NADH and APADH. *Biochemistry*, *44*(49), 16221-8.

Coghlan, D. R., Mackintosh, J. A., & Karuso, P. (2005). Mechanism of reversible fluorescent staining of protein with epicocconone. *Org Lett, 7*(12), 2401-2404.

Colin, D. Y., Deprez-Beauclair, P., Silva, N., Infantes, L., & Kerfelec, B. (2010). Modification of pancreatic lipase properties by directed molecular evolution. *Protein Eng Des Sel, 23*(5), 365-373.

Colman, P. M., Varghese, J. N., & Laver, W. G. (1983). Structure of the catalytic and antigenic sites in influenza virus neuraminidase. *Nature, 303*(5912), 41-44.

Combet, C., Jambon, M., Deleage, G., & Geourjon, C. (2002). Geno3D: automatic comparative molecular modelling of protein. *Bioinformatics, 18*(1), 213-214.

Coquelle, N., Fioravanti, E., Weik, M., Vellieux, F., & Madern, D. (2007). Activity, stability and structural studies of lactate dehydrogenases adapted to extreme thermal environments. *J Mol Biol, 374*(2), 547-562.

Coulton, J. W., & Kapoor, M. (1973). Studies on the kinetics and regulation of glutamate dehydrogenase of *Salmonella typhimurium*. *Can J Microbiol, 19*(4), 439-450.

Cunningham, B.A., Hoffman, S., Rutishauser, U., Hemperly, J.J., & Edelman, G.M. (1983). Molecular topography of the neural cell adhesion molecule N-CAM: surface orientation and location of sialic acid-rich and binding regions. *Proceedings of the National Academy of Sciences*, *80*(10), 3116-3120.

Chaikuad, A., Fairweather, V., Conners, R., Joseph-Horne, T., Turgut-Balik, D., & Brady, R. L. (2005). Structure of lactate dehydrogenase from *Plasmodium vivax*: complexes with NADH and APADH. *Biochemistry, 44*(49), 16221-16228.

Chen, X., & Varki, A. (2010). Advances in the biology and chemistry of sialic acids. *ACS Chem Biol, 5*(2), 163-176.

Cheng, S. J., Thibert, L., Sanchez, T., Heifets, L., & Zhang, Y. (2000). pncA mutations as a major mechanism of pyrazinamide resistance in *Mycobacterium tuberculosis*: spread of a monoresistant strain in Quebec, Canada. *Antimicrob Agents Chemother, 44*(3), 528-532.

Cheng, W., & Roth, J. (1995). Isolation of NAD cycle mutants defective in nicotinamide mononucleotide deamidase in *Salmonella typhimurium*. *J Bacteriol, 177*(23), 6711-6717.

Chenu, S., Gregoire, A., Malykh, Y., Visvikis, A., Monaco, L., Shaw, L., Schauer, R., Marc, A., & Goergen, J. L. (2003). Reduction of CMP-*N*-acetylneuraminic acid hydroxylase activity in engineered Chinese hamster ovary cells using an antisense-RNA strategy. *Biochim Biophys Acta, 1622*(2), 133-144.

Dai, D., Nanthkumar, N.N., Newburg, D.S., Walker, W.A. 2000. Role of oligosaccharides and glycoconjugates in intestinal host defense. *J Pediatr Gastroenterol Nutr*, **30 Suppl 2**, S23-33.

Dower, W.J., Miller, J.F., Ragsdale, C.W. 1988. High efficiency transformation of *E. coli* by high voltage electroporation. *Nucleic Acids Res*, **16**(13), 6127-45.

Du, X., Wang, W., Kim, R., Yakota, H., Nguyen, H., & Kim, S. H. (2001). Crystal structure and mechanism of catalysis of a pyrazinamidase from *Pyrococcus horikoshii*. *Biochemistry, 40*(47), 14166-14172.

Eichner, R. D., & Kaplan, N. O. (1977). Catalytic properties of lactate dehydrogenase in *Homarus americanus*. *Arch Biochem Biophys, 181*(2), 501-507.

Fan, Y., Ludewig, R., & Scriba, G. K. (2009). 9-Fluorenylmethoxycarbonyl-labeled peptides as substrates in a capillary electrophoresis-based assay for sirtuin enzymes. *Anal Biochem, 387*(2), 243-248.

Feng, Y., Wu, J., Chen, L., Luo, C., Shen, X., Chen, K., Jiang, H., & Liu, D. (2009). A fluorometric assay of SIRT1 deacetylation activity through quantification of nicotinamide adenine dinucleotide. *Anal Biochem, 395*(2), 205-210.

Fergusson, D.M., Beautrais, A.L., & Silva, P.A. (1982). Breast-feeding and cognitive development in the first seven years of life. *Social Science & Medicine, 16*(19), 1705-1708.

Ferrero, M. A., Reglero, A., Fernandez-Lopez, M., Ordas, R., & Rodriguez-Aparicio, L. B. (1996). *N*-acetyl-D-neuraminic acid lyase generates the sialic acid for colominic acid biosynthesis in *Escherichia coli* K1. *Biochem J, 317 (Pt 1)*, 157-165.

Felsenstein, J. (1989). Mathematics vs. evolution: mathematical evolutionary theory. *Science*, *246*(4932), 941-2.

Ford, E., Voit, R., Liszt, G., Magin, C., Grummt, I., & Guarente, L. (2006). Mammalian Sir2 homolog SIRT7 is an activator of RNA polymerase I transcription. *Genes Dev, 20*(9), 1075-1080.

Foster, J. W. (1981). Pyridine nucleotide cycle of *Salmonella typhimurium*: in vitro demonstration of nicotinamide adenine dinucleotide glycohydrolase, nicotinamide mononucleotide glycohydrolase, and nicotinamide adenine dinucleotide pyrophosphatase activities. *J Bacteriol, 145*(2), 1002-1009.

Foster, J. W., & Baskowsky-Foster, A. M. (1980). Pyridine nucleotide cycle of *Salmonella typhimurium*: in vivo recycling of nicotinamide adenine dinucleotide. *J Bacteriol, 142*(3), 1032-1035.

Foster, J. W., & Brestel, C. (1982). NAD metabolism in *Vibrio cholerae*. *J Bacteriol, 149*(1), 368-371.

Foster, J. W., Kinney, D. M., & Moat, A. G. (1979a). Pyridine nucleotide cycle of *Salmonella typhimurium*: isolation and characterization of pncA, pncB, and pncC mutants and utilization of exogenous nicotinamide adenine dinucleotide. *J Bacteriol, 137*(3), 1165-1175.

Foster, J. W., Kinney, D. M., & Moat, A. G. (1979b). Pyridine nucleotide cycle of *Salmonella typhimurium*: regulation of nicotinic acid phosphoribosyltransferase and nicotinamide deamidase. *J Bacteriol, 138*(3), 957-961.

Foster, J. W., & Moat, A. G. (1980). Nicotinamide adenine dinucleotide biosynthesis and pyridine nucleotide cycle metabolism in microbial systems. *Microbiol Rev, 44*(1), 83-105.

French, J. B., Cen, Y., Sauve, A. A., & Ealick, S. E. (2010). High-resolution crystal structures of *Streptococcus pneumoniae* nicotinamidase with trapped intermediates provide insights into the catalytic mechanism and inhibition by aldehydes. *Biochemistry, 49*(40), 8803-8812.

French, J. B., Cen, Y., Vrablik, T. L., Xu, P., Allen, E., Hanna-Rose, W., & Sauve, A. A. (2010). Characterization of nicotinamidases: steady state kinetic parameters, classwide inhibition by nicotinaldehydes, and catalytic mechanism. *Biochemistry, 49*(49), 10421-10439.

Friede, R. (1989). *Developmental neuropathology*. Springer-Berlag, Berlin, New York.

Friedmann, H. C., & Garstki, C. (1973). The pyridine nucleotide cycle: presence of a nicotinamide mononucleotide-specific amidohydrolase in *Propionibacterium shermanii*. *Biochem Biophys Res Commun, 50*(1), 54-58.

Fyfe, P. K., Rao, V. A., Zemla, A., Cameron, S., & Hunter, W. N. (2009). Specificity and mechanism of *Acinetobacter baumanii* nicotinamidase: implications for activation of the front-line tuberculosis drug pyrazinamide. *Angew Chem Int Ed Engl, 48*(48), 9176-9179

Fukuda, M. (1996). Possible Roles of Tumor-associated Carbohydrate Antigens. *Cancer Research*, *56*(10), 2237-2244

Galeazzi, L., Bocci, P., Amici, A., Brunetti, L., Ruggieri, S., Romine, M., Reed, S., Osterman, A. L., Rodionov, D. A., Sorci, L., & Raffaelli, N. (2011). Identification of nicotinamide mononucleotide deamidase of the bacterial

pyridine nucleotide cycle reveals a novel broadly conserved amidohydrolase family. *J Biol Chem, 286*(46), 40365-40375.

Gallo, C. M., Smith, D. L., Jr., & Smith, J. S. (2004). Nicotinamide clearance by Pnc1 directly regulates Sir2-mediated silencing and longevity. *Mol Cell Biol, 24*(3), 1301-1312.

Garrity, J., Gardner, J. G., Hawse, W., Wolberger, C., & Escalante-Semerena, J. C. (2007). *N*-lysine propionylation controls the activity of propionyl-CoA synthetase. *J Biol Chem, 282*(41), 30239-30245.

Garvie, E. I. (1980). Bacterial lactate dehydrogenases. *Microbiol Rev, 44*(1), 106-139.

Gazanion, E., Garcia, D., Silvestre, R., Gerard, C., Guichou, J. F., Labesse, G., Seveno, M., Cordeiro-Da-Silva, A., Ouaissi, A., Sereno, D., & Vergnes, B. (2011). The *Leishmania* nicotinamidase is essential for $NAD^{(+)}$ production and parasite proliferation. *Mol Microbiol, 82*(1), 21-38.

Ghislain, M., Talla, E., & Francois, J. M. (2002). Identification and functional analysis of the *Saccharomyces cerevisiae* nicotinamidase gene, PNC1. *Yeast, 19*(3), 215-224.

Gottschalk, A. 1955. Structural Relationship between Sialic Acid, Neuraminic Acid and 2-Carboxy-Pyrrole. *Nature*, **176**(4488), 881-882

Gottschling, D. E., Aparicio, O. M., Billington, B. L., & Zakian, V. A. (1990). Position effect at *S. cerevisiae* telomeres: reversible repression of Pol II transcription. *Cell, 63*(4), 751-762.

Goldman, N., & Whelan, S. (2000). Statistical tests of gamma-distributed rate heterogeneity in models of sequence evolution in phylogenetics. *Mol Biol Evol*, *17*(6), 975-8.

Gouet, P., Courcelle, E., Stuart, D. I., & Metoz, F. (1999). ESPript: analysis of multiple sequence alignments in PostScript. *Bioinformatics, 15*(4), 305-308.

Grose, J. H., Bergthorsson, U., Xu, Y., Sterneckert, J., Khodaverdian, B., & Roth, J. R. (2005). Assimilation of nicotinamide mononucleotide requires periplasmic AphA phosphatase in *Salmonella enterica*. *J Bacteriol, 187*(13), 4521-4530.

Guindon, S., & Gascuel, O. (2003). A simple, fast, and accurate algorithm to estimate large phylogenies by maximum likelihood. *Syst Biol*, **52**(5), 696-704.

Harduin-Lepers, A., Vallejo-Ruiz, V., Krzewinski-Recchi, M.-A., Samyn-Petit, B., Julien, S., & Delannoy, P. (2001). The human sialyltransferase family. *Biochimie, 83*(8), 727-737

Hayden, F.G., Treanor, J.J., Betts, R.F., Lobo, M., Esinhart, J.D., & Hussey, E.K. (1996). Safety and efficacy of the neuraminidase inhibitor GG167 in experimental human influenza. *JAMA*, *275*(4), 295-9.

Hemmila, I. A., & Mantsala, P. I. (1978). Purification and properties of glutamate synthase and glutamate dehydrogenase from *Bacillus megaterium*. *Biochem J, 173*(1), 45-52.

Hillyard, D., Rechsteiner, M., Manlapaz-Ramos, P., Imperial, J. S., Cruz, L. J., & Olivera, B. M. (1981). The pyridine nucleotide cycle. Studies in *Escherichia coli* and the human cell line D98/AH2. *J Biol Chem, 256*(16), 8491-8497.

Ho, M., Gutierrez, J. A., Almo, S. C., & Schramm, V. L. (2009). Crystal structure of Lactate dehydrogenase from *Staphylococcus aureus.* In).

Holbrook, J. J., Liljas, A., Steindel, S. J., & M.G., R. (1975). *Lactate Dehydrogenase* (Vol. 11). New York: P.D. Boyer, editor. Academic Press.

Holland, L. Z., McFall-Ngai, M., & Somero, G. N. (1997). Evolution of lactate dehydrogenase-A homologs of barracuda fishes (genus *Sphyraena*) from different thermal environments: differences in kinetic properties and thermal stability are due to amino acid substitutions outside the active site. *Biochemistry, 36*(11), 3207-3215.

Hooft, R.W., Sander, C., & Vriend, G. (1996). Positioning hydrogen atoms by optimizing hydrogen-bond networks in protein structures. *Proteins*, *26*(4), 363-76.

Hu, G., Taylor, A. B., McAlister-Henn, L., & Hart, P. J. (2007). Crystal structure of the yeast nicotinamidase Pnc1p. *Arch Biochem Biophys, 461*(1), 66-75.

Huang, S., Yu, H., & Chen, X. (2007). Disaccharides as sialic acid aldolase substrates: synthesis of disaccharides containing a sialic acid at the reducing end. *Angew Chem Int Ed Engl, 46*(13), 2249-2253.

Huelsenbeck, J.P., & Ronquist, F. (2001). MRBAYES: Bayesian inference of phylogenetic trees. *Bioinformatics*, *17*(8), 754-5.

Huson, D.H., & Bryant, D. (2006). Application of phylogenetic networks in evolutionary studies. *Mol Biol Evol*, *23*(2), 254-67.

Imai, S. (2010). A possibility of nutriceuticals as an anti-aging intervention: activation of sirtuins by promoting mammalian NAD biosynthesis. *Pharmacol Res, 62*(1), 42-47.

Imai, T. (1973). Purification and properties of nicotinamide mononucleotide amidohydrolase from *Azotobacter vinelandii*. *J Biochem, 73*(1), 139-153.

Inoue, T., Hiratsuka, M., Osaki, M., & Oshimura, M. (2007). The molecular biology of mammalian SIRT proteins: SIRT2 in cell cycle regulation. *Cell Cycle, 6*(9), 1011-1018.

Izard, T., Lawrence, M. C., Malby, R. L., Lilley, G. G., & Colman, P. M. (1994). The three-dimensional structure of *N*-acetylneuraminate lyase from *Escherichia coli*. *Structure, 2*(5), 361-369.

Jensen, V. J., & Rugh, S. (1987). Industrial-scale production and application of immobilized glucose isomerase. In M. Klaus (Ed.), *Methods in Enzymology*, vol. Volume 136 (pp. 356-370): Academic Press.

Joerger, A. C., Mayer, S., & Fersht, A. R. (2003). Mimicking natural evolution in vitro: an *N*-acetylneuraminate lyase mutant with an increased dihydrodipicolinate synthase activity. *Proc Natl Acad Sci U S A, 100*(10), 5694-5699.

Joshi, J. G., & Handler, P. (1962). Purification and properties of nicotinamidase from *Torula cremoris*. *J Biol Chem, 237*, 929-935.

Karlin, S. (2001). Detecting anomalous gene clusters and pathogenicity islands in diverse bacterial genomes. *Trends Microbiol*, *9*(7), 335-43.

Kawai, N., Ikematsu, H., Iwaki, N., Maeda, T., Kawashima, T., Hirotsu, N., & Kashiwagi, S. (2009). Comparison of the effectiveness of Zanamivir and Oseltamivir against influenza A/H1N1, A/H3N2, and B. *Clin Infect Dis, 48*(7), 996-997.

Kazatchkine, M.D., Fearon, D.T., & Austen, K.F. (1979). Human alternative complement pathway: membrane-associated sialic acid regulates the competition between B and beta1 H for cell-bound C3b. *J Immunol*, *122*(1), 75-81.

Kilbourne, E.D. (2006). Influenza pandemics of the 20th century. *Emerg Infect Dis*, *12*(1), 9-14.

Kim, S., Kurokawa, D., Watanabe, K., Makino, S., Shirahata, T., & Watarai, M. (2004). *Brucella abortus* nicotinamidase (PncA) contributes to its

intracellular replication and infectivity in mice. *FEMS Microbiol Lett, 234*(2), 289-295.

Kinney, D. M., Foster, J. W., & Moat, A. G. (1979). Pyridine nucleotide cycle of *Salmonella typhimurium*: in vitro demonstration of nicotinamide mononucleotide deamidase and characterization of pnuA mutants defective in nicotinamide mononucleotide transport. *J Bacteriol, 140*(2), 607-611.

Kleene, R., & Schachner, M. (2004). Glycans and neural cell interactions. *Nat Rev Neurosci., 5*(3), 195-208.

Knapp, S., de Vos, W. M., Rice, D., & Ladenstein, R. (1997). Crystal structure of glutamate dehydrogenase from the hyperthermophilic eubacterium *Thermotoga maritima* at 3.0 A resolution. *J Mol Biol, 267*(4), 916-932.

Korber, F. C., Rizkallah, P. J., Attwood, T. K., Wootton, J. C., McPherson, M. J., North, A. C., Geddes, A. J., Abeysinghe, I. S., Baker, P. J., Dean, J. L., & et al. (1993). Crystallization of the NADP(+)-dependent glutamate dehydrogenase from *Escherichia coli*. *J Mol Biol, 234*(4), 1270-1273.

Kragl, U., Gygax, D., Ghisalba, O., & Wandrey, C. (1991). Enzymatic Two-Step Synthesis of *N*-Acetyl-neuraminic Acid in the Enzyme Membrane Reactor. *Angewandte Chemie International Edition in English*, *30*(7), 827-828

Kruger, D., Schauer, R., & Traving, C. (2001). Characterization and mutagenesis of the recombinant *N*-acetylneuraminate lyase from *Clostridium perfringens*: insights into the reaction mechanism. *Eur J Biochem, 268*(13), 3831-3839.

Kuchner, O., & Arnold, F. H. (1997). Directed evolution of enzyme catalysts. *Trends Biotechnol, 15*(12), 523-530.

Kuhn, R., Brossmer, R. (1962). *Angewandte Chemie*, *74*(7), 252-253.

Laemmli, U.K. (1970). Cleavage of structural proteins during the assembly of the head of bacteriophage T4. *Nature*, *227*(5259), 680-5.

Lanave, C., Preparata, G., Saccone, C., & Serio, G. (1984). A new method for calculating evolutionary substitution rates. *J Mol Evol*, *20*(1), 86-93.

Landry, J., Slama, J. T., & Sternglanz, R. (2000). Role of NAD(+) in the deacetylase activity of the SIR2-like proteins. *Biochem Biophys Res Commun, 278*(3), 685-690.

Lasky, L.A. (1995). Selectin-Carbohydrate Interactions and the Initiation of the Inflammatory Response. *Annual Review of Biochemistry*, *64*(1), 113-140.

Lawrence, M. C., Barbosa, J. A., Smith, B. J., Hall, N. E., Pilling, P. A., Ooi, H. C., & Marcuccio, S. M. (1997). Structure and mechanism of a sub-family of enzymes related to *N*-acetylneuraminate lyase. *J Mol Biol, 266*(2), 381-399.

LeVan, K. M., & Goldberg, E. (1991). Properties of human testis-specific lactate dehydrogenase expressed from *Escherichia coli*. *Biochem J, 273 (Pt 3)*, 587-592.

Li, Y., & Chen, X. (2012). Sialic acid metabolism and sialyltransferases: natural functions and applications. *Appl Microbiol Biotechnol, 94*(4), 887-905.

Li, Y., Yu, H., Cao, H., Lau, K., Muthana, S., Tiwari, V. K., Son, B., & Chen, X. (2008). *Pasteurella multocida* sialic acid aldolase: a promising biocatalyst. *Appl Microbiol Biotechnol, 79*(6), 963-970.

Liese, A., Seelbach, K., & Wandrey, C. (2001). *Putting Enzymes to Work: Industrial Biotransformations.* (Vol. 19). Weinheim.

Lilley, G. G., Barbosa, J. A., & Pearce, L. A. (1998). Expression in *Escherichia coli* of the putative *N*-acetylneuraminate lyase gene (nanA) from *Haemophilus influenzae:* overproduction, purification, and crystallization. *Protein Expr Purif, 12*(3), 295-304.

Lin, S. J., Defossez, P. A., & Guarente, L. (2000). Requirement of NAD and SIR2 for life-span extension by calorie restriction in *Saccharomyces cerevisiae*. *Science, 289*(5487), 2126-2128.

Liu, G., Foster, J., Manlapaz-Ramos, P., & Olivera, B. M. (1982). Nucleoside salvage pathway for NAD biosynthesis in *Salmonella typhimurium*. *J Bacteriol, 152*(3), 1111-1116.

Liu, Y., Gerber, R., Wu, J., Tsuruda, T., & McCarter, J. D. (2008). High-throughput assays for sirtuin enzymes: a microfluidic mobility shift assay and a bioluminescence assay. *Anal Biochem, 378*(1), 53-59.

Lowe, J.B., Stoolman, L.M., Nair, R.P., Larsen, R.D., Berhend, T.L., & Marks, R.M. (1990). ELAM-1-dependent cell adhesion to vascular endothelium determined by a transfected human fucosyltransferase cDNA. *Cell*, *63*(3), 475-484.

Ma, K., Robb, F. T., & Adams, M. W. (1994). Purification and characterization of NADP-specific alcohol dehydrogenase and glutamate dehydrogenase from the hyperthermophilic archaeon *Thermococcus litoralis*. *Appl Environ Microbiol, 60*(2), 562-568.

Mackintosh, J. A., Choi, H. Y., Bae, S. H., Veal, D. A., Bell, P. J., Ferrari, B. C., Van Dyk, D. D., Verrills, N. M., Paik, Y. K., & Karuso, P. (2003). A fluorescent natural product for ultra sensitive detection of proteins in one-dimensional and two-dimensional gel electrophoresis. *Proteomics, 3*(12), 2273-2288.

Maggio-Hall, L. A., & Escalante-Semerena, J. C. (2003). Alpha-5,6-dimethylbenzimidazole adenine dinucleotide (alpha-DAD), a putative new intermediate of coenzyme B12 biosynthesis in *Salmonella typhimurium*. *Microbiology, 149*(Pt 4), 983-990.

Mahmoudian, M., Noble, D., Drake, C. S., Middleton, R. F., Montgomery, D. S., Piercey, J. E., Ramlakhan, D., Todd, M., & Dawson, M. J. (1997). An efficient process for production of *N*-acetylneuraminic acid using *N*-acetylneuraminic acid aldolase. *Enzyme Microb Technol, 20*(5), 393-400.

Malawski, G. A., Hillig, R. C., Monteclaro, F., Eberspaecher, U., Schmitz, A. A., Crusius, K., Huber, M., Egner, U., Donner, P., & Muller-Tiemann, B. (2006). Identifying protein construct variants with increased crystallization propensity-a case study. *Protein Sci, 15*(12), 2718-2728.

Maloy, S., Stewart, V., & Taylor, R. (1996). *Genetic analysis of pathogenic bacteria.* New York: Cold Spring Harbor Laboratory Press.

Martinez-Martinez, I., Kaiser, C., Rohde, A., Ellert, A., Garcia-Carmona, F., Sanchez-Ferrer, A., & Luttmann, R. (2007). High-level production of *bacillus subtilis* glycine oxidase by fed-batch cultivation of recombinant *Escherichia col*i Rosetta (DE3). *Biotechnol Prog, 23*(3), 645-651.

Maru, I., Ohnishi, J., Ohta, Y., & Tsukada, Y. (2002). Why is sialic acid attracting interest now? complete enzymatic synthesis of sialic acid with *N*-acylglucosamine 2-epimerase. *Journal of Bioscience and Bioengineering*, *93*(3), 258-265.

McPherson, M. J., & Wootton, J. C. (1983). Complete nucleotide sequence of the Escherichia coli *gdhA* gene. *Nucleic Acids Res, 11*(15), 5257-5266.

Meinke, S., Schroven, A., & Thiem, J. (2011). Sialic acid C-glycosides with aromatic residues: Investigating enzyme binding and inhibition of *Trypanosoma cruzi* trans-sialidase. *Org Biomol Chem*.

Mendez, C., & Salas, J. A. (2001). Altering the glycosylation pattern of bioactive compounds. *Trends Biotechnol, 19*(11), 449-456.

Meysick, K. C., Dimock, K., & Garber, G. E. (1996). Molecular characterization and expression of a N-acetylneuraminate lyase gene from *Trichomonas vaginalis*. *Mol Biochem Parasitol, 76*(1-2), 289-292.

Michalopoulos, I., Torrance, G. M., Gilbert, D. R., & Westhead, D. R. (2004). TOPS: an enhanced database of protein structural topology. *Nucleic Acids Res, 32*(Database issue), D251-254.

Michan, S., & Sinclair, D. (2007). Sirtuins in mammals: insights into their biological function. *Biochem J, 404*(1), 1-13.

Michishita, E., McCord, R. A., Berber, E., Kioi, M., Padilla-Nash, H., Damian, M., Cheung, P., Kusumoto, R., Kawahara, T. L., Barrett, J. C., Chang, H. Y., Bohr, V. A., Ried, T., Gozani, O., & Chua, K. F. (2008). SIRT6 is a histone H3 lysine 9 deacetylase that modulates telomeric chromatin. *Nature, 452*(7186), 492-496.

Milne, J. C., Lambert, P. D., Schenk, S., Carney, D. P., Smith, J. J., Gagne, D. J., Jin, L., Boss, O., Perni, R. B., Vu, C. B., Bemis, J. E., Xie, R., Disch, J. S., Ng, P. Y., Nunes, J. J., Lynch, A. V., Yang, H., Galonek, H., Israelian, K., Choy, W., Iffland, A., Lavu, S., Medvedik, O., Sinclair, D. A., Olefsky, J. M., Jirousek, M. R., Elliott, P. J., & Westphal, C. H. (2007). Small molecule activators of SIRT1 as therapeutics for the treatment of type 2 diabetes. *Nature, 450*(7170), 712-716.

Mitrasinovic, P. M. (2010). Advances in the structure-based design of the influenza A neuraminidase inhibitors. *Curr Drug Targets, 11*(3), 315-326.

Montoro-Garcia, S., Gil-Ortiz, F., Navarro-Fernandez, J., Rubio, V., Garcia-Carmona, F., & Sanchez-Ferrer, A. (2010). Improved cross-linked enzyme aggregates for the production of desacetyl beta-lactam antibiotics intermediates. *Bioresour Technol, 101*(1), 331-336.

Mulkiewicz, E., Zietara, M. S., Stachowiak, K., & Skorkowski, E. F. (2000). Properties of lactate dehydrogenase from the isopod, *Saduria entomon*. *Comp Biochem Physiol B Biochem Mol Biol, 126*(3), 337-346.

Murphy, D.J. 2004. Determination of accurate KI values for tight-binding enzyme inhibitors: an in silico study of experimental error and assay design. *Anal Biochem*, **327**(1), 61-7.

Navarro-Fernandez, J., Martinez-Martinez, I., Montoro-Garcia, S., Garcia-Carmona, F., Takami, H., & Sanchez-Ferrer, A. (2008). Characterization of a new

rhamnogalacturonan acetyl esterase from *Bacillus halodurans* C-125 with a new putative carbohydrate binding domain. *J Bacteriol, 190*(4), 1375-1382.

Nees, S., Schauer, R., & Mayer, F. (1976). Purification and characterization of *N*-acetylneuraminate lyase from *Clostridium perfringens*. *Hoppe Seylers Z Physiol Chem, 357*(6), 839-853.

Negi, S.S., Kolokoltsov, A.A., Schein, C.H., Davey, R.A., Braun, W. 2006. Determining functionally important amino acid residues of the E1 protein of Venezuelan equine encephalitis virus. *J Mol Model*, **12**(6), 921-9.

Oberdoerffer, P., & Sinclair, D. A. (2007). The role of nuclear architecture in genomic instability and ageing. *Nat Rev Mol Cell Biol, 8*(9), 692-702.

Ohshima, T., & Nishida, N. (1993). Purification and properties of extremely thermostable glutamate dehydrogenases from two hyperthermophilic archaebacteria, *Pyrococcus woesei* and *Pyrococcus furiosus*. *Biosci Biotechnol Biochem, 57*(6), 945-951.

Ohta, Y., Shinosaka, K., Murata, Y., Tsukada, Y., & Kimura, A. (1986). Molecular cloning of the *N*-acetylneuraminate lyase gene from *Escherichia coli* K-12. *Appl Microbiol Biotechnol, 24*, 386-391.

Ohta, Y., Watanabe, K., & Kimura, A. (1985). Complete nucleotide sequence of the *E. coli N*-acetylneuraminate lyase. *Nucleic Acids Res, 13*(24), 8843-8852.

Olivera, B. M., & Lehman, I. R. (1967). Diphosphopyridine nucleotide: a cofactor for the polynucleotide-joining enzyme from *Escherichia coli*. *Proc Natl Acad Sci U S A, 57*(6), 1700-1704.

Op den Camp, H. J., Liem, K. D., Meesters, P., Hermans, J. M., & Van der Drift, C. (1989). Purification and characterization of the NADP-dependent glutamate dehydrogenase from *Bacillus fastidiosus*. *Antonie Van Leeuwenhoek, 55*(4), 303-311.

Ota, K., Kiyomiya, A., Koyama, N., & Noso, Y. (1975). The basis of the alkalophilic property of a species of *bacillus*. *J Gen Microbiol, 86*(2), 259-266.

Outeiro, T. F., Kontopoulos, E., Altmann, S. M., Kufareva, I., Strathearn, K. E., Amore, A. M., Volk, C. B., Maxwell, M. M., Rochet, J. C., McLean, P. J., Young, A. B., Abagyan, R., Feany, M. B., Hyman, B. T., & Kazantsev, A. G. (2007). Sirtuin 2 inhibitors rescue alpha-synuclein-mediated toxicity in models of Parkinson's disease. *Science, 317*(5837), 516-519.

Oxford, J.S. (2000). Influenza A pandemics of the 20th century with special reference to 1918: virology, pathology and epidemiology. *Reviews in Medical Virology*, *10(*2), 119-133.

Pacholec, M., Bleasdale, J. E., Chrunyk, B., Cunningham, D., Flynn, D., Garofalo, R. S., Griffith, D., Griffor, M., Loulakis, P., Pabst, B., Qiu, X., Stockman, B., Thanabal, V., Varghese, A., Ward, J., Withka, J., & Ahn, K. (2010). SRT1720, SRT2183, SRT1460, and resveratrol are not direct activators of SIRT1. *J Biol Chem, 285*(11), 8340-8351.

Pardee, A.B., Benz, E.J., Jr., St Peter, D.A., Krieger, J.N., Meuth, M., & Trieshmann, H.W., Jr. (1971). Hyperproduction and purification of nicotinamide deamidase, a microconstitutive enzyme of Escherichia coli. *J Biol Chem*, *246*(22), 6792-6.

Park, U. E., Olivera, B. M., Hughes, K. T., Roth, J. R., & Hillyard, D. R. (1989). DNA ligase and the pyridine nucleotide cycle in *Salmonella typhimurium*. *J Bacteriol, 171*(4), 2173-2180.

Pearcy, J.O., Lee, T.D. 2001. MoWeD, a computer program to rapidly deconvolute low resolution electrospray liquid chromatography/mass spectrometry runs to determine component molecular weights. *J Am Soc Mass Spectrom*, **12**(5), 599-606.

Petrella, S., Gelus-Ziental, N., Maudry, A., Laurans, C., Boudjelloul, R., Sougakoff, W. (2011). Crystal structure of the pyrazinamidase of *Mycobacterium tuberculosis:* insights into natural and acquired resistance to pyrazinamide. *PLoS One*, *6*(1), e15785.

Phillips, M.L., Nudelman, E., Gaeta, F.C., Perez, M., Singhal, A.K., Hakomori, S., & Paulson, J.C. (1990). ELAM-1 mediates cell adhesion by recognition of a carbohydrate ligand, sialyl-Lex. *Science*, *250*(4984), 1130-2.

Plumbridge, J., Vimr, E. 1999. Convergent Pathways for Utilization of the Amino Sugars *N*-Acetylglucosamine, *N*-Acetylmannosamine, and *N*-Acetylneuraminic Acid by *Escherichia coli*. *J. Bacteriol.*, *181*(1), 47-54.

Porcu, M., & Chiarugi, A. (2005). The emerging therapeutic potential of sirtuin-interacting drugs: from cell death to lifespan extension. *Trends Pharmacol Sci, 26*(2), 94-103.

Posada, D., & Crandall, K.A. (1998). MODELTEST: testing the model of DNA substitution. *Bioinformatics*, *14*(9), 817-8.

Preiss, J., & Handler, P. (1958a). Biosynthesis of diphosphopyridine nucleotide. I. Identification of intermediates. *J Biol Chem, 233*(2), 488-492.

Preiss, J., & Handler, P. (1958b). Biosynthesis of diphosphopyridine nucleotide. II. Enzymatic aspects. *J Biol Chem, 233*(2), 493-500.

Preston, A., Mandrell, R.E., Gibson, B.W., Apicella, M.A. 1996. The Lipooligosaccharides of Pathogenic Gram-Negative Bacteria. *Critical Reviews in Microbiology*, *22*(3), 139-180.

Purser, J. E., Lawrenz, M. B., Caimano, M. J., Howell, J. K., Radolf, J. D., & Norris, S. J. (2003). A plasmid-encoded nicotinamidase (PncA) is essential for infectivity of *Borrelia burgdorferi* in a mammalian host. *Mol Microbiol, 48*(3), 753-764.

Read, J. A., Winter, V. J., Eszes, C. M., Sessions, R. B., & Brady, R. L. (2001). Structural basis for altered activity of M- and H-isozyme forms of human lactate dehydrogenase. *Proteins, 43*(2), 175-185.

Rice, D. W., Baker, P. J., Farrants, G. W., & Hornby, D. P. (1987). The crystal structure of glutamate dehydrogenase from *Clostridium symbiosum* at 0.6 nm resolution. *Biochem J, 242*(3), 789-795.

Rice, D. W., Hornby, D. P., & Engel, P. C. (1985). Crystallization of an NAD+-dependent glutamate dehydrogenase from *Clostridium symbiosum*. *J Mol Biol, 181*(1), 147-149.

Rich, J. O., Michels, P. C., & Khmelnitsky, Y. L. (2002). Combinatorial biocatalysis. *Curr Opin Chem Biol, 6*(2), 161-167.

Ringenberg, M.A., Steenbergen, S.M., & Vimr, E.R. (2003). The first committed step in the biosynthesis of sialic acid by *Escherichia coli* K1 does not involve a phosphorylated *N*-acetylmannosamine intermediate. *Molecular Microbiology*, *50*(3), 961-975.

Rodgers, B. (1978). Feeding in infancy and later ability and attainment: a longitudinal study. *Dev Med Child Neurol*, *20*(4), 421-6.

Rogers, P. L., Jeon, Y. J., & Svenson, C. J. (2001). *The Application of Biotechnology to Industrial Sustainability.* Paris, France.

Russell, P. J., Williams, A., Amador, X., & Vargas, R. (2004). Aldolase and actin protect rabbit muscle lactate dehydrogenase from ascorbate inhibition. *J Enzyme Inhib Med Chem, 19*(1), 91-98.

Salazar, O., & Sun, L. (2003). Evaluating a screen and analysis of mutant libraries. *Methods Mol Biol, 230*, 85-97.

Sambrook, J., Fritsch, E. P., & Maniatis, T. (1989). *Molecular cloning: a laboratory manual 2nd ed.* Cold Spring harbor, NY: Cold Spring harbor Laboratory Press.

Sanchez-Carron, G., Garcia-Garcia, M. I., Lopez-Rodriguez, A. B., Jimenez-Garcia, S., Sola-Carvajal, A., Garcia-Carmona, F., & Sanchez-Ferrer, A. (2011). Molecular characterization of a novel *N*-acetylneuraminate lyase from *Lactobacillus plantarum* WCFS1. *Appl Environ Microbiol, 77*(7), 2471-2478.

Sanwal, B. D. (1970). Allosteric controls of amphilbolic pathways in bacteria. *Bacteriol Rev, 34*(1), 20-39.

Sauve, A. A. (2008). NAD+ and vitamin B3: from metabolism to therapies. *J Pharmacol Exp Ther, 324*(3), 883-893.

Sauve, A. A., Wolberger, C., Schramm, V. L., & Boeke, J. D. (2006). The biochemistry of sirtuins. *Annu Rev Biochem, 75*, 435-465.

Scorpio, A., & Zhang, Y. (1996). Mutations in pncA, a gene encoding pyrazinamidase/nicotinamidase, cause resistance to the antituberculous drug pyrazinamide in tubercle *bacillus*. *Nat Med, 2*(6), 662-667.

Schauer, R. (1982). Chemistry, metabolism, and biological functions of sialic acids. *Adv Carbohydr Chem Biochem, 40*, 131-234.

Schauer, R. (2000). Achievements and challenges of sialic acid research. *Glycoconj J, 17*(7-9), 485-499.

Schauer, R., Sommer, U., Kruger, D., van Unen, H., & Traving, C. (1999). The terminal enzymes of sialic acid metabolism: acylneuraminate pyruvate-lyases. *Biosci Rep, 19*(5), 373-383.

Schlicker, C., Gertz, M., Papatheodorou, P., Kachholz, B., Becker, C. F., & Steegborn, C. (2008). Substrates and regulation mechanisms for the human mitochondrial sirtuins Sirt3 and Sirt5. *J Mol Biol, 382*(3), 790-801.

Schmid, A., Dordick, J. S., Hauer, B., Kiener, A., Wubbolts, M., & Witholt, B. (2001). Industrial biocatalysis today and tomorrow. *Nature, 409*(6817), 258-268.

Schrodinger, L. (2010). The PyMOL Moleuclar Graphics System. Version 1.3rl.

Schultheisz, H. L., Szymczyna, B. R., & Williamson, J. R. (2009). Enzymatic synthesis and structural characterization of 13C, 15N-poly(ADP-ribose). *J Am Chem Soc, 131*(40), 14571-14578.

Schwarz, G., Mendel, R. R., & Ribbe, M. W. (2009). Molybdenum cofactors, enzymes and pathways. *Nature, 460*(7257), 839-847.

Severi, E., Hood, D. W., & Thomas, G. H. (2007). Sialic acid utilization by bacterial pathogens. *Microbiology, 153*(Pt 9), 2817-2822.

Shafikhani, S., Siegel, R. A., Ferrari, E., & Schellenberger, V. (1997). Generation of large libraries of random mutants in *Bacillus subtilis* by PCR-based plasmid multimerization. *Biotechniques, 23*(2), 304-310.

Sharkey, M. A., & Engel, P. C. (2009). Modular coenzyme specificity: a domain-swopped chimera of glutamate dehydrogenase. *Proteins, 77*(2), 268-278.

Shi, T., Wang, F., Stieren, E., & Tong, Q. (2005). SIRT3, a mitochondrial sirtuin deacetylase, regulates mitochondrial function and thermogenesis in brown adipocytes. *J Biol Chem, 280*(14), 13560-13567.

Smith, B. C., Hallows, W. C., & Denu, J. M. (2009). A continuous microplate assay for sirtuins and nicotinamide-producing enzymes. *Anal Biochem, 394*(1), 101-109.

Smith, E. L., Austen, B. M., Blumenthal, K. M., & Nyc, J. F. (1975). Glutamate dehydrogenases. In P. D. 3rd Edn (Boyer, ed) (Ed.), *The Enzymes*, vol. 11 (pp. 293-367). New York: Academic Press.

Smith, J. S., & Boeke, J. D. (1997). An unusual form of transcriptional silencing in yeast ribosomal DNA. *Genes Dev, 11*(2), 241-254.

Smith, P.W., Sollis, S.L., Howes, P.D., Cherry, P.C., Starkey, I.D., Cobley, K.N., Weston, H., Scicinski, J., Merritt, A., Whittington, A., Wyatt, P., Taylor, N., Green, D., Bethell, R., Madar, S., Fenton, R.J., Morley, P.J., Pateman, T., & Beresford, A. (1998). Dihydropyrancarboxamides Related to Zanamivir: A New Series of Inhibitors of Influenza Virus Sialidases. 1. Discovery, Synthesis, Biological Activity, and Structure−Activity Relationships of 4-

Guanidino- and 4-Amino-4H-pyran-6-carboxamides. *Journal of Medicinal Chemistry*, *41*(6), 787-797.

Soundararajan, V., Tharakaraman, K., Raman, R., Raguram, S., Shriver, Z., Sasisekharan, V., & Sasisekharan, R. (2009). Extrapolating from sequence[mdash]the (2009) H1N1 'swine' influenza virus. *Nat Biotech*, *27*(6), 510-513.

Spivak, C.T., Roseman, S. (1959). Preparation of N-Acetyl-D-mannosamine (2-Acetamido-2-deoxy-D-mannose) and D-Mannosamine Hydrochloride (2-Amino-2-deoxy-D-mannose)1. *Journal of the American Chemical Society, 81*(10), 2403-2404.

Stillman, T. J., Baker, P. J., Britton, K. L., & Rice, D. W. (1993). Conformational flexibility in glutamate dehydrogenase. Role of water in substrate recognition and catalysis. *J Mol Biol, 234*(4), 1131-1139.

Suzuki, M., Christians, F. C., Kim, B., Skandalis, A., Black, M. E., & Loeb, L. A. (1996). Tolerance of different proteins for amino acid diversity. *Mol Divers, 2*(1-2), 111-118.

Taguchi, H., & Ohta, T. (1995). Role of histidine 188 in fructose 1,6-bisphosphate- and divalent cation-regulated L-lactate dehydrogenase of *Lactobacillus casei*. *Biosci Biotechnol Biochem, 59*(3), 451-458.

Tamura, K., Dudley, J., Nei, M., & Kumar, S. (2007). MEGA4: Molecular Evolutionary Genetics Analysis (MEGA) software version 4.0. *Mol Biol Evol, 24*(8), 1596-1599.

Tanigawa, Y., Shimoyama, M., & Ueda, I. (1980). Nicotinamide deamidase from *Flavobacterium peregrinum*. *Methods Enzymol, 66*, 132-136.

Tao, N., DePeters, E.J., German, J.B., Grimm, R., & Lebrilla, C.B. (2009). Variations in bovine milk oligosaccharides during early and middle lactation stages analyzed by high-performance liquid chromatography-chip/mass spectrometry. *Journal of Dairy Science*, *92*(7), 2991-3001.

Taylor, N.R., Cleasby, A., Singh, O., Skarzynski, T., Wonacott, A.J., Smith, P.W., Sollis, S.L., Howes, P.D., Cherry, P.C., Bethell, R., Colman, P., & Varghese, J. (1998). Dihydropyrancarboxamides Related to Zanamivir: A New Series of Inhibitors of Influenza Virus Sialidases. 2. Crystallographic and Molecular Modeling Study of Complexes of 4-Amino-4H-pyran-6-

carboxamides and Sialidase from Influenza Virus Types A and B. *Journal of Medicinal Chemistry*, **41**(6), 798-807.

Thompson, J. D., Higgins, D. G., & Gibson, T. J. (1994). CLUSTAL W: improving the sensitivity of progressive multiple sequence alignment through sequence weighting, position-specific gap penalties and weight matrix choice. *Nucleic Acids Res, 22*(22), 4673-4680.

Traving, C., Roggentin, P., & Schauer, R. (1997). Cloning, sequencing and expression of the acylneuraminate lyase gene from *Clostridium perfringens* A99. *Glycoconj J, 14*(7), 821-830.

Traving, C., Schauer, R. 1998. Structure, function and metabolism of sialic acids. *Cell Mol Life Sci*, **54**(12), 1330-49.

Uchikoba, H., Fushinobu, S., Wakagi, T., Konno, M., Taguchi, H., & Matsuzawa, H. (2002). Crystal structure of non-allosteric L-lactate dehydrogenase from *Lactobacillus pentosus* at 2.3 A resolution: specific interactions at subunit interfaces. *Proteins, 46*(2), 206-214.

Ugorski, M., & Laskowska, A. (2002). Sialyl Lewis(a): a tumor-associated carbohydrate antigen involved in adhesion and metastatic potential of cancer cells. *Acta Biochim Pol*, *49*(2), 303-11.

van Beilen, J. B., & Li, Z. (2002). Enzyme technology: an overview. *Curr Opin Biotechnol, 13*(4), 338-344.

van der Horst, A., Schavemaker, J. M., Pellis-van Berkel, W., & Burgering, B. M. (2007). The *Caenorhabditis elegans* nicotinamidase PNC-1 enhances survival. *Mech Ageing Dev, 128*(4), 346-349.

Vancurova, I., Vancura, A., Volc, J., Kopecky, J., Neuzil, J., Basarova, G., & Behal, V. (1989). Purification and properties of NADP-dependent glutamate dehydrogenase from *Streptomyces fradiae*. *J Gen Microbiol, 135*(12), 3311-3318.

Varki, A., Diaz, S., & Taylor, R. (2011). Elimination of a contaminating non-human sialic acid by metabolic competition. In, vol. 062069).

Varki, N. M., Strobert, E., Dick, E. J., Jr., Benirschke, K., & Varki, A. (2011). Biomedical differences between human and nonhuman hominids: potential roles for uniquely human aspects of sialic acid biology. *Annu Rev Pathol, 6*, 365-393.

Varki, A. 1997. Sialic acids as ligands in recognition phenomena. *The FASEB Journal*, **11**(4), 248-255.

Varki, A. 1993. Biological roles of oligosaccharides: all of the theories are correct. *Glycobiology*, **3**(2), 97-130.

Veh, R.W., Michalski, J.C., Corfield, A.P., Sander-Wewer, M., Gies, D., Schauer, R. 1981. New chromatographic system for the rapid analysis and preparation of colostrum sialyloligosaccharides. *J Chromatogr*, **212**(3), 313-22.

Vestweber, D., Blanks, J.E. 1999. Mechanisms That Regulate the Function of the Selectins and Their Ligands. *Physiological Reviews*, **79**(1), 181-213.

Veronese, F. M., Nyc, J. F., Degani, Y., Brown, D. M., & Smith, E. L. (1974). Nicotinamide adenine dinucleotide-specific glutamate dehydrogenase of *Neurospora.* I. Purification and molecular properties. *J Biol Chem, 249*(24), 7922-7928.

Vimr, E. R., Kalivoda, K. A., Deszo, E. L., & Steenbergen, S. M. (2004). Diversity of microbial sialic acid metabolism. *Microbiol Mol Biol Rev, 68*(1), 132-153.

Vimr, E.R., & Troy, F.A. (1985a). Identification of an inducible catabolic system for sialic acids (nan) in *Escherichia coli. J. Bacteriol.*, *164*(2), 845-853.

Vimr, E. R., & Troy, F. A. (1985b). Regulation of sialic acid metabolism in *Escherichia coli*: role of *N*-acylneuraminate pyruvate-lyase. *J Bacteriol, 164*(2), 854-860.

Vimr, E.R., Troy, F.A. 1985c. Regulation of sialic acid metabolism in *Escherichia coli*: role of *N*-acylneuraminate pyruvate-lyase. *J. Bacteriol.*, **164**(2), 854-860.

Vogel, U., Hammerschmidt, S., & Frosch, M. (1996). Sialic acids of both the capsule and the sialylated lipooligosaccharide of *Neisseria meningitis* serogroup B are prerequisites for virulence of meningococci in the infant rat. *Med Microbiol Immunol*, *185*(2), 81-7.

Von Itzstein, M., Wu, W.-Y., Kok, G.B., Pegg, M.S., Dyason, J.C., Jin, B., Phan, T.V., Smythe, M.L., White, H.F., Oliver, S.W., Colman, P.M., Varghese, J.N., Ryan, D.M., Woods, J.M., Bethell, R.C., Hotham, V.J., Cameron, J.M., & Penn, C.R. (1993). Rational design of potent sialidase-based inhibitors of influenza virus replication. *Nature, 363*(6428), 418-423.

Vrablik, T. L., Huang, L., Lange, S. E., & Hanna-Rose, W. (2009). Nicotinamidase modulation of NAD^+ biosynthesis and nicotinamide levels separately affect reproductive development and cell survival in *C. elegans. Development, 136*(21), 3637-3646.

Wada, M., Hsu, C. C., Franke, D., Mitchell, M., Heine, A., Wilson, I., & Wong, C. H. (2003). Directed evolution of *N*-acetylneuraminic acid aldolase to catalyze enantiomeric aldol reactions. *Bioorg Med Chem, 11*(9), 2091-2098.

Waldvogel, S., Weber, H., & Zuber, H. (1987). Structure and function of L-lactate dehydrogenases from thermophilic and mesophilic bacteria. VII. Nucleotide sequence of the lactate dehydrogenase gene from the mesophilic bacterium *Bacillus megaterium*. Preparation and properties of a hybrid lactate dehydrogenase comprising moieties of the *B. megaterium and B. stearothermophilus* enzymes. *Biol Chem Hoppe Seyler, 368*(10), 1391-1399.

Wang, G., & Pichersky, E. (2007). Nicotinamidase participates in the salvage pathway of NAD biosynthesis in Arabidopsis. *Plant J, 49*(6), 1020-1029.

Wang, T. H., & Lee, W. C. (2005). Production of 2-keto-3-deoxy-D-glycero-D-galacto-nonopyranulosonic acid (KDN) using fusion protein of *N*-acetyl-D-neuraminic acid aldolase. *Biochem. eng. J., 29*, 75-80.

Wang, B. 2009. Sialic Acid Is an Essential Nutrient for Brain Development and Cognition. *Annual Review of Nutrition*, **29**(1), 177-222.

Wang, B., Brand-Miller, J. 2003. The role and potential of sialic acid in human nutrition. *Eur J Clin Nutr*, **57**(11), 1351-1369.

Wang, B., Brand-Miller, J., McVeagh, P., Petocz, P. 2001. Concentration and distribution of sialic acid in human milk and infant formulas. *The American Journal of Clinical Nutrition*, **74**(4), 510-515.

Wegener, D., Hildmann, C., Riester, D., & Schwienhorst, A. (2003). Improved fluorogenic histone deacetylase assay for high-throughput-screening applications. *Anal Biochem, 321*(2), 202-208.

Wigley, D. B., Gamblin, S. J., Turkenburg, J. P., Dodson, E. J., Piontek, K., Muirhead, H., & Holbrook, J. J. (1992). Structure of a ternary complex of an allosteric lactate dehydrogenase from *Bacillus stearothermophilus* at 2.5 A resolution. *J Mol Biol, 223*(1), 317-335.

Williams, J.D., Weiner, B.E., Ormand, J.R., Brunner, J., Thornquest, A.D., Jr., Burinsky, D.J. 2001. Automated molecular weight assignment of

electrospray ionization mass spectra. *Rapid Commun Mass Spectrom*, **15**(24), 2446-55.

Wong, C. H., & Whitesides, G. M. (1994). *Enzymes in synthetic organic chemistry*. Oxford, United Kingdom: Elsevier.

Wu, S., Acevedo, J. P., & Reetz, M. T. (2010). Induced allostery in the directed evolution of an enantioselective Baeyer-Villiger monooxygenase. *Proc Natl Acad Sci U S A, 107*(7), 2775-2780.

Xu, P., Qiu, J.H., Zhang, Y.N., Chen, J., Wang, P.G., Yan, B., Song, J., Xi, R.M., Deng, Z.X., & Ma, C.Q. (2007). Efficient Whole-Cell Biocatalytic Synthesis of *N*-Acetyl-D-neuraminic Acid. *Advanced Synthesis & Catalysis*, *349(*10), 1614-1618.

Yan, C., & Sloan, D.L. (1987). Purification and characterization of nicotinamide deamidase from yeast. *J Biol Chem, 262*(19), 9082-7.

Yu, H., & Chen, X. (2006). Aldolase-catalyzed synthesis of beta-D-galp-(1-->9)-D-KDN: a novel acceptor for sialyltransferases. *Org Lett, 8*(11), 2393-2396.

Yu, H., Karpel, R., & Chen, X. (2004). Chemoenzymatic synthesis of CMP-sialic acid derivatives by a one-pot two-enzyme system: comparison of substrate flexibility of three microbial CMP-sialic acid synthetases. *Bioorg Med Chem, 12*(24), 6427-6435.

Zerez, C. R., Roth, E. F., Jr., Schulman, S., & Tanaka, K. R. (1990). Increased nicotinamide adenine dinucleotide content and synthesis in *Plasmodium falciparum*-infected human erythrocytes. *Blood, 75*(8), 1705-1710.

Zhang, H., Deng, J. Y., Bi, L. J., Zhou, Y. F., Zhang, Z. P., Zhang, C. G., Zhang, Y., & Zhang, X. E. (2008). Characterization of *Mycobacterium tuberculosis* nicotinamidase/pyrazinamidase. *FEBS J, 275*(4), 753-762.